
# Attachment of peri-implant pathogens to laser melted abutments and the development of a novel antimicrobial coating

Clotilde Haury

A thesis submitted to Cardiff University for the degree of Doctor of Philosophy

School of Dentistry

2019

# Declaration

This work has not been submitted in substance for any other degree or award at this or any other university or place of learning, nor is being submitted concurrently in candidature for any degree or other award.

Signed:.....Clotilde Haury.....(Clotilde Haury) Date: 14/02/20

# Statement 1

This thesis is being submitted in partial ful_llment of the requirements for the degree of PhD.

Signed:.....Clotilde Haury.....(Clotilde Haury) Date: 14/02/20

# Statement 2

This thesis is the result of my own independent work/investigation, except where otherwise stated. Other sources are acknowledged by explicit references. The views expressed are my own.

Signed:.....Clotilde Haury.....(Clotilde Haury) Date: 14/02/20

# Statement 3

I hereby give consent for my thesis, if accepted, to be available for photocopying and for inter-library loan, and for the title and summary to be made available to outside organisations.

Signed:.....Clotilde Haury.....(Clotilde Haury) Date: 14/02/20

*To Mum and Pierrot*
*Who always supported my decisions,*
*Sometimes with tears,*
*Always with love.*

# Acknowledgements

I would like to express my gratitude to my supervisors for giving me the opportunity to carry out this research project as well as for their support and guidance over the course of my PhD. Thank you, Dr. Wayne Ayre, for your patience and your time. I know it was not always easy. Many thanks to Prof. Alastair Sloan for teaching me patience and diplomacy, and for re-motivating me when it was hard to keep going. I would like to thank Mr. Quentin Jones, for advising me on the clinical side of my PhD and for helping me attend an implant placement at the School of Dentistry. I would like to thank Renishaw PLC Medical and Dental Products Division for supporting my research. Without the funding, expertise and help from Renishaw, this project would never have been possible. I also would like to thank NEXUS at Newcastle University for helping me analyse the samples by XPS and Dr. Aurélie Beal and Prof. Roger Phan-Tan-Luu from NemrodW for helping me with the DoE.

I owe sincere thankfulness to Prof. David Williams whose knowledge in microbiology and assistance, especially during my third year were invaluable.

I would like to thank everyone in the School of Dentistry for their constant help and support: Fiona, without whom the labs would just not run; Daf, Helen and Sarah B. for helping me so much in micro; Mathieu for his assistance in using the HPLC; Martin for helping me use the centrifuge and the freeze-dryer (I failed the first time!); Wendy for teaching me how to use the microscopes. Thank you all for your assistance and know-how in the lab. Thanks to Sarah Y. and Sarah B. for the lab chats and the tech office chats, especially during my third year! Vera, thank you so much for your continuous support. I would not have made it without you!
Life at the Dental School would not have been as enjoyable and I would have been much less knowledgeable without Amr, Elen, Dan, Emma, Genevieve, Richard, Steven A., Steven M., and Zahraa. Rhiannon, Sharon, Helen, thank you for being my “foster office mates”!
Last but not least, thank you Josh for being here every single day, for thinking out loud with me, for troubleshooting, for laughing at me and with me, for daily support.

Merci Maroua pour avoir toujours été là, pour avoir tant papoté sur la vie à l’étranger, pour m’avoir toujours encouragée et aidée pour finir ma thèse. Merci à tout le reste de ma famille pour votre support et votre intérêt dans ma thèse. J’ai adoré tout vous expliquer ! Merci à Mum et Pierrot pour leur support constant et leur amour. Merci de m’avoir suivie dans mes choix : pharma, Master à Angers, vivre aux US, au UK… Je vous aime de tout mon cœur et je ne pourrai jamais vous remercier suffisamment.

# Abstract

Dental implant placement is undertaken increasingly frequently to restore the function and aesthetics of missing teeth. The abutment forms the interface between the implant and overlying crown, bridge or denture prosthesis. Despite reasonable long-term survival of dental implants overall, inflammation of peri-implant tissues may develop in response to chronic insult from microbial biofilms formed on implant surfaces, leading to implant failure. Despite efforts in developing novel treatments, progression and recurrence of peri-implantitis is a major clinical problem. Therefore, focus on prevention rather than treatment of peri-implant conditions is crucial.

This project aimed to investigate the early, direct attachment of peri-implant pathogens *Fusobacterium nucleatum* (FN) and *Porphyromonas gingivalis* (PG) to laser melted Ti6Al4V. Subsequently, a novel antimicrobial abutment coating was developed to reduce bacterial attachment. Both microbes attached readily to Ti6Al4V without the aid of early colonisers in the presence and absence of artificial saliva (AS). Interestingly, AS reduced FN attachment and encouraged the attachment of the more pathogenic PG to laser melted surface. The developed antimicrobial coating was composed of triclosan-loaded liposomes, tethered to the Ti6Al4V oxide layer by the amphiphilic molecule octadecylphosphonic acid. Liposomes were composed of phosphatidylcholine and cholesterol at a 7:1 w/w ratio and encapsulated 300 µg/mL triclosan in 3 mg/mL lipids. Triclosan demonstrated efficacy in inhibiting both FN and PG. The liposomes were successfully adsorbed to the laser melted surfaces, although this coating was not uniform. The triclosan-loaded liposomal coating showed high antimicrobial efficacy against FN and PG in the absence of AS. However, preconditioning of coated surfaces with AS reduced liposomal antimicrobial activity.

This work indicates that bacterial attachment to oral metallic implants may differ from the successive process described in the literature. A novel liposomal coating demonstrated potential in preventing attachment and proliferation of clinically relevant implant pathogens which may reduce peri-implantitis risk.

# List of Abbreviations

AATCC: American association of textile chemists and colorists

ACTC: American type culture collection

AFM: Atomic force microscopy

ANOVA: Analysis of variance

AS: Artificial saliva

ASTM: American society for testing and materials

AUC: Area under the curve

BCA: Bicinchoninic acid

$CaCl_2$: Calcium chloride

CLSM: Confocal laser scanning microscopy

CoCr: Cobalt chromium

CYP: Cytochrome P450

DAC®: Defensive antimicrobial coating

DLVO: Derjaguin, Landau, Verwey, and Overbeek

DoE: Design of experiments

EMA: European medicine agency

FAA: Fastidious anaerobe agar

FAB: Fastidious anaerobe broth

FDA: Food and drug administration

FTIR: Fourier-transform infrared spectroscopy

FTIR-ATR: Fourier-transform infrared spectroscopy-attenuated total reflectance

ICS: Ion chromatography system

IL: Interleukin

IPA: Isopropanol

IUPAC: International union of pure and applied chemistry

KCl: Potassium chloride

K2CO3: Potassium carbonate

LUV: Large unilamellar vesicle

MIC: Minimum inhibitory concentration

MLV: Multilamellar vesicle

MVV: Multivesicular vesicle

NaCl: Sodium chloride

NCTC: National collection of type cultures

ODPA: Octadecylphosphonic acid

$OD_{600}$: Optical density at 600 nm

PBS: Phosphate buffered saline

PCR: Polymerase chain reaction

PICF: Peri-implant crevicular fluid

PVM/MA: Polyvinylmethylether maleic acid

$R_a$: Arithmetic mean of the height

$R_y$: Maximum height

SAM: Self-assembled monolayer

SEM: Scanning electron microscopy

SUV: Small unilamellar vesicle

THF: Tetrahydrofuran

Ti: Titanium

$TiO_2$: Titanium oxide layer, also called titania

Ti6Al4V: Titanium-6 aluminium-4 vanadium

TNFα: Tumour necrosis factor α

XPS: X-ray photoelectron spectroscopy

XRD: X-ray diffraction

# Contents

# List of Figures

# List of Tables

# Chapter 1. Introduction

## 1.1 Introduction

Dental implant placement has become an increasingly common procedure used in the management of tooth loss as it allows the restoration of function and aesthetics. Albrektsson and colleagues (2014) as well as Klinge et al (2018) estimated that approximately 12 million dental implants are placed yearly. Despite the relatively high rate of success reported to be between 90 % and 95 % (Pye *et al.*, 2009), implants may fail and this can be divided into two main categories:

- early failure, due to inability to establish osseointegration,
- late failure, due to inability to maintain osseointegration (Esposito *et al.*, 1998).

Late failure is mostly caused by infection of the tissues surrounding the implant and the subsequent inflammation leading to bone destruction and implant loss (Lindhe and Meyle, 2008). This condition is called peri-implantitis and its prevalence is currently estimated at 22 % (Derks and Tomasi, 2015). Peri-implantitis has a severe impact on patients' quality of life: high levels of anxiety and limitation in social life and intimate relationships were reported (Insua *et al.*, 2017). The outcome of peri-implantitis treatment is unfortunately still considered unpredictable due to the lack of consensus on diagnosis and treatment methods (Lindhe and Meyle, 2008). The 11$^{th}$ European Workshop on Periodontology highlighted the necessity to focus on preventing rather than treating peri-implantitis (Derks and Tomasi, 2015). As peri-implantitis is caused by the proliferation of pathogenic bacteria on all the parts constituting the dental implant, its prevention must involve the reduction of bacterial adhesion and proliferation onto the material directly.

Several materials are used to manufacture dental implants, including metals such as titanium (Ti) and its alloys like titanium-6 aluminium-4 vanadium (Ti6Al4V). The main manufacturing process of metallic dental implants is milling, however engineering companies, such as Renishaw PLC, manufacture implants by additive manufacturing. Additive manufacturing is divided in several processes such as selective laser-

melting, selective laser sintering, or electron beam melting. They all build objects using a layer-by-layer approach, although each process differs and diverse equipment is needed. These techniques allow the manufacturing of a range of patient-specific medical implants and are nowadays increasingly used to manufacture all types of medical implants.

The current project aims to characterise the surface properties of laser melted Ti6Al4V used in clinic and compares them with the surface properties of milled Ti6Al4V samples. This project will also characterise the early attachment of peri-implantitis associated pathogens *Fusobacterium nucleatum* and *Porphyromonas gingivalis* to the laser melted samples. This investigation is building on previous work conducted by Jordan and colleagues (Jordan *et al.*, 2016) in which the early attachment of several pathogenic bacteria involved in peri-implantitis to laser melted cobalt chromium (CoCr) was examined. Jordan showed that these bacteria were able to attach to smooth metallic surfaces without the aid of early colonisers or salivary proteins. It is therefore clinically relevant to study their early attachment to Ti6Al4V, as this alloy is frequently used in dental clinics. Finally, based on the above investigations, this project aims to develop an antimicrobial coating onto laser melted Ti6Al4V that will release triclosan in a sustainable manner and to assess its efficacy against *F. nucleatum* and *P. gingivalis*. Previous work has demonstrated that liposome containing triclosan loaded into a hydrogel can prevent and treat infection by *Streptococcus anginosus* and *Enterococcus faecalis* of root canals (Everett, 2017). Triclosan is also used in toothpastes and mouthwashes and is efficacious against the proliferation of numerous oral bacteria (Gilbert *et al.*, 2007; Janani and Kumar, 2018). This project aims to expand the investigation conducted by Everett on the efficacy of triclosan liposomes coated to Ti6Al4V against the peri-implantitis associated pathogens *F. nucleatum* and *P. gingivalis*.

## 1.2 Oral cavity

### 1.2.1 Dental anatomy and function

The tooth is a mineralised, hard, non-shedding structure anatomically composed of a crown and a root (Figure 1.1). The tooth comprises several different tissues: the

enamel, the dentine, the pulp and the cementum. The enamel forms the external layer, and is composed almost entirely of hydroxyapatite, making it the most highly mineralised tissue in the body. This makes enamel a very strong but brittle tissue. Below the enamel is a layer of dentine, a mineralised and elastic tissue composed mostly of hydroxyapatite and collagen. Its composition provides flexural strength by absorbing masticatory forces on the enamel. It is a sensitive tissue, as its tubular structure makes it continuous with the pulp. The pulp is situated in the centre of each tooth and receives innervation and blood supply via the terminal portion of the root – the apex. The neurons within the pulp respond to stimulation, such as pain, and thus are responsible for symptoms of sensitivity. The cementum attaches the tooth root to the bone by providing a tissue onto which periodontal ligament fibres are attached, anchoring the tooth to the bone while allowing some physiological movement (Nanci, 2012).

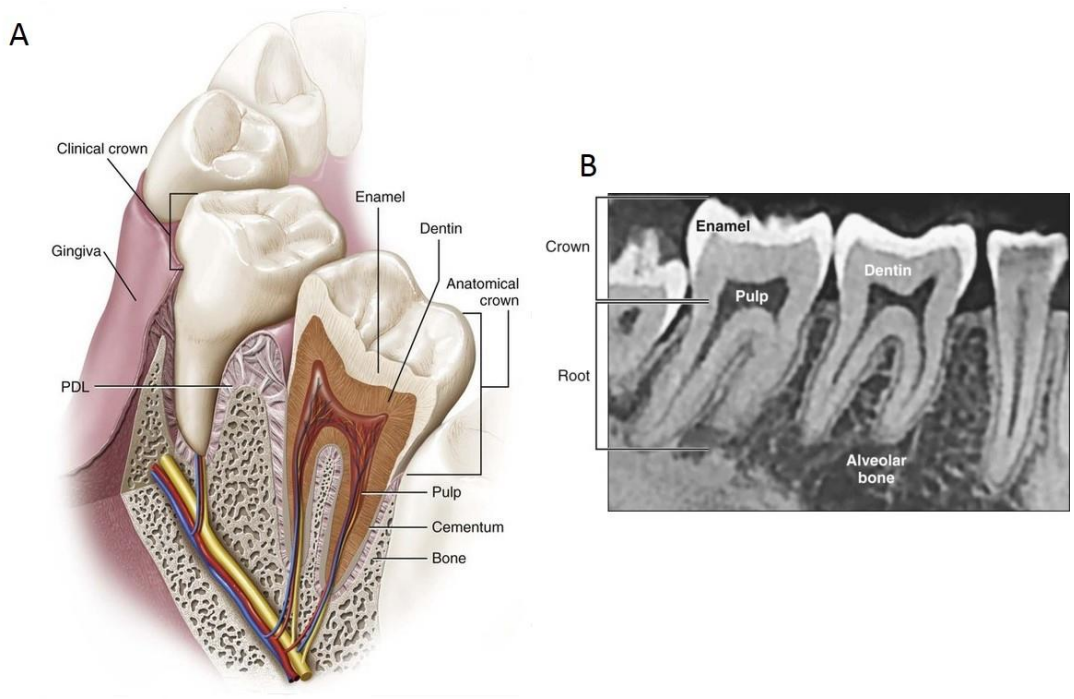


**Figure 1.1. Structure of the oral tissues (A) and radiograph of a patient (B) (Nanci, 2012).**

Teeth facilitate digestion through mastication, the mechanical disruption of the food, to transform it into the alimentary bolus prior to swallowing (Pedersen *et al.*, 2002). They also have a significant social function as they play a role in speech and are considered aesthetically important (Eli *et al.*, 2001; Arhakis *et al.*, 2017). It has also been shown that in the absence of teeth the oral microbiota is modified and a

development of anaerobic bacteria appears (Sachdeo *et al.*, 2008). Teeth therefore play a role in maintaining a balance in the oral bacterial composition.

### 1.2.2 Oral microbiota in health and disease

In health, the oral microbiome predominantly comprises microorganisms which are considered commensal. Most of the bacterial species observed in high proportion in health are Gram positive aerobic cocci: *Streptococcus* species, *Granulicatella* species, *Abiotrophia* species, and *Gemella* species. Other types are also likely to be present, such as Gram positive filamentous (*Actinomyces*), and Gram negative cocci (*Veillonella* and *Neisseria*) (Aas et al. 2005). Most of the bacteria detected in lower proportions are Gram negative anaerobes, including *Porphyromonas* and *Prevotella* (bacillo-cocci), and *Fusobacterium* (bacilli) (Zaura et al. 2009). However, *Lactobacillus* - a Gram positive facultative anaerobic bacillus; and *Staphylococcus* - a Gram positive coccal species (Smith et al. 2001) may also be identified (Marsh & Martin 2009; Dewhirst et al. 2010). It has been shown that this microbial balance is essential to health (Cho & Blaser 2012). For example, bacteria support the immune system by acting as a barrier against exogenous populations. This phenomenon is called “colonisation resistance” (Marsh & Percival 2006). It also has been shown that oral bacteria reduce nitrate into nitrite, which is, then transported in the bloodstream and converted into nitric oxide, a natural anti-hypertensive molecule (Govoni et al. 2008; Petersson et al. 2009). However oral homeostasis may be disturbed due to a number of physiological and environmental factors, such as chronic or acute immune dysregulation, implant placement, or antibiotic therapy. This is known as dysbiosis, and facilitates disease/infection progression. Other organisms such as keystone pathogens (*Porphyromonas gingivalis*) or other opportunistic pathogens (which may or may not be commensals) have the opportunity to thrive and induce diseases.

In disease, perturbations of the oral microbiome composition occur (Wade 2013). Species diversity is often reduced and an increase in anaerobic bacilli and bacillo-cocci Gram negative bacteria are detected in plaque-mediated diseases (Meffert 1996); such as caries, periodontal disease or peri-implantitis. The most common pathogenic bacteria in peri-implantitis, for example, are *P. gingivalis*, *F. nucleatum*, *Prevotella spp*, *Aggregatibacter actinomycetemcomitans*, *Treponema denticola*, and *Tannerella forsythia* (Lindhe et al. 2008).

In the oral cavity, bacteria tend to grow in communities, known as plaque, on surfaces.

### 1.2.3 Dental plaque

The dental plaque is the biofilm that can be found at the tooth surface. Plaque formation is a sequential process involving several steps. A conditioning film formed by the salivary proteins and called “acquired enamel pellicle” appears immediately following cleaning, modifies the tooth surface properties and directly influences the early microbial colonisation (Marsh, 2004). Initial microorganism attachment depends primarily on weak, long-range physicochemical interactions between the cell membrane and the pellicle-coated tooth and results in a reversible attachment. This phenomenon is conventionally modelled by the Derjaguin-Landau-Verwey-Overbeek (DLVO) theory (Figure 1.2), which has been first suggested to describe nano- and micro-particle aggregation. As bacteria are within the same size range as microparticles, the DLVO theory may be applied to model bacterial attachment (Marshall *et al.*, 1971). This theory states that, in aqueous solution, the energy of interaction between a particle subject to Brownian motion and a surface is composed of the attractive Van der Waals forces, and the repulsive electrostatic forces. All surfaces are charged, and balanced by an equivalent number of counter ions, called the electrical double layer. When a bacterium approaches a surface, it experiences a weak attraction due to the dipole fluctuation within the molecules of the two surfaces. Then the particle experiences a strong repulsion caused by an overlap of the two electric double layers (Hori and Matsumoto, 2010). The net result of the strength of the forces results in either attachment or repulsion from the surface. Although the DLVO theory is considered as the gold standard, van Oss (1995) took into account another significant factor in bacterial attachment: hydrophobicity. It has been shown that hydrophobic surfaces attract bacteria with hydrophobic cell membranes, such as Gram negative which contains lipopolysaccharide, hydrophobicity being linked to H+ (van Loosdrecht *et al.*, 1987). Thus, in the DLVO extended theory, bacterial attachment to surfaces is led by three major physical forces: van der Waals, Lewis acid-base and electric double layer interaction forces.

The weak physicochemical interactions quickly become irreversible due to the strong interactions between specific molecules on the bacterial cell surface called adhesins and complementary receptors present in the pellicle (Marsh, 2004). The first species

adhering to the acquired enamel pellicle are called ‘early colonisers’, Streptococcus being the predominant genus, followed by Actinomyces. Bacterial metabolism removes oxygen from the film surface, and produces specific metabolites used as nutrients (lactate), or as receptors for further bacterial adhesion, such as glucans, favouring the second phase of colonisation.

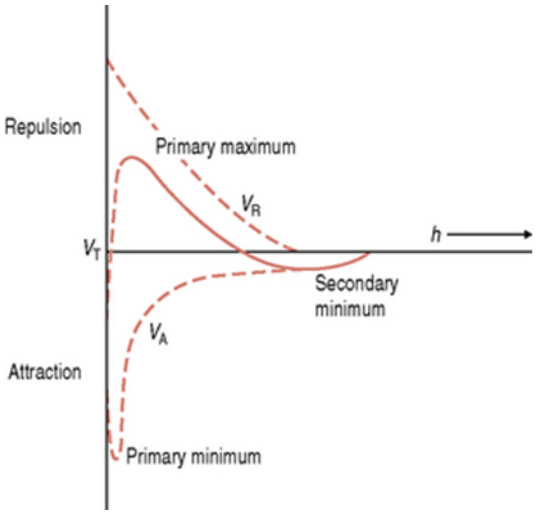


Primary maximum: repulsion is greater than attraction resulting in particle dispersion.
Primary minimum: attraction is greater than repulsion at low molecular distance resulting in aggregation.
$V_T$: total interactive energy between a particle and a surface, sum of attractive curve, $V_A$, and repulsive curve, $V_R$.

**Figure 1.2. Energetic interaction between a particle and a surface according to the DLVO theory (Marsh *et al.*, 2016).**

Oral bacteria usually possess several types of adhesins and can consequently participate in multiple interactions both with the host molecules and the complementary receptors on other bacterial membranes. This phenomenon is called co-adhesion or co-aggregation and corresponds to the second phase of bacterial colonisation. ‘Late colonisers’ co-aggregate with ‘early colonisers’ via cellular interactions, leading to an increase in the biofilm diversity. *F. nucleatum* plays a key role in the co-adhesion of late colonisers by the multiplicity of its co-aggregation mechanisms: it is called the ‘bridging bacterium’ (Kolenbrander *et al.*, 2010; Marsh *et al.*, 2016). This bridging ability is mediated mainly through the PK1594 galactose-binding adhesin (Shaniztki *et al.*, 1997) and is an essential milestone in the development of dental plaque (Figure 1.3). The bacterial proliferation eventually leads to the formation of an organised three-dimensional structure composed of microorganisms embedded in a largely self-produced matrix, containing salivary constituents and extracellular bacterial products. The matrix has multiple functions: it controls movement of water and nutrients, acts as a scaffold to maintain a three-dimensional structure, and facilitates the community response to environmental changes, including the acquisition of antimicrobial resistance. A well-known example

for microbiologists is the emergence of persister cells, which present a dormant phenotype allowing resistance to antimicrobials (Lewis, 2010). Shear forces and bacteria themselves can detach from the biofilm to colonise other areas. This final stage of biofilm maturation is known as the dispersal phase (Marsh *et al.*, 2016).

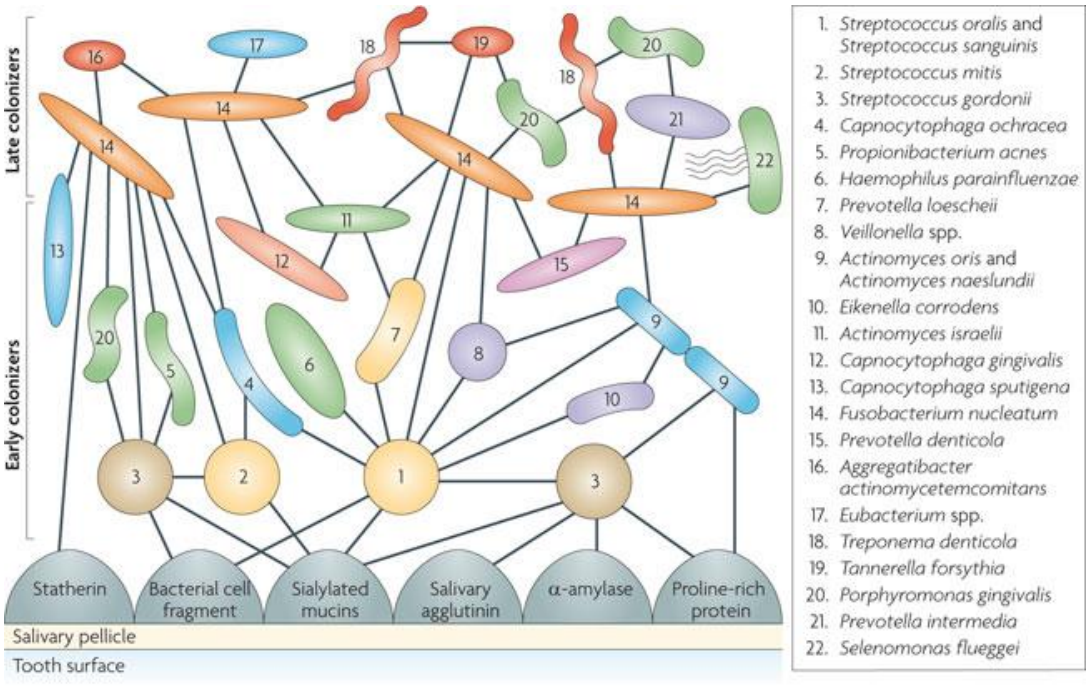


**Figure 1.3. Schematic representation of bacterial adhesion and co-aggregation in dental plaque formation (Kolenbrander et al., 2010).**

## 1.3 Dental implants

### 1.3.1 Structure and function

Dental implants are employed to restore function and aesthetics of missing teeth. The medical device is composed of three parts: the screw, also known as the implant, is surgically inserted into the alveolar bone; the abutment, placed on top of the implant, is the link between the screw and the external part of the medical device, the crown, bridge or denture (Figure 1.4). Implants can be manufactured using metals and their alloys, ceramics, or polymers. Metallic implants may be composed of Ti, Ti alloys, CoCr alloys, stainless steel, gold alloys or tantalum. Titanium and its alloys are considered the standard for the implant screw due to their high biocompatibility, lack

of reactivity and fatigue strength. TiAl6V4 is the most commonly used alloy in dentistry because it provides better compressive strength, resistance to fatigue and corrosion, and has a lower density (Osman and Swain, 2015). Surface structures have been investigated in order to improve osseointegration and prevent infection. Nowadays, most implants are roughened to encourage osseointegration, whilst abutments are manufactured as smooth as possible to prevent bacterial colonisation. A Cochrane review, however did not find evidence of superior long-term success for roughened implants currently available on the market (Esposito *et al.*, 2014).

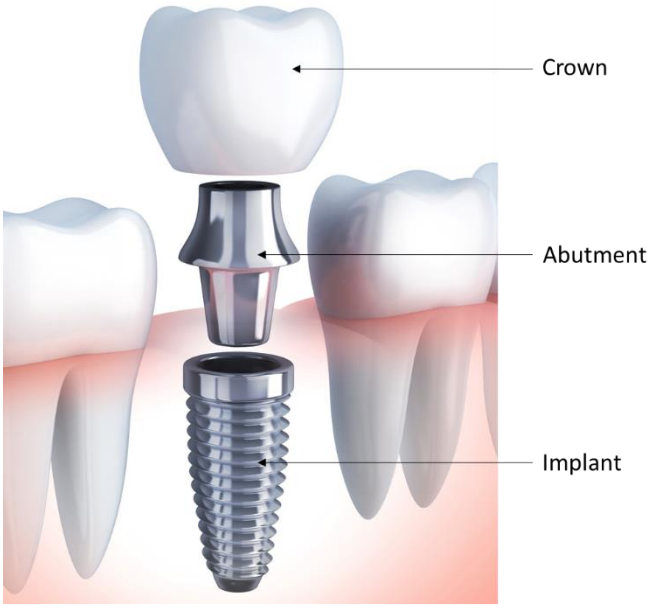


**Figure 1.4. The different parts of a dental implant (Aspen Dental, 2017).**

### 1.3.2 Implant placement and maintenance

The placement of a dental implant starts with a diagnosis which aids the clinician in choosing the most suitable treatment option for the patient. The diagnosis requires periodontal and radiographic examinations that include the assessment of the quality, quantity and morphology of the hard and soft tissues surrounding the site to be implanted. Once the whole diagnosis is performed, the treatment plan can be developed, followed by the start of the surgical procedures (Hämmerle *et al.*, 2004). After tooth extraction, an implant can be placed immediately (‘immediate’ implants), a few weeks to two months after the extraction (‘immediate-delayed’ implants), or when the bone is completely or almost completely healed (‘delayed implant’). A Cochrane meta-analysis did not find evidence supporting one protocol over the others (Esposito

*et al.*, 2011). A hole is drilled into the jawbone to place the implant. Different protocols to place the implant are currently available, including:

- The two-stage approach, also called the Brånemark protocol, during which an incision is performed into the soft tissues to expose and drill into the underlying bone. The screw is placed into the bone and covered by a flap of soft tissues made during the initial incision. This surgery is followed by a healing period of 3 to 6 months prior to re-incision of the flap to expose the osseointegrated implant and to place the abutment.
- The one-stage approach, in which the soft and hard tissues are directly drilled into and the placed implant extends through the soft tissues during the healing period (Handelsman, 2006).

So far, no conclusion indicating which approach gives best outcomes at population or sub-population levels could be reached (Chrcanovic *et al.*, 2014; Wadhwa *et al.*, 2015; Lemos *et al.*, 2018). A Cochrane systematic review conducted in 2012 could not demonstrate a significant difference between either protocol (Esposito, *et al.*, 2012). Both approaches are consequently used, and several pros and cons are detailed in Table 1.1.

The prosthesis is then fitted to the abutment, which is called 'loading'. The International Team for Implantology has defined three loading protocols that are currently used (Gallucci *et al.*, 2014):

- Immediate loading: the prothesis is attached to the implant earlier than one week after implant placement
- Early loading: the prothesis is attached to the implant between 1 week and 2 months subsequently to implant placement
- Conventional loading: the prothesis is attached to the implant after at least two months following implant placement.

A Cochrane meta-analysis showed no evidence of a clinically important difference in implant failure due to different loading times (Esposito *et al.*, 2013). The suitability of each protocol must be assessed according to each implanted site and situation.

**Table 1.1. Pros and cons of open flap and flapless surgery.**

| Open flap surgery | | Flapless surgery | |
|---|---|---|---|
| **Advantages** | **Drawbacks** | **Advantages** | **Drawbacks** |
| Visualisation of the surgical area allowing identification and protection of anatomical landmarks | Patient discomfort (pain, swelling) and suturing | Reduction of surgical symptoms (swelling, pain) | Inability for the surgeon to see anatomical landmarks and vital structures |
| Optimisation of implant positioning | Longer duration of the surgical act | Reduction of bleeding during surgery | Risk of thermal trauma to the bone due to lack of preparation of the osteotomy |
| Minimisation of bone fenestration when the amount of bone is limited | Longer treatment time, two surgical interventions | Reduction of surgical time and no need for suturing | Inability to visualise the vertical endpoint of the implant placement |
| More control over the implantation process | Bleeding during surgery | Preservation of soft tissues | Reduced access to bone contours for alveoloplasty |

Finally, after implant placement, a maintenance program is recommended to avoid complications. It should include numerous clinical examinations of the implant such as visual assessment of inflammation, probing depth and bleeding on probing, stability of the soft tissue margin, plaque index and mobility. If signs of inflammation are observed, a radiographic examination of the bone level should be performed. A 3-month regimen is the recommended protocol during the first year after implantation, and can be extended to 6 months if the patient is compliant to oral hygiene, assessments and risk factors (Humphrey, 2006; Todescan *et al.*, 2012; Gulati *et al.*, 2014).

### 1.3.3 Differences between teeth and implants

A number of differences can be observed between tissues surrounding the implant and the tooth. These differences may have an influence on the bacterial colonisation of the abutment and implant, the microbiota composition, the host response, and the

development of peri-implant diseases. The first anatomical observation to be noted is that there is no periodontium or cementum around a dental implant. Berglundh and co-workers (1991) showed the impact of implantation on the mucosa using biopsies from dogs. They found that the collagen fibre orientation around the tooth and the implant differs: the fibres run in a parallel and circular pattern around the implant, whilst they run perpendicularly and obliquely to the tooth enamel and are firmly inserted into the root cementum and the bone, constituting the dento-gingival junction (Figure 1.5). Berglundh et al hypothesised that the parallel orientation of the collagen fibres cannot protect the body from bacterial colonisation and migration as well as the gingiva. The composition of the fibres was also modified with a much higher ratio of collagen to fibroblasts of 109 in peri-implant mucosa against 4 in the gingival tissue surrounding the tooth. They finally observed that the peri-implant mucosa composition was more uniform and hypothesised that healed tissues may originate from the mucosa of the edentulous ridge only.

As for teeth and implants, microbiota differs between periodontitis and peri-implantitis. Peri-implantitis appears to show a greater diversity in bacterial species than periodontitis (Listgarten and Lai, 1999; Ebadian *et al.*, 2012; Koyanagi *et al.*, 2013; Maruyama *et al.*, 2014; Albertini *et al.*, 2015) . Koyanagi and his team (2013) found 192 bacterial taxa in peri-implantitis sites versus 148 in periodontal sites using 16S rRNA and real-time polymerase chain reaction. *P. gingivalis*, *T. denticola* and *T. forsythia*, the key pathogens of the 'red complex', as well as *F. nucleatum* were found to be abundant in both diseases (Koyanagi *et al.*, 2013; Maruyama *et al.*, 2014). Other species such as *Prevotella nigrescens*, *Prevotella oris*, *Pseudomonas aeruginosa*, *Staphylococcus aureus,* and *Candida albicans* were found in higher numbers in peri-implantitis sites than in periodontitis (Koyanagi *et al.*, 2013; Maruyama *et al.*, 2014; Albertini *et al.*, 2015), whilst periodontitis showed a higher frequency of *P. intermedia*, *Proteobacteria*, including *Salmonella spp* and *Enterobacter*, as well as *Firmicutes* and *Bacteroidetes* (Koyanagi and Ebadian).

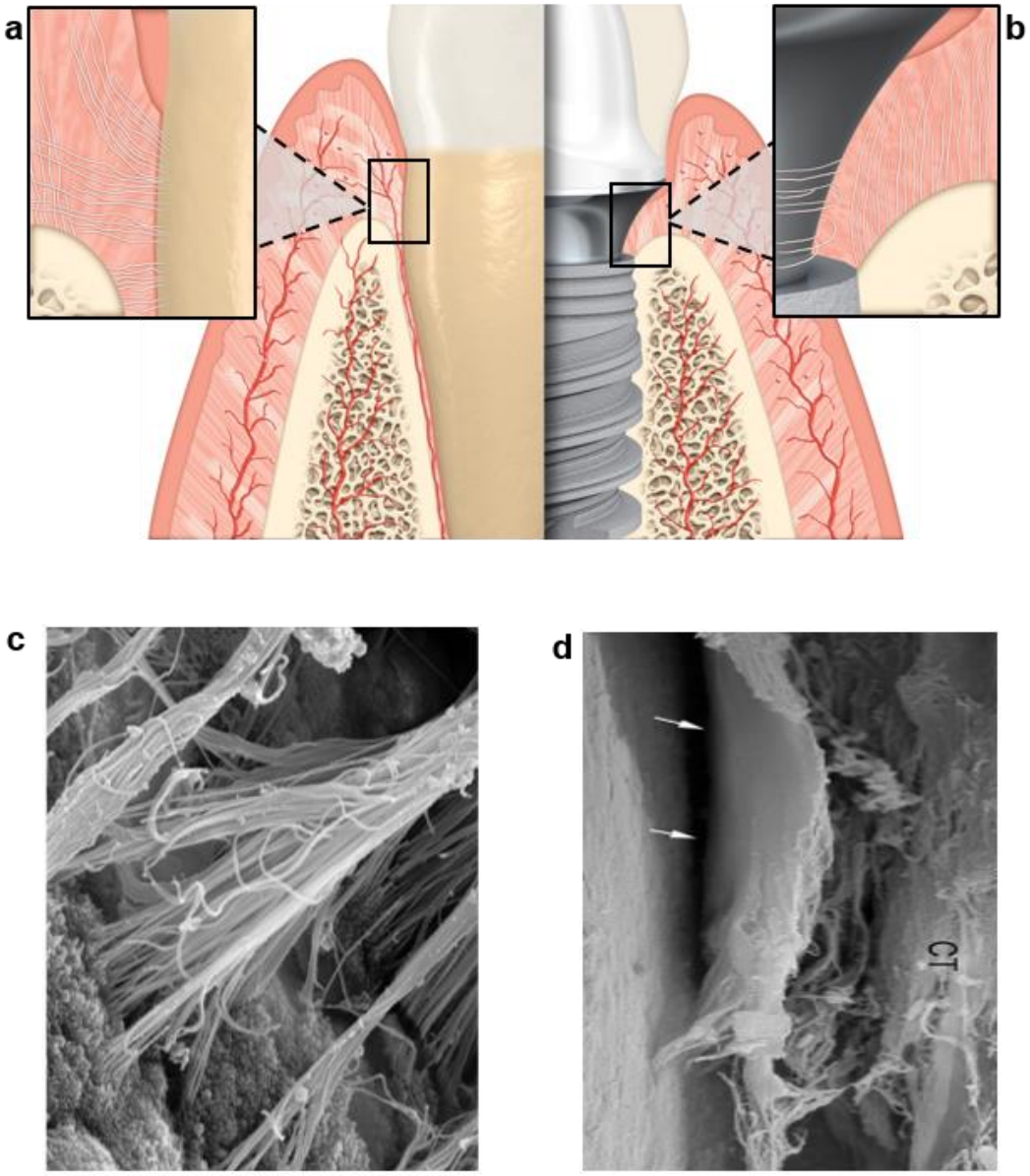


**Figure 1.5. Anatomical differences between gingiva and peri-implant mucosa. The end of the periodontal ligaments, perpendicularly oriented, are attached to the cementum of the tooth root (a and c), whilst the peri-implant connective fibres run parallel and in a circular manner around the intramucosal part of the abutment (b and d) (Lambert, 2018).**

In another *in vivo* study involving dogs, Ericsson and Lindhe (1993) observed a much deeper probe penetration in healthy implanted sites than around healthy teeth (Figure 1.6). It is thought that the orientation of the collagen fibres around the implant and the adhesion of the peri-implant mucosa at the apical region leads to poor mechanical resistance. The gingiva surrounding the tooth presents resilience due to the connection between the bone, the periodontium and the cementum (Stern, 1981). The periodontium allows tooth movement, but also plays a role in proprioception and

tactile sensitivity, which implanted sites do not present (Jacobs and van Steenberghe, 1994).

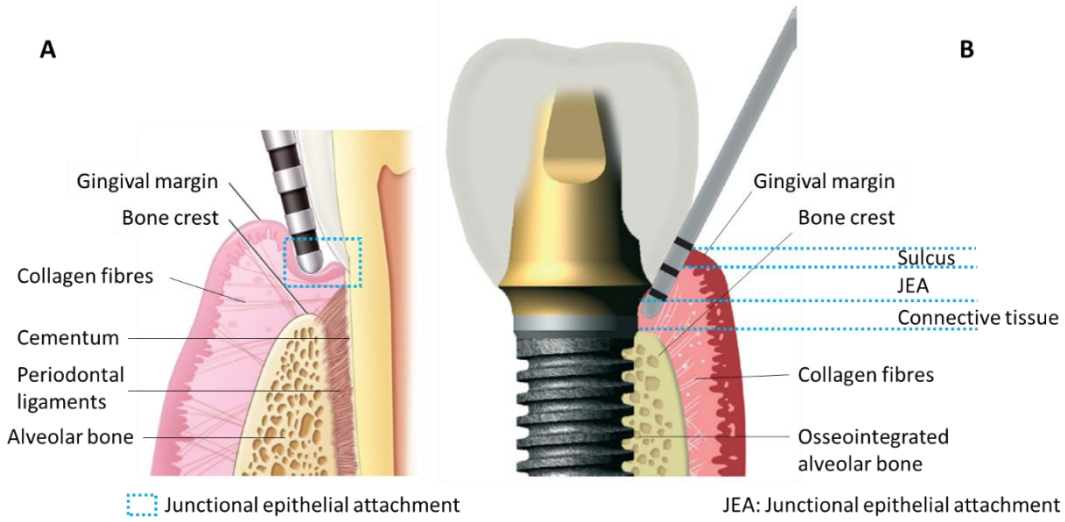


**Figure 1.6. Probing gingiva supporting a healthy tooth (A) and peri-implant mucosa supporting a healthy implant (B). The probe goes beyond the junctional epithelial attachment at the implant site, which may trigger a blood dot (modified from Suzuki and Misch, 2018).**

The early inflammatory response was found to be similar between gingiva surrounding teeth and peri-implant mucosa, however a more pronounced inflammatory response was noticed in peri-implant mucosa after a long-lasting bacterial insult. Inflammatory lesions around implants were reported to be twice as large than inflammatory lesions around teeth in dogs and humans (Carcuac *et al.*, 2012; Carcuac and Berglundh, 2014). Qualitative differences were also observed with many more macrophages, polymorphonuclear neutrophils, plasma cells, IL-6, IL-8 and TNFα detected, indicating an intensification of the inflammatory response by activating both innate and acquired immune systems (Venza *et al.*, 2010; Becker *et al.*, 2014). Two histopathologic differences were also detected during the biopsies between inflammation of tissues surrounding teeth and implants: inflammatory lesions surrounding teeth were found to be walled off from the alveolar bone by a zone of non-infiltrated connective tissue, and the biofilm was separated from the connective tissue by an epithelial pocket (Carcuac *et al.*, 2012).

Kalykakis and colleagues (1998) found differences in microbiota composition and ratio in partially edentulous patients compared to edentulous patients with an increase in anaerobic pathogens, such as *P. gingivalis* and *Prevotella intermedia*. Although Hultin et al (2012) have not found a significant difference in bacterial population, a

significant difference in neutrophil secretion was noticed. These findings show that differences exist between fully dentate, partially edentulous and edentulous patients in terms of physiological function that need to be further investigated.

### 1.3.4 Dental abutments

Abutments have an essential role in the interface between the medical device and the body: it links the crown, situated within the oral cavity and the implant, in the body, through the mucosa. The abutment therefore disrupts the normal integrity between the oral cavity and the body. Abutments must consequently maintain a healthy peri-implant mucosa. This role encompasses the prevention of bacterial colonisation and migration towards the implant and the bone and the withstanding of mechanical forces created by mastication. Unfortunately, prevention of bacterial colonisation and leakage frequently fails and biofilms are found on the abutment, leading sometimes to migration towards the implant (Gross *et al.*, 2000). It was also noticed that depending on the technique used to place the implant and screw the abutment, an early, persistent inflammation may occur (Broggini *et al.*, 2003; Cochran *et al.*, 2009) and may lead to early crestal bone recession (Abrahamsson, Berglundh, Glantz, *et al.*, 1998; Lindhe and Berglundh, 1998). It is currently understood that the abutment plays a crucial role in the long-term success of the implant, however limited data is available and additional studies need to be performed to understand all interactions at the abutment-mucosa interface (Abrahamsson and Cardaropoli, 2007; Linkevicius and Apse, 2008).

Abutments must be biocompatible and can be made of metal-based compounds, such as gold or Ti-derived and cobalt-derived alloys, zirconium or aluminium oxide ceramics (Linkevicius and Apse, 2008). Metallic abutments can be manufactured according to two main techniques: milling and 3D printing. Currently, most abutments are still milled, however an increasing number of implants and abutments are 3D printed, due to the higher degree of design freedom and subsequently the possibility to shape the device to fit each patient.

Abutments are categorised as class IIb medical devices according to the rule 8, Annex IX of the Medical Devices Directive 93/42/EEC (European Commission, 2007), as they are implantable and long-term (> 30 days) surgically invasive devices. They are considered to present a moderate risk to the patient.

### 1.3.5 Additive manufacturing

Additive manufacturing refers to a process that employs 3D computer-assisted design to build a component layer by layer through deposition of material. Additive manufacturing comprises multiple techniques including selective laser melting used during this project. During selective laser melting, the powder particles are heated and fused together by lasers on selected locations of the powder bed. The bed is then lowered, allowing the deposition of a new layer of powder to be melted. The non-melted material remains in place to support the structure until the construction has been completed. The powder is then cleaned and can be used for the next production cycle. The whole process is carried out in an inert gas filled chamber, such as argon, to ensure the highest purity possible by minimising the quantity of oxygen and other contaminants present. From an engineering point of view, additive manufacturing allows the production of highly complex geometries that remain light weight yet robust (Gebhardt, 2012; Bikas *et al.*, 2016; Figure 1.7).

The conventional manufacturing process to build dental implants is milling each part from a solid block of material. Additive manufacturing is however increasingly used in implantology, as this process allows clinicians to customise the shape of every parts of the implant specifically to fit each patient. The patient's anatomical data is recorded by radiography, reconstructed in 3D using a medical imaging software and fitted to an implant modelled specifically to the patient's characteristics. After verifications in terms of quality of fit and design, the implant can be printed (Sing *et al.*, 2016). A systematic literature review performed by Kapos and Evans (2014) compared clinical outcomes of dental implants produced by additive manufacturing and conventional manufacturing. The short- to medium-term studies included in this review showed that crowns, abutments, and frameworks produced by additive manufacturing provided comparable results to milled implant components in terms of implant survival, prosthesis survival, technical, and biologic complications. Additive manufacturing is, however, still a new process and further investigation needs to be performed, including the comparison of surface characteristics between milled and 3D printed structures.

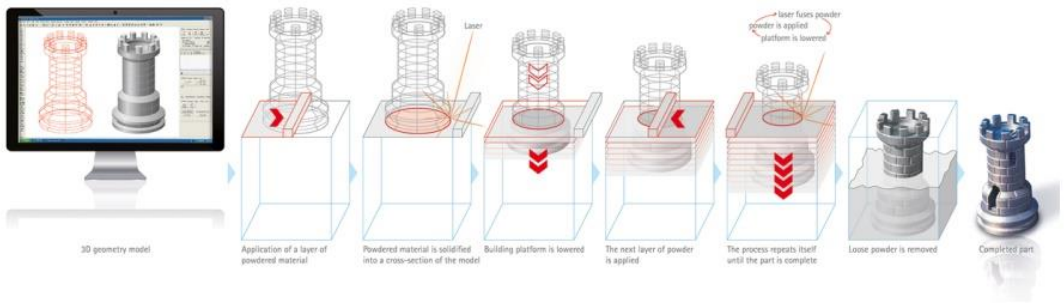


**Figure 1.7. The principle of selective laser-melting (EOS, 2019).**

## 1.4 Pathologies associated with dental implants

During the 2017 World Workshop on Periodontology, a new classification for peri-implant diseases and conditions was developed. Peri-implant health was characterised, peri-implant mucositis and peri-implantitis defined and the category named “peri-implant soft and hard tissue deficiencies” was established (Caton *et al.*, 2018).

### 1.4.1 Peri-implant health

Peri-implant health requires the absence of clinical signs of inflammation, including a probing depth ≤ 5 mm (Araujo and Lindhe, 2017; Renvert *et al.*, 2018). An increase in probing depth over time is a sign of a diseased implant site (Figure 1.8). If a bleeding dot on probing appears, this may be due to traumatic handling of the probe as peri-implant mucosa is less firmly attached than the gingiva around teeth, as stated in Section 1.3.3. A diffuse bleeding on probing observed with clinical signs of inflammation however indicates disease. Finally, an absence of bone loss ≥ 2 mm characterises peri-implant health.

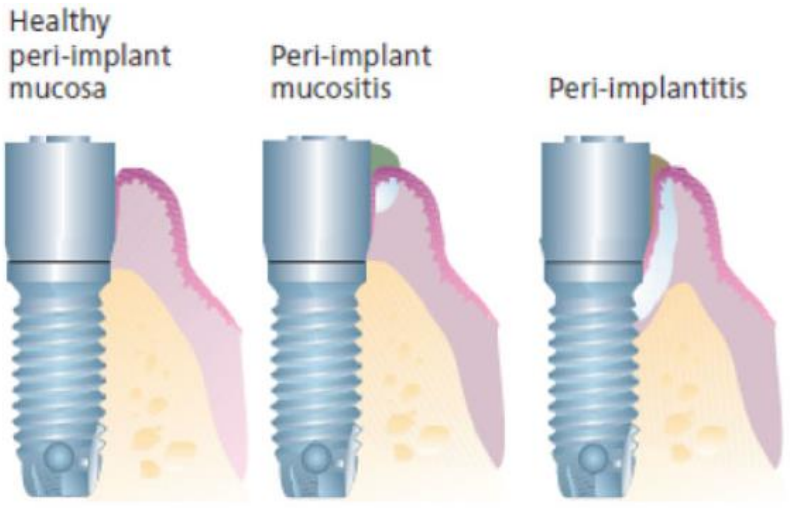


**Figure 1.8. Healthy peri-implant mucosa, peri-implant mucositis, and peri-implantitis** (Lindhe, Lang and Karring, 2008)**.**

### 1.4.2 Peri-implant mucositis

Peri-implant mucositis is defined as a bacterial induced, reversible inflammatory process affecting peri-implant soft tissues, without marginal peri-implant bone loss (Heitz-Mayfield and Salvi, 2018; Renvert *et al.*, 2018). It is a common and reversible condition affecting 80 % of implanted patients. It is generally accepted that this reversible process known as peri-implant mucositis has the potential to be a precursor to the establishment of peri-implantitis and ultimate failure of the implant and its supported prosthesis (Lindhe and Meyle, 2008). Although a potential precursor, peri-implant mucositis does not inevitably lead to peri-implantitis, which is described as an irreversible inflammatory process characterised by inflammatory lesions of the peri-implant mucosa and progressive loss of supporting peri-implant bone (Renvert *et al.*, 2018). Several studies have shown that peri-implant mucositis is directly caused by the accumulation of biofilm around the abutment (Pontoriero *et al.*, 1994; Zitzmann *et al.*, 2001; Salvi *et al.*, 2012). Studies in humans have also associated three general risk factors with an increased risk of developing peri-implant mucositis: smoking, radiation therapy, and diabetes mellitus (Karbach *et al.*, 2009; Rinke *et al.*, 2011; Gómez-Moreno *et al.*, 2015).

In clinical settings, diagnosis of peri-implant mucositis is mostly made with the presence of bleeding on probing of the peri-implant tissues. A complete diagnosis of peri-implant mucositis however was clarified by Renvert and colleagues (2018) during the World Workshop on Periodontology, and requires:

- A visual inspection showing signs of inflammation such as red, swollen and soft tissues; the patient may also report soreness
- The presence of bleeding and/or suppuration on probing
- An increase in probing depth compared to baseline (a probing depth must be taken after the implant placement)
- An absence of bone loss compared to baseline (a radiograph must be taken after implant placement)
- Bleeding on probing without any other sign of inflammation should not be considered as a criterion of peri-implant mucositis, as the peri-implant mucosa is not firmly attached to the implant like the gingiva around the tooth and it is common that the probe injures slightly the peri-implant mucosa, as explained in Section 1.3.3.

There is a lack of consensus on the treatment of peri-implant mucositis, a gold standard treatment is consequently not in place (Mattheos *et al.*, 2012; Zeza and Pilloni, 2012). Mechanical non-surgical therapy associated with antimicrobial mouthwashes has demonstrated efficacy in treating peri-implant mucositis and is the most commonly used method (Renvert *et al.*, 2008).

### 1.4.3 Peri-implantitis

It is currently considered that peri-implantitis originates from the conversion of peri-implant mucositis to peri-implantitis (Figure 1.9). According to the proceedings of the 11th European Workshop on Periodontology, 22 % of patients with implants suffer from peri-implantitis. This prevalence was calculated from multiple studies reporting their own prevalence ranging from 1 % to 47 % (Derks and Tomasi, 2015). The risk of bias is high when estimating the prevalence of peri-implantitis, as there is no consensus on the extent of tissue damage and modifications corresponding to a diagnosis of peri-implantitis. The use of different thresholds in clinical features indicating the disease can lead to very different values regarding the prevalence of peri-implantitis. Studies also use different units to report treatment outcomes: some studies use the implant as a unit, whilst other studies use the patient, who can have several implants, as a unit (Klinge *et al.*, 2018). The prevalence of peri-implantitis is consequently challenging to estimate nowadays: as an example, by using different thresholds for the diagnosis, Daubert et al (2015) reported a development of peri-

implantitis in 26 % of cases over eleven years follow-up, whereas van Velzen and colleagues (2015) related a prevalence between 4 % and 7 % over ten years.
Costa et al (2012) followed up implanted patients over 5 years and noted that the incidence of peri-implantitis was lower for patients that complied to a regular maintenance program, with 18 % of patients experiencing peri-implantitis, against 43 % patients who did not adhere regularly to a maintenance program. The term of 'success' in the treatment of peri-implantitis is however at high risk of bias. It was observed that the success of peri-implantitis treatment decreases with the increase in follow-up duration. As an example, Cecchinato et al (2013) showed 8 % cases of peri-implantitis over 4 to 5 years follow-up, Konstantinidis and colleagues (2015) reported that 13 % of participants developed peri-implantitis over a 6-year follow-up, whilst longer studies showed around 20 % cases developed peri-implantitis (Koldsland *et al.*, 2010; Marrone *et al.*, 2013; Daubert *et al.*, 2015). The percentages indicated in each study are, as stated above, highly dependent on the definition of peri-implantitis given by the authors.

There is a general concern that the incidence of peri-implantitis may increase as implant placement is becoming more common and performed by a greater number of clinicians with varying expertise in implantology and its complications (Roccuzzo *et al.*, 2018).


**Figure 1.9. Peri-implant mucositis (A) and peri-implantitis (B) (Suzuki and Misch, 2018).**

Derks and colleagues (2016) demonstrated that peri-implantitis may occur early after implantation: 52 % and 66 % of patients presented bone loss after two and three years following implantation, respectively. Fransson and co-workers (2010) showed that the progression of peri-implantitis is not linear and tends to follow an accelerating pattern.

In studies investigating the histopathology of this condition, inflammatory lesions biopsied from peri-implantitis differed from peri-implant mucositis sites and harboured more neutrophil granulocytes and B lymphocytes (Gualini and Berglundh, 2003). They also presented a denser vascular network outside and lateral to the cell infiltrate (Carcuac and Berglundh, 2014). It was noticed that the majority of lesions were located laterally to the barrier epithelium and separated from the crestal bone by an area of healthy connective tissue (Ericsson *et al.*, 1995; Abrahamsson *et al.*, 1998). The lesions presented a high number of neutrophil granulocytes, lymphocytes, and plasma cells (Sanz *et al.*, 1991; Cornelini *et al.*, 2001; Bullon *et al.*, 2004), with much larger proportions of macrophages and leukocytes (Berglundh *et al.*, 2004, 2011). Konttinen et al (2006) also found interleukin 1α (IL-1α) as a dominant cytokine that activates osteoclasts in the peri-implantitis lesions. The release of IL-1β was also detected to be significantly increased in peri-implantitis and peri-implant mucositis, compared with healthy implanted sites (Faot *et al.*, 2015). Peri-implantitis was associated with a high increase of tumour necrosis factor α (TNFα) levels compared with healthy implants (Faot *et al.*, 2015). Peri-implantitis is often compared to periodontitis, however, we have shown in Section 1.3.2 that numerous differences exist between teeth and implants. Although periodontitis is defined by similar clinical symptoms such as inflammation of the gingiva surrounding the diseased tooth and progressive loss of supporting bone, the progression of peri-implantitis appears to be faster and presents larger inflammatory lesions (Carcuac *et al.*, 2012).

Peri-implantitis is an inflammatory disease due to prolonged bacterial infection (Table 1.2). The analysis of several studies led to the conclusion that peri-implantitis is a very complex and heterogeneous infection. An increase of the proliferation of nineteen bacterial species was associated with diseased sites compared with healthy sites, including *P. gingivalis* (Persson and Renvert, 2014). Opportunistic pathogens such as *P. aeruginosa* and *S. aureus* were also detected (Leonhardt *et al.*, 1999; Mombelli and Décaillet, 2011), as well as fungi, like *Candida spp* or *Penicillum spp* (Leonhardt *et al.*, 1999; Albertini *et al.*, 2015; Schwarz *et al.*, 2015), and viruses, including human cytomegalovirus and Epstein-Barr virus (Jankovic *et al.*, 2011). A recent meta-analysis by Akram and co-workers (2019) showed that the Epstein-Barr virus appears to be significantly increased between diseased and healthy sites. Although not significant, most studies assessed in this meta-analysis observed an increase in human cytomegalovirus and herpes simplex virus in diseased sites compared with healthy sites. A difference in the composition of the peri-implant microflora between deep and shallow pockets was also demonstrated (Mombelli and Décaillet, 2011; Yeh

*et al.*, 2019). Yeh and colleagues (2019) showed that most anaerobic bacteria were found at 8 mm and deeper, whilst aerobic microbes were found at 7 mm maximum. Pockets 5 mm deep or more are believed to be protected from oxygen and may be favourable niches for putative pathogens involved in peri-implant diseases (Figure 1.10). Studies also found fungi in diseased implanted sites (Leonhardt *et al.*, 1999; Albertini *et al.*, 2015; Schwarz *et al.*, 2015; Yeh *et al.*, 2019). Fungi were detected in healthy sites as well, however Schwartz and colleagues (2015) detected different species between health and diseased: peri-implantitis sites presented *C. albicans* and *Candida boidinii* in majority, whilst healthy implant sites were mainly associated with *Candida dubliniensis* and *Candida cladosporioides*. Schwartz et al also reported for the first time the detection of *Penicillium spp*, *Rhadotorula laryngis* and *Paelicomyces spp* in peri-implantitis sites.

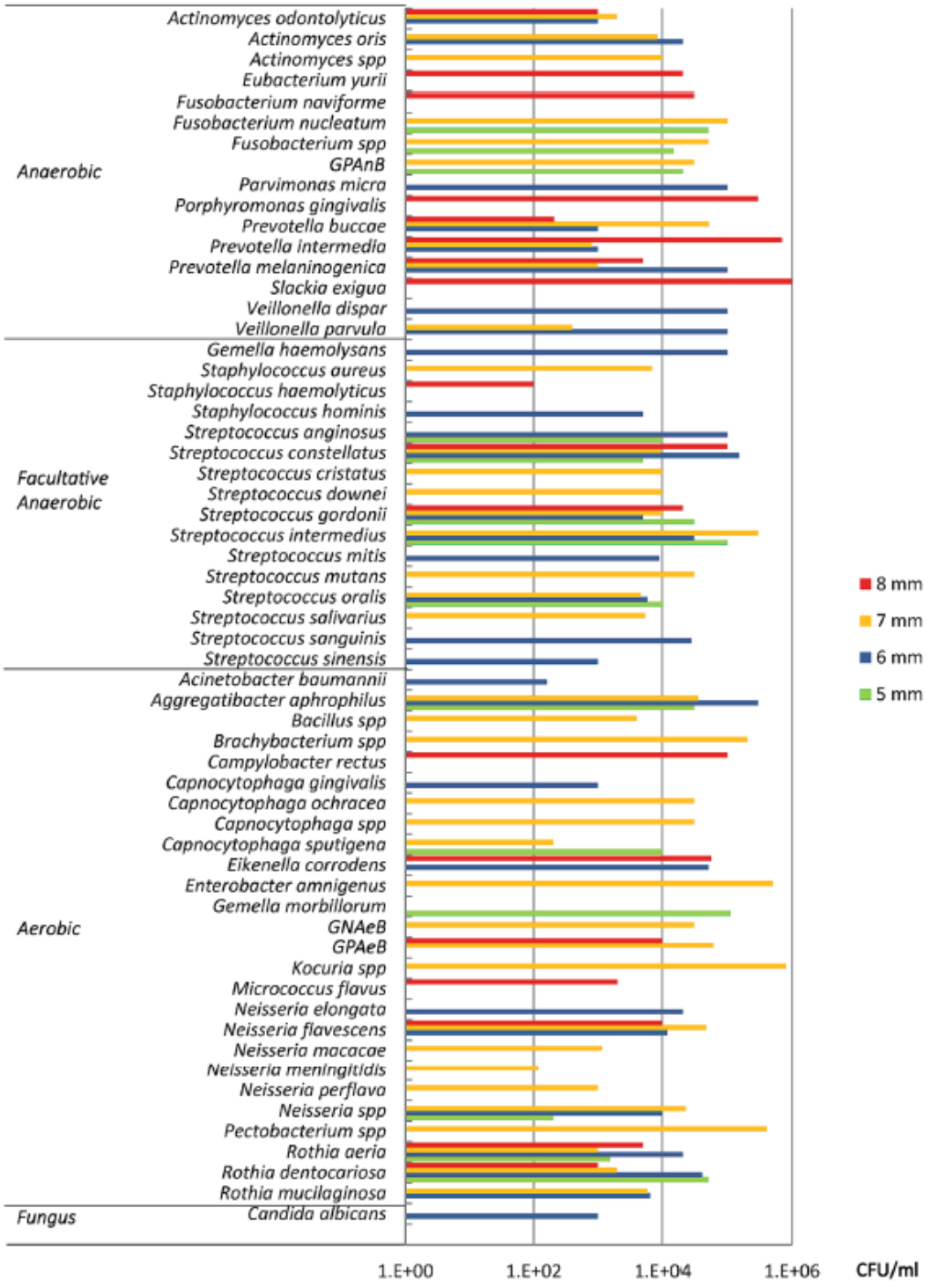


**Figure 1.10. Bacterial and fungal species found in different pocket depths (Yeh *et al.*, 2019).**

**Table 1.2. Bacterial, fungal species and viruses found in peri-implantitis sites.**

| Microorganisms | References |
|---|---|
| **Bacterial species** | |
| *Actinomyces odontolyticus* | Mombelli and Décaillet, 2011; Persson and Renvert, 2014; Yeh *et al.*, 2019 |
| *A. actinomycetemcomitans* | Leonhardt *et al.*, 1999; Mombelli and Décaillet, 2011; Albertini *et al.*, 2015; Schwarz *et al.*, 2015 |
| *Campylobacter rectus* | Mombelli and Décaillet, 2011; Persson and Renvert, 2014; Yeh *et al.*, 2019 |
| *Campylobacter showae* | Persson and Renvert, 2014 |
| *F. nucleatum* | Mombelli and Décaillet, 2011; Persson and Renvert, 2014; Albertini *et al.*, 2015; Schwarz *et al.*, 2015; Yeh *et al.*, 2019 |
| *sp. naviforme* | Persson and Renvert, 2014; Yeh *et al.*, 2019 |
| *sp. nucleatum* | Persson and Renvert, 2014; Yeh *et al.*, 2019 |
| *sp. polymorphum* | Persson and Renvert, 2014 |
| *F. periodonticum* | Mombelli and Décaillet, 2011; Persson and Renvert, 2014 |
| *Haemophilus influenzae* | Mombelli and Décaillet, 2011; Persson and Renvert, 2014 |
| *Helicobacter pylori* | Mombelli and Décaillet, 2011; Persson and Renvert, 2014 |
| *Parvimonas micra* | Mombelli and Décaillet, 2011; Persson and Renvert, 2014; Albertini *et al.*, 2015; Schwarz *et al.*, 2015; Yeh *et al.*, 2019 |
| *Prevotella intermedia* | Leonhardt *et al.*, 1999; Mombelli and Décaillet, 2011; Persson and Renvert, 2014; Albertini *et al.*, 2015; Schwarz *et al.*, 2015; Yeh *et al.*, 2019 |
| *Prevotella nigrescens* | Leonhardt *et al.*, 1999; Mombelli and Décaillet, 2011; Albertini *et al.*, 2015 |
| *Porphyromonas gingivalis* | Leonhardt *et al.*, 1999; Mombelli and Décaillet, 2011; Persson and Renvert, 2014; Albertini *et al.*, 2015; Schwarz *et al.*, 2015; Yeh *et al.*, 2019 |
| *Pseudomonas aeruginosa* | Mombelli and Décaillet, 2011; Persson and Renvert, 2014; Albertini *et al.*, 2015; Schwarz *et al.*, 2015 |
| *Staphylococcus spp* | Mombelli and Décaillet, 2011; Persson and Renvert, 2014 |
| *Staphylococcus aureus* | Mombelli and Décaillet, 2011; Persson and Renvert, 2014; Albertini *et al.*, 2015; Schwarz *et al.*, 2015; Yeh *et al.*, 2019 |
| *Streptococcus epidermidis* | Mombelli and Décaillet, 2011 |
| *Streptococcus intermedius* | Persson and Renvert, 2014; Yeh *et al.*, 2019 |
| *Streptococcus mitis* | Persson and Renvert, 2014; Yeh *et al.*, 2019 |
| *Tannerella forsythia* | Leonhardt *et al.*, 1999; Mombelli and Décaillet, 2011; Persson and Renvert, 2014; Albertini *et al.*, 2015; Schwarz *et al.*, 2015 |

| | |
|---|---|
| *Treponema denticola* | Leonhardt *et al.*, 1999; Mombelli and Décaillet, 2011; Persson and Renvert, 2014; Albertini *et al.*, 2015; Schwarz *et al.*, 2015 |
| *Treponema socranskii* | Mombelli and Décaillet, 2011; Persson and Renvert, 2014 |
| *Veillonella parvula* | Mombelli and Décaillet, 2011; Persson and Renvert, 2014; Schwarz *et al.*, 2015; Yeh *et al.*, 2019 |
| Enterococci | Leonhardt *et al.*, 1999; Mombelli and Décaillet, 2011 |
| **Fungal species** | |
| *Candida albicans* | Leonhardt *et al.*, 1999; Albertini *et al.*, 2015; Schwarz *et al.*, 2015; Yeh *et al.*, 2019 |
| *Candida boidinii* | Schwarz *et al.*, 2015 |
| *Penicillum spp* | Schwarz *et al.*, 2015 |
| *Rhadotorula laryngis* | Schwarz *et al.*, 2015 |
| *Paelicomyces spp* | Schwarz *et al.*, 2015 |
| **Viruses** | |
| HCMV alone or in co-infection with EPB | Jankovic *et al.*, 2011; Akram *et al.*, 2019 |
| EPB alone or in co-infection with HCMV | Jankovic *et al.*, 2011; Verdugo *et al.*, 2015; Canullo *et al.*, 2018; Akram *et al.*, 2019 |

HCMV: human cytomegalovirus, EPB: Epstein-Barr virus

Due to the complexity of the disease stated above, the diagnosis of peri-implantitis has still not reached a consensus. Renvert and colleagues (2018) have summarised the current requirements to diagnose peri-implantitis. A clinician must detect:

- The same symptoms as mucositis:
    - Visible signs of inflammation, including redness, mucosal enlargement, oedema and softness of the tissues
    - Bleeding upon probing
- Associated with progressive loss of supporting bone compared with the baseline bone level on the initial radiograph.

If no initial radiograph and probing depth were performed after implant placement, Renvert and co-workers advise that a radiographic evidence of bone loss ≥ 3 mm and/or a probing depth ≥ 6 mm should be diagnosed as peri-implantitis. A recent study however described high variability, between 1.6 mm and 7.0 mm, of the vertical mucosal thickness before crestal bone at healthy implanted sites (Fuchigami *et al.*, 2017). It has been shown that with increasing severity of peri-implantitis, the frequency of implants presenting a probing depth ≥ 6 mm increases (Derks *et al.*, 2016). The complexity of this condition makes defining peri-implant health, peri-

implant mucositis and peri-implantitis crucial to diagnose and treat implanted sites accordingly.

A potential mean to reach a consensus on the characteristics of implant health, peri-implant mucositis and peri-implantitis is to measure the expression of biochemical markers in peri-implant crevicular fluid (PICF) or saliva as a tool alongside clinical and radiographic data to define each condition. Clinical measurements are needed in determining peri-implant mucositis as well as peri-implantitis, however they may be challenged by subjective factors such as the force applied and the direction of probing or the patients' soft tissue characteristics (Yakar *et al.*, 2019). Multiple studies have been measuring the modifications of biomarker levels in PICF. Two literature reviews were published in 2016, Zani and co-workers (2016) highlighted the numerous studies reporting increased levels of IL-1β, IL-2, IL-6, TNFα, IL-10, IL-12 and IL-17 in PICF during peri-implantitis compared with healthy sites, whereas Duarte et al (2016) concluded that there was only moderate evidence regarding a correlation between levels of proinflammatory cytokines and peri-implantitis. Conflicting results can be found in the literature about IL-1β, IL-6, RANKL and OPG: some studies have found a significant increase of these markers in peri-implantitis, whilst others have not (Murata *et al.*, 2002; Monov *et al.*, 2006; Huynh-Ba *et al.*, 2008; Kajale and Mehta, 2014; Yaghobee *et al.*, 2014; Severino *et al.*, 2016; Al-Askar *et al.*, 2018; Lira-Junior *et al.*, 2019). Studies however appear to agree regarding the increase in activated matrix metalloproteinase-8 expression in peri-implantitis compared with healthy sites (Al-Majid *et al.*, 2018). Recent studies have also observed a promising rise in sclerostin and CFS-1, molecules involved in bone resorption, in PICF that could help differentiate peri-implant mucositis from early peri-implantitis (Lira-Junior *et al.*, 2019; Yakar *et al.*, 2019). These tools however need further long-term investigation in order to be used in a reliable manner in the diagnosis of peri-implant diseases (Heitz-Mayfield, 2008).

Due to the complex and not yet completely understood aetiology of peri-implantitis, multiple treatment protocols exist, including surgical, non-surgical, regenerative and combined regimens (Roccuzzo *et al.*, 2018). Non-surgical treatment includes manual debridement followed by delivery of adjunctive local antibiotics and/or chlorhexidine. Manual surface debridement can be performed using scalers, curettes, air-powder abrasion or ultrasonic devices. Local antibiotics used in non-surgical treatments include minocycline, doxycycline and tetracycline. Systemic antibiotics such as ornidazole are sometimes employed (Mombelli *et al.*, 2001; De Araújo Nobre *et al.*, 2006; Renvert *et al.*, 2006; Salvi *et al.*, 2007; Renvert *et al.*, 2008). Prior to surgical

therapies, the acute infection must have been resolved (Heitz-Mayfield and Lang, 2004). The majority of surgical therapies include flap elevation, implant surface debridement followed by chlorhexidine irrigation, and systemic antibiotics. Numerous systemic antibiotics are used, including metronidazole, amoxicillin and clavulanic acid, tetracycline, ciprofloxacin, and clindamycin. Removal of the inflammatory lesions, called resection, is often performed as well. Bone regeneration is also used to treat the bone defect (Hämmerle *et al.*, 1995; Behneke *et al.*, 2000; Haas *et al.*, 2000; Khoury and Buchmann, 2001; Varghese *et al.*, 2015). All treatments include oral hygiene instructions. In a Cochrane meta-analysis, Esposito and co-workers (2012) demonstrated that none of the current treatments proves significantly better outcomes than the others. Despite the efforts made in finding treatment methods, Heitz-Mayfield and Mombelli (2014) showed in a systematic review cases of progression, recurrence or non-resolution of peri-implantitis. An analysis of studies published in the literature showed a high rate of resolution when a thorough maintenance regimen was followed, with 90 % of implants and 85 % of patients expected to retain their implants at five years. In the same review at seven years this rate decreased with 80 % of patients following regular professional peri-implant maintenance (Roccuzzo *et al.*, 2018). If not treated and in some cases despite treatment, peri-implantitis may lead to implant failure, which requires implant removal. Between 5 % and 20 % of patients affected by peri-implantitis experience implant failure (Rosenberg *et al.*, 2004; Moy *et al.*, 2005). Failure is characterised by pain during function, mobility, which indicates the presence of connective tissue between implant and bone, and crestal bone loss. As a result, removal of the failed implant is necessary (Misch *et al.*, 2008). Several options are available to patients who experienced implant failure and removal: implant replacement, short arch, fixed partial denture, implant tooth-supported removable partial denture, or removable denture. Although most patients prefer replacing a failed implant with another implant, survival rates are lower with a replacing implant (Levin, 2008). Grossman and Levin (2007) reported a 71 % survival rate of replaced implants compared with 93 % for the first implants in the original cohort, whilst Machtei and colleagues (2011) reported 60 % survival rate of the second implants. After the first implant removal, it is traditionally thought that a healing time of nine to twelve months is needed (Levin, 2008; Zhou *et al.*, 2016), however some studies have shown a similar survival rate after immediate reimplantation (Mardinger *et al.*, 2008, 2012; Kim *et al.*, 2010). Again, no consensus has been reached so far and further investigation is needed regarding reimplantation after first implant failure.

All the clinical studies and publications are at high risk of bias. Systematic literature reviews and meta-analysis cited in this work assessed risks of bias during their review of the literature. Common bias in the investigation of peri-implant supportive care, peri-implantitis treatment and implant survival were extracted from the bias assessment form published by Roccuzzo et al (2018):

- The patient selection:
    - Were the patients selected during the study representative of patients suffering from peri-implantitis?
    - Was the medical act performed on patients reported in detail and how was it reported (surgical record, clinical notes, structure interviews, self-report…)
    - Did the study report clearly that the outcome of interest was not present at the beginning of the study?
- The comparability of the cohorts:
    - Were the patients from the same cohort comparable with each other? Did the authors consider and act on the confounding factors?
    - Were the patients from different cohorts comparable with each other? Was the study randomised? Did the authors consider and act on the confounding factors?
- Outcomes:
    - How were the outcomes assessed: (blinded assessment with calibrated examiners, non-blinded assessment and why, patient self-reporting…)?
    - Were the clinical procedures examining signs of peri-implantitis such as probing, or radiographs standardised?
    - Were criteria for clinical conditions, such as ‘recurrence’ and ‘failure’, as well as terms including ‘treatment success’ clearly defined?
    - Was the follow-up long enough and adequate?

### 1.4.4 Current research to prevent peri-implant infections using antimicrobials and antifouling coatings

Two main research fields can be distinguished in peri-implant health and diseases: clinical research that involves comparisons between different protocols of treatment

or maintenance already used in clinical practice, and laboratory research including the *in vitro* and *in vivo* development and characterisation of new methods of preventing peri-implant mucositis and peri-implantitis. Research in preventing peri-implantitis mainly involves the functionalisation of the implant surface to obtain an antimicrobial and or antifouling activity. Functionalisation can be classified into drug- and peptide-loaded surfaces, metallic coatings, antifouling polymeric coatings, anodically oxidized and ion-implanted surfaces, UV-activatable titanium oxide ($TiO_2$) surfaces, and surface topography modification.

Drug-loaded surfaces include the direct attachment of the drug to the implant surface and the use of delivery systems, such as nanoparticles or hydrogels deposited onto the surface. The advantage of coating the metal directly with antimicrobials is the control of the microbial burden from the implantation of the device over time. The disadvantages though are the release of antibiotics below the minimum inhibitory concentration (MIC) level which can create resistance and, if the objective is a prolonged release over several months, the burst release observed with most of these systems. Several techniques can be used to coat a medical device with an antimicrobial. The simplest technique is the direct adsorption of an antimicrobial or a nanoparticle encapsulating an antimicrobial to Ti (Barbour *et al.*, 2009; Wood *et al.*, 2015). Kim and co-workers (2008), Lee and colleagues (2013), and Moon et al (2012) used the electrospray deposition technique to coat commercially pure Ti with poly(lactic-co-glycolic acid) mixed with an antibiotic or antimicrobial. The use of the self-assembled monolayer technique can also be used to construct a multilayer coating to Ti: Kang et al (2012) used calcium phosphate mixed with cefalotin, whilst Lv (2014) and colleagues used a mixture of chitosan/alginate associated to minocycline. Finally, covalent binding and polymer film directly dried onto the Ti surface are also methods that can be employed (Cortizo *et al.*, 2012; Davidson *et al.*, 2015; Karacan *et al.*, 2017). Polymers can also be coated without antimicrobial molecules to the dental implant surface as some present antifouling properties, such as polyethylene glycol (Tanaka *et al.*, 2010; Kawabe *et al.*, 2014), or antimicrobial properties, such as chitosan (Ignjatovi *et al.*, 2016) or polypyrrole (Mîndroiu *et al.*, 2013).

Metallic nanoparticles as dental implant coatings have been reported to present effective antimicrobial properties. The antimicrobial effect of metallic nanoparticles is not always fully elucidated, however it is due to their corrosion releasing high concentrations of ions which often form reactive oxygen species, damaging the bacterial membrane (Campoccia *et al.*, 2013). An increasing body of research on

metal-based antimicrobials can be found due to their chemical stability, thermal resistance and prolonged action, as well as the alarming increase in antibiotic resistance (Grischke *et al.*, 2016). The main metallic nanoparticles studied are silver-based, copper-based, zinc-based and Ti-based nanoparticles. They still present limitations however, mainly due to the lack of information regarding their impact on both human health and environment, in terms of toxicity and accumulation. It was shown that they can react with cell components resulting in the formation of reactive oxygen species, leading to the initiation of an inflammatory response. *In vivo* studies showed accumulation in organs after intravenous or oral administration (Schrand *et al.*, 2010; Espinosa-Cristobal *et al.*, 2013; Yang *et al.*, 2017). As an example, studies found that zinc oxide nanoparticles exhibit a significant cytotoxicity *in vitro* on numerous cell lines and signs of general toxicity such as lethargy and weight loss *in vivo* (Jeng and Swanson, 2006; Wang *et al.*, 2006; Srakaew *et al.*, 2011). Interestingly however, its toxicity was reduced when conjugated to iron or chitosan (George *et al.*, 2010; Srakaew *et al.*, 2011). Studies have also demonstrated that association between metallic nanoparticles or metallic thin films with antimicrobial molecules can create a synergistic antimicrobial effect (Mo *et al.*, 2008; Vogel *et al.*, 2014; Janković *et al.*, 2015; Divakar *et al.*, 2018).

Ions can also be used through the ionization of surfaces: elements such as calcium, Ti, silver, copper, chlorine, fluorine and zinc ions can be coated to Ti or hydroxyapatite and exert an antimicrobial activity (Grischke *et al.*, 2016). The mechanism of action, as well as the toxicity, appear to be comparable to the ions released from the metallic nanoparticles: highly reactive components, including hydrochloric acid, hypochlorous acid, hydrogen peroxide or superoxide are formed after interacting with the environment and react with the bacterial membrane leading to an increased cell permeability and death (Petrini *et al.*, 2006; Yue *et al.*, 2009; Deng *et al.*, 2010).

Finally, antimicrobial peptides are new antimicrobials of great interest as they possess a broad-spectrum activity and spare the host's flora while killing only pathogenic bacteria (Grischke *et al.*, 2016). A few compounds have been specifically researched in peri-implantitis. GL13K peptide coating presented a bactericidal effect on *P. gingivalis* and *F. nucleatum* and the biofilm formation of *P. aeruginosa* and *S. gordonii*, after covalent binding to commercially pure Ti (Holmberg *et al.*, 2013; Chen *et al.*, 2014; Li *et al.*, 2017). HHC-36 peptide was loaded into commercially pure Ti nanotubes and inhibited *S. aureus* growth (Ma *et al.*, 2011). Yoshinari and colleagues (Yoshinari *et al.*, 2010) demonstrated that covalently bound histatin 5 and lactoferricin induced a reduction in *P. gingivalis* biofilm development.

During this project triclosan, a broad-spectrum antimicrobial, was used to develop a novel lipidic antimicrobial coating.

## 1.5 Triclosan

### 1.5.1 Physico-chemical properties and structure

Triclosan is a synthetic, broad-spectrum antimicrobial agent. The name given by the International Union of Pure and Applied Chemistry (IUPAC) is 5-chloro-2-(2,4-dichlorophenoxy)phenol. Due to its structure composed of two aromatic moieties (Figure 1.11), triclosan is a hydrophobic compound with a logP of 4.76. LogP is the partition coefficient of a molecule between a lipophilic and an aqueous phase, usually octanol and water: a negative logP means the tested compound is hydrophilic, whereas a positive logP indicates a lipophilic compound. Triclosan is consequently soluble in solvents, such as tetrahydrofuran (THF), methanol, or acetone. Its solubility in water reaches 10 mg/L at 20 °C. Its molecular weight is 289.536 g/mol (U.S. National Library of Medicine, 2019). Triclosan has two mechanisms of action: at low concentrations it presents a bacteriostatic effect by inhibition of fatty acid production at the enoyl-acyl carrier protein reductase step (McMurry et al., 1998; Heath *et al.*, 1999); at high concentrations a bactericidal effect is observed by incorporation into the bacterial membrane followed by destabilisation of the membrane structure and leakage of intracellular components (Villalaín *et al.*, 2001; Russell, 2004).

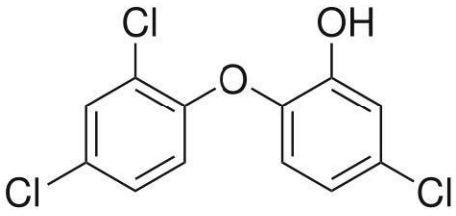


**Figure 1.11. Triclosan structure, extracted (Wu *et al.*, 2010).**

### 1.5.2 Metabolism in the human body

Triclosan can be absorbed in the body through the mucosa, the skin and the gastro-intestinal tract after ingestion (Lin, 2000; Moss *et al.*, 2000; Sandborgh-Englund *et al.*, 2006). After absorption, it has been detected in majority in the liver, followed by the adipose tissue and the brain with an extremely low detection (Geens *et al.*, 2012). Triclosan undergoes first a hydroxylation, followed by a glucuronidation or a sulfonation. Depending on the conjugation pathway the molecule takes, the glucuronic acid or the sulphate moiety is added to the hydroxyl group of triclosan, which adds a highly charged moiety to the structure (Wu *et al.*, 2010). Provencher and colleagues (2014) analysed the urine samples of 46 patients and found that the main conjugation pathway was the glucuronidation with 97.7 % of triclosan found as triclosan glucuronide. Lin (2000) also found much higher concentrations of triclosan glucuronide in plasma after mucosal absorption. Although the main organ metabolising triclosan is the liver, it was noticed that when triclosan was applied on the skin, it was partially metabolised in the skin. Moss and co-workers (2000) found that triclosan sulphate was the only metabolite detected up to 8 h after application, and both triclosan sulphate and glucuronide were found after 24 h. The unmetabolized, parent molecule triclosan was, however, found in vast majority in the skin at 24 h after application compared with its metabolites. Triclosan also appears to undergo a metabolism through the cytochrome P450 (CYP). Wu et al (2017) used a range of human HepG2-derived cell lines, each overexpressing one CYP isoform. They found that the main isoform metabolising triclosan was CYP 1A2, followed in decreasing order by CYP 2B6, CYP 2C19, CYP 2D6, CYP 1B1, CYP 2C18, and CYP 1A1. The team analysed the metabolites by high-performance liquid chromatography (HPLC) and found three breakdown products: 4-chlorocatechol, 5'-hydroxytriclosan and 2,4-dichlorophenol.

The main route of elimination of triclosan is via urine and secondary faeces, mainly as triclosan metabolites (Moss *et al.*, 2000; Sandborgh-Englund *et al.*, 2006). Sandborgh-Englund and colleagues showed that excretion through urine increased up to 24 h, and after four days 24 and 83 % of the orally administered triclosan was excreted. Triclosan approached baseline concentrations after 8 days subsequent oral administration. It was noticed that after oral exposure, the triclosan half-life was 21 h (Sandborgh-Englund et al. 2006).

### 1.5.3 Use in oral care

Triclosan is contained in toothpastes and mouthwashes. A few literature reviews and meta-analyses have been conducted in order to assess the benefits of triclosan in oral care products. In toothpaste formulations, triclosan was added in combination with the copolymer polyvinylmethylether maleic acid (PVM/MA). Davies and co-workers (2004) first conducted a literature review about the benefits of triclosan/PVM/MA in improving plaque control and gingival health. After analysing the outcomes of 16 studies they concluded that triclosan/PVM/MA toothpastes reduced subgingival plaque compared with a normal fluoride toothpaste. Blinkhorn and colleagues (2009) conducted a similar literature review, however more focused on the PVM/MA and the management of periodontal disease. They concluded that without the copolymer, triclosan toothpaste did not show any difference from a fluoride toothpaste. The PVM/MA appears to enhance and prolong the antimicrobial activity of triclosan. It was hypothesised that the copolymer acts as a bioadhesive reservoir of triclosan in the oral cavity (Nabi *et al.*, 1989; Renvert and Birkhed, 1995; Furuichi and Birkhed, 1999; Irache *et al.*, 2005). In 2013 a Cochrane meta-analysis compared the efficacy of triclosan/copolymer-fluoride toothpaste with fluoride toothpastes and indicated that a 22 % reduction in plaque and in gingivitis, as well as a 48 % reduction in bleeding gums and a 5 % reduction in tooth decay could be observed. There was, however, insufficient evidence showing a difference between both types of toothpastes in preventing periodontal disease (Riley and Lamont, 2013). Further investigations were conducted, and new formulations of triclosan-containing toothpastes were developed but are at an early stage of research (Jannesson *et al.*, 2002; Wara-Aswapati *et al.*, 2005; Moran *et al.*, 2010; Geidel *et al.*, 2017).

Studies specifically focused on triclosan toothpaste and peri-implant diseases have also been conducted. A meta-analysis performed by the Cochrane group compared methods used in clinical settings to maintain and recover health of the peri-implant mucosa in peri-implant mucositis. No significant difference was noticed between the triclosan-containing toothpaste and the fluoride toothpaste (Grusovin *et al.*, 2010). Since this publication a few studies have been conducted regarding the efficacy of triclosan-containing toothpastes in peri-implant maintenance. Sreenivasan and colleagues (2011) demonstrated a reduction in bleeding on probing and dental plaque after 6 months use of triclosan/copolymer toothpaste. Stewart et al (2018) further investigated its efficacy over two years and showed a greater reduction in bleeding

on probing and pocket depth compared with fluoride toothpaste. Although Riley and Lamont (2013) have shown the efficacy of triclosan/copolymer-containing toothpaste in reducing dental plaque, gingivitis, bleeding and caries, further investigation is needed to confirm the efficacy of this formulation in maintaining peri-implant health and reducing inflammation and microbial burden.

A low number of studies have investigated the effects of triclosan-containing mouthwashes in patients and they have been focusing mostly on plaque re-growth. Limited evidence of triclosan efficacy was found when the molecule was contained in mouthwashes. Moran and colleagues (2000) did not find plaque reduction after its use. Arweiler and co-workers (2001, 2002) and Welk et al (2005) noted a significant reduction in plaque growth with the use of triclosan-containing mouthwash, however less significant than when using chlorhexidine-containing mouthwashes.

Triclosan, as a highly hydrophobic compound, may be more efficacious in reducing plaque if used in a formulation composed of hydrophobic excipients. Liposomes might be an interesting alternative to aqueous media as their bilayer allows a high encapsulation of triclosan and their hydrophilic heads lead to the triclosan miscibility in hydrophilic environments.

## 1.6 Liposomes as drug delivery systems

Liposomes are artificially produced, self-assembled, spherical vesicles prepared from phospholipids forming a lipid bilayer surrounding an aqueous core. The amphiphilic properties of phospholipids trigger the self-assembly process forming liposomes in water. The amphiphilic properties of phospholipids come from their structure: they are formed of a polar head and hydrophobic alkyl chains linked by a glycerol molecule group (Figure 1.12A). Phospholipids are the main constituent of cell membranes and are therefore biocompatible (Li *et al.*, 2015). The liposome structure, although much simpler, is similar to the cell membrane and is consequently used as a simplistic cell model in numerous fields. Liposomes can vary greatly in terms of composition, charge, size, and structure. Their charge depends on their composition, whilst their size and structure depend on the treatment they undergo after their preparation. With no post-preparation treatment, liposomes can be observed as multilamellar vesicles (MLV) or multivesicular vesicles (MVV) measuring up to five microns (Minisini, 2016). They usually are extruded or sonicated after preparation, which decreases their size

and triggers a structure modification of the lipids into unilamellar vesicles that can be large (LUV) or small (SUV). The greatest strength of liposomes as a drug delivery system is their versatility: all their characteristics can be adapted for the intended application, such as the modification of their composition, and the post-preparation treatments, the functionalisation of their surface and the wide range of molecules that can be encapsulated.

### 1.6.1 Composition

The hydrophilic head charge of phospholipids will affect the liposome overall charge. The phospholipids also influence the membrane fluidity by their alkyl chain structures and their gel-liquid crystalline transition temperatures (Gregory Gregoriadis and Florence, 1993). The length and saturation of the alkyl chains modify the interaction between chains which results in a modulation of the membrane permeability: saturated chains will lead to a less permeable membrane whilst liposomes composed of phospholipids with unsaturated alkyl chains will present a higher permeability. The transition temperature is defined as the temperature at which the phospholipids change state from gel phase to liquid phase. In gel phase, phospholipids are more organised, resulting in a stiffer and less permeable membrane (Figure 1.12B). Thus, a high transition temperature leads to greater stability and lower permeability, decreasing the risk of encapsulated active substance leakage (Pattni *et al.*, 2015). Some compounds can increase the transition temperature of phospholipids, such as cholesterol.

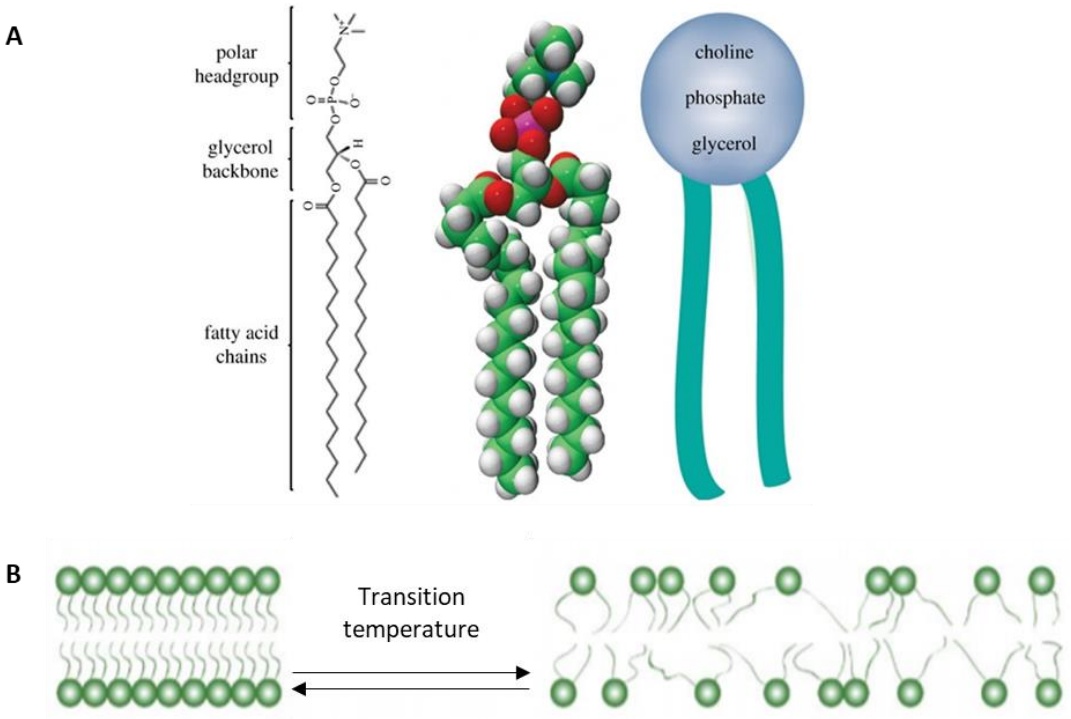


**Figure 1.12. Phosphatidylcholine structure (A) and phospholipid bilayer configuration under and above transition temperature (B) (adapted from Monteiro *et al.*, 2014 and Minisini, 2016).**

Cholesterol is a rigid molecule which inserts itself between the phospholipid tails, increasing the rigidity of the membrane and inhibiting phospholipid "flip-flop" (Figure 1.13). The addition of cholesterol leads to the increase of the phase transition temperature and decrease of the membrane permeability improving the overall liposome stability (Yeagle, 1985; Sułkowski *et al.*, 2005; van Meer *et al.*, 2008).

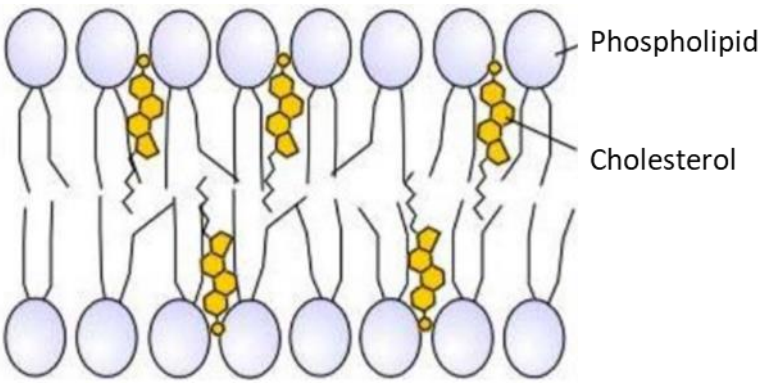


**Figure 1.13. Lipid bilayer composed of phospholipids and cholesterol (Minisini, 2016).**

The type of phospholipid can modify the physico-chemical behaviour of liposomes as well as the drug release pattern. pH-sensitive liposomes can be made using a synthetic phospholipid known as dioleoylphosphatidylethanolamine (Simões *et al.*, 2001), whilst thermosensitive liposomes can be prepared based on dipalmitoylphosphatidylcholine (Yatvin *et al.*, 1978). Time in the bloodstream can also be partially controlled with the composition in phospholipids: Allen et al. (2006) showed that a longer circulation time can be achieved by mimicking an erythrocyte outer membrane mostly made of phosphatidylcholine and sphingomyelin.

The addition of polymers and other constituents can act in synergy with the phospholipids, modulating existing properties or adding properties to a liposome. Wu and colleagues (1992, 1993) showed that adding a pH-sensitive polymer to liposomes containing dioleoylphosphatidylethanolamine led to liposomes becoming much more sensitive to pH. Johnsson and Edwards (2001) modulated the pH-responsiveness of dioleoylphosphatidylethanolamine-based liposomes by using polyethylene glycol that helped the membrane stabilisation, leading to a later release of the encapsulated molecule. Huang and MacDonald (2004) prepared liposomes composed of mannitol and diheptanolyphosphatidylcholine that reacted to ultrasound stimuli and released their content. They hypothesised that the mannitol and the diheptanolyphosphatidylcholine allowed the encapsulation of air which destabilised the liposome membrane when exposed to ultrasound.

### 1.6.2 Preparation methods and structure

Numerous processes are available to prepare liposomes (Table 1.3). The most common preparation method used in research laboratories is the thin film hydration method. Most preparation methods result in the formation of MLVs or MVVs. Liposome size and structure can thereafter be modified using post-preparation techniques such as sonication or extrusion, resulting in the formation of SUVs.

Liposomes are usually categorised by their size and lamellarity or their overall charge. As explained above, many preparation methods lead to the formation of MLVs and MVVs. Both can encapsulate a larger amount of drug as they are wider (up to five microns) with multiple bilayers and aqueous cores. LUVs and SUVs can be obtained after post-preparation techniques and present only one bilayer (Figure 1.14).

**Table 1.3. Liposome preparation methods (Keservani *et al.*, 2016).**

| Preparation methods | Description of the methods |
|---|---|
| **Thin film hydration** | The lipids and hydrophobic drug are dissolved in a solvent, which is then evaporated under vacuum, leaving a thin lipid layer at the bottom of the flask. The film is hydrated with an aqueous solution containing the hydrophilic drug. The hydration can be performed passively over a long period of time (days), under an electric field, or under vigorous shaking. |
| **Solvent injection** | The lipids and hydrophobic drug are dissolved in a solvent miscible with water, which is then injected into the aqueous phase under vigorous stirring. The solvent is then removed. |
| **Solvent spherule method** | The lipids and hydrophobic drug are dissolved in a solvent immiscible with water. The aqueous phase containing the hydrophilic drug is added to the solvent. The resulting suspension is vigorously shaken to create an oil in water emulsion. The solvent is subsequently removed. |
| **Reverse phase evaporation** | Similar to the solvent spherule method, however a water in oil emulsion is created. |
| **Microfluidic-based methods** | The lipids and hydrophobic drugs are dissolved in a solvent and the hydrophilic drug in the aqueous solution. Both solutions are mixed in a microfluidic cell, allowing better control over the mix and a faster liposome preparation. |
| **Supercritical fluids** | The lipids, solvent and hydrophobic drugs are mixed with the supercritical fluid under high pressure. The aqueous solution containing the hydrophilic drug is then slowly introduced into the cell and the pressure is released to evaporate the supercritical fluid. |

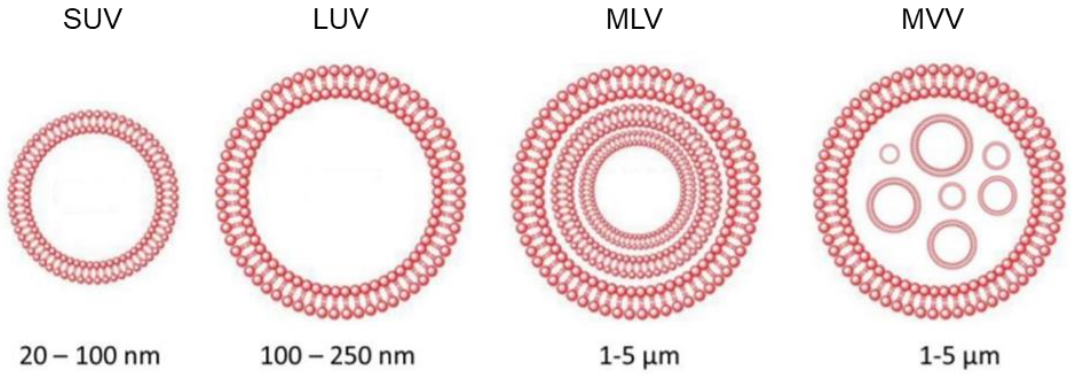


**Figure 1.14. Structures of liposomes (Minisini, 2016).**

### 1.6.3 Liposomes currently on the market

The first liposome formulation receiving a marketing authorisation was AmBisome®, an injectable liposomal formulation of the antifungal amphotericin B. The authorisation was delivered in Europe in 1990. The drug is dissolved in the lipid bilayer of unilamellar liposomes composed of soy phosphatidylcholine, cholesterol, and distearoylphosphatidylglycerol. Liposomes have shown a significant reduction in adverse effect without decreasing the amphotericin B efficacy (Stone *et al.*, 2016). In 1995, Doxil, a liposomal doxorubicin used in the treatment of ovarian and breast cancers, as well as Kaposi sarcoma, was authorised on the market by the Food and Drug Administration (FDA), making this anticancer drug the first nanomedicine authorised in the USA. Table 1.4 shows a range of commercially available liposome formulations.

**Table 1.4. Liposomal formulations currently on the market (adapted from Oliveira Eloy *et al.*, 2014; Bulbake *et al.*, 2017 and Food and Drug Administration, 2018).**

| Commercial name | Molecule encapsulated | Indication | Lipids used |
|---|---|---|---|
| **Abelcet®** | Amphotericin B | Fungal infection | DMPC, DMPG |
| **AmBisome®** | Amphotericin B | Fungal infection | HSPC, DSPG, chol |
| **DaunoXome** | Daunorubicin | Kaposi's sarcoma | DSPC, chol |
| **Depocyt** | Cytarabine | Neoplastic meningitis | DOPC, chol, triolein, DPPG |
| **Doxil®/Caelyx®** | Doxorubicin | Ovarian cancer<br>Breast cancer<br>Kaposi's sarcoma | HSPC, chol, PEG, DSPE |
| **Exparel®** | Bupivacaine | Pain management | DPPG, tricaprylin, DEPC, chol |
| **Lipodox®** | Doxorubicin | Ovarian cancer<br>Kaposi's sarcoma | DSPC, chol, PEG, DSPE |
| **Marqibo®** | Vincristine | Acute lymphoblastic leukaemia | Sphingomyelin, chol |
| **Mepact®** | Mifamurtide | High-grade, resectable, non-metastatic osteosarcoma | DOPS, POPC |

| | | | |
|---|---|---|---|
| **Myocet®** | Doxorubicin | Metastatic breast cancer | EPC, chol |
| **Onivyde™** | Irinotecan | Metastatic adenocarcinoma of the pancreas | DSPC, MPEG, DSPE |
| **Visudyne®** | Verteporphin | Choroidal neovascularisation | DMPC, EPG |
| **Arikayce®** | Amikacin | *Mycobacterium avium* complex lung disease | DPPC, chol |

Chol: cholesterol, DEPC: dierucoyl phosphatidylcholine, DMPC: dimyristoyl phosphatidylcholine, DMPG: dimyristoyl phosphatidylglycerol, DOPC: dioleoyl phosphatidylcholine, DOPS: dioleoyl phosphatidylserine, DPPC: 1,2-dipalmitoyl-sn-glycero-3-phosphocholine, DPPG: dipalmitoyl phosphatidylglycerol, DSPC: distearoyl phosphatidylcholine, DSPE: distearoyl-sn-glycero-phosphoethanolamine, DSPG: distearoyl phosphatidylglycerol, EPC: egg phosphatidylcholine, HSPC: hydrogenated soy phosphatidylcholine, MPEG: methoxy polyethylene glycol, PEG: polyethylene glycol, POPC: palmitoyloleoyl phosphatidylcholine.

### 1.6.4 Liposomes as antimicrobial delivery systems

There is currently one antimicrobial liposomal formulation on the market: the amikacin liposomal suspension, Arikayce®, indicated in adults who have no alternative options for the treatment of mycobacterium avium complex lung disease (Food and Drug Administration, 2018). Arikayce® has been authorised since 2018. Three liposomal ciprofloxacin suspensions are under investigation within the company Aradigm and are at different stages of development. The most advanced in its development has successfully finished phase 3 clinical trials and is currently being examined by the FDA and the European Medicine Agency (EMA), under the name Apulmiq® (FDA)/Linhaliq® (EMA). Apulmiq® is indicated in the treatment of non-cystic fibrosis bronchiectasis patients with chronic lung infection to *P. aeruginosa* (Aradigm, 2019a; Haworth *et al.*, 2019). The ARD-3100 is currently in phase 2 clinical trials and intended to treat patients suffering from cystic fibrosis. The last formulation has successfully finished pre-clinical tests and is intended to treat patients infected by *Coxiella burnetii* and suffering from Q fever (Norville *et al.*, 2014; Aradigm, 2019b). A liposomal tobramycin was developed and obtained a marketing authorisation by the EMA in

2006 in the treatment of *P. aeruginosa* lung infection in cystic fibrosis but was withdrawn in 2013 (European Medicines Agency, 2013). Many other antimicrobial liposomes are under investigation, however at very early stages of research. Among the multiple studies, several liposomal triclosan formulations have been developed and tested *in vitro*. As early as 1993, Jones and colleagues (1993, 1994) saw the interest of encapsulating triclosan into liposomes to inhibit oral biofilm formation, and prepared targeted liposomes against *S. gordonii*, *S. sanguinis*, *S. mutans* and *S. epidermidis* using triclosan as the antimicrobial agent. They showed a growth inhibition from 14 % to 58 % compared with control, depending on the bacteria tested and the liposomal formulation used. Robinson and co-workers (2001) studied the adsorption of liposomes by bacteria and noticed that the adsorption varied from species to species: a greater liposomal adsorption was detected by *Streptococcus salivarius* than *S. sanguinis*. The adsorption, however, did not reflect the growth inhibition as triclosan liposomes failed to inhibit *S. salivarius* growth. Finally, El-Zawawy et al (2015a, 2015b) studied the effect of liposomal triclosan against *Toxoplasma gondii* and found that the inhibition of the parasite growth was higher with liposomal triclosan than with free triclosan.

Overall, few studies have been performed on liposomal triclosan but all of them showed encouraging results.

### 1.6.5 Liposomes as coatings

As stated above, liposomes are versatile formulations that can be adapted to many applications. They have been used as drug delivery systems, but also as additives in cosmetics and in the food industry (Fakhravar *et al.*, 2015; Vélez *et al.*, 2017). As entities to be coated onto a surface, liposomes have been investigated as an antimicrobial carrier, gene delivery system and joint lubricant. Catuogno and Jones (2003) coated liposomes encapsulating triclosan and penicillin onto zinc citrate particles and their antimicrobial activity was assessed against *S. oralis*. They found that the zinc citrate particles combined with the free drugs had an antagonistic effect and inhibited the overall antimicrobial activity, whilst the particles in conjunction with the free liposomes had a synergistic effect. Ganly and co-workers (2013) studied the *in vitro* and *in vivo* effects of liposomes coated onto metallic stents as a gene delivery system to prevent in-stent restenosis. They found that the use of phosphatidylethanolamine yielded higher transfection efficiencies than

phosphatidylcholine. The best formulations showed transfection efficiencies up to 28 days that were higher than previously reported with other viral and non-viral delivery systems. Klein's research team investigated new ways to allow joint lubrication and developed a liposomal coating onto mica bearing lubrication properties. The adsorbed phosphatidylcholine-based liposomes could withstand pressures similar to those encountered in human hips and knees. The lubrication properties were attributed to the hydration layers surrounding the phosphatidylcholine heads, allowing the liposomes to slide against each other with very low friction forces. The soft character of the liposomes also led to their easy deformation without breaking their structure (Goldberg, *et al.*, 2011a, 2011b; Sorkin *et al.*, 2013, 2016; Gaisinskaya-Kipnis and Klein, 2016). Duan and colleagues (2018) investigated the mechanism of lubrication of liposomes by coating phosphatidylcholine-based liposomes onto Ti6Al4V and testing the robustness of liposomes, lipid bilayers, and lipid double bilayers against pressure. They showed that liposomes withstood repetitive high pressure better than bilayers and double bilayers. Liposome membranes in their liquid configuration were easily damaged and reassembled as flattened vesicles just after one cycle of pressure, whilst in their gel phase they could withstand up to 34 cycles of pressure. They hypothesised that the weakness of the liquid phase was due to the disorganised characteristics of the alkyl chains and the rupture of the hydrophobic interactions. They also showed that the coating was not easily penetrated by the AFM cantilever tips.

These studies show the considerable adaptability of liposomes and the wide range of medical and non-medical fields that could gain from their use.

## 1.7 Aims and objectives

The main aim of this research project was to investigate the direct and early attachment of two key pathogens involved in peri-implantitis and implant failure, *F. nucleatum* and *P. gingivalis*, to laser melted Ti6Al4V. The secondary aim of this project was to develop an antimicrobial coating onto laser melted and polished Ti6Al4V in order to prevent biofilm formation.

These two aims were achieved by studying:

- The surface properties of laser melted compared with milled Ti6Al4V using techniques such as contact angle measurement and Fourier-transform infrared spectroscopy (FTIR)
- The attachment of *F. nucleatum* and *P. gingivalis* in single and dual species with and without the presence of artificial saliva (AS) using culture and live/dead staining techniques
- The suitability of liposomes to encapsulate and release triclosan using fluorescent imaging and high performance liquid chromatography (HPLC) and the development of a triclosan-containing liposomal coating onto laser melted Ti6Al4V
- The assessment of the antimicrobial coating against *F. nucleatum* and *P. gingivalis* in single and dual species, with and without the presence of AS, using culture and live/dead staining techniques.

# Chapter 2. Characterisation of metallic surfaces

## 2.1 Introduction

According to the rule 8, Annex IX of the Medical Devices Directive 93/42/EEC (European Commission, 2007), dental abutments are categorised as class IIb medical devices. This class includes implantable and long-term (> 30 days) surgically invasive devices. Class IIb indicates that the concerned device is considered to present a moderate risk to the patient. Dental abutments are a necessary link between the osseointegrated implant and the crown and are exposed to the oral cavity. In this sense, their mechanical function is not their only purpose, they must also keep a healthy interface with the mucosal tissues. This implies biocompatibility and features that minimise microbial attachment. Bacterial attachment and biofilm formation onto abutments lead to a high risk of inflammatory host response that may be followed by subsequent destruction of the tissues surrounding the implant. This disease is known as peri-implantitis (Lindhe and Meyle, 2008). Consequently, abutment surfaces should be as smooth as possible. Moreover, a better understanding of the relationship between surface properties and bacterial attachment is necessary to obtain a reduction in biofilm formation on dental abutments. Physico-chemical surface properties, such as topography, charge, and wettability considerably affect interactions between microorganisms and the material surface (Boulange-Petermann *et al.*, 1993; Rimondini *et al.*, 1997; Lorenzetti *et al.*, 2015).

Surface roughness is considered to be one of the most important parameters influencing bacterial attachment. Rough surfaces favour microbial attachment through microscopic depressions which shelter adherent microbes from mechanical forces which might otherwise remove them (De Avila *et al.*, 2014). Numerous methods are available to measure surface roughness. The main techniques are summarised in Table 2.1.

**Table 2.1. Examples of surface topography characterisation methods.**

| Technique | Relevant information provided | Reference |
|---|---|---|
| **Stylus profilometry** | Profilometry<br>Topographic tracing<br>Morphology | Poon and Bhushan, 1995; Vorburger et al., 1998; Kazuhisa, 2002 |
| **Optical profiler and interferometry** | 3D and 2D imaging<br>Morphology<br>Profilometry<br>Topographic mapping | Poon and Bhushan, 1995; Vorburger et al., 1998; Kazuhisa, 2002 |
| **Confocal microscopy** | 3D and 2D imaging<br>Morphology<br>Profilometry<br>Topographic imaging | Vorburger et al., 1998; Kazuhisa, 2002; Al-Nawas et al., 2001 |
| **AFM** | Topographic imaging<br>Friction force mapping<br>Morphology<br>Profilometry | Poon and Bhushan, 1995; Vorburger et al., 1998; Kazuhisa, 2002 |
| **Scanning tunneling microscopy** | Topographic imaging<br>Compositional mapping<br>Morphology<br>Profilometry | Vorburger et al., 1998; Kazuhisa, 2002 |
| **SEM** | Morphology<br>Profilometry<br>Topographic imaging | Al-Nawas et al., 2001; Kazuhisa, 2002 |
| **Light microscopy** | Imaging<br>Morphology | Kazuhisa, 2002 |

AFM: Atomic Force Microscopy; SEM: Scanning Electron Microscopy.

Initial microbial attachment depends also on physico-chemical interactions. The three major forces involved in bacterial attachment to surfaces are van der Waals, Lewis acid-base and the electric double layer according to the DLVO extended theory discussed in Chapter 1 Section 1.2.3. Consequently, the surface hydrophilicity is of crucial importance in the bacterial attachment and subsequent adhesion. Surface hydrophilicity is measured by contact angle. The two main techniques used to assess contact angles are the sessile drop method using a goniometer, and the indirect contact angle measurement using the Wilhelmy balance technique.

The overall charge of a surface is affected by its elemental and chemical composition. Titanium forms a natural oxide layer, called titania ($TiO_2$), with which bacteria and cells are in direct contact. The main techniques used to analyse surface elemental composition are: X-ray photoelectron spectroscopy (XPS; Kazuhisa, 2002; Watts and Wolstenholme, 2005), FTIR (Kazuhisa, 2002) and Raman spectroscopy (Kazuhisa, 2002).

The crystal structure of a material affects its physical and mechanical properties and is therefore of high importance for medical devices (Callister and Rethwisch, 2007). Crystal structure can be described as the ordered atomic architecture within one crystal constituting the material (Figure 2.1) and is studied by X-ray diffraction (XRD). The grain boundaries appear where crystals of different orientation meet.

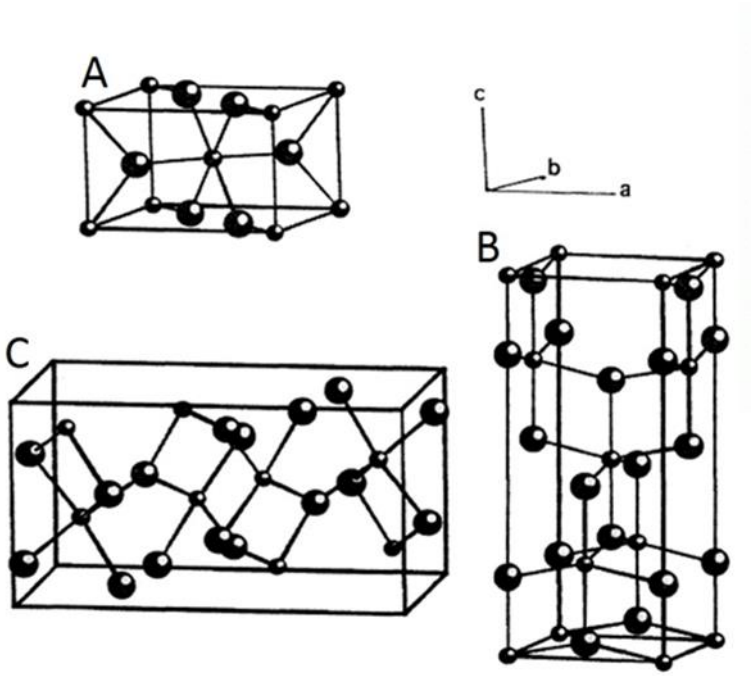


**Figure 2.1. Crystal structures formed by $TiO_2$ called rutile (A), anatase (B), and brookite (C) (Mo and Ching, 1995).**

### 2.1.1 Aims and Objectives

This chapter focused on the characterisation of the physico-chemical properties of a metallic alloy frequently employed in dental abutments manufacturing: grade 5 Ti, Ti6Al4V. Physico-chemical properties of milled Ti6Al4V surfaces were also compared

to the surfaces produced by laser melting to investigate the potential differences in surface properties between these two manufacturing processes. In this chapter, surface topography was assessed using a stylus profilometer and scanning electron microscopy (SEM), the Wilhelmy balance method was employed to investigate surface hydrophilicity, and XRD was used to study material crystal structure.

## 2.2 Materials and methods

### 2.2.1 Materials

Medical grade Ti6Al4V laser melted discs were supplied by Renishaw PLC – Medical and Dental Products Division (Gloucestershire, UK). Medical grade milled Ti6Al4V discs were purchased from GoodFellow (Cambridgeshire, UK).

### 2.2.2 Manufacture of metallic discs

Renishaw PLC uses laser melting to manufacture dental implants and implant abutments. Briefly, using a Renishaw AM250 laser melting equipment (Renishaw PLC, Gloucestershire, UK) a layer of metallic microparticles of 21.5 µm diameter is placed onto a build platform. Selected areas are melted at high temperature using a laser, the temperature and cooling rate are proprietary details kept by Renishaw PLC. The building platform is then moved downwards with a step height of 0.04 mm to allow the placement of a new layer of metallic microparticles. Laser melting is performed under inert atmosphere using argon at a minimum ratio of 99.998 %. The specifications of the Ti6Al4V powder meets the requirements of the ASTM B348-11 standard (Table 2.2; ASTM International, 2011).

Cylindrical Ti6Al4V discs of fixed dimensions (14 mm diameter, 1 mm thick) were used as a model for dental abutments, to allow standardisation and a flat surface topography for ease of study. Melting can proceed at different orientations by altering the position of the sample. Five orientations were built and studied: 0 °, 30 °, 45 °, 60 ° and 90 ° in order to investigate the influence of the manufacturing angle on the surface

properties of the laser melted metals. An angle of 0 ° corresponded to the horizontal position of the sample, and an orientation of 90 ° indicated a vertical position.

**Table 2.2. Chemical composition of the Ti6Al4V powder used. Details provided by Renishaw PLC.**

| Element | Requirements | | Actual % |
|---|---|---|---|
| | wt% minimum | wt% maximum | |
| **C** | | 0.08 | 0.02 |
| **O** | | 0.13 | 0.11 |
| **N** | | 0.03 | 0.02 |
| **H** | | 0.0125 | 0.0023 |
| **Fe** | | 0.25 | 0.2 |
| **Al** | 5.5 | 6.5 | 6.2 |
| **V** | 3.5 | 4.5 | 3.9 |

wt%: weight percent

### 2.2.3 Sample preparation

The laser melted surfaces were polished using a rotary polisher Forcipol 1V (Kemet International Ltd, Maidstone, UK) and silicon carbide abrasive from P120 to P4000 grade (Agar Scientific Ltd, Stansted, UK). The surfaces were polished sequentially at each grade until Renishaw's abutment specifications were reached in terms of surface roughness: the arithmetic mean of the height ($R_a$) must remain within this range: 0.03 µm < $R_a$ < 0.1 µm.

Prior to use, the samples were brushed for 30 seconds each side under tap water to remove any adherent particles. The discs were then immersed three times in 70 % ethanol for 30 seconds, followed by three rinses in sterile water. The samples were finally sterilised by autoclaving.

### 2.2.4 Profilometry

Surface roughness was assessed using a Surftest SV-2000 profilometer (Mitutoyo, Hampshire, UK) across a distance of 8.5 mm, at a speed of 0.1 mm/s and a range of 800.0 µm. The arithmetic average and maximum roughness peak-to-trough height

($R_y$) values of the profile were calculated by Surfpak-SV software (Mitutoyo, Hampshire, UK), using the standard method OLDMIX.

### 2.2.5 Scanning electron microscopy imaging

Images of randomly selected fields of view of the Ti6Al4V surfaces were obtained using a Vega Tescan microscope (Brno, Czech Republic), under vacuum, with voltage set at 5 kV and 10 kV. No tilt of the platform was used. No preparation was required prior to imaging. Images were recorded at magnifications x850, x650 and x420 using ATLAS software (Tescan, Brno, Czech Republic).

### 2.2.6 Fourier-transform infrared spectroscopy analysis

Functional groups were detected by Fourier-transform infrared spectroscopy-attenuated total reflectance (FTIR-ATR). Spectra were recorded on a Nicolet 380® Thermo Fisher Scientific Inc. (Madison, WI USA) using EZOMNIC 7.4 software (Thermo Fisher Scientific Inc., Madison, WI USA). The scanning range used was 500 $cm^{-1}$ – 4000 $cm^{-1}$, 36 scan averaging, and a resolution of 4 $cm^{-1}$.

### 2.2.7 Contact angle measurement

Surface hydrophobicity was measured by contact angle using a Dynamic Contact Angle analyser (DCA-312, Thermo Cahn Instruments, Madison, USA) and the WinDCA 32 software (Thermo Cahn Instruments, Madison, USA). Samples were dipped 7 mm in water at a speed of 264 µm/s. Measurements were recorded at 21 °C. Sample contact angles were assessed before and after autoclave.

### 2.2.8 X-ray diffraction analysis

Crystal structure was investigated using a Philips PW3830 X-ray generator (Philips Research, Eindhoven, The Netherlands) and X'pert Industry software (PANalytical B.V., Almelo, The Netherlands). The scan was run between 5 ° and 90 ° (2θ) at a scan speed of 0.040 °/s.

### 2.2.9 Grains boundaries formed by laser melted and milled Ti6Al4V

Grain boundaries of the laser melted and milled Ti6Al4V surfaces were imaged. Discs were polished following the protocol described in Chapter 2, Section 2.2.3. The surfaces were then etched using a 5 % hydrofluoric acid for 1 min (VITA Zahnfabrik, Bad Säckingen, Germany). Five images of randomly selected fields of view (479x359 µm) were obtained by optical microscopy using a Leica DMRX microscope fitted to a camera Leica MC190 HD. The software used was Leica Application Suite V4.9.0 software (Leica Microsystems CMS GmbH, Switzerland). The settings were set as follow:

- Exposure 16.5ms
- Gain 1.0x
- Saturation 100.00
- High sharpening
- Magnification x20.

### 2.2.10 Statistical analysis

Unless stated otherwise, all the experiments described above were performed three times including internal triplicates. One-way analysis of variance (ANOVA) was performed for the analysis of the sample profilometry. Repeated measures ANOVA was performed for the analysis of the sample contact angle. When a p value of $< 0.05$ was found, a Bonferroni multiple comparisons post-test was performed between all groups.

## 2.3 Results

### 2.3.1 Profilometry

After undergoing the standardised polishing process, the $R_a$ and $R_y$ of the two types of surfaces were compared (Table 2.3). No significant differences were observed in $R_a$ and $R_y$ between polished laser melted and polished milled Ti6Al4V with a $R_a$ of 0.059 µm (± 0.003) and a $R_y$ of 0.286 µm (± 0.005) for laser melted surfaces, and a $R_a$ of 0.071 µm (± 0.001; $p > 0.9999$) and $R_y$ of 0.272 µm (± 0.003; $p = 0.7598$) for milled Ti6Al4V. No difference was identified between manufacturing orientations.

**Table 2.3. Surface roughness characterisation of laser melted and milled Ti6Al4V. Mean $R_a$ and $R_y$ are presented.**

| Manufacturing technique | Sample | Roughness (µm) | |
|---|---|---|---|
| | | **$R_a$ (± SEM)** | **$R_y$ (± SEM)** |
| **Laser melted, polished** | Ti6Al4V 0 ° | 0.059 (± 0.004) | 0.285 (± 0.009) |
| | Ti6Al4V 30 ° | 0.053 (± 0.003) | 0.276 (± 0.004) |
| | Ti6Al4V 45 ° | 0.068 (± 0.002) | 0.290 (± 0.008) |
| | Ti6Al4V 60 ° | 0.056 (± 0.002) | 0.282 (± 0.010) |
| | Ti6Al4V 90 ° | 0.062 (± 0.002) | 0.299 (± 0.009) |
| **Milled, polished** | Ti6Al4V | 0.071 (± 0.003) | 0.293 (± 0.002) |

SEM: Standard Error of the Mean

### 2.3.2 Scanning electron microscopy imaging

SEM images (Figure 2.2) showed a smooth topography for the laser melted and milled samples. No distinction between manufacturing orientations, or manufacturing process could be made.

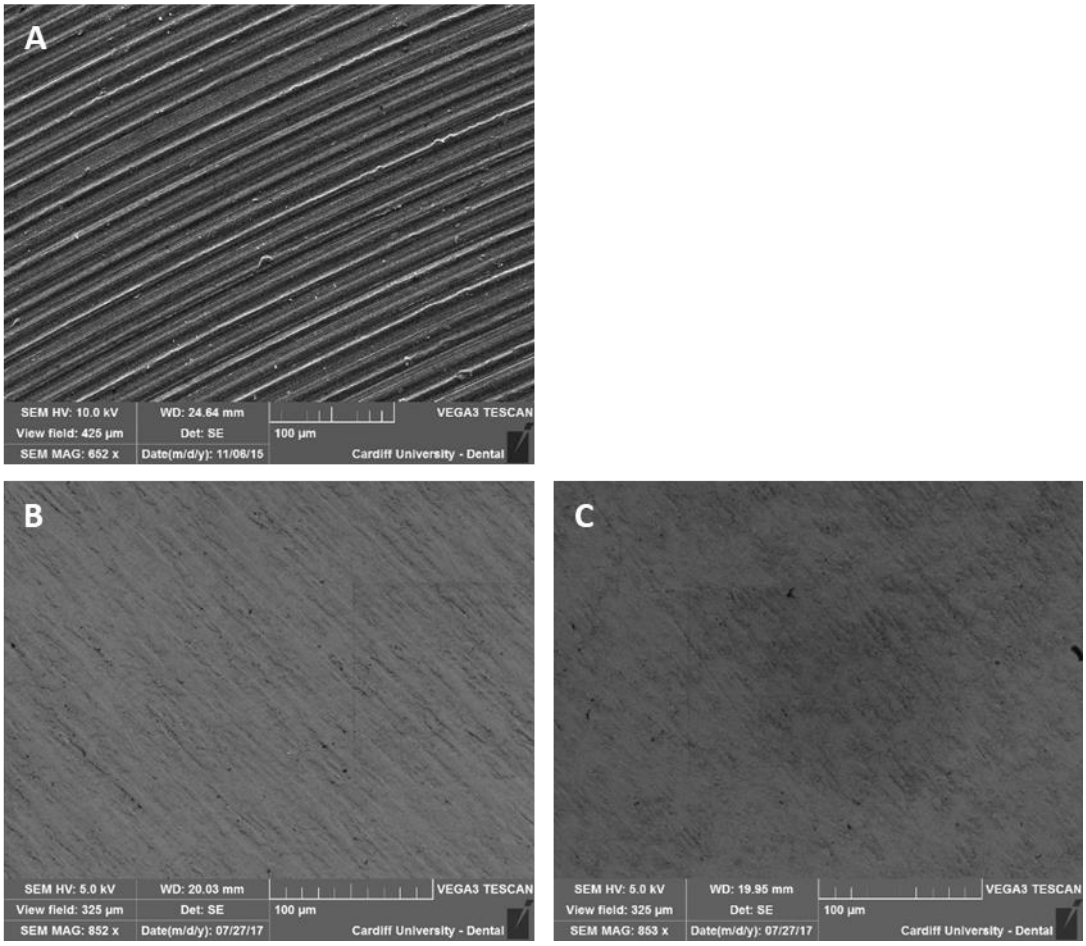


**Figure 2.2. Representative SEM images of unpolished milled Ti6Al4V (A; magnification x450), polished milled Ti6Al4V (B, magnification x850) and polished laser melted Ti6Al4V (C, magnification x850).**

### 2.3.3 Fourier-transform infrared spectroscopy analysis

The laser melted and milled Ti6Al4V spectra showed a large number of bands between 1000 $cm^{-1}$ and 500 $cm^{-1}$ corresponding to various Ti, Al and V oxides (Figure 2.3; Ashok *et al.*, 2015; Chellappa *et al.*, 2015). Attribution of each peak to a specific metal oxide group was challenging, however the band at 619 $cm^{-1}$ corresponded to the V-O bond (Chen *et al.*, 2004); whilst the 588 $cm^{-1}$ peak was identified as Al-O bond (Öhman *et al.*, 2006). The bands detected at 663 $cm^{-1}$ and and 640 $cm^{-1}$ could be attributed to Al-O and Ti-O, and Al-O and V-O respectively (Sarker, 2014; Chen *et al.*, 2004), whilst the peak at 610 $cm^{-1}$ corresponded to Ti (Yaseen *et al.*, 2017). The same bands were detected on the laser melted and milled Ti6Al4V. Most bands presented a slight shift towards the left between both manufacturing processes. No

difference in FTIR spectra was identified between manufacturing orientations of laser melted discs.

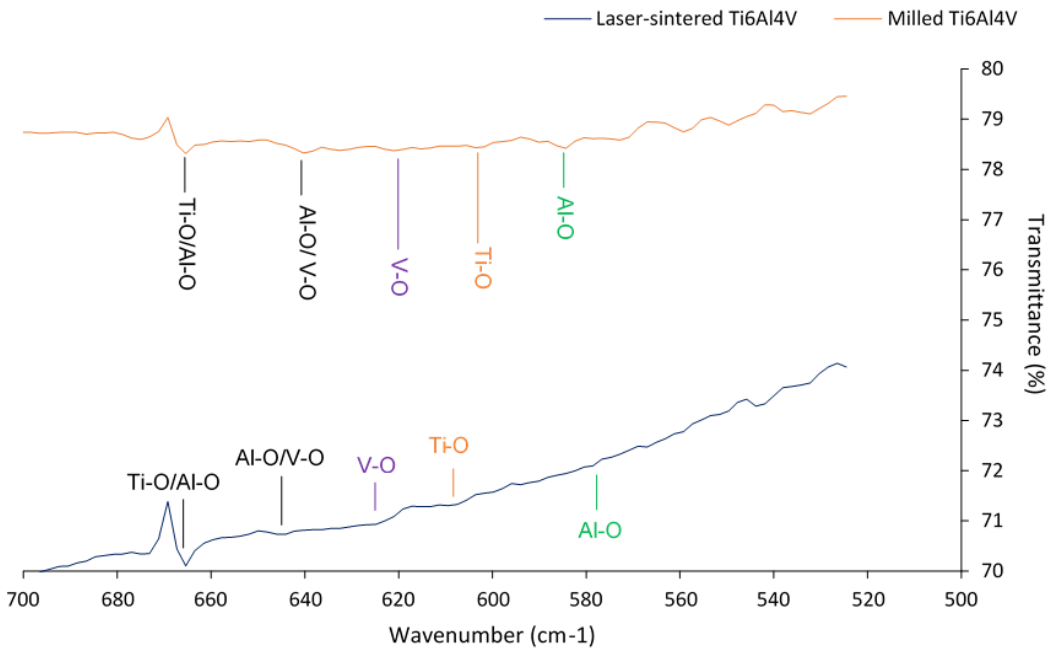


**Figure 2.3. FTIR spectra of laser melted and milled Ti6Al4V surfaces. Spectra representative of all manufacturing angles of laser melted discs.**

## 2.3.4 Contact angle measurement

Laser melted Ti6Al4V presented a moderate wetting capacity of 64 ° (± 1.026), that significantly decreased after autoclaving with a mean contact angle of 48 ° (± 1.178), regardless of manufacturing angle (Table 2.4). Milled Ti6Al4V discs demonstrated a similar behaviour to the laser melted discs with a significant reduction from 63 ° (± 1.398) to 40 ° (± 1.079) after autoclaving. No significant difference was observed between milled and laser melted discs before autoclaving. After autoclaving, however, the difference between milled and laser melted discs was significant for every manufacturing angles, with a p value of 0.0409 (milled vs laser melted at 90 °), 0.0031 (milled vs laser melted at 45 °), 0.0013 (milled vs laser melted at 0 °) and 0.0011 (milled vs laser melted at 60 °).

**Table 2.4. Contact angle measurements before and after autoclaving of laser melted Ti6Al4V for all manufacturing angles and of milled Ti6Al4V.**

| Manufacturing process | Sample | Mean advancing contact angle (°) | | Significance |
|---|---|---|---|---|
| | | Before autoclave ° (± SEM) | After autoclave ° (± SEM) | |
| **Laser melted, polished** | Ti6Al4V 0° | 64 (± 1.697) | 49 (± 0.519) | $p < 0.0001$ |
| | Ti6Al4V 30° | 66 (± 1.186) | 47 (± 3.384) | $p < 0.0001$ |
| | Ti6Al4V 45° | 61 (± 1.823) | 50 (± 1.697) | $p = 0.0003$ |
| | Ti6Al4V 60° | 62 (± 1.709) | 51 (± 1.633) | $p = 0.0003$ |
| | Ti6Al4V 90° | 66 (± 1.168) | 47 (± 0.865) | $p < 0.0001$ |
| **Milled, polished** | Ti6Al4V | 63 (± 1.398) | 40 (± 1.079) | $p < 0.0001$ |

SEM: Standard Error of the Mean

### 2.3.5 X-ray diffraction analysis

XRD peaks detected at 16 °, 42 °, 52 °, and 63 ° at the surface of the Ti6Al4V samples were assigned to the α phase, also called hexagonal close-packed, whilst the peak detected at 85 ° corresponded to the β phase, also known as body-centered cubic (Rinner *et al.*, 2000; Lapovok and Tomus, 2007; Facchini *et al.*, 2010). These peaks were identified regardless of manufacturing orientation. Milled Ti6Al4V presented the same peaks as the laser melted discs, indicating predominantly an α phase with a slight contribution of β phase (Figure 2.4 and Figure 2.5).

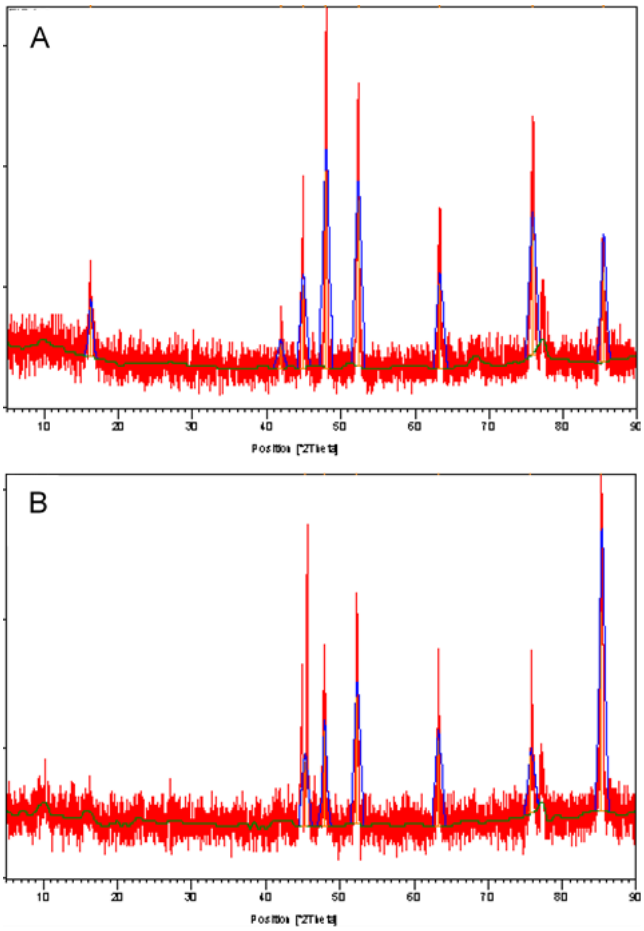


**Figure 2.4. Representative graphs of XRD spectra of laser melted Ti6Al4V (A) and milled Ti6Al4V (B).**

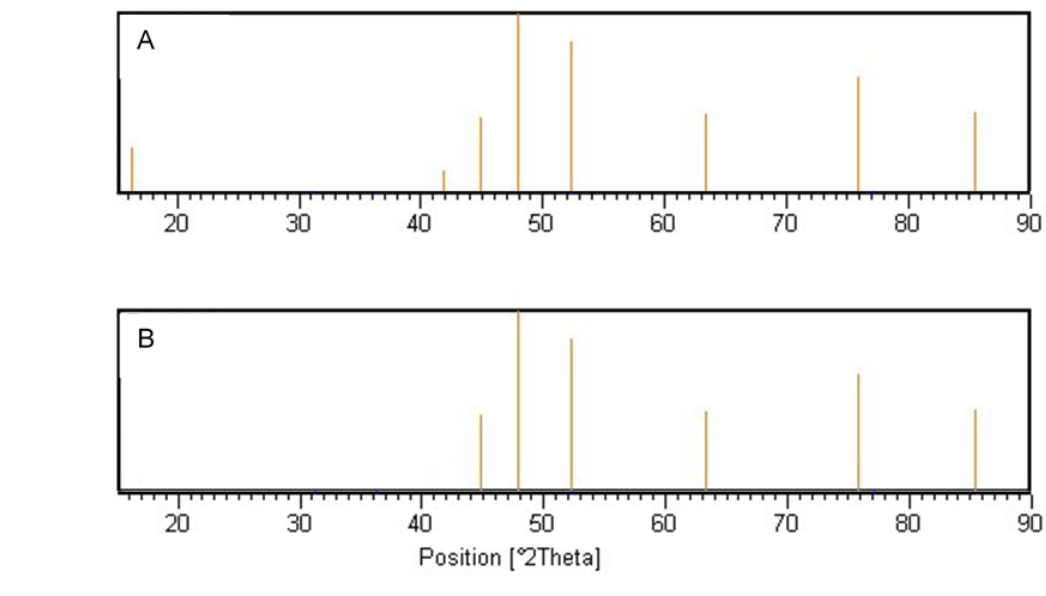


**Figure 2.5. Representative graphs of XRD analysis of laser melted Ti6Al4V (A) and milled Ti6Al4V (B).**

### 2.3.6 Grain boundary imaging

Laser melted and milled discs presented very different grain boundaries. Laser melted disc boundaries formed lamellar structures and branching patterns, whereas milled disc boundaries showed colonies of irregular shapes that were not lamellar (Figure 2.6). *F. nucleatum* patterns were remarkably similar to the grain boundaries of the laser melted discs.

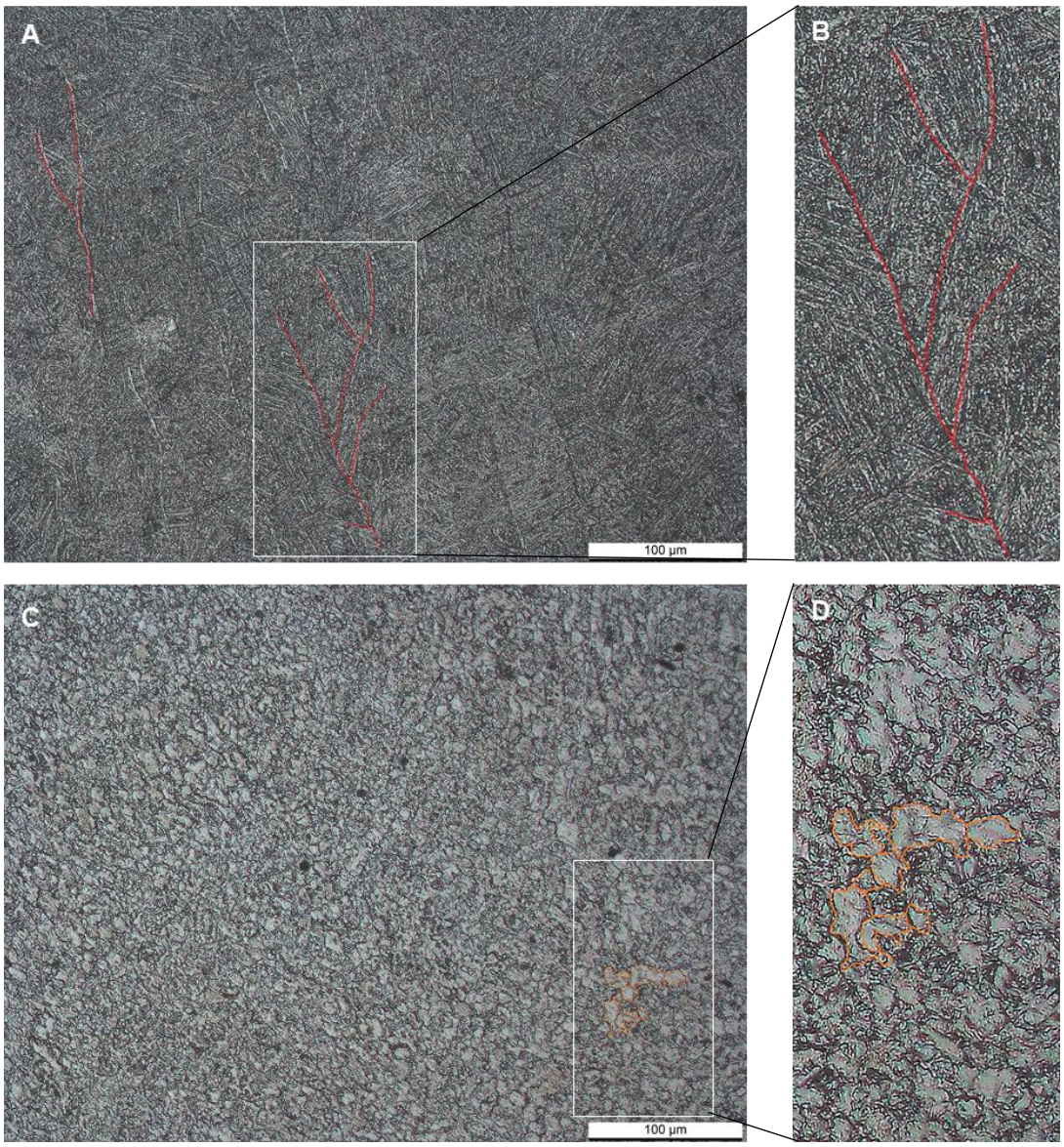


**Figure 2.6. Representative images (magnification x20) of grain boundaries on laser melted disc (A), zoomed in laser melted disc (B), milled disc (C), and zoomed in milled disc. Laser melted surfaces presented lamellar structures and branching patterns as highlighted in red in images A and B, whilst the grain boundaries of the milled surfaces formed colonies of irregular delimitations as highlighted in orange.**

## 2.4 Discussion

Dental abutment surface characteristics can affect long-term implant success by influencing microbial attachment and subsequent migration and leakage through the implant-abutment interface, leading to host inflammation (Gross et al., 2000; Dibart et al., 2005; Aloise et al., 2010; Lopes de Chaves e Mello Dias et al., 2017). Physico-

chemical properties affect non-specific, early bacterial attachment through physical forces (Hori and Matsumoto, 2010). A bacterium can attach to the surface if the overall surface charge, comprised of attractive van der Waals, repulsive electrostatic and Lewis acid-base forces, is favourable to attraction (van Loosdrecht *et al.*, 1987; Van Oss, 1989). This preliminary, non-specific attachment is soon replaced by specific adhesion via bacterial appendages, such as flagella and pili, that pierce through the electric barrier. Covalent bonds are then formed between membrane receptors and proteins embedded in the conditioning film present at the material surface (Hori and Matsumoto, 2010).

In this chapter, the surface characteristics of medical grade laser melted and milled Ti6Al4V surfaces were analysed. The $R_a$ values of all manufacturing orientations met Renishaw's requirements in terms of surface roughness: 0.03 µm < $R_a$ < 0.1 µm. Previous research *in vivo* by Bollen and co-workers performed a split-mouth study design in which they compared biofilm formation on two abutments presenting different roughnesses with $R_a$ of 0.21 µm and 0.06 µm at three and twelve months after insertion. The study failed to identify a significant difference in bacterial attachment between the two surface roughnesses (Bollen *et al.*, 1996). A later literature review performed by Bollen and colleagues (1997) showed that a threshold in surface roughness below which bacterial attachment was reduced may exist. It was determined that the threshold appeared to be around a $R_a$ of 0.2 µm. This finding was consistent with the previous *in vivo* study from 1996, as abutments of $R_a$ close to and under the threshold ($R_a$ of 0.21 µm and 0.06 µm) were used. Amoroso et al (2006), however studied the *in vitro* attachment of *P. gingivalis* to commercially pure Ti and found a decrease in attachment only under 0.03 µm. Attachment was not reduced above this threshold. The surfaces used during the present study showed a $R_a$ below the threshold published by Bollen et al (1997) and close to the threshold determined by Amoroso and co-workers (2006) with $R_a$ of 0.059 µm and 0.071 µm for laser melted Ti6Al4V and milled Ti6Al4V, respectively. The SEM imaging visually confirmed the smooth topography of the polished discs.

An additional parameter affecting early bacterial attachment is surface wettability and the corresponding hydrophilicity (Bayoudh *et al.*, 2006; Pereni *et al.*, 2006). Hydrophilicity is the capacity to form hydrogen bonds. A surface is hydrophilic if hydrogen bonds can be formed with water molecules. A bacterial membrane that is electrically neutral will therefore attach to a hydrophobic surface, whilst a charged membrane will preferentially be attracted to a hydrophilic surface (Hori and Matsumoto, 2010). All samples demonstrated a moderate wetting capacity regardless

of manufacturing process or manufacturing orientation. Mean advancing contact angles in water were 64 ° and 63 ° before autoclaving for laser melted and milled Ti6Al4V, respectively. Ti oxide was detected by FTIR, as well as Al and V oxides, which may have led to the formation of a naturally homogeneous oxide layer throughout the sample surface. Medical devices must however be sterilised before use. Consequently, we also investigated the laser melted and milled Ti6Al4V contact angles after sterilisation in order to assess the effects of sterilisation on the surface properties. Several sterilisation methods are available, such as autoclaving, gamma irradiation, ultraviolet, and oxygen plasma. Autoclaving was selected as this is a commonly used technique that all research teams can reproduce. This is also clinically relevant as most medical devices are autoclaved or gamma irradiated. The autoclaving process decreased the Ti6Al4V contact angles, increasing their hydrophilicity. This may be due to an increase in oxide layer formation or a modification in oxidation state during the autoclaving cycle. Smith and co-workers (1991) showed that autoclaving altered the surface structure of their TiAl6V4 samples, and noticed a reduction in contact angle of the surfaces. However, outcomes are variable in terms of contact angle before and after autoclaving from one study to another: some studies noticed an increase in contact angle after autoclaving (Baier *et al.*, 1982; Serro and Saramago, 2003; Pegueroles *et al.*, 2008). Three possible causes responsible for differences in contact angle can be speculated:

1. Factors relating to the autoclaving process itself: the minimum conditions required are heating at 121 °C, pressure of 100 kPa and saturated steam for 15 min. However, the duration of heating can often last up to 30 min and variations in pressure and temperature may be noticed from one autoclave setting to another.
2. Studies detecting an increase in contact angle also found an increase in surface carbon content after autoclaving (Baier *et al.*, 1982; Serro and Saramago, 2003; Pegueroles *et al.*, 2008). The variability in samples, such as elemental percentage, crystallographic phase, grain boundaries and surface chemistry may generate extensive disparities (Park *et al.*, 2011).
3. Contact angle measurement itself may trigger inconsistencies as this technique is sensitive to external conditions such as ambient temperature.

Roughness is also a factor that may influence contact angle. It was shown that a rougher surface may amplify the substrate surface hydrophilicity or hydrophobicity (Marmur, 2009) due to the extended surface involved in the solid-liquid exchanges of a liquid drop. The wetting character of the surface was shown to be increased

(Wenzel, 1936). As their roughness was similar, contact angle data of laser melted and milled Ti6Al4V surfaces could be compared in a reliable manner.

Ti is an allotropic metal, meaning that it can be composed of several crystal structures. The α phase is the common form found at room temperature, whilst the β phase is formed when Ti is cooled from liquid state to solid state or heated above 883 °C (Brunette *et al.*, 2001). Alloying Ti allows manufacturers to stabilise the metal in α, β, or α-β form at room temperature and modify the metal properties. Al is an α stabiliser, whereas V is a β stabiliser. Selective laser melting usually presents high cooling rates that transform the β phase into α' martensite (Vrancken *et al.*, 2012; Rafi *et al.*, 2013). The cooling rates are proprietary details kept by Renishaw PLC. The different phases are however showed by the XRD spectrum. According to the XRD data, peaks corresponding to the β phase were present for all the laser melted Ti6Al4V surfaces, as well as the milled samples. A predominent α phase was also observed (Lapovok and Tomus, 2007; Facchini *et al.*, 2010). The presence of the β phase indicates that the cooling rates of the samples were slowed to avoid a full transformation from the β phase to the α' martensite phase (Rafi *et al.*, 2013).

The grain boundaries observed on the melted and milled samples appeared very different. The melted Ti6Al4V grain boundaries presented branching patterns, whilst the milled samples showed shapes irregularly delineated. These two types of grain boundaries are typical of these manufacturing processes (Rafi *et al.*, 2013; Liu and Shin, 2019).

## 2.5 Conclusion

In conclusion, manufacturing orientations did not modify the surface properties in terms of surface roughness, wettability or crystal structure. Abutments can therefore be manufactured at any orientation and the surface properties identified in this study can be maintained. All polished discs demonstrated surfaces below or similar to the $R_a$ thresholds which have been shown to reduce bacterial attachment. All surfaces also showed a moderate wetting capacity related to the metallic oxide layers.

Having characterised the Ti6Al4V samples in this chapter, the next chapter will focus on attachment of *F. nucleatum* and *P. gingivalis* to laser melted surfaces.

# Chapter 3. Attachment of peri-implantitis associated bacteria to titanium alloy

## 3.1 Introduction

Implantable medical devices are made of materials that are considered compatible with the body, or biocompatible, due to their mechanical, chemical and biological properties. Ti and its alloys are biocompatible and are the most frequently employed materials to manufacture medical implants where strength for load bearing is required, such as orthopaedic and dental implants. Currently, medical implants can be milled, or 3D printed. The latter is also referred to as additive manufacturing, and is increasingly used due to its numerous benefits, such as reducing material waste, its high potential for customisation due to greater freedom of design, and its increase in production speed. Additive manufacturing includes numerous techniques including selective laser melting used during this project. Despite its clinical relevance, few studies have been conducted regarding the interaction between laser melted materials and host cells and microbiota. There is consequently a need to study these interactions *in vitro* and *in vivo*.

Attachment and adhesion of microorganisms can occur in any environment, including some of the human body (Donlan, 2001) and surfaces, such as medical implants, and often lead to biofilm formation (O'Toole et al., 2000). The bacterial genera and species attaching to implants and forming biofilms differ depending on the implant location within the body. Orthopaedic implants are predominantly colonised by staphylococci, particularly *S. aureus* and *S. epidermidis*, whereas dental implants and abutments are colonised by a wider variety of microorganisms, including Gram positive aerobic bacteria, Gram negative anaerobic bacteria and fungi (Aas *et al.*, 2005; Campoccia *et al.*, 2006; Ribeiro *et al.*, 2012). If not removed, attached bacteria will allow further attachment and proliferation, leading to the structuration and development of a biofilm. Biofilms can trigger host inflammatory responses due to the presence of virulence

factors (Costerton *et al.*, 1999). If the biofilm is left to develop and mature, a constant inflammatory response may take place and lead to implant failure. Biofilm formation starts with early bacterial attachment to surfaces, which is governed by three major physical forces: van der Waals, Lewis acid-base and electric double layer interaction forces (Van Oss, 1989). The initial weak physicochemical interactions are followed by adhesion, involving the expression of adherence-associated proteins with surface receptors, such as adhesins. The interaction between these proteins and the substrate surface lead to irreversible adhesion of bacteria to the substrate (Hori and Matsumoto, 2010). Oral plaque develops in a series of defined and sequential stages. The process involves the adsorption of salivary proteins to the surface, followed by the initial attachment of early colonisers, involving early attachment mechanisms and subsequent adhesion. Early colonisers, such as *S. oralis* and *S. gordonii*, co-aggregate and build a favourable environment for the adhesion of late colonisers, including *F. nucleatum* and *P. gingivalis*. This development of oral plaque by succession is not restricted to the enamel but extends to all surfaces in the mouth. Interestingly, previous work by Jordan et al (2016) has revealed that the late colonisers *F. nucleatum*, *P. gingivalis*, *P. intermedia*, and *A. actinomycetemcomitans* can attach directly to smooth ($R_a$ = 0.028 ± 0.0067; $R_y$ = 0.165 ± 0.0.034) laser melted CoCr alloy surfaces. These bacteria are traditionally considered to only be able to adhere to other bacteria, not to surfaces directly. As most dental implants and abutments are made of Ti6Al4V alloy it might be anticipated that similar surface interactions may arise between these late colonisers and Ti6Al4V.

This chapter consequently investigated for the first time the early attachment and viability of the peri-implant pathogens *F. nucleatum* and *P. gingivalis* to laser melted Ti6Al4V surface. A high number of methods are available to characterise attachment and adherence of microbes to surfaces. Table 3.1 presents some of them along with their advantages and drawbacks.

**Table 3.1. Examples of characterisation methods of bacterial attachment to surfaces.**

| Technique | Advantages | Drawbacks | References |
|---|---|---|---|
| **CLSM/Fluorescent microscopy** | Quantifiable; Species detection; Biofilm structure analysis | Autofluorescence/background staining | Asadishad et al., 2011; Hannig et al., 2010; Hoppe et al., 2010 |
| **SEM** | High resolution of bacterial morphology | Desiccation of biological sample – modification of structure; Cost | Hannig et al., 2010 |
| **AFM** | Measurement of binding strength; Generation of 3D images of the surface | Cost | Dorobantu & Gray, 2010; Dufrene et al., 2002 |
| **Micromanipulation** | Direct measurement of binding strength | Cost | Garrett et al., 2008 |
| **Microbalance** | Direct measurement of binding strength | Cost | Marcus et al., 2012 |
| **Culture** | Quantification of attachment and viability | Reliability and accuracy issues | Del Curto et al., 2005; Duarte et al., 2009; Shi et al., 2006 |
| **PCR** | DNA/RNA quantification; Tracking microbial gene expression and its modifications | Amplification process – an error in early steps may result in major variations | Wong & Medrano, 2005 |
| **Tetrazolium salts** | Quick colorimetric assay; Viability quantification | Reliability and accuracy issues | Berridge et al., 2005 |

| | | | |
|---|---|---|---|
| **Resazurin** | Quick colorimetric assay; Viability quantification | Reliability and accuracy issues | Sandberg et al., 2009 |
| **Bioluminescence** | Quick assay; Viability quantification; Repeatable; Specific; Sensitive | Cost | Fan & Wood, 2007 |
| **Crystal violet** | Quick colorimetric assay; Biomass quantification | Non-specific; Non-sensitive | Peeters et al., 2008 |

CLSM: Confocal Laser Scanner Microscopy, SEM: Scanning Electron Microscopy, AFM: Atomic Force Microscopy, PCR: Polymerase Chain Reaction

The two techniques used during this research project were imaging using fluorescent microscopy and culture. Both techniques are widely employed and comparison with other scientific publications can be performed. They also are complementary as culture involves the mechanical removal and displacement of microorganisms that are then cultured on solid agar medium and enumerated. This is an indirect measurement method of microbial attachment and viability to a surface. The number of colonies recovered indicates the number of live bacteria that had attached and could survive the removal and displacement process. This technique does not indicate the quantity of attached bacteria that have died on the surface or during the removal. The use of live/dead stains and fluorescent microscopy helps confirm the outcome found via culture and allows the direct measurement of live and dead attached bacteria to the surface through specific fluorochromes and subsequent image analysis. Measurement of attachment can be then expressed as bacterial counts per unit area, percentage surface coverage, or an estimated biomass (Hannig et al., 2010; Hoppe et al., 2010; Muller et al., 2007).

### 3.1.1 Aims and objectives

This chapter investigated the ability of *F. nucleatum* and *P. gingivalis* to attach directly to unconditioned and AS-preconditioned laser melted Ti6Al4V surfaces using culture and imaging combined with the image analysis software Comstat2.

## 3.2 Materials and methods

### 3.2.1 Strains and culture media

*F. nucleatum* subsp. *vincentii* ATCC® 49256™ (originally isolated from a human periodontal pocket) and *P. gingivalis* NCTC 11834 (originally isolated from a human gingival sulcus) were used in these studies. Fastidious Anaerobe Agar (FAA) and Fastidious Anaerobe Broth (FAB) were obtained from Lab M (Lancashire, UK). Defibrinated horse blood was obtained from TCS Biosciences (Buckingham, UK). The LIVE/DEAD™ BacLight™ Bacterial Viability Kit stain was purchased from ThermoFisher Scientific (Eugene, Oregon, USA). Glass beads (500-750 µm) were obtained from Acros Organics (Thermo Fisher Scientific, Geel, Belgium).

### 3.2.2 Culture

All bacteria were initially cultured under anaerobic conditions (anaerobic gas mixture: 10 % $CO_2$, 10 % $H_2$, 80 % $N_2$) on FAA supplemented with 5 % (v/v) defibrinated horse blood, at 37 °C for 72 h to 96 h. A loop of bacterial colonies was transferred to 5 mL pre-reduced FAB at 37 °C for 15 h without agitation. Broth cultures were then diluted in 20 mL of pre-reduced FAB to an optical density at 600 nm ($OD_{600}$) of 0.08 and further diluted to an optimal starting concentration.

### 3.2.3 Correlation between $OD_{600}$ and colony counts

Bacterial suspensions were cultured in FAB to stationary phase as determined by optical density. This process involved preparing dilutions of the cultures to obtain a range of $OD_{600}$ values from 0.6 to 0.02 as measured with a spectrophotometer (Implen GmbH, Munich, Germany). Volumes corresponding to each $OD_{600}$ were then serial diluted in phosphate buffered saline (PBS) and plated onto FAA using a spiral plater (Whitley Automatic Spiral Plater, Don Whitley Scientific, West Yorkshire, UK). Inoculated agar plates were cultured as previously described and the resulting colony forming units/mL (CFU/mL) used to correlate total number of viable bacteria with the previous optical density values.

### 3.2.4 Investigation of bacterial growth with and without supplementation in artificial saliva

Bacterial suspensions were standardised at $OD_{600}$ 0.08 using a spectrophotometer (Implen GmbH, Munich, Germany). Half the suspensions were diluted with FAB, the other half with 50 % (v/v) AS (Artificial Saliva) in FAB, corresponding to $6 \times 10^9$ CFU/mL. Aliquots were sampled and cultured using a spiral plater (Whitley Automatic Spiral Plater, Don Whitley Scientific, West Yorkshire, UK) every 4 h until stationary phase.

### 3.2.5 Assessment of *Fusobacterium nucleatum* and *Porphyromonas gingivalis* viability over time under aerobic conditions

Handling anaerobic bacteria in an aerobic environment required preliminary controls regarding their viability. The mean viability of *F. nucleatum* and *P. gingivalis* was assessed over time under aerobic conditions prior to further experiment. To do so, bacterial suspensions were grown in FAB to mid-log phase ($OD_{600}$ of 0.30 for *F. nucleatum* and 0.65 for *P. gingivalis*). Ti6Al4V discs were then incubated in

bacterial suspensions for 2 h, rinsed in 0.9 % (w/v) NaCl solution to remove the loosely attached microorganisms and stained using the LIVE/DEAD™ BacLight™ kit. Five images from random fields of view (658x551 µm, magnification x20) were obtained using a fluorescent microscope Provis AX-70 (Olympus, Tokyo, Japan) at 5 min, 15 min, and 30 min periods after the discs had been removed from the anaerobic environment. Bacterial viability was measured using Comstat2 software (Heydorn *et al.*, 2000; Vorregaard, 2008), with green fluorescence (SYTO9) corresponding to live microorganisms, and red (propidium iodide) to dead bacteria. Prior to quantification, a threshold was applied on images to remove fluorescent background that can be caused by the metal or stain aggregates. The thresholding process sets pixels of equal or higher value than the threshold as ONE, and the pixels of value below the threshold as ZERO. Thresholds were manually set and remained the same for each bacterial species and condition (e.g. *F. nucleatum* single species on untreated Ti6Al4V was processed with a threshold of 60 for all time points). Once the thresholding was performed, green and red areas were calculated in $\mu m^2$ by Comstat2 and divided by the total surface area of the image to obtain a percentage coverage. The percentage of area covered by bacteria, as well as the viability ratio could therefore be analysed.

### 3.2.6 Surface charge measurements of bacterial membranes

Overnight bacterial suspensions were centrifuged at 13,000 *g* for 5 min using a Heraeus Pico 17 (ThermoFisher Scientific, Waltham, Massachusetts, USA). The supernatant was discarded, and the pellet resuspended in PBS at $OD_{600}$ equal to 0.08. A 1-mL volume of the suspension was added to a cuvette and the zeta potential measured using a Zetasizer Nano ZS (Malvern, Malvern, UK). Three independent measurements were recorded in triplicate. Twelve runs per replicate were performed.

### 3.2.7 Attachment of *Fusobacterium nucleatum* and *Porphyromonas gingivalis* to Ti6Al4V

#### 3.2.7.1 Pre-conditioning of Ti6Al4V with artificial saliva

AS was prepared according to Wilson and co-workers (Wilson, 1999). The AS was composed of 5 g/L proteose peptone, 2.5 g/L porcine stomach mucin, 2 g/L yeast extract, 1 g/L lab lemco powder, 0.35 g/L NaCl, 0.2 g/L KCl and 0.2 g/L $CaCl_2$ in distilled water. AS was autoclaved and stored at room temperature for up to one month. Prior to use, 40 % (w/v) urea solution was filter sterilised and added at a ratio of 12.5 µL urea solution per 10 mL of AS.

Incubation time of the discs in AS was determined by measuring the total concentration of proteins on the Ti6Al4V surfaces after 1 h and 24 h incubation using a Pierce™ bicinchoninic acid assay (BCA) protein assay kit (ThermoFisher Scientific, Waltham, Massachusetts, USA). Discs were immersed in AS for 1 h and 24 h at 37 °C, then rinsed in deionised, sterile water for 1 min. 2 mL of the prepared reagent were added directly onto the discs and incubated at 37 °C for 30 min, following the manufacturer's instructions. 225 µL of the resulting purple solution was transferred into a 96-well plate that was shaken for 30 seconds and absorption was read at 562 nm.

#### 3.2.7.2 Contact angle of Ti6Al4V discs after preconditioning with AS

Laser melted Ti6Al4V discs were incubated in AS for 15 h. Surface hydrophobicity of laser melted Ti6Al4V was assessed before autoclaving, after autoclaving and after preconditioning with AS by contact angle measurement using a Dynamic Contact Angle analyser (DCA-312, Thermo Cahn Instruments, Madison, USA) and the WinDCA 32 software (Thermo Cahn Instruments, Madison, USA). Samples were dipped 7 mm in water at a speed of 264 µm/s. Measurements were recorded at 21 °C.

#### 3.2.7.3 Investigation of bacterial attachment and viability to Ti6Al4V using fluorescent imaging and live/dead stain

For single species experiments, bacterial suspensions were cultured in FAB to mid-log phase, corresponding to $OD_{600}$ = 0.30 for *F. nucleatum* and $OD_{600}$ = 0.65 for *P. gingivalis*. For dual species experiments, equal proportions of bacteria were added to the suspension, corresponding to $OD_{600}$ = 0.30 and $OD_{600}$ = 0.25 for *F. nucleatum* and *P. gingivalis*, respectively. Ti6Al4V surfaces were incubated in bacterial suspensions for 10 min, 30 min, 60 min and 120 min, then rinsed in 0.9 % (w/v) NaCl. Adherent bacteria were stained using the LIVE/DEAD™ BacLight™ kit. Five images of randomly selected fields of view (658x551 µm, magnification x20) were obtained using a fluorescent microscope. The percentage coverage and bacterial viability were then assessed by image analysis using Comstat2 software as stated in Section 3.2.5.

#### 3.2.7.4 Investigation of bacterial attachment and viability to Ti6Al4V using microbial counts

Bacterial suspensions were cultured in FAB to mid-log phase. Ti6Al4V discs were incubated in suspension for 10 min, 30 min, 60 min and 120 min, rinsed in sterile PBS and placed in a bijou bottle. The discs were vortexed for 1 min with 200 mg of sterile glass beads (500-750 µm) in 1 mL of sterile PBS. The resulting bacterial suspension was serially diluted and plated onto FAA using a spiral plater (Whitley Automatic Spiral Plater, Don Whitley Scientific, West Yorkshire, UK). *F nucleatum* and *P. gingivalis* were then cultured anaerobically at 37 °C for 3 and 7 days, respectively. Colony forming units from the Ti6Al4V discs were enumerated. Both species were differentiated by colony morphology: *F. nucleatum* formed white colonies, whilst *P. gingivalis* colonies appeared black.

#### 3.2.7.5 Investigation of residual bacterial coverage of Ti6Al4V surfaces after vortexing

To investigate the efficacy of the removal protocol (i.e. 1 min vortexing with 200 mg glass beads – 500-750 µm, and 1 mL PBS), discs were subsequently stained using

the BacLight™ dead stain and five images of randomly selected fields of view (658x551 µm, magnification x20) were obtained by fluorescent microscopy. The remaining bacterial percentage coverage was analysed using Comstat2 software and compared to the results found during the attachment studies.

### 3.2.8 Statistical analysis

Unless stated otherwise, all experiments described above were performed three times including internal triplicates and all data were subject to a two-way analysis of variance (ANOVA) to test for statistical significance. When a p value of $< 0.05$ was found, a Bonferroni post-test was performed between all groups. All data were expressed as the mean together with the standard error of the mean.

## 3.3 Results

### 3.3.1 Correlation between $OD_{600}$ and colony counts

Both species yielded similar bacterial numbers at equal $OD_{600}$ values, with a slightly higher number of *P. gingivalis*, e.g. $OD_{600} = 0.30$ corresponded to $6 \times 10^9$ CFU/mL ($\pm 8 \times 10^8$) for *F. nucleatum*, and $9 \times 10^9$ CFU/mL ($\pm 1 \times 10^9$) for *P. gingivalis* (Figure 3.1). A linear correlation between $OD_{600}$ and colony count was found for both species with a $R^2$ of 0.9950 and 0.9879 for *F. nucleatum* and *P. gingivalis*, respectively.

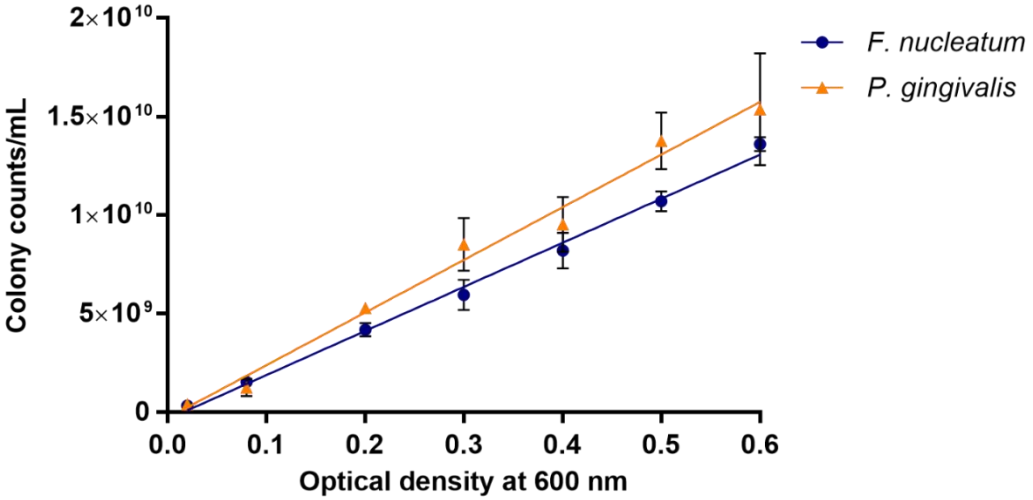


**Figure 3.1. Correlation between colony counts/mL and $OD_{600}$. Mean values of 3 independent experiments in triplicate are shown. Error bars represent standard error of the mean.**

### 3.3.2 Investigation of bacterial growth with and without supplementation in artificial saliva

No significant difference was observed in the proliferation trends of *F. nucleatum* and *P. gingivalis* with and without supplementation in AS. At 24 h incubation, *F. nucleatum* presented 1.27 x $10^{10}$ CFU/mL (± 8.22 x $10^{8}$) and 1.10 x $10^{10}$ CFU/mL (± 1.67 x $10^{9}$), without and with supplementation in AS, respectively, whilst *P. gingivalis* showed 8.13 x $10^{9}$ CFU/mL (± 7.31 x $10^{8}$) and 9.56 x $10^{9}$ CFU/mL (± 1.74 x $10^{9}$) without and with supplementation in AS, respectively (Figure 3.2A and B, $p > 0.999$).

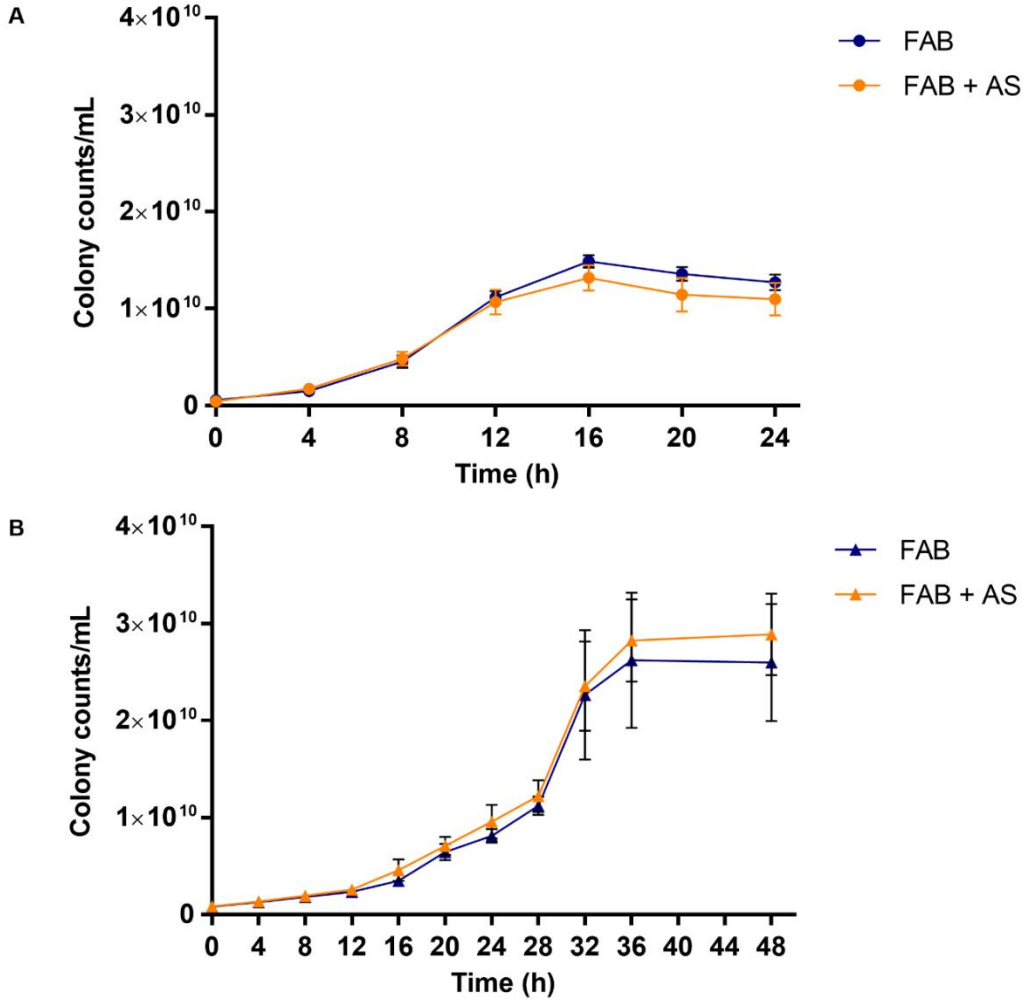


**Figure 3.2. *F. nucleatum* (A) and *P. gingivalis* (B) proliferation with and without artificial saliva supplementation. Mean values of 3 independent experiments in triplicate are shown. Error bars represent standard error of the mean.**

**Key** **FAB: Fastidious Anaerobe Broth**

**AS: Artificial Saliva**

### 3.3.3 Assessment of *Fusobacterium nucleatum* and *Porphyromonas gingivalis* viability over time under aerobic conditions

The percentage of live *F. nucleatum* and *P. gingivalis* at 5 min, 15 min and 30 min under aerobic conditions was measured (Figure 3.3). Both species showed

comparable viability at 5 min in aerobic conditions with 88 % (± 3) and 93 % (± 3) viability for *F. nucleatum* and *P. gingivalis*, respectively. *F. nucleatum* viability however dropped significantly at each time point, with 63 % (± 2; p = 0.0003) viability at 15 min and 40 % (± 2; p = 0.0006 compared with 15 min; p < 0.0001 compared with 5 min) viability at 30 min. *P. gingivalis* viability decreased in a less significant manner, with 84 % (± 2; p = 0.2486) and 58 % (± 5; p = 0.0058 compared with 15 min; p = 0.0006 compared with 5 min) viability at 15 min and 30 min, respectively. The differences in viability between both species were significant at 15 min (p = 0.0008) and 30 min (p < 0.0001) in aerobic conditions.

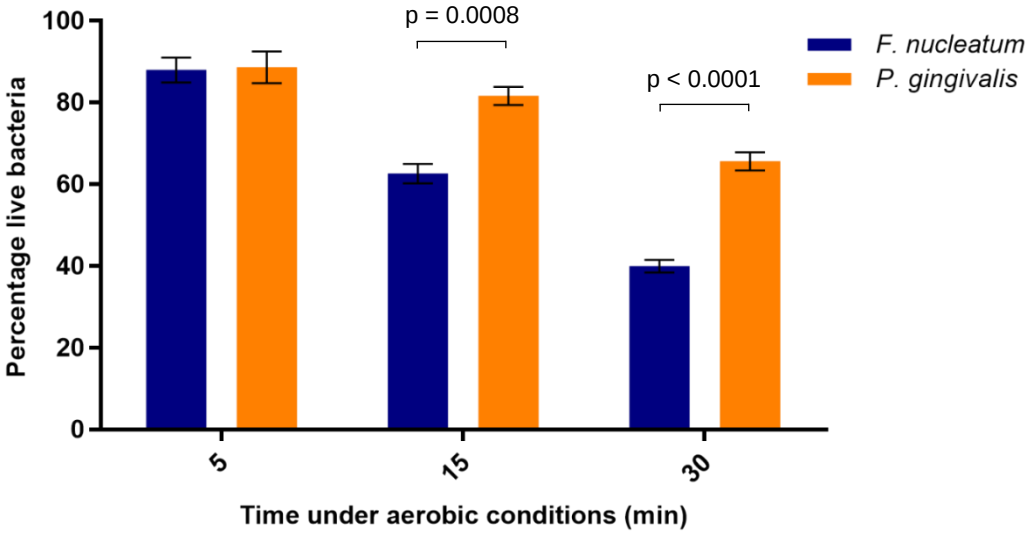


**Figure 3.3. Percentage of live bacteria on untreated Ti6Al4V surfaces under aerobic conditions. Mean values of 3 independent experiments in triplicate are shown. Error bars represent standard error of the mean.**

### 3.3.4 Surface charge measurements of bacterial membranes

*F. nucleatum* and *P. gingivalis* presented a significant difference (p < 0.0001) in zeta potentials at - 3.35 mV (± 0.126) and - 5.47 mV (± 0.138), respectively (Figure 3.4).

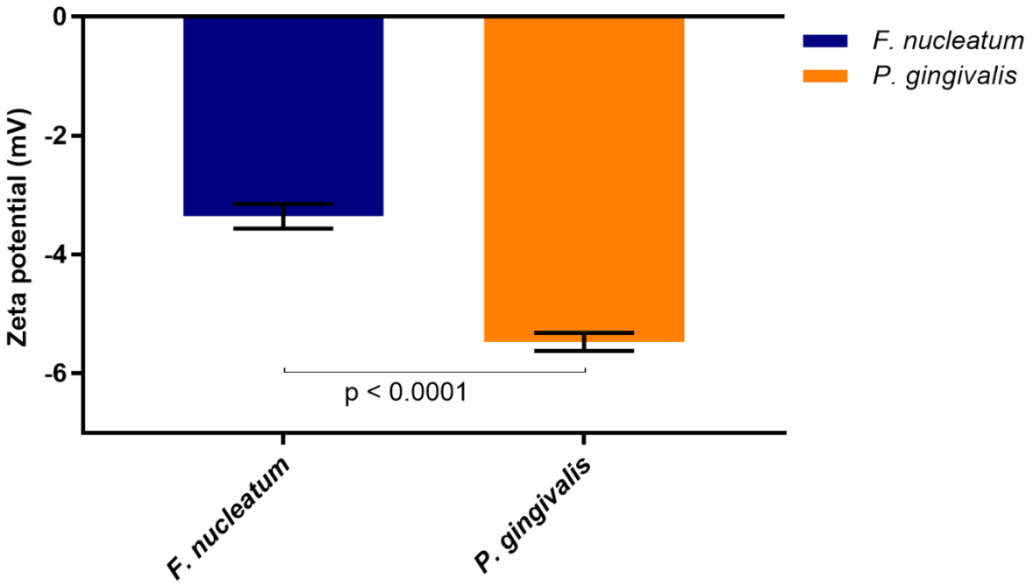


**Figure 3.4. Zeta potential of *F. nucleatum* and *P. gingivalis*. Three independent measurements were recorded in triplicate. Twelve runs per replicate were performed.**

### 3.3.5 Attachment of *Fusobacterium nucleatum* and *Porphyromonas gingivalis* to Ti6Al4V

#### 3.3.5.1 Pre-conditioning of Ti6Al4V with artificial saliva

Using the BCA assay, similar amounts of protein were found after incubation in AS for 1 h and 24 h with concentrations of 21.32 µg/mL (± 1.20) and 23.42 µg/mL (± 3.99), respectively. A fourth order polynomial was used to obtain the calibration curve (Figure 3.5). The equation was as follows:

$y = -31.971x^4 + 48.414x^3 + 197.59x^2 + 650.36x - 59.178$

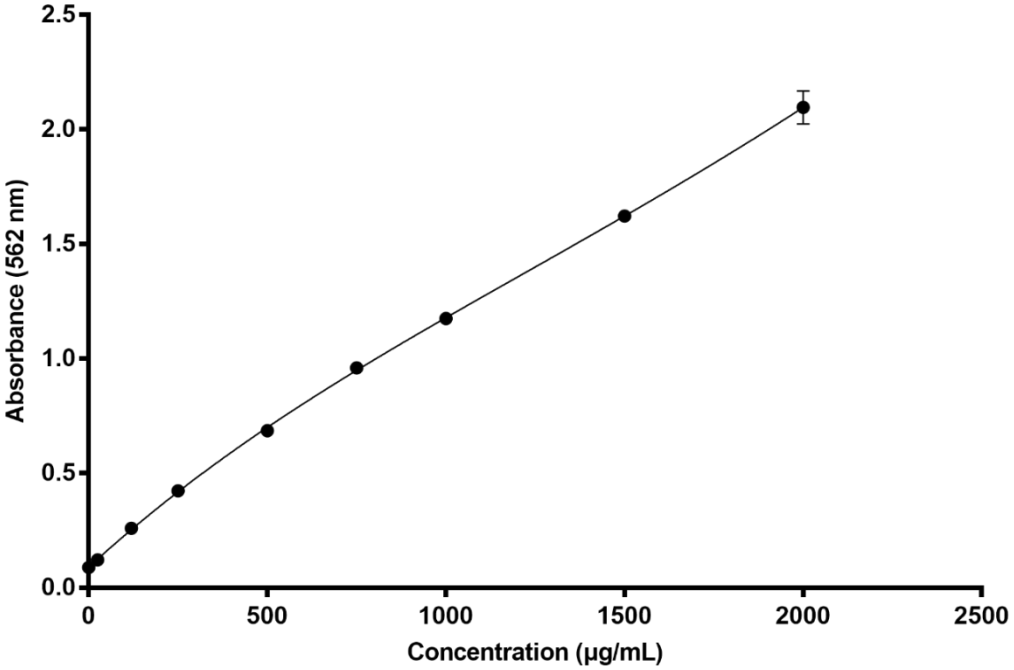


**Figure 3.5. Standard curve of protein concentration according to absorbance at 562 nm. Mean values of 3 independent experiments are shown. Error bars represent standard error of the mean.**

The contact angle of preconditioned surfaces was measured and compared to the contact angles of untreated Ti6Al4V before and after autoclaving (Figure 3.6). Prior to autoclaving, Ti6Al4V surfaces had a contact angle of 64 ° (± 1.026). A significant reduction ($p = 0.0059$) to 48 ° (± 1.178) was observed after autoclaving. AS preconditioning further reduced the contact angle to 34 ° (± 2.719, $p = 0.0119$ compared with contact angle measured after autoclaving; $p = 0.0002$ compared with contact angle measured before autoclaving).

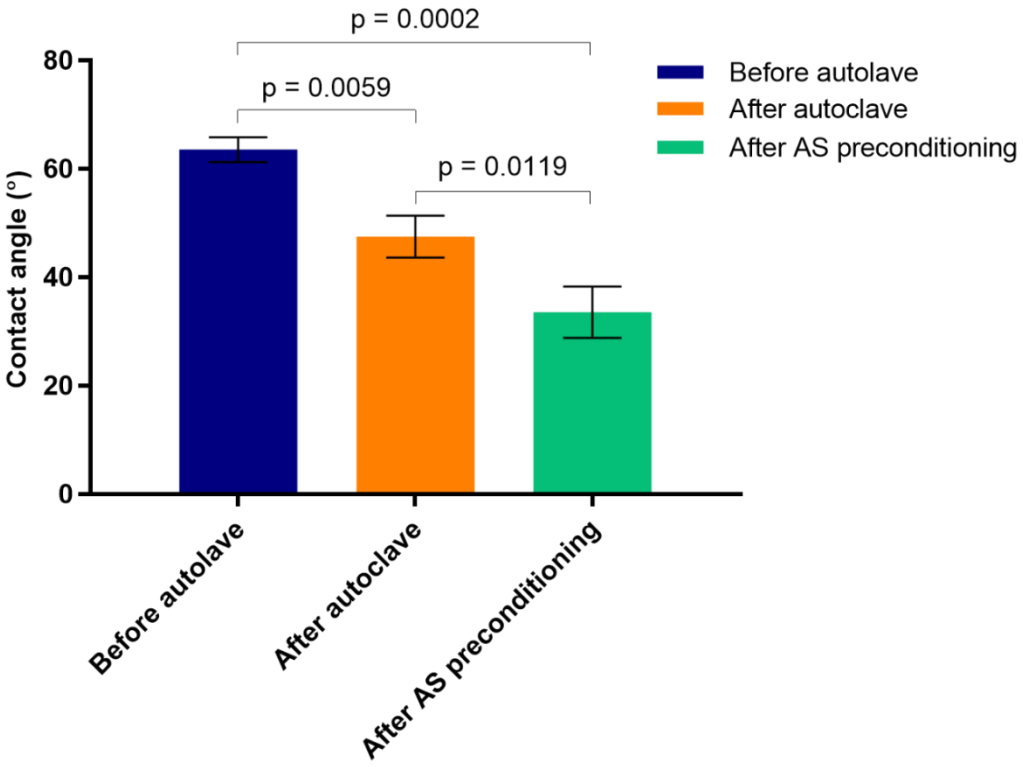


**Figure 3.6. Ti6Al4V surfaces before autoclaving, after autoclaving and after preconditioning with AS. Mean values of 3 independent experiments in triplicate are shown. Error bars represent standard error of the mean.**

### 3.3.5.2 Fluorescent imaging of *F. nucleatum* and *P. gingivalis* to untreated Ti6Al4V

Bacterial attachment and viability were measured using fluorescent microscopy and a live/dead stain. *F. nucleatum* attachment to untreated Ti6Al4V increased linearly ($R^2$ = 0.9837) from 13 % coverage at 10 min incubation to 42 % at 120 min (Figure 3.7). *P. gingivalis* attachment remained constant from 10 % coverage at 10 min to 13 % at 120 min (

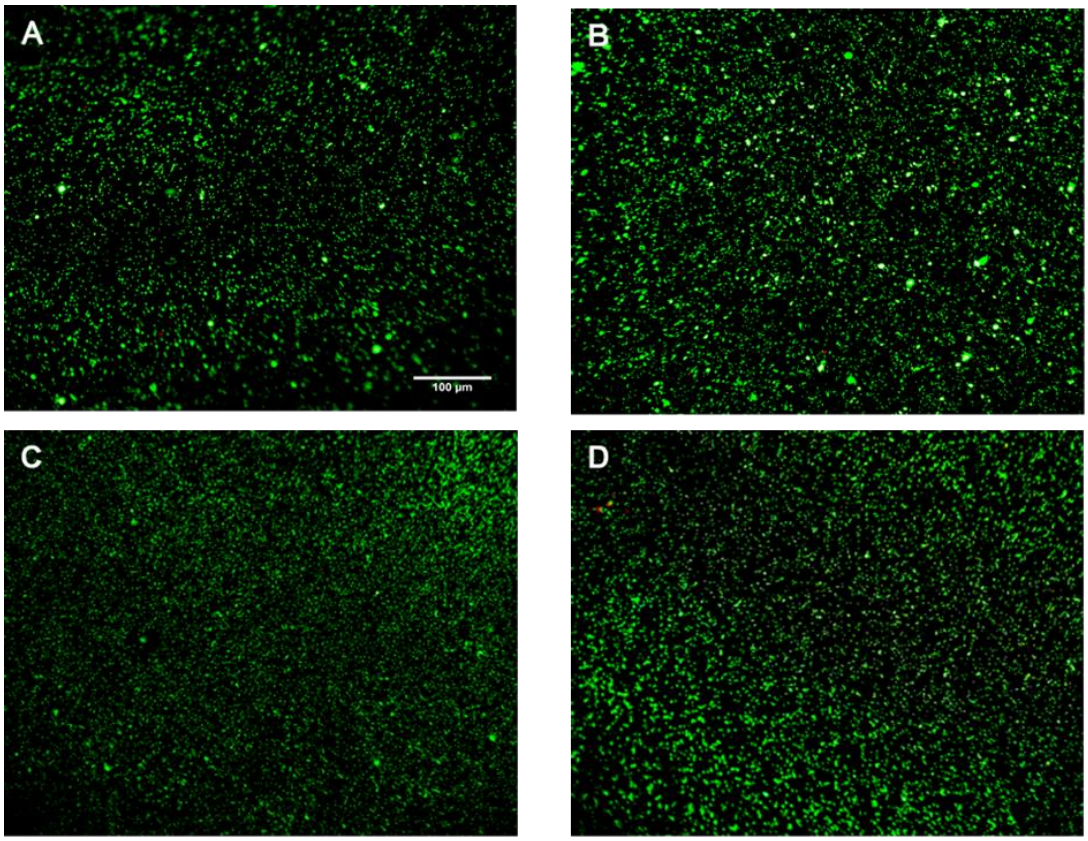


Figure 3.8). At 10 min incubation, both inoculums presented a comparable percentage coverage with 13 % and 10 % coverage for *F. nucleatum* and *P. gingivalis*, respectively (Figure 3.10). Significant differences were measured however at the next time points between both species. At 60 min incubation, 25 % coverage and 11 % coverage were detected for *F. nucleatum* and *P. gingivalis*, respectively ($p = 0.0083$), and at 120 min incubation *F. nucleatum* presented 42 % versus 13 % coverage for *P. gingivalis* ($p < 0.0001$).

At 10 min incubation, dual species showed an attachment of 10 % coverage, increasing to 25 % at 120 min (Figure 3.9). This coverage was significantly lower than single species *F. nucleatum* with 42 % coverage ($p = 0.0066$) and higher than single species *P. gingivalis* presenting 13 % coverage ($p = 0.0125$) at 120 min incubation. No distinction between *F. nucleatum* and *P. gingivalis* in the dual species attachment was achieved using Comstat2.

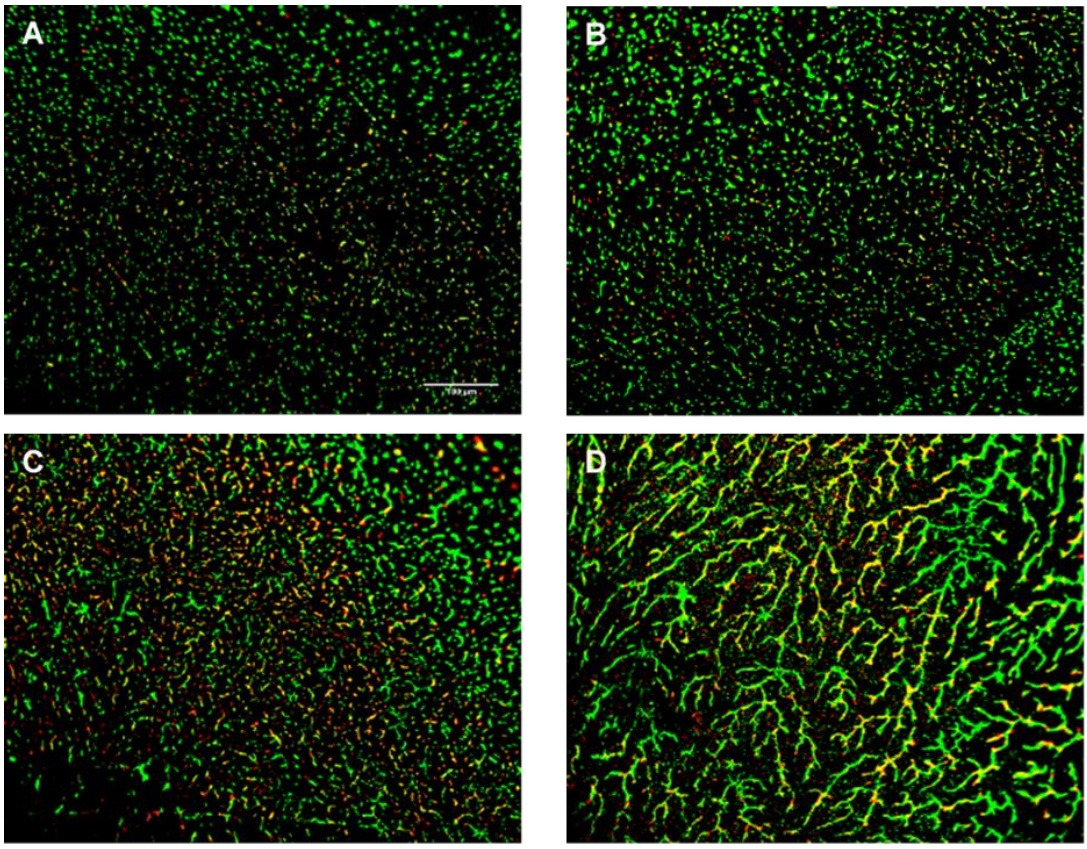


**Figure 3.7. *F. nucleatum* attachment to untreated Ti6Al4V. Images (magnification x20) at 10 min (A), 30 min (B), 60 min (C), 120 min (D) were used to calculate the percentage coverage and live ratio with Comstat2 software.**

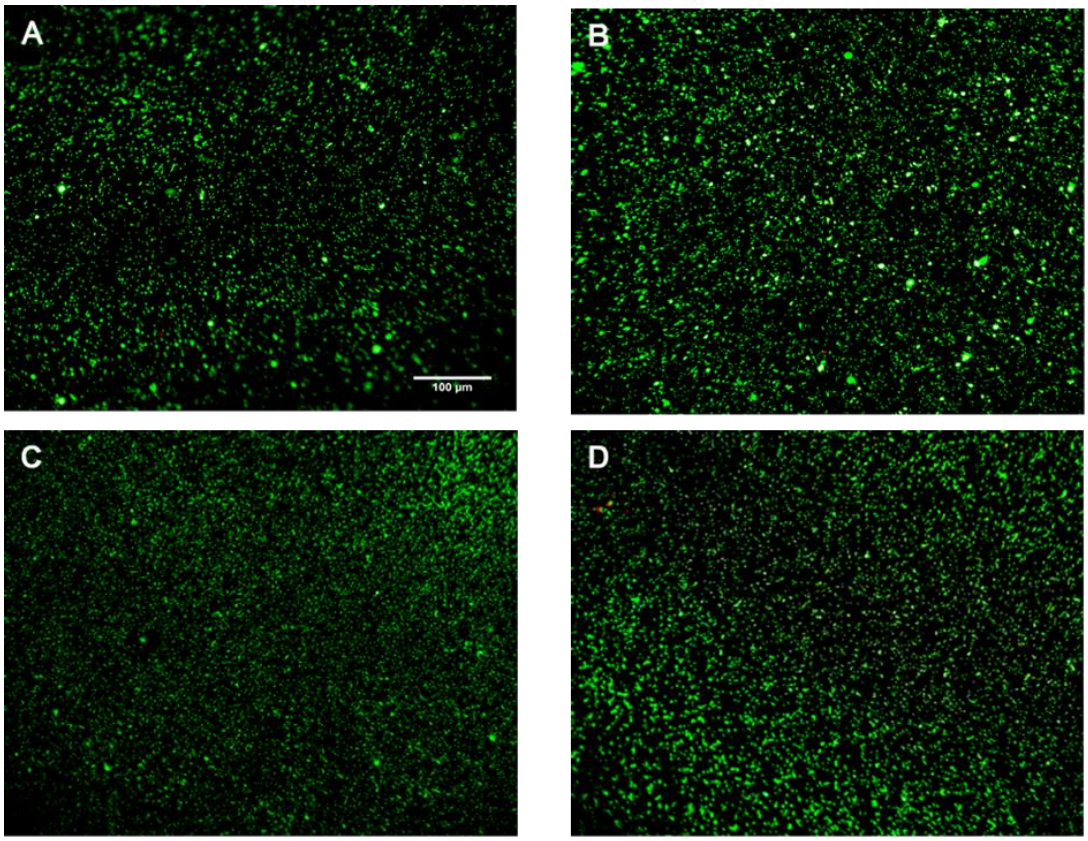


**Figure 3.8. *P. gingivalis* attachment to untreated Ti6Al4V. Images (magnification x20) at 10 min (A), 30 min (B), 60 min (C), 120 min (D) were used to calculate the percentage coverage and live ratio with Comstat2 software.**

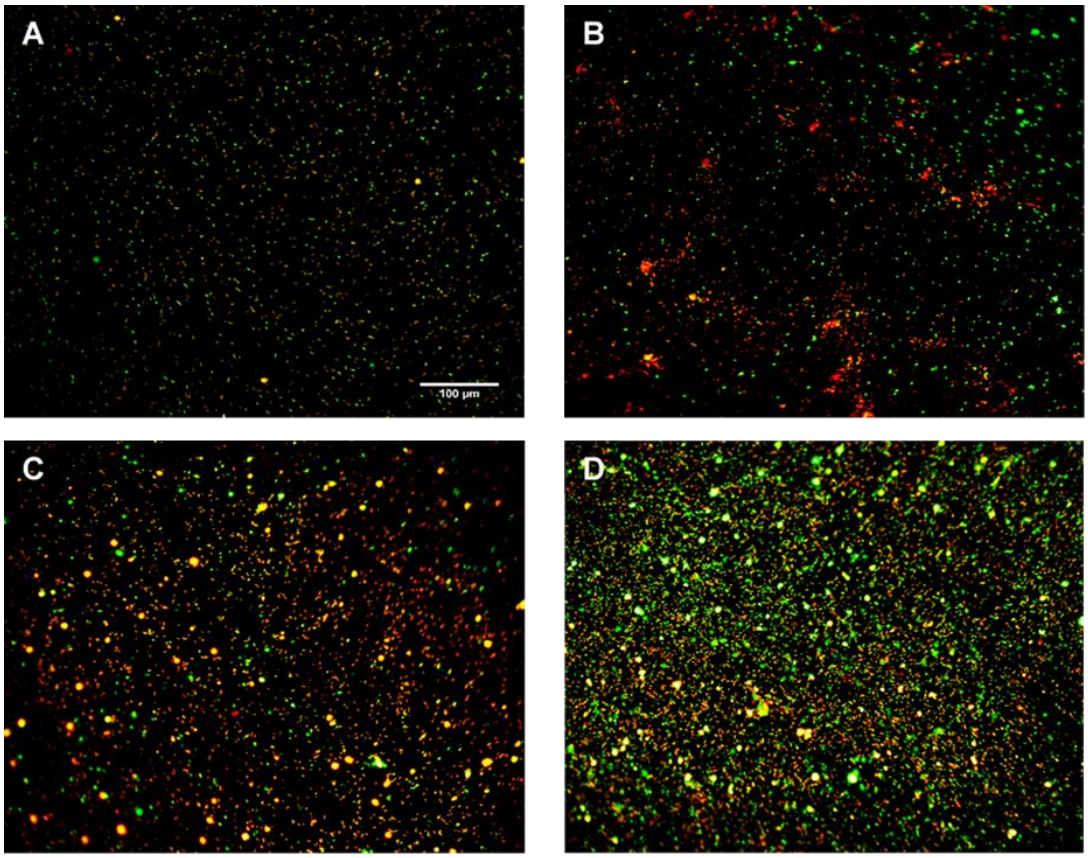


**Figure 3.9. Dual species attachment to untreated Ti6Al4V. Images (magnification x20) at 10 min (A), 30 min (B), 60 min (C), 120 min (D) were used to calculate the percentage coverage and live ratio (E) with Comstat2 software.**

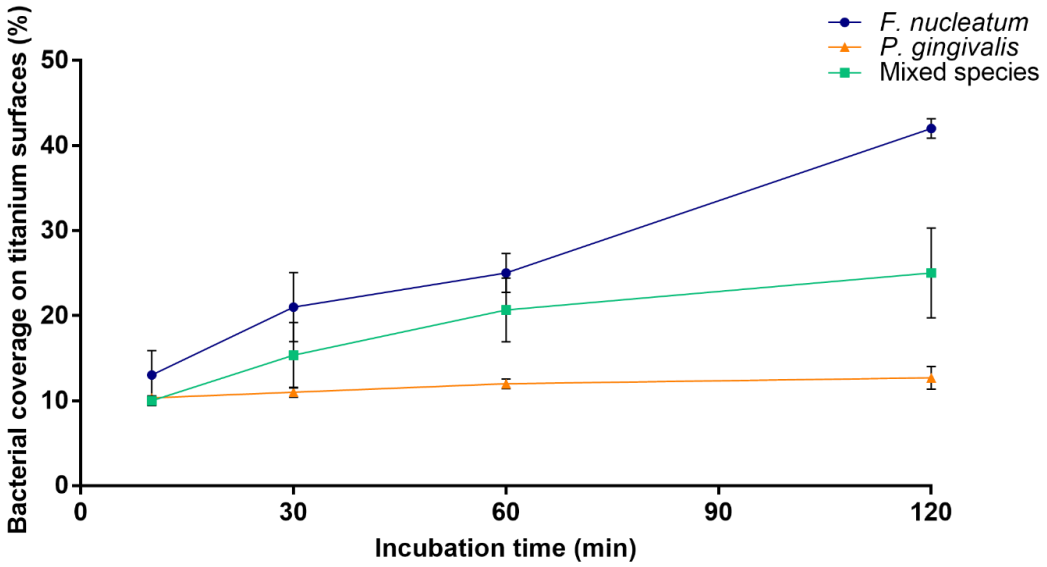


**Figure 3.10. Bacterial percentage coverage on untreated Ti6Al4V surfaces. Mean values of 3 independent experiments in triplicate are shown. Error bars represent standard error of the mean.**

*P. gingivalis* exhibited a significantly higher viability than *F. nucleatum* at 10 min ($p = 0.0003$), 30 min ($p = 0.0052$) and 60 min ($p = 0.0161$) incubation. No significant difference was detected at 120 min incubation (Figure 3.11). *F. nucleatum* viability increased over time from 67 % at 10 min incubation to 90 % at 120 min, whereas *P. gingivalis* viability remained constant at all time points, with 92 % viability at 10 min and 98 % at 120 min. Incubated together, however, *F. nucleatum* and *P. gingivalis* demonstrated a significant reduction in viability compared with *P. gingivalis* single species and a non-significant reduction compared with *F. nucleatum* single species. The viability at 10 min was detected at 55 % ($p = 0.2880$ compared with *F. nucleatum*; $p < 0.0001$ compared with *P. gingivalis*) and increased to 78 % ($p = 0.1143$ compared with *F. nucleatum*; $p = 0.0045$ compared with *P. gingivalis*) at 120 min incubation.

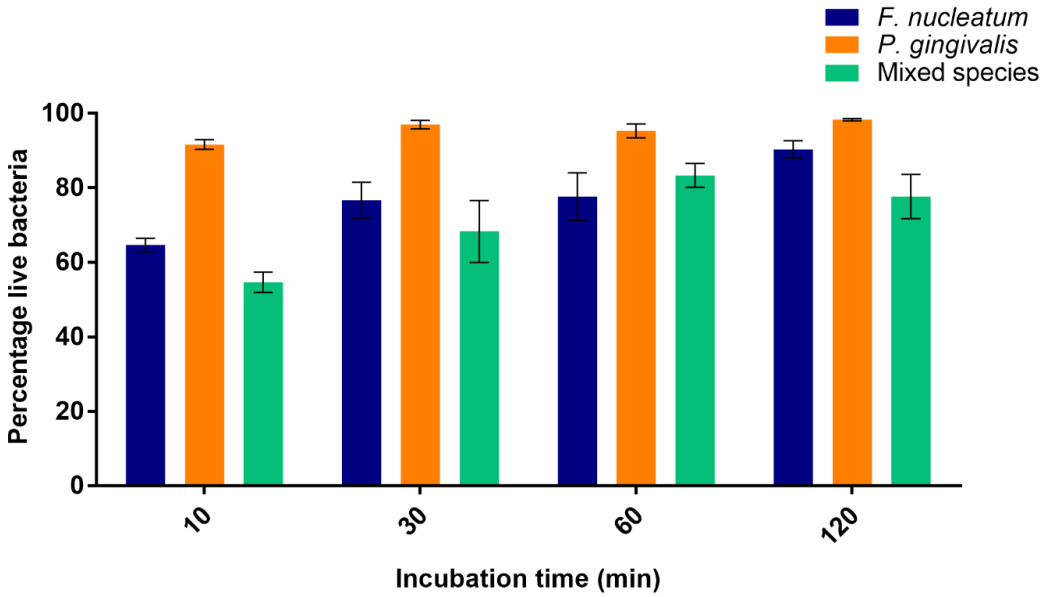


**Figure 3.11. Percentage of live bacteria on untreated Ti6Al4V surfaces. Mean values of 3 independent experiments in triplicate are shown. Error bars represent standard error of the mean.**

### 3.3.5.3 Fluorescent imaging of *Fusobacterium nucleatum* and *Porphyromonas gingivalis* to Ti6Al4V preconditioned with artificial saliva

Preconditioning with AS dramatically modified attachment of bacteria. *F. nucleatum* attachment was detected at 3 % at 10 min incubation and reached 14 % at 120 min incubation (Figure 3.12). In contrast, 23 % area coverage was measured at 10 min for *P. gingivalis* and appeared to plateau between 30 min and 120 min with 39 % and

43 % area coverage, respectively. In these conditions, *F. nucleatum* and *P. gingivalis* attachment differed significantly at all time points ($p < 0.0001$). Differences between single species *P. gingivalis* and dual species were also significant at all time points, with 8 % area coverage at 10 min ($p = 0.0009$) and 31 % at 120 min ($p = 0.0150$) for dual species. Significant differences were observed between dual species and *F. nucleatum* after 30 min incubation. Although the percentage area of bacterial coverage significantly differed at most time points for both single species, the same trend was noticed for each species indifferently of Ti6Al4V treatment: *F. nucleatum* attachment increased at each time point, whilst *P. gingivalis* plateaued from early time points.

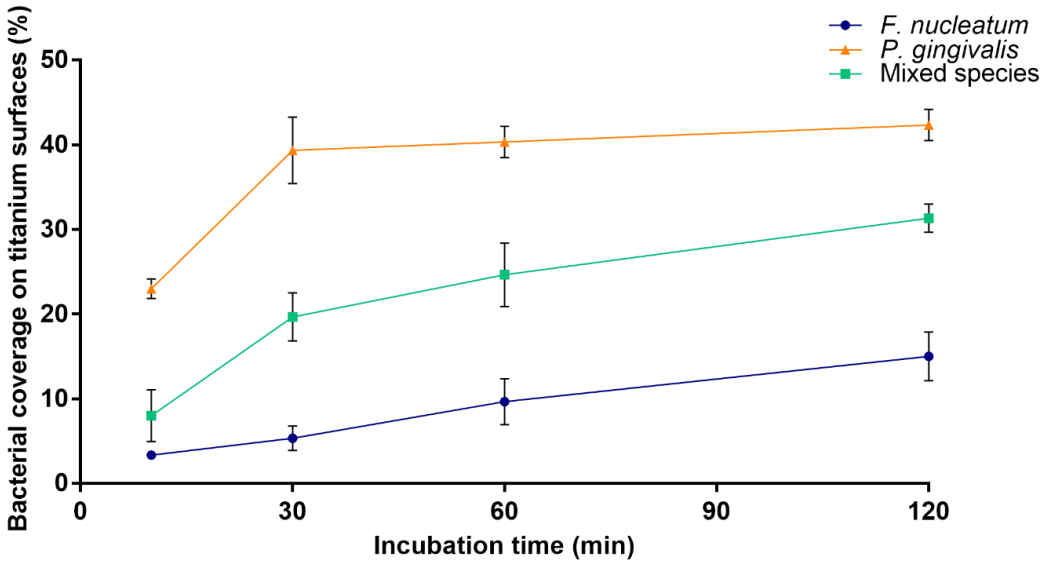


**Figure 3.12. Bacterial percentage coverage on Ti6Al4V surfaces preconditioned with AS. Mean values of 3 independent experiments in triplicate are shown. Error bars represent standard error of the mean.**

*P. gingivalis* and dual species presented viabilities that were comparable between untreated and preconditioned Ti6Al4V (Figure 3.13). *P. gingivalis* exhibited viability ratios of 86 % at 10 min, 93 % at 30 min and 60 min and 88 % viability at 120 min incubation, and dual species showed 52 %, 71 %, 78 % and 68 % viability at 10 min, 30 min, 60 min and 120 min incubation. However, *F. nucleatum* viability significantly decreased at all time points compared with *P. gingivalis* ($p < 0.0001$), presenting 48 % at 10 min, 46 % at 30 min, 53 % at 60 min and 49 % at 120 min incubation. The viability ratio remained constant over time for *F. nucleatum*.

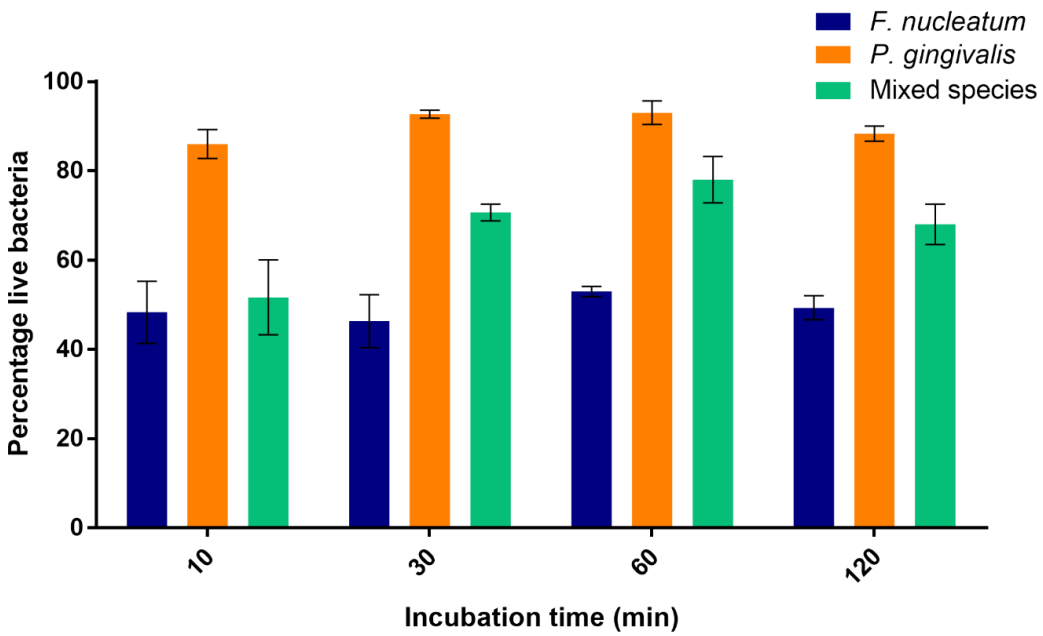


**Figure 3.13. Percentage of live bacteria on Ti6Al4V surfaces preconditioned with AS. Mean values of 3 independent experiments in triplicate are shown. Error bars represent standard error of the mean.**

### 3.3.5.4 Culture of *Fusobacterium nucleatum* and *Porphyromonas gingivalis* from untreated Ti6Al4V

At each time point, *P. gingivalis* presented a higher colony count than *F. nucleatum*, with the greatest difference at 120 min incubation with $1.35 \times 10^8$ CFU/mL ($\pm 1.20 \times 10^6$) and $7.82 \times 10^7$ CFU/mL ($\pm 2.99 \times 10^7$), respectively ($p = 0.0012$, Figure 3.14). This is consistent with the viability found using fluorescent microscopy and live/dead stain: *P. gingivalis* was more viable than *F. nucleatum*. When incubated concomitantly, *F. nucleatum* yielded a higher colony count than *P. gingivalis*, with a significant difference at 120 min incubation ($p = 0.0055$). However, both species showed reduced microbial counts compared with single species experiments, which again is in line with previous experimental findings. The reduction was significant for *P. gingivalis* at 60 min ($p = 0.0263$) and 120 min incubation ($p < 0.0001$).

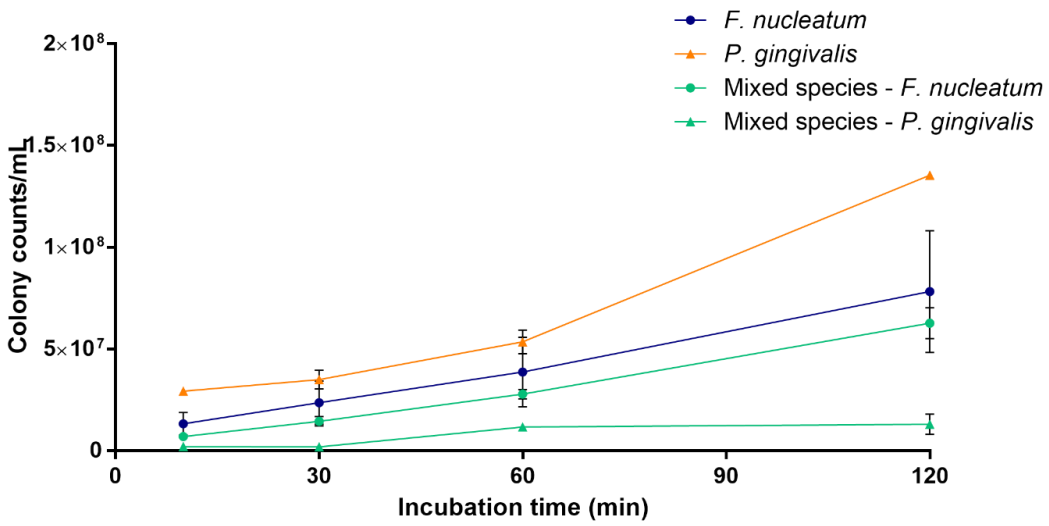


**Figure 3.14. Colony counts/mL recovered from untreated Ti6Al4V surfaces. Mean values of 3 independent experiments in triplicate are shown. Error bars represent standard error of the mean.**

### 3.3.5.5 Culture of *Fusobacterium nucleatum* and *Porphyromonas gingivalis* from Ti6Al4V preconditioned with artificial saliva

The CFU/mL observed from preconditioned Ti6Al4V was lower than from untreated surfaces for *F. nucleatum*, presenting 6.96 x $10^6$ CFU/mL (± 3.63 x $10^5$), 1.38 x $10^7$ CFU/mL (± 4.49 x $10^6$), 2.48 x $10^7$ CFU/mL (± 7.22 x $10^6$) and 4.39 x $10^7$ CFU/mL (± 5.24 x $10^6$) at 10 min, 30 min, 60 min and 120 min incubation, respectively (Figure 3.15). In contrast, *P. gingivalis* colony number increased from 2.09 x$10^7$ CFU/mL (± 6.23 x $10^6$) at 10 min incubation to 1.51 x $10^8$ CFU/mL (± 4.81 x $10^6$) at 30 min, followed by a reduction at 60 min and 120 min with 1.01 x $10^8$ CFU/mL (± 1.66 x $10^7$) and 8.82 x $10^7$ CFU/mL (± 1.57 x $10^7$), respectively. When incubated together, *F. nucleatum* and *P. gingivalis* counts were reduced compared to single species. The reduction in CFU/mL was significant ($p < 0.0001$) for *P. gingivalis* at 30 min, 60 min and 120 min, whereas the colony numbers remained close for *F. nucleatum* between dual species and single species experiments.

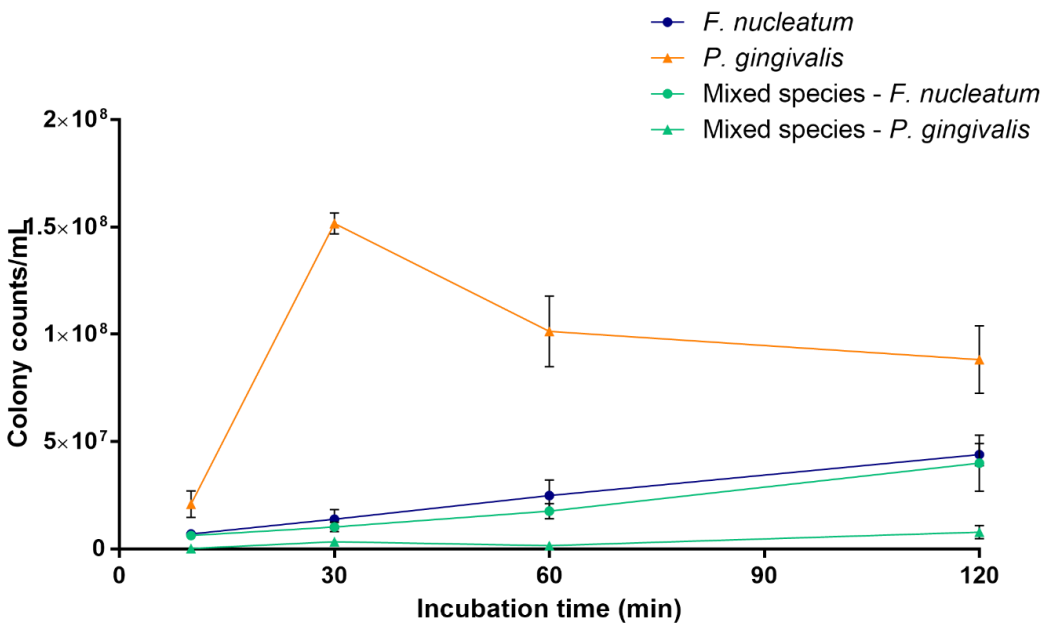


**Figure 3.15. Colony counts/mL recovered from preconditioned Ti6Al4V surfaces. Mean values of 3 independent experiments in triplicate are shown. Error bars represent standard error of the mean.**

### 3.3.5.6 Residual bacterial coverage of untreated Ti6Al4V after vortexing

An increase in *F. nucleatum* percentage coverage was observed at each time point, reaching 7 % (± 1) and 9 % (± 1) at 60 min and 120 min incubation, respectively (Figure 3.16A). The same removal method consequently lost its efficacy with the increase in Ti6Al4V surfaces incubation time in *F. nucleatum* suspensions. *P. gingivalis* percentage coverage remained at 1 % at all time points (Figure 3.16B). Dual species presented a percentage coverage lower than single species *F. nucleatum* and higher than single species *P. gingivalis* (Figure 3.16C).

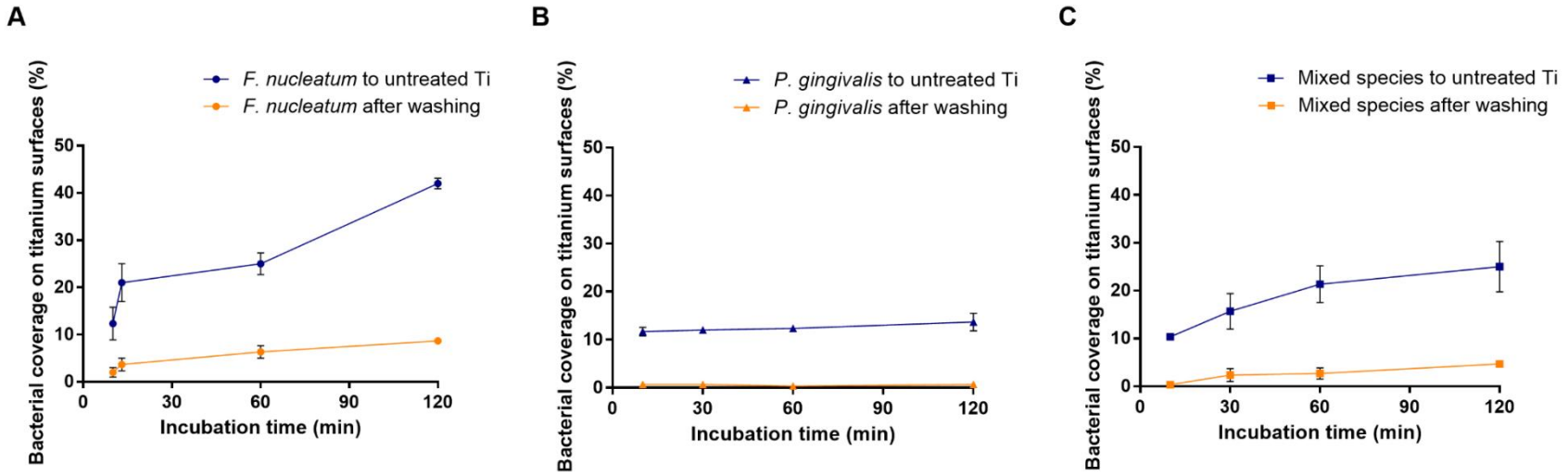


**Figure 3.16. Bacterial percentage coverage on untreated Ti6Al4V surfaces: comparison between attachment and recovery after vortexing of *F. nucleatum* (A), *P. gingivalis* (B) and dual species (C). Mean values of 3 independent experiments in triplicate are shown. Error bars represent standard error of the mean.**

#### 3.3.5.7 Residual bacterial coverage of Ti6Al4V preconditioned with artificial saliva after vortexing

After vortexing *F. nucleatum* percentage area coverage on preconditioned Ti6Al4V was comparable to that of the untreated Ti6Al4V. Preconditioned Ti6Al4V presented 3 % (± 2), 6 % (± 0), 7 % (± 3) and 8 % (± 2) coverage, whilst 2 % (± 1), 4 % (± 1), 7 % (± 1) and 9 % (± 1) coverage were found on untreated Ti at 10 min, 30 min, 60 min and 120 min, respectively (Figure 3.17A). Compared with untreated Ti6Al4V, *P. gingivalis* attachment showed a significant increase ($p < 0.0001$) after 60 min and 120 min incubation on AS preconditioned Ti6Al4V (Figure 3.17B). This corresponded to the reduction in *P. gingivalis* colony counts removed from the surfaces by vortexing. Dual species presented non-significant differences between residual percentage coverage on untreated (Figure 3.16C) and preconditioned Ti6Al4V (Figure 3.17C), with 0 % (± 0), 2 % (± 1), 3 % (± 1) and 5 % (± 0) residual percentage coverage on untreated surfaces and 3 % (± 1; $p > 0.9999$), 2 % (± 1; $p > 0.9999$), 6 % (± 2; $p = 0.5611$) and 8 % (± 4; $p = 0.7099$) residual coverage on surfaces preconditioned with AS.

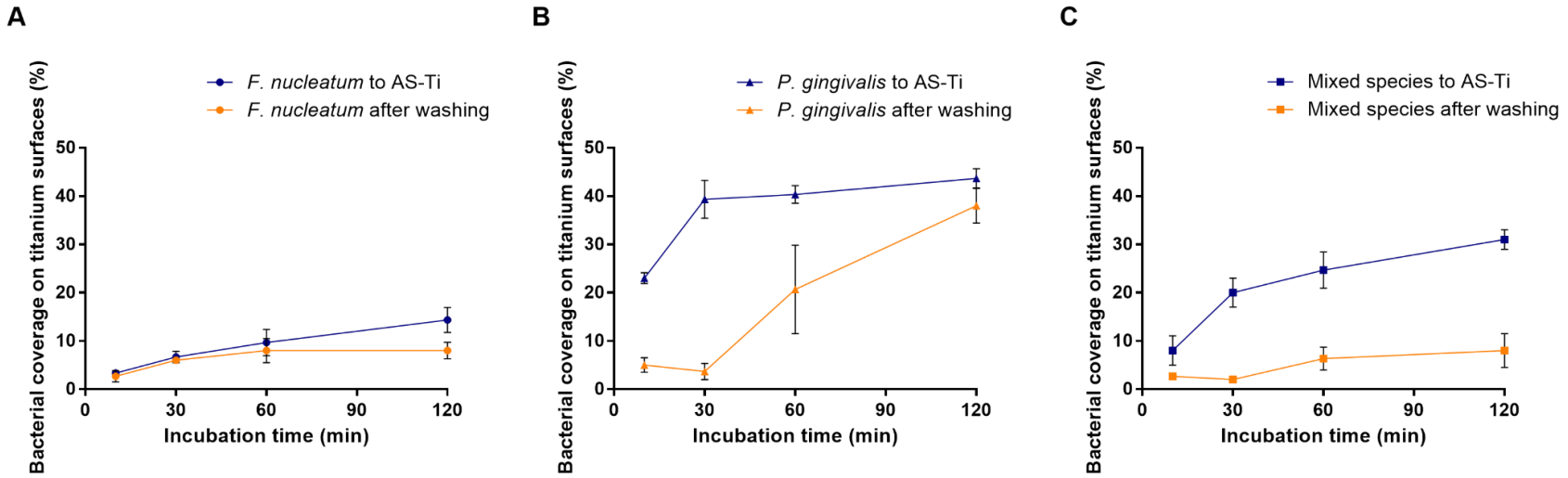


**Figure 3.17. Bacterial percentage coverage on Ti6Al4V surfaces preconditioned with AS: comparison attachment and recovery after vortexing of *F. nucleatum* (A), *P. gingivalis* (B) and dual species (C). Mean values of 3 independent experiments in triplicate are shown. Error bars represent standard error of the mean.**

### 3.3.6 Patterns formed by *Fusobacterium nucleatum* on untreated laser melted Ti6Al4V

#### 3.3.6.1 Adherence patterns of bacteria on laser melted discs

*F. nucleatum* formed branching patterns at 120 min incubation on untreated laser melted Ti6Al4V. Although at earlier time points no patterns were observed, seven out of nine untreated laser melted discs showed initial branching patterns at 60 min incubation (Figure 3.18). No pattern was observed on milled discs or on discs preconditioned with AS. Table 3.2 presents the coverage and live bacteria on laser melted and milled discs. A non-significant, higher coverage was detected on milled discs with 47 % and 42 %, respectively. Bacterial viability was significantly lower ($p = 0.017$) on milled than on laser melted discs. *P. gingivalis* and dual species were not found to form patterns (Figure 3.19). However, it can be noted that *P. gingivalis* predominantly formed aggregates and chains when attaching to the untreated Ti6Al4V surfaces (Figure 3.20).

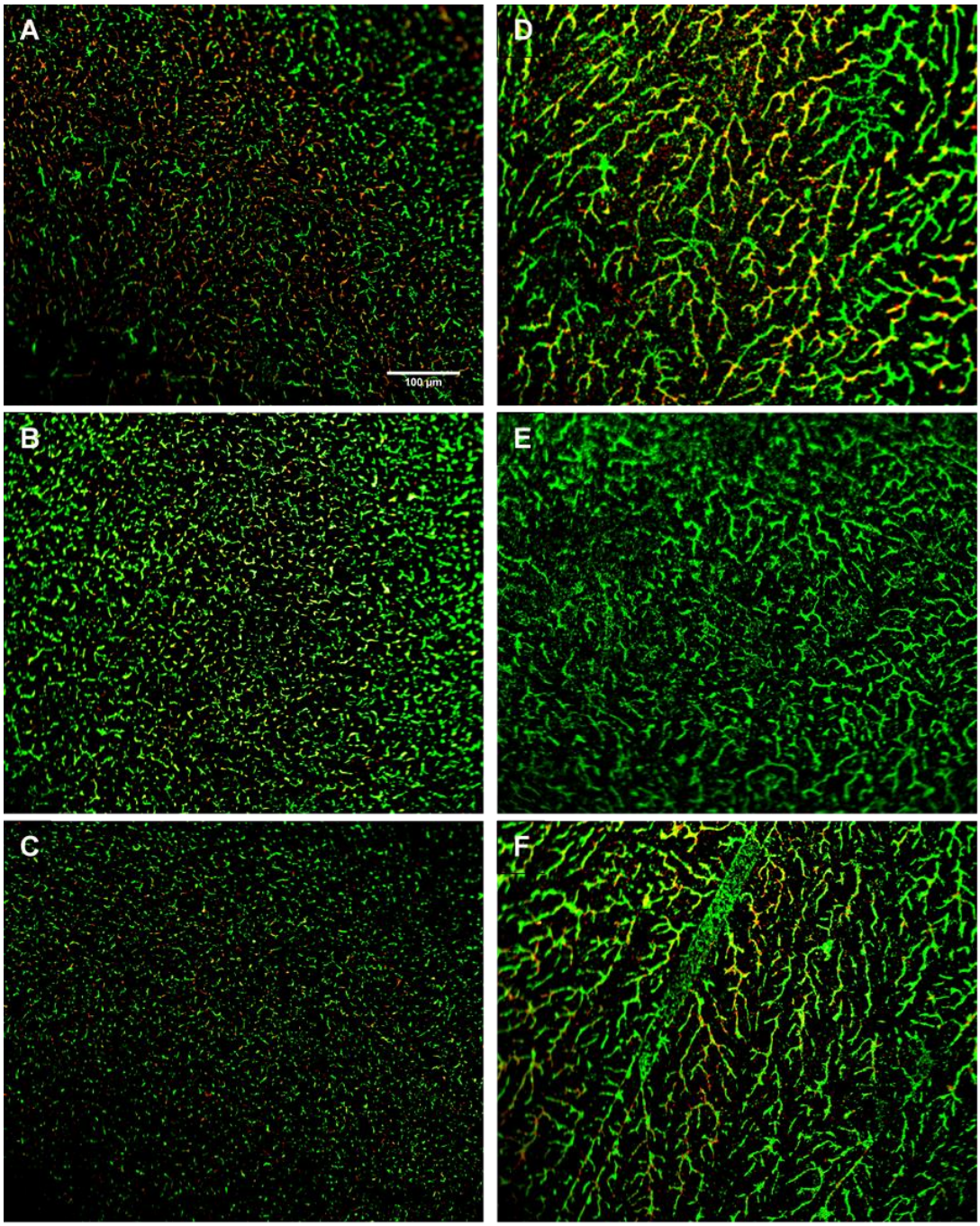


**Figure 3.18. Representative images (magnification x20) of *F. nucleatum* patterns at 60 min (A, B, C) and 120 min (D, E, F) on untreated Ti6Al4V.**

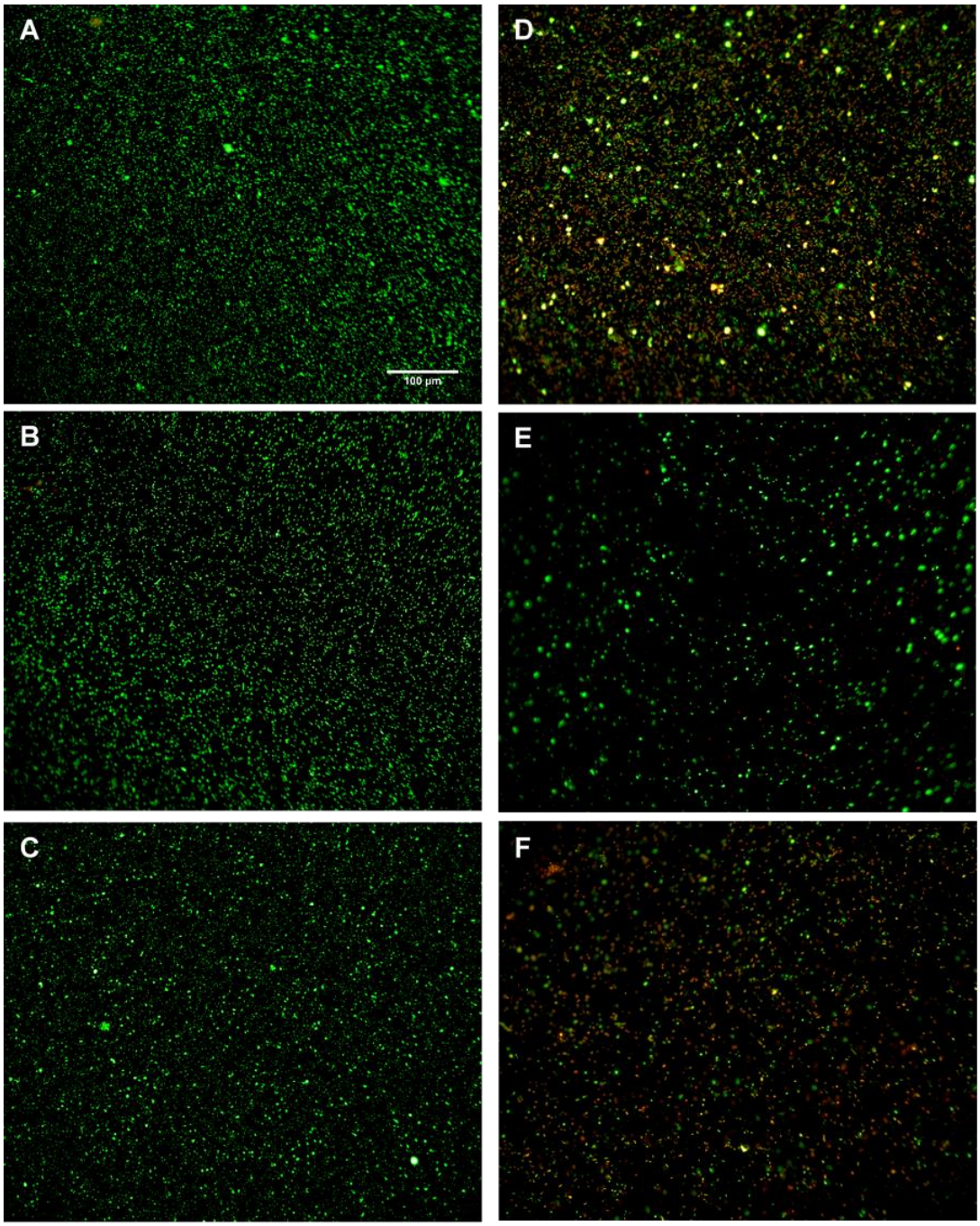


**Figure 3.19. Representative images (magnification x20) of *P. gingivalis* (A, B, C) and dual species (D, E, F) attachment at 120 min attachment to untreated Ti6Al4V.**

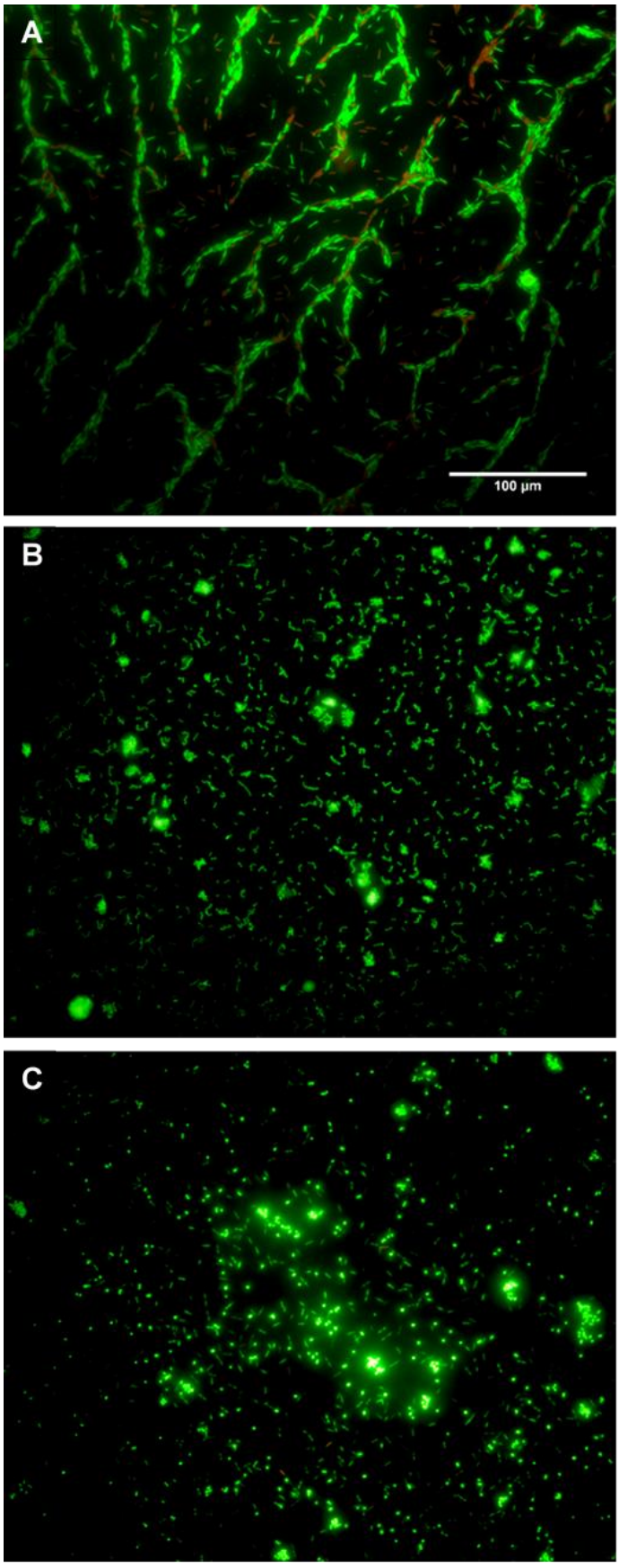


**Figure 3.20. Representative images (magnification x60) of *F. nucleatum* (A), *P. gingivalis* (B), and dual species (C) on untreated Ti6Al4V.**

**Table 3.2. *F. nucleatum* percentage coverage and viability at 120 min incubation on laser melted and milled Ti6Al4V.**

| Manufacturing process | Mean coverage (%) | SEM (%) | Mean live bacteria (%) | SEM (%) |
|---|---|---|---|---|
| **Laser melted disc** | 42 | 2 | 90 | 4 |
| **Milled disc** | 47 | 4 | 73 | 3 |

SEM: Standard Error of the Mean.

## 3.4 Discussion

Attachment of microorganisms to surfaces is a pre-requisite for biofilm formation and may facilitate host cell invasion and subsequent infection (Costerton et al., 1999). Implant-associated infections can be initiated by many microbial species. Staphylococci, especially *S. aureus* and *S. epidermidis*, account for two thirds of bacteria-associated orthopaedic implant infections (Campoccia et al., 2006; Ribeiro et al., 2012). In contrast, dental implants bear a comparatively high microbial burden, in terms of number of species and actual microbial number (Aas *et al.*, 2005). The aetiology of dental implant infection is therefore highly complex and often associated with Gram negative anaerobic bacteria such as *F. nucleatum*, *P. gingivalis*, *A. actinomycetemcomitans* and *P. intermedia*. *F. nucleatum* and *P. gingivalis* play a key role in the pathogenesis of peri-implantitis (Mombelli and Décaillet, 2011). *F. nucleatum* can participate in the architecture of the biofilm by acting as a bridge that links early and late colonisers (Bolstad et al., 1996), whilst *P. gingivalis* has been reported as a 'keystone' pathogen in peri-implantitis (Hajishengallis et al., 2012; Kolenbrander & London, 1993). Although both species are thought to need the help of early colonisers to adhere to surfaces (Kolenbrander et al., 2006), Jordan and co-workers (2016) demonstrated their direct attachment to smooth laser melted CoCr after 120 min incubation. The ability of pathogens involved in peri-implantitis to attach directly to CoCr, material used to produce dental abutments, is of clinical importance as the composition and pathogenicity of the plaque might differ from current expectations. As Ti6Al4V is more often used than CoCr in the construction of dental implants and abutments, part of this research sought to investigate early attachment of these two species to laser melted Ti6Al4V surfaces. Two conditions were studied: attachment to untreated Ti6Al4V and to Ti6Al4V preconditioned with AS. AS was used to study potential changes in attachment trends, as shown with other species on

different surfaces. The use of AS over human saliva to precondition the Ti6Al4V surfaces during this project was decided by the possibility of a better standardisation of saliva composition and an easier sterilisation of AS.

The contact angle of the Ti6Al4V surfaces was measured before and after preconditioning with AS. Preconditioning reduced the contact angle of autoclaved discs from 48 ° to 34 °, which represented a significant ($p = 0.0119$) increase in surface hydrophilicity. This phenomenon can be explained by the adsorption of proteins contained in AS to the material surface. Protein adsorption to surfaces is driven by non-covalent bonds, such as electrostatic and hydrophobic interactions (Kyriakides, 2015). After autoclaving, the Ti6Al4V surface hydrophilicity increased. It can therefore be hypothesised that proteins, particularly mucin, may have been adsorbed to the surface $TiO_2$ layer through electrostatic interactions. This phenomenon may have led to an increase of the surface overall charge, subsequently increasing the surface hydrophilicity. Mabboux and co-workers (2004) compared the contact angles of Ti6Al4V to commercially pure Ti preconditioned with human saliva. The contact angle for the saliva-coated Ti6Al4V found by Mabboux et al (2004) was higher than the Ti6Al4V used in this project, with 56 ° vs 34 °, respectively. However, they did not compare preconditioned with untreated surfaces, and did not mention the disc manufacturing process, making the comparison between both studies challenging. During this study, the same amount of protein was detected on the Ti6Al4V surfaces after 1 h and 24 h incubation in AS. Protein adsorption to a surface is a dynamic process, different types of proteins continuously adsorb to and desorb from the surface until reaching an equilibrium. The most motile and abundant proteins adsorb first to the surface, followed by their displacement by proteins with higher chemical and electrical affinities for the exposed surface moieties. This phenomenon is called the “Vroman effect” and has been studied with serum proteins (Li et al., 2017). Thus, the same amount of protein found after 1 h and 24 h incubation may not indicate the same composition on the Ti6Al4V surface. The identification of the proteins could be performed by electrophoresis in order to verify the composition after these two incubation times.

Initial studies using *F. nucleatum* and *P. gingivalis* explored the correlation between $OD_{600}$ and CFU/mL for both strains to ensure the use of the same number of bacteria in experiments when both species were employed together. *P. gingivalis* showed a slightly higher bacterial number than *F. nucleatum*, which may be attributed to the relative difference in shape and size of these two species: *P. gingivalis* is a bacterium of approximately 2 µm in diameter and has a bacillo-cocci shape (Zhou and Li, 2015),

whereas *F. nucleatum* has a larger cell size (5-10 µm) and an elongated bacillus shape (Bolstad, Jensen and Bakken, 1996).

Attachment of *F. nucleatum* and *P. gingivalis* to untreated and AS preconditioned Ti6Al4V was investigated using fluorescent imaging and the subsequent measurement of bacterial percentage coverage on images and bacterial colony count following removal from the surface and culture. Using the fluorescent imaging and bacterial percentage coverage technique, *F. nucleatum* showed an increase in attachment and viability over time to untreated Ti6Al4V reaching 42 % and 90 % at 120 min incubation, respectively. On surfaces preconditioned with AS however, despite presenting an increase in attachment over time, at 120 min *F. nucleatum* reached 15 % coverage, less than half its attachment to untreated Ti6Al4V, and its viability was much lower and remained constant, reaching 49 %. These data were confirmed by culture as *F. nucleatum* colony number also increased over time indifferently of the surface treatment but was lower after incubation with Ti6Al4V preconditioned with AS than with untreated surfaces. The low viability observed for *F. nucleatum* on untreated Ti6Al4V at 10 min incubation may have been caused by its sensitivity to $TiO_2$, as titania is recognised to have antimicrobial properties. (Adams et al, 2006; Fu et al., 2005; Trapalis et al., 2003). Although the mechanism of action still remains unclear, $TiO_2$ appears to disrupt the cell wall, increase cell stress and oxygen reactive species that damages intracellular structures (Kubacka *et al.*, 2014). The steady increase in viability after 10 min incubation may have been due to the build-up of bacterial layers, lowering the interaction between the bacteria and the oxide layer. The full mechanism of action of $TiO_2$ antimicrobial activity is not fully elucidated, however studies showed that the antimicrobial activity is contact-dependant, with an oxidative attack of the bacterial membrane and DNA (Foster et al., 2011; Gogniat & Dukan, 2007; Kiwi & Nadtochenko, 2005). Kubacka and co-workers (2014) investigated *P. aeruginosa* response to $TiO_2$ antimicrobial activity and observed numerous defence responses, such as an activation of DNA repair mechanisms and a stimulation of anti-oxidant production, that appeared to be triggered when *P. aeruginosa* was in contact with $TiO_2$. This antimicrobial activity is enhanced with exposure to UV. It can also be hypothesized that $TiO_2$ has an antimicrobial activity against anaerobes due to the presence of oxygen. The use of confocal microscopy and focus stacking could help assessing this hypothesis by measuring the build-up of *F. nucleatum* layers from 10 min to 120 min incubation.

The analysis of the Ti6Al4V surfaces after bacterial removal and culture showed an increase of bacterial coverage with increasing incubation time on untreated and AS

preconditioned Ti6Al4V. This outcome suggests that the vortexing process did not remove all bacteria from the discs, and consequently underestimated *F. nucleatum* attachment. This reduction in removal treatment efficacy may also indicate a strengthening of *F. nucleatum* bond to the Ti6Al4V surface, which could show the shift between reversible, electrochemical and irreversible, protein-driven attachment. Further work needs to be performed to assess bacterial strength of attachment. This could be undertaken with AFM: the tip of the AFM cantilever, coated with bacteria, can measure the force-distance strength of interaction with the surface through a series of approach-and-retract cycles (Dammer et al., 1995; Dufrene, 2014; Fang et al., 2000). Furthermore, despite a reduction in *F. nucleatum* attachment on preconditioned Ti6Al4V, bacterial coverage measured by fluorescence microscopy after vortexing was the same as with untreated Ti6Al4V after vortexing (8% and 9% coverage, respectively after vortexing). This may imply that *F. nucleatum* binding remained as strong at 120 min incubation, despite modifications in environmental conditions.

The percentage coverage of *P. gingivalis* remained constant on untreated Ti6Al4V, however a significant increase in attachment was observed when *P. gingivalis* was incubated in the presence of the preconditioned surfaces. The greatest differences were observed at 10 min and 30 min incubation and were followed by a reduction in *P. gingivalis* colony number at 60 min and 120 min that remained higher than on untreated surfaces. The preconditioning did not affect *P. gingivalis* viability, which stayed higher than *F. nucleatum* on both Ti6Al4V surfaces. Culture showed a high viability and attachment to both surfaces as well, confirming the imaging results. The analysis of the disc surfaces after vortexing and culture showed a low percentage coverage of *P. gingivalis* remaining on the untreated surfaces. The culture data can consequently be considered reliable. A surprisingly high percentage of *P. gingivalis* however remained on the preconditioned surfaces after vortexing, at 60 min and 120 min incubation especially. This corresponded to the reduction in colony number observed at 60 min and 120 min. This outcome may be explained by *P. gingivalis* mechanisms of attachment: this bacterium is a late coloniser and its attachment is consequently thought to occur to an already formed biofilm. Four types of structures and proteins have been found to mediate *P. gingivalis* co-aggregation: the fimbriae, the LPS O-antigen, the internalin family protein InlJ and the polysaccharidic capsule (Gerits et al., 2017a). In the presence of extracellular arginine, the fimbriae (long and short) enhance *P. gingivalis* co-aggregation with other early (*S. gordinii*, *S. oralis*) and late (*T. denticola*, *A. viscosus*) colonisers (Goulbourne & Ellen, 1991; Hashimoto et

al., 2003; Lamont et al., 1993; Maeda et al., 2004), as well as auto-aggregation (Kuboniwa *et al.*, 2009). The LPS O-antigen appears to affect the biofilm formation negatively: it is thought to be a physical hindrance to attachment (Kuboniwa *et al.*, 2009). The protein InlJ promotes *P. gingivalis* auto-aggregation (Capestany *et al.*, 2006). Finally the role of the capsule has not been fully clarified yet as it has been found to mediate negatively (Davey and Duncan, 2006) or positively (Rosen and Sela, 2006) the biofilm formation. The preconditioning with proteins may have created numerous sites favouring *P. gingivalis* attachment via a range of structures and proteins, as described above: the fimbriae, and the protein InlJ promote co- and auto-aggregation. During longer incubations, the favourable sites would become occupied, which could have led to a slower colonisation process and the apparition of a plateau. After AS preconditioning, reduced attachment and viability were observed for *F. nucleatum*, whilst *P. gingivalis* viability was unchanged and attachment increased. These changes may be due to the modifications in electrostatic charges associated with the presence of proteins and the subsequent increase in Ti6Al4V surface hydrophilicity. The membrane of *F. nucleatum* was found closer to neutrality than *P. gingivalis*. This neutrality may be the cause of *F. nucleatum* decrease in attachment and viability. The *P. gingivalis* membrane, however, was found to be more electrostatically charged, which would consequently be more attracted by other charged surfaces. Tavares and co-workers (2018) studied the adhesion of *F. nucleatum* NCTC 11326 and *P. gingivalis* ATCC 32277, single and dual species, for 24 and 48 h to saliva-coated polystyrene by crystal violet staining and scanning electron microscopy. Higher attachment of *F. nucleatum* was evident compared with *P. gingivalis*. Moreover, when incubated together, total adhesion was found higher than for single species experiments. It was hypothesised that the incubation of both species together resulted in a synergistic effect in terms of attachment. This is contrary to the results found in the current study. The same strain of *P. gingiv*alis was employed by Tavares et al and the current research, however the strain of *F. nucleatum* was different: Tavares et al used *F. nucleatum* subspecies *fusiforme*. The use of a different *F. nucleatum* subspecies, growth media and substrate can change attachment results greatly. Differences in genome are present between every subspecies that lead to different metabolisms, attachment trends, as well as virulence (Kapatral *et al.*, 2003). Interactions between strains have also been shown to differ greatly (Bachrach et al., 2005; Park et al., 2016; Xie et al., 1991).

Attachment of *F. nucleatum* and *P. gingivalis* in combination was also investigated by fluorescence microscopy and culture. Fluorescence microscopy showed that when

combined, *F. nucleatum* and *P. gingivalis* did not show a synergistic attachment. The coverage was lower than *F. nucleatum* single species, but higher than *P. gingivalis* single species. When mixed, cell viability on untreated Ti6Al4V decreased compared with single species experiments. However, AS preconditioning did not affect viability of the dual species; a trend similar to that seen with *P. gingivalis* viability. A decrease in colony counts was observed for dual species experiments compared with single species ones. Co-aggregation between these species could be the cause of the observed reduction in attachment. *F. nucleatum* has been shown to co-aggregate with numerous species, especially late colonisers, such as *P. gingivalis* (P. Kolenbrander & Andersen, 1989; Metzger et al., 2009; Park et al., 2016). During the culture experiments, no method capable of breaking bacterial aggregates were used, which could have led to the deposition of aggregates onto the agar during the plating process. As *F. nucleatum* is a faster growing bacterium than *P. gingivalis*, the colonies appearing white may have contained smaller colonies of *P. gingivalis*. The use of a MALDI-TOF mass spectrometry (Matrix Assisted Laser Desorption/Ionisation-Time Of Flight) equipment could help detect the presence of *P. gingivalis* in the white-*F. nucleatum* like colonies observed from dual species experiments. To identify microbial species, the mass spectrum of the unknown species is compared to spectra known within a mass range of 2-20 kDa. This mass range is used to target predominantly ribosomal peptides, the most abundant proteins in a microorganism. The 2-20 kDa spectra are very specific and can allow identification to the strain (Singhal et al., 2015).

Microbial attachment to surfaces has mostly been studied using staphylococcal, streptococcal species, and *C. albicans* (Bürgers et al., 2010; Chandra et al., 2008; Corbin et al., 2011; Dorkhan et al., 2012; Xiao et al., 2012). Commercially pure Ti has been studied more often than Ti6Al4V alloy and the majority of studies use bacterial cell counts, fluorescence microscopy or scanning electron microscopy to measure attachment (Del Curto *et al.*, 2005; Hu *et al.*, 2010; Truong *et al.*, 2010; Lorenzetti *et al.*, 2015). No previous studies investigating *F. nucleatum* and *P. gingivalis* attachment to laser melted Ti6Al4V were found. Xie and co-workers (1991) studied attachment of *F. nucleatum* ATCC 49256 to hydroxyapatite (HA). Untreated HA and HA preconditioned with various proteins, including proline-rich proteins and statherin, and stimulated human saliva was used. Preconditioned and untreated HA beads were incubated in suspensions of radiolabelled *F. nucleatum* in PBS at a concentration of $5x10^7$ CFU/mL for 1 h. Saliva and statherin increased *F. nucleatum* attachment to HA compared to untreated HA. However, proline-rich proteins did not increase

*F. nucleatum* attachment. An increase in attachment was observed with increase in statherin concentration, whilst *F. nucleatum* attachment plateaued despite the increase in proline-rich protein concentration.

To ensure that AS did not influence bacterial viability, growth was monitored in FAB supplemented with or without AS. Neither the growth of *F. nucleatum* or *P. gingivalis* was affected by the presence of AS in the medium. The effect of AS on *F. nucleatum* viability and attachment was therefore not due to hypothesised antimicrobial properties of AS. Both *F. nucleatum* and *P. gingivalis* membranes presented a negative zeta potential. An increase in negative charge on the Ti6Al4V surface may consequently have had a repulsive effect on *F. nucleatum* membrane, whereas *P. gingivalis* attachment may not have been hindered due to the presence of fimbriae. *F. nucleatum* formed patterns of attachment to laser melted discs at 120 min incubation. It was hypothesised that *F. nucleatum* attached following the grain boundaries within the discs formed during laser melting. After etching with hydrofluoric acid, grain boundaries were imaged, showing the same branching patterns. The mean roughness ($R_a$) of the polished surfaces was 0.059 µm (± 0.003), which is below the threshold found to have an impact on microbial attachment in patients (Bollen *et al.*, 1996). However, the surface topography may follow the grain boundaries at a nanometre level, below the limit of detection of the profilometer used (no limit of detection reported, resolution 0.001 µm). No study was found to support this hypothesis, and further investigation using an AFM is needed to understand the cause of this phenomenon. A difference in chemical composition on the grain boundary could also be possible: the surfaces are composed of α + β phases (Gammon *et al.*, 2004). *F. nucleatum* appeared to exploit some slight modifications present at the surface and adhered primarily within the contours formed by the grain boundaries.

## 3.5 Conclusion

Plaque formation is a sequential process: ‘early colonisers’ such as certain streptococcal species adhere to the acquired pellicle on enamel surfaces and build a favourable environment for the further attachment of ‘late colonisers’. *F. nucleatum* is key in the biofilm maturation as it allows late colonisers to bind to early colonisers. *P. gingivalis*, is a Gram-negative late colonising bacterium and plays a crucial role in inducing host inflammatory response leading to peri-implantitis. Both species are

thought to need the help of early colonisers to attach. Here, attachment and viability of *F. nucleatum* ATCC 49256 and *P. gingivalis* NCTC 11834 were investigated. First, both species were found to be able to attach directly to laser melted Ti6Al4V without the aid of early colonisers. *F. nucleatum* presented a higher attachment to untreated Ti6Al4V surfaces than *P. gingivalis*. Preconditioning the Ti6Al4V surfaces with AS modified the attachment trend significantly: *F. nucleatum* attachment decreased whilst *P. gingivalis* attachment increased. The preconditioning appeared to have had an influence on *P. gingivalis* binding strength as a significant increase in bacteria was found after vortexing. Despite a significant decrease in attachment in the presence of preconditioned surfaces, *F. nucleatum* binding strength appeared not to have been modified, as in both conditions the same percentage coverage was detected after bacterial removal from the surfaces for culture. *P. gingivalis* viability was found to be constant and very high on untreated and preconditioned Ti6Al4V. *F. nucleatum* viability trends differed greatly depending on conditions. An increase in viability was observed over time on untreated surfaces, whilst a reduced but constant viability was shown on preconditioned Ti6Al4V.

Of clinical importance, the ability of late colonisers to attach directly to Ti6Al4V surface may have a significant impact on the composition of the dental abutment-associated plaque. These unexpected *in vitro* findings need further investigation to assess whether such a difference in colonisation sequence can happen in patients or not, as this would lead to further understanding of microbiota-host interaction in patients with dental implants and peri-implantitis pathogenesis.

# Chapter 4. Antimicrobial coating development

## 4.1 Introduction

Peri-implantitis is a pathology characterised by the inflammation of the peri-implant mucosa and loss of supporting bone. The aetiology of the disease is not completely understood yet, however, plaque formation is always observed in the gingival sulcus (Schwarz *et al.*, 2018a). A shift in bacterial population occurs and Gram negative anaerobes, such as *P. gingivalis* and *F. nucleatum* are found in a greater proportion in diseased sites compared with healthy sites (Persson and Renvert, 2014). The treatment of peri-implantitis is long (Wang *et al.*, 2017) and has a severe impact on patients' quality of life with high levels of anxiety reported, associated with limitations in daily activities, social life and intimate relationships (Insua *et al.*, 2017). Treatment of peri-implantitis is also costly: in 2015 a study in the US showed that implant placement costs on average $5800, whilst peri-implantitis treatment costs on average $2200, a third of the initial procedure (Froum and Summerford, 2015). Consequently, novel solutions to prevent the development of this pathology are required.

An antimicrobial that has proved its efficacy in reducing the microbial burden in the context of peri-implantitis (Stewart *et al.*, 2018) and peri-implant mucositis (Ribeiro *et al.*, 2018; Peres Pimentel *et al.*, 2019) is triclosan. Triclosan is extensively used in consumer products, including toothpastes, due to its broad spectrum of antimicrobial and antifungal activity (Zhou *et al.*, 2017). It has a concentration-dependent mode of action: at low concentrations it is bacteriostatic by inhibition of fatty acid production at the enoyl-acyl carrier protein reductase step (McMurry et al., 1998; Heath *et al.*, 1999), while at high concentrations it is bactericidal by incorporation into the bacterial membrane followed by destabilisation of the membrane structure and leakage of intracellular components (Villalaín *et al.*, 2001; Russell, 2004). A recent Cochrane systematic review showed that triclosan reduced plaque formation by 22 %, gingivitis by 22 % (n = 2743 participants) and the proportion of bleeding sites by 48 % (n = 1998 participants) when administered in combination with a copolymer to decrease drug

dilution by mouth rinsing or saliva (Riley *et al.*, 2013). Triclosan appears to be efficacious against peri-implantitis associated bacteria, such as *P. gingivalis* (Farsi and Tanner, 2016) and has also been successfully encapsulated in liposomes (Kim *et al.*, 2002; Catuogno and Jones, 2003; El-Zawawy *et al.*, 2015b). Jones and colleagues (1997) found that liposomal triclosan inhibited bacterial biofilm formation with greater efficacy when compared to free triclosan. This outcome is thought to be related to a deeper diffusion of liposomal triclosan within the biofilm.

As stated in Chapter 1, Section 1.6, liposomes are spherical, artificially-synthesised vesicles composed of an aqueous core delimited by one or more lipid bilayer(s) (van Rooijen, 1998; Patil and Jadhav, 2014). Liposomes are multifunctional and versatile platforms for drug delivery (Figure 4.1) due to:

- their structural similarities to cell membranes,
- their amphiphilic properties, that allow the encapsulation of both hydrophilic and hydrophobic molecules (G Gregoriadis and Florence, 1993),
- the ease of manipulation of the bilayer composition, leading to the controlled release of the encapsulated molecule or the development of triggered release (Allen and Cullis, 2013),
- the ability to functionalise the liposome surface, leading to properties such as stealth in the bloodstream and targeting specific receptors (Immordino et al., 2006).

Liposomes are predominantly composed of phospholipids and cholesterol making them biodegradable and biocompatible (G Gregoriadis and Florence, 1993). They can be prepared according to numerous different methods; the most common being the thin-film hydration (Laouini *et al.*, 2012). Liposomes are then physico-chemically characterised. The main characterisation methods performed on liposomes are size, zeta potential, encapsulation efficiency, concentration of phospholipids, drug release and stability over time (Laouini *et al.*, 2012). Liposomes are used to deliver a wide range of medications, such as the antifungal amphotericin B (McMillan et al., 2011), the antitumoral anthracyclines doxorubicin and daunorubicin, as well as the inactivated hepatitis A virus and inactivated hemagglutinin of influenza virus strains A and B as vaccines (Bozzuto and Molinari, 2015).

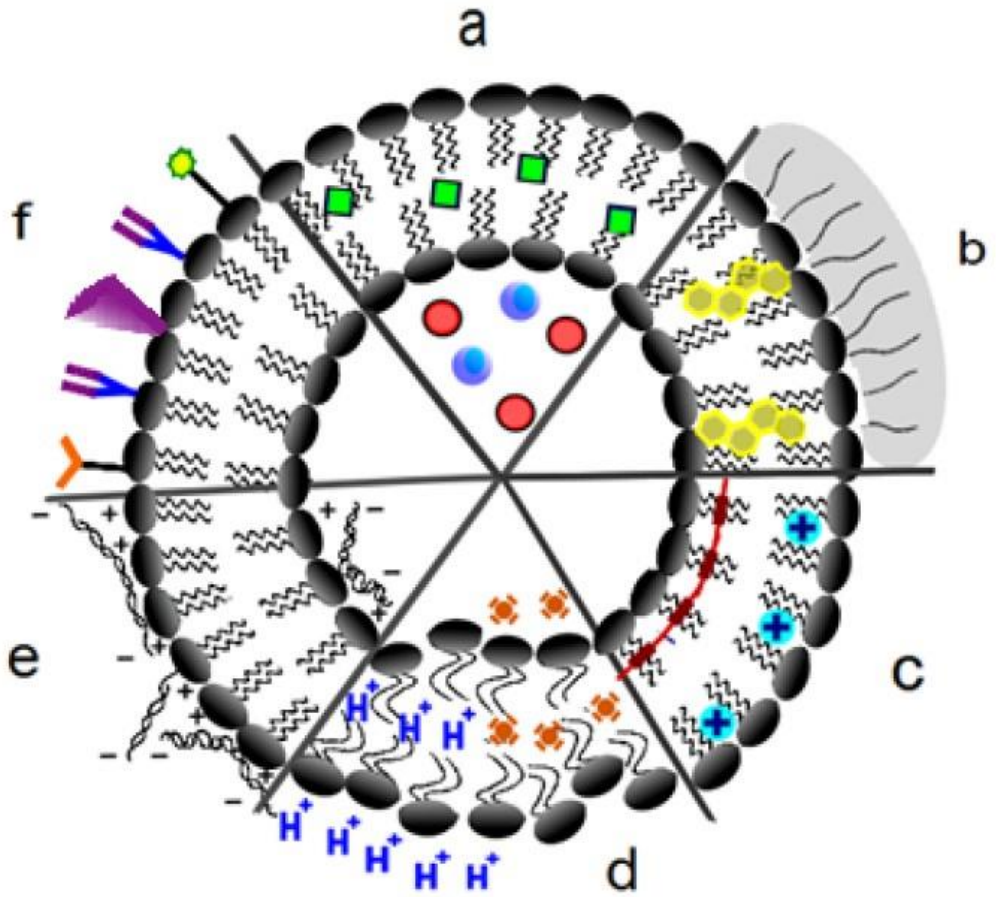


**Figure 4.1. Liposomes as multifunctional and versatile platforms. Hydrophilic (a, red) and lipophilic (a, green) molecules, as well as gas bubbles (a, blue) can be encapsulated in liposomes. The bilayer can be stabilised by the incorporation of cholesterol (b, yellow), or multivalent cations (c, blue), or by polymerisation (c, red). The membrane surface can be functionalised to increase the circulation time in the bloodstream by grafting hydrophilic polymers (b, grey) or negatively charged DNA (e). Functionalisation can also allow the specific targeting of receptors by grafting targeting molecules (f) or the development of a release system by membrane destabilisation in acidic medium (d, blue $H^+$) or by increase in temperature (d, orange) (Madni et al., 2014).**

Numerous methods and materials are used to develop efficacious antimicrobial coatings on Ti-based implants. Antimicrobial/antibiotic-loaded hydroxyapatite has been considerably investigated in orthopaedic and dental implants research due to the osseointegration properties of hydroxyapatite (Mohseni et al., 2014). However, it was reported that the release profile of compounds from hydroxyapatite presented a burst release pattern (Stigter *et al.*, 2004; Boonsongrit *et al.*, 2008). In the context of peri-implantitis the release of an initial large bolus of active substance is not advantageous. After the implant surroundings are healed, dental appointments are planned every 3 to 12 months (Gay *et al.*, 2016). Furthermore, peri-implantitis usually

appears several years after implantation (Schwarz *et al.*, 2018a). To manage the bacterial burden in an efficient manner, a sustainable release over several months to a year would consequently be of more interest than a burst release after placement of the abutment. Kang and colleagues (2012) and Karacan et al (2017) developed a multilayer coating that showed interesting long-term release trends. Kang used the self-assembling monolayer technique to coat Ti with several layers of cefalotin-associated apatite. A burst release could be observed the first day, however not hindering an increasing release over 60 days. Karacan prepared poly-lactic acid/hydroxyapatite/gentamycin composites prior to dipping the Ti samples into the composite solution. Four release phases were observed that, according to Karacan's hypothesis, corresponded to:

1. the release of the gentamycin at the surface of the coating, lasting one week,
2. the dissolution of the poly-lactic acid matrix and the release of the gentamycin embedded within this matrix, lasting two weeks,
3. the breakdown of the hydroxyapatite particles, lasting 2 weeks,
4. the final dissolution of all remaining particles and matrix, lasting two weeks.

A plateau was then observed from week 7. Multilayer and multi-composite coatings appear to be a beneficial technique to obtain a prolonged release.

Finally, metallic-based antimicrobial coatings, such as silver or copper coatings, are thoroughly investigated to try to overcome the bacterial resistance to antibiotics (Mattos Corrêa *et al.*, 2015; Norambuena *et al.*, 2017).

Multiple factors have to be considered when developing an antimicrobial coating. First, a broad-spectrum antimicrobial, such as chlorhexidine or triclosan, allows the targeting of a wider variety of bacterial species (Regos *et al.*, 1979). The covalent attachment of an antimicrobial directly to the surface may be effective against the first bacterial colonisers, however, the formation of salivary pellicle and the successive bacterial adhesion might become a hindrance to the antimicrobial efficacy (Rosan and Lamont, 2000; Lindh *et al.*, 2014). Therefore, the encapsulation of an antimicrobial into nano- or micro-particles that are weakly attached to the surface may be a valuable alternative. The delivery system may release the compound near the surface, as well as detach from the surface and release the active agent within the gingival sulcus.

### 4.1.1 Aims and objectives

This chapter presents for the first time the development of a triclosan-loaded liposomal coating onto laser melted Ti6Al4V surfaces and the characterisation of its physico-chemical and antimicrobial properties.

## 4.2 Materials and methods

### 4.2.1 Materials and bacterial strains

ODPA, anhydrous tetrahydrofuran (THF), L-α-phosphatidylcholine (extracted from egg yolk, Type XVI-E), and cholesterol were purchased from Sigma Aldrich-Merck (Haverhill, UK). Chloroform, potassium carbonate ($K_2CO_3$) and ethanol were purchased from ThermoFisher Scientific (Eugene, Oregon, USA).
*F. nucleatum* subsp. *vincentii* ATCC® 49256™ (originally isolated from a human periodontal pocket; American Type Culture Collection, 2019) and *P. gingivalis* NCTC 11834 (originally isolated from a human gingival sulcus; National Collection of Type Cultures, 2019) were used in these studies. FAA and FAB were obtained from Lab M (Lancashire, UK). Defibrinated Horse blood was obtained from TCS Biosciences (Buckingham, UK). The LIVE/DEAD™ BacLight™ Bacterial Viability Kit stain was purchased from ThermoFisher Scientific (Eugene, Oregon, USA). Glass beads (500-750 µm) were obtained from Acros Organics (Thermo Fisher Scientific, Geel, Belgium).

### 4.2.2 Culture

All bacteria were initially cultured under anaerobic conditions (anaerobic gas mixture: 10 % $CO_2$, 10 % $H_2$, 80 % $N_2$) on FAA supplemented with 5 % (v/v) defibrinated horse blood, at 37 ºC for 72 h to 96 h. A loop of bacterial colonies was transferred to 5 mL pre-reduced FAB at 37 ºC for 15 h without agitation. Broth cultures were then diluted

in 20 mL of pre-reduced FAB to an $OD_{600}$ of 0.08 and further diluted to an optimal starting concentration.

### 4.2.3 Attachment of ODPA to Ti6Al4V

The attachment of ODPA to Ti6Al4V involved three main steps (Hanson *et al.*, 2003; Ayre *et al.*, 2016). ODPA was dissolved in THF at concentrations of 0.5 mM, 1 mM and 5 mM. The Ti6Al4V discs were immersed in the ODPA-THF solution from 1 h to 24 h (five discs in 10 mL) and air-dried prior to baking at 180 °C for 1 h to 5 h to convert the phosphonic acid into phosphonate and bind to the $TiO_2$ via a covalent bond (Gouzman *et al.*, 2006). Finally, the rinsing step involved the immersion of the discs in a solution containing 5 mL 1.5 M $K_2CO_3$ in 10 mL ethanol for 20 min, followed by three washes in water.
Preliminary experiments were performed before a design of experiment (DoE) was implemented. The details of the concentrations, incubation and baking times will be presented in the corresponding sections below.

#### 4.2.3.1 Preliminary experiments

During the preliminary experiments the incubation time of the surfaces in ODPA-THF solution was tested. The ODPA solution was fixed at concentration 1 mM (Ayre *et al.*, 2016). The discs were incubated for 1 h or 24 h (five discs in 10 mL), air-dried, and baked for 1 h at 180 °C. They were then immersed in the rinsing solution, composed of 5 mL 1.5 M $K_2CO_3$ in 10 mL ethanol for 20 min, followed by three washes in water, as stated in 4.2.3.

FTIR

Functional groups were detected by FTIR-ATR. Spectra were recorded on a Nicolet 380® Thermo Fisher Scientific Inc. (Madison, WI USA) using EZOMNIC 7.4 software (Thermo Fisher Scientific Inc., Madison, WI USA). The scanning range used was 500 $cm^{-1}$ – 4000 $cm^{-1}$, averaged over 36 scans with a resolution of 4 $cm^{-1}$. Three experiments were performed.

XPS

The phosphorus present at the disc surface was quantified by XPS using an AXIS Nova XPS, Kratos Analytical (Manchester, UK), coupled to CasaXPS software, Casa Software LTD (Devon, UK). The atomic percentages were measured using a monochromatic AlKα source with an X-ray energy of 1486.6 eV and a voltage, current and power of 15 kV, 15 mA, and 225 W, respectively. The pass energy was fixed at 20 eV with a pressure below $7.5 \times 10^{-9}$ mbar. The analysis area comprised slots of 700 x 300 µm. Ten sweeps were performed per scan, each sweep lasting 60 seconds. Three runs were performed on each test sample. One test sample was used per condition.

#### 4.2.3.2 Design of experiments and characterisation by XPS

The ODPA solution was prepared in THF at concentrations of 0.5 mM, 1 mM and 5 mM. The discs were then incubated in ODPA-THF for 1 h, 1 h 30 min, 3 h, 4 h 30 min or 5 h (five discs in 10 mL). The samples were air-dried prior to baking for 1 h, 1 h 30 min, 3 h, 4 h 30min or 5 h at 180 °C to convert the phosphonic acid in phosphonate and bind to the $TiO_2$ via a covalent bond. Finally, the discs were immersed in the rinsing solution containing 5 mL 1.5 M $K_2CO_3$ in 10 mL ethanol for 20 min, followed by three washes in water, as stated in 4.2.3. Experiments performed for the DoE and analysed by XPS were performed one time, with each surface analysed three times.

The DoE was undertaken using NemrodW software (NemrodW, Marseille, France) in order to investigate the effect of the following factors involved in the different steps of the coating process: concentration of ODPA, incubation time in ODPA-THF solution, and baking time.

The ultimate goal was to maximise the quantity of ODPA attached to the surface of the discs.

The three factors were renamed as follow:

- Concentration of ODPA = factor A
- Incubation time = factor B
- Baking time = factor C.

A field of investigation was chosen, delimited by two levels for each factor: a low and a high level represented by -1 and +1 (Table 4.1).

**Table 4.1. Field of investigation delimited by low and high levels for each factor.**

| | Low (-1) | High (+1) |
|---|---|---|
| **ODPA concentration (A)** | 0.5 mM | 5 mM |
| **Incubation time (B)** | 1 h | 5 h |
| **Baking time (C)** | 1 h | 5 h |

To run a full factorial systematic experiment including all combinations ($2^3$), 8 experiments were needed. A matrix of experiments was designed to reflect this (Table 4.2).

**Table 4.2. Matrix of experiments.**

| Run | A | B | C | AB | AC | BC | ABC | Y |
|---|---|---|---|---|---|---|---|---|
| **1** | -1 | -1 | -1 | 1 | 1 | 1 | -1 | |
| **2** | 1 | -1 | -1 | -1 | -1 | 1 | 1 | |
| **3** | -1 | 1 | -1 | -1 | 1 | -1 | 1 | |
| **4** | 1 | 1 | -1 | 1 | -1 | -1 | -1 | |
| **5** | -1 | -1 | 1 | 1 | -1 | -1 | 1 | |
| **6** | 1 | -1 | 1 | -1 | 1 | -1 | -1 | |
| **7** | -1 | 1 | 1 | -1 | -1 | 1 | -1 | |
| **8** | 1 | 1 | 1 | 1 | 1 | 1 | 1 | |

With:

- AB: the interaction between the factors A and B, calculated by multiplying A and B
- AC: the interaction between the factors A and C, calculated by multiplying A and C
- BC: the interaction between the factors B and C, calculated by multiplying B and C
- ABC: the interaction between the factors A, B and C, calculated by multiplying A, B and C
- Y: the outcome, found experimentally. In this experiment, the outcome was the atomic percentage of phosphorus on the Ti6Al4V surfaces.

The effect of each factor on the outcome was calculated according to Equation 1 below.

**Equation 1**

$$\alpha = \frac{\Sigma(Y\ at\ A = +1)}{Number\ of\ experiments\ at\ A = +1} - \frac{\Sigma(Y\ at\ A = -1)}{Number\ of\ experiments\ at\ A = -1}$$

In this experiment, more than two levels were investigated: three concentrations, and five incubation and baking times were tested. Consequently, the resulting matrix of experiments should have been composed of seventy-five experiments if a full factorial

was used. Here a fractional factorial design was used, leading to a factorial composed of sixteen experiments (Table 4.3).

**Table 4.3. Matrix of experiments containing more than two levels per factor.**

| Experimentation number | Concentration of ODPA (mM) | Incubation time | Baking time | Mean atomic % of phosphorus |
|---|---|---|---|---|
| 1 | 0.5 | 1 h 30 min | 1 h 30 min | |
| 2 | 0.5 | 4 h 30 min | 1 h 30 min | |
| 3 | 0.5 | 1 h 30 min | 4 h 30 min | |
| 4 | 0.5 | 4 h 30 min | 4 h 30 min | |
| 5 | 1 | 1 h | 3 h | |
| 6 | 1 | 5 h | 3 h | |
| 7 | 1 | 3 h | 1 h | |
| 8 | 1 | 3 h | 5 h | |
| 9 | 1 | 3 h | 3 h | |
| 10 | 5 | 1 h 30 min | 1 h 30 min | |
| 11 | 5 | 4 h 30 min | 1 h 30 min | |
| 12 | 5 | 1 h 30 min | 4 h 30 min | |
| 13 | 5 | 4 h 30 min | 4 h 30 min | |
| 14 | 5 | 1 h | 3 h | |
| 15 | 5 | 3 h | 1 h | |
| 16 | 5 | 3 h | 3 h | |

As experiments were planned to be performed one time (n = 1), one experiment was selected to be repeated five times in order to obtain a variability inter-experiment. Experiment number 7 was repeated on different days from a freshly prepared ODPA solution for each repeat. The exact same protocol was used by the same operator: clean discs were immersed in 1 mM ODPA-THF solution for 3 h, air-dried, then baked for 1 h at 180 °C, and rinsed in 5 mL 1.5 M $K_2CO_3$ in 10 mL ethanol for 20 min, followed by three washes in water.

#### 4.2.3.3 Contact angle measurement

The surfaces were incubated in 5 mM ODPA for 1 h, baked for 1 h at 180 °C and rinsed in 5 mL 1.5 M $K_2CO_3$ in 10 mL ethanol for 20 min. The discs were then dried, and their contact angle was measured using a Dynamic Contact Angle analyser

(DCA-312, Thermo Cahn Instruments, Madison, USA) with WinDCA 32 software (Thermo Cahn Instruments, Madison, USA). Samples were dipped 7 mm, corresponding to half the disc diameter, in water at a speed of 264 µm/s. Measurements were taken at 21 °C in triplicate.

### 4.2.4 Preparation and characterisation of liposomes

#### 4.2.4.1 Preparation of liposomes

Liposomes were prepared using phosphatidylcholine extracted from egg yolk and cholesterol. Both lipids were weighed at a ratio of 7:1 w/w phosphatidylcholine:cholesterol. 0 µg/mL or 300 µg/mL triclosan was added, mixed and dissolved with the lipids in chloroform in a round-bottom flask. The chloroform was then removed using a rotary evaporator (Büchi Rotavap R300, Büchi Labortechnik AG, Flawil, Switzerland) at 50 °C, leading to the formation of a thin lipid film in the flask. Sterile, distilled water was added to obtain a concentration of 3 mg/mL lipids prior to vortexing the flask, which allowed the formation of liposomes. The liposomes were stored at +4 °C prior to use.

#### 4.2.4.2 Size and polydispersity

The hydrodynamic diameter and polydispersity index of the liposomes were measured using dynamic light-scattering in a Zetasizer Nano ZS (Malvern, Malvern, UK). Liposomes were diluted approximately 1:9 in water and placed in a 2 mL quartz cuvette. Three independent measurements were recorded in triplicate.

#### 4.2.4.3 Zeta potential

The zeta potential of the liposomal formulations was measured using a Zetasizer Nano ZS (Malvern, Malvern, UK). Liposomes were diluted approximately 1:9 in water

and placed in a 1 mL folded capillary zeta cell. Three independent measurements were recorded in triplicate. Twelve runs per replicate were performed.

#### 4.2.4.4 Heat stability of liposomes

Liposome stability in heat was assessed to ensure their capacity to withstand incorporation in molten agar during the Minimal Inhibitory Concentration (MIC) testing (Section 4.2.4.8). Liposomes were prepared as stated in 4.2.4.1 and incubated in a water bath at 80 °C for 10 min. The liposomes were allowed to cool to room temperature before measurement of their size and polydispersity was performed. Three independent measurements were performed.

#### 4.2.4.5 Phospholipid concentration

The phospholipid concentration of liposomal suspensions was measured to identify a loss of phospholipids during the preparation process. A phospholipid assay kit (Sigma Aldrich, Gillingham, UK) was used to determine the phospholipid concentration once the liposomes were prepared. In this assay phosphatidylcholine was enzymatically hydrolysed into choline. The presence of choline oxidase and a $H_2O_2$-specific dye triggered a change in colour proportional to the concentration of choline.

A standard solution of phosphatidylcholine was prepared and diluted in Triton™ X-100 (0.5 % v/v) to obtain concentrations of 0 µmol/L, 60 µmol/L, 100 µmol/L and 200 µmol/L as stated in the assay protocol. The test liposome suspensions were diluted in 1:7 0.5 % (v/v) Triton™ X-100. 20 µL of each standard and sample were placed into a 96 well plate and mixed with 80 µL of the assay reaction mix, prepared according to the manufacturer's instructions (Sigma-Aldrich, 2018). The plate was protected from light and incubated for 35 min prior to measuring the absorbance at 570 nm using a plate reader (FLUOstar Omega, BMG Labtech, Ortenberg, Germany). Sample concentrations were calculated from the absorbance detected using the standard curve. Three independent repeats were performed.

#### 4.2.4.6 Triclosan concentration

Triclosan concentration in the liposomes was measured using an ion chromatography system (ICS 3000 Dionex™, Thermofisher, Waltham, Massachusetts, USA) and a column Phase GEMINI NX 5 µm C18 110 Å (Phenomenex, Torrance, California, USA). Data collection and subsequent analysis was performed using the software Chromeleon™ 7.2 (Dionex™, Thermofisher, Waltham, Massachusetts, USA). 10 µL of the test solution was injected and analysed by isocratic elution of the mobile phase composed of acetonitrile:water 30:70 at a flow rate of 1 mL/min. The analytical wavelength was set at 285 nm (Everett, 2017). Standard solutions of triclosan were prepared in methanol from 0 µg/mL to 100 µg/mL. The area under the curve (AUC) measured from the detected peak ($y$) was plotted in a graph against the known concentration ($x$). The equation of the produced calibration curve was used to calculate the concentration of the samples from the AUC. Liposomes were diluted in 1:4 methanol (v/v) in order to break the lipid bilayer, release and measure the quantity of free triclosan. Three independent repeats were performed.

#### 4.2.4.7 Intrinsic activity of triclosan against *Fusobacterium nucleatum* and *Porphyromonas gingivalis*

Previous research showed a higher antimicrobial activity against *Enterococcus faecalis* and *Streptococcus anginosus* with liposomes containing 300 µg/mL and 500 µg/mL triclosan compared with liposomes containing 100 µg/mL triclosan (Everett, 2017). The highest antimicrobial activity demonstrated was from triclosan liposomes containing 300 µm/mL triclosan and 3 mg/mL lipids (phosphatidylcholine and cholesterol). To assess the intrinsic activity of triclosan and triclosan liposomes against *F. nucleatum* ATCC® 49256™ (American Type Culture Collection, 2019) and *P. gingivalis* NCTC 11834 (National Collection of Type Cultures, 2019) solutions containing triclosan and triclosan liposomes were prepared (Table 4.4). PBS was used for the experiments involving the culture of bacteria, whilst 0.9 % NaCl solution (w/v) was employed when bacteria were imaged using the LIVE/DEAD™ BacLight™ kit. Three independent repeats were performed in triplicate.

**Table 4.4. Solutions prepared to investigate the intrinsic activity of triclosan against *F. nucleatum* and *P. gingivalis*.**

| Solutions prepared for culture | Solutions prepared for imaging |
|---|---|
| Triclosan (300 µg/mL) liposomes (3 mg/mL phosphatidylcholine and cholesterol) in PBS | Triclosan (300 µg/mL) liposomes (3 mg/mL phosphatidylcholine and cholesterol) in 0.9 % NaCl solution (w/v) |
| Triclosan (300 µg/mL) in 1 % isopropanol (IPA)/PBS (v/v) | Triclosan (300 µg/mL) in 1 % IPA (v/v)/0.9 % NaCl solution (w/v) |
| Blank liposomes (3 mg/mL phosphatidylcholine and cholesterol) in PBS | Blank liposomes (3 mg/mL phosphatidylcholine and cholesterol) in 0.9 % NaCl solution (w/v) |
| 1 % IPA in PBS (v/v) | 1 % IPA (v/v) in 0.9 % NaCl solution (w/v) |
| PBS | 0.9 % NaCl solution (w/v) |

PBS: phosphate buffered saline; IPA: isopropanol

Bacterial suspensions were cultured in FAB to mid-log phase and $OD_{600}$ set at 0.30 and 0.65 for *F. nucleatum* and *P. gingivalis*, respectively. The suspensions were then centrifuged at 13,000 *g* for 5 min using a Heraeus Pico 17 (ThermoFisher Scientific, Waltham, Massachusetts, USA). The supernatant was discarded, the pellet resuspended in 1 mL of the different solutions and placed in the anaerobic cabinet. After 1 h incubation, the resulting suspensions were cultured or imaged. Imaging offered complementary information on the triclosan bacteriostatic or bactericidal activity against *F. nucleatum* and *P. gingivalis* at this concentration. Suspensions that were cultured were serially diluted and plated onto FAA using a spiral plater (Whitley Automatic Spiral Plater, Don Whitley Scientific, West Yorkshire, UK). *F. nucleatum* and *P. gingivalis* were then cultured anaerobically at 37 ºC for 3 and 7 days, respectively, prior to CFU/mL enumeration. Suspensions that were imaged were deposited on a microscope slide, stained using the LIVE/DEAD™ BacLight™ kit and imaged using a fluorescent microscope (Provis AX-70, Olympus, Tokyo, Japan) at magnifications x20 and x60.

#### 4.2.4.8 Minimum inhibitory concentrations

FAA was used to determine MICs during this project as it was found to be more suitable than the recommended Brucella agar (Clinical and Laboratory Standards

Institute, 2012) for *F. nucleatum (*Brazier *et al.,* 1990*)* The following stocks of antimicrobial solutions were prepared:

- Triclosan (630 µg/mL) liposomes (6.3 mg/mL) in sterile water
- Triclosan (630 µg/mL) in 2 % IPA/sterile water (v/v)
- Blank liposomes (6.3 mg/mL lipids) in sterile water
- 2 % IPA in sterile water (v/v).

A double strength stock of FAA was prepared. The stock antimicrobial and stock FAA were mixed at a 1:1 volumetric ratio. 5 % horse blood (v/v) was added to the resulting molten agar. The obtained concentration, corresponding to 300 µg/mL triclosan, 3 mg/mL lipids and 1 % IPA, was the highest concentration tested. The following antimicrobial agar plates were then prepared by 1:2, 1:4, and 1:8 dilutions in molten agar. FAA control plates were also prepared.

Bacterial suspensions were cultured in FAB to mid-log phase and $OD_{600}$ set at 0.08, as recommended by the standard M11-A8 (Clinical and Laboratory Standards Institute, 2012). 1 µL bacterial suspension was deposited onto the test plates. The inoculated plates were placed under anaerobic conditions for 3 days and 7 days for *F. nucleatum* and *P. gingivalis*, respectively prior to analysis. Three independent repeats were performed in triplicate.

### 4.2.5 Attachment of liposomes to ODPA-coated Ti6Al4V

#### 4.2.5.1 Quantification of liposomal coverage by confocal laser scanning microscopy

In order to assess the attachment of liposomes to the ODPA-coated Ti6Al4V surfaces by CLSM, a fluorophore was incorporated into the prepared liposomes according to the manufacturer's protocol with slight modifications due to the high concentration in lipids (Molecular Probes Inc, 2011). 15 µL Vybrant™ DiO (3-octadecyl-2-[3-(3-octadecyl-2(3H)-benzoxazolylidene)-1-propenyl]-, perchlorate 34215-57-1) was added per 1 mL of liposomal suspension of concentration 3 mg/mL. The suspension was placed at 37 °C for 20 min and centrifuged at 100,000 *g* for 1 h at 4 °C. The supernatant was discarded, the pellet containing the liposomes was washed and centrifuged one more time. The resuspended liposomal suspension was left to warm up to room temperature prior to immersion with the ODPA-coated Ti6Al4V for 1 h.

This process was performed protected from light. Two conditions were investigated: the concentration of ODPA used to coat the Ti6Al4V surfaces and the incubation time of the ODPA-coated discs in liposomal suspensions. The different concentrations of ODPA were first tested: discs were incubated in 0.5 mM, 1 mM or 5 mM ODPA for 1 h, baked for 1 h at 180 °C, rinsed and incubated for 1 h in 3 mg/mL fluorescent liposomal suspension. The incubation times in liposomal suspensions were then tested: the samples were coated with ODPA at a concentration of 5 mM for 1 h, baked at 180 °C for 1 h, rinsed and incubated in 3 mg/mL fluorescent liposomal suspension for 1 h, 5 h, or 24 h. After attachment of liposomes, the surfaces were rinsed in water to detach loosely attached liposomes, and observed under a CLSM (Leica TCS SP5, Leica Microsystems, Wetzlar, Germany) using Leica Application Suite X software (Leica Microsystems, Wetzlar, Germany).

#### 4.2.5.2 Quantification of total triclosan coverage by HPLC

ODPA-coated Ti6Al4V surfaces were prepared as described in Section 4.2.3 using a concentration of 5 mM ODPA and immersed in liposomal suspension (300 µg/mL triclosan; 3 mg/mL lipids) or in free triclosan solution (300 µg/mL in 1 % IPA in water) for 1 h at room temperature. The discs were then rinsed in water to detach loosely attached liposomes prior to immersion in 100 µL methanol in order to detach the lipids from the surfaces. The samples were transferred to HPLC vials and analysed by HPLC as stated in 4.2.4.6. Untreated discs were immersed in 100 µL methanol and analysed by HPLC as a negative control.

#### 4.2.5.3 Release study

Ti6Al4V surfaces were coated with 5 mM ODPA as mentioned in Section 4.2.3, prior to incubating in liposomal suspensions. Surfaces were coated with triclosan-loaded liposomes at 300 µg/mL triclosan; 3 mg/mL lipids, or with blank liposomes at 3 mg/mL lipids as a control. Liposome-coated discs were immersed in 1 mL water for 1 h to 140 h. The entire water samples were taken at each time point and frozen at -80 °C. All samples were then lyophilised using a Scanvac CoolSafe 55-4 (Labogene ApS, Lynge, DK), resuspended in 100 µL methanol and analysed by HPLC. As mentioned

in 4.2.4.64.2.5.2, standard solutions of triclosan were also prepared and analysed by HPLC in order to produce a calibration curve for triclosan concentration calculation. Three independent repeats were performed.

### 4.2.6 Statistical analysis

Unless stated otherwise, all the experiments described above were performed three times including internal triplicates. A T-test was performed to analyse differences between liposome size and zeta potential before and after heat treatment. Linear regression analysis was performed on all calibration curves. One-way analysis of variance (ANOVA) was performed for the analysis of all other experiments. When a p value of $< 0.05$ was found, a Bonferroni multiple comparisons post-test was performed between all groups.

## 4.3 Results

### 4.3.1 Attachment of ODPA to Ti6Al4V

#### 4.3.1.1 Preliminary experiments

ODPA powder was analysed by FTIR (Table 4.5, Figure 4.2). Characteristic peaks of P-O and P=O were detected from 715 $cm^{-1}$ to 1213 $cm^{-1}$. P-O-H bands were found between 2116 $cm^{-1}$ and 2359 $cm^{-1}$. Finally, C-H vibrations were identified at 1400 $cm^{-1}$, 1471 $cm^{-1}$, 2848 $cm^{-1}$ and 2914 $cm^{-1}$.

**Table 4.5. Assignments of FTIR peaks for ODPA powder.**

| Wavenumber ($cm^{-1}$) | Assignment | Reference |
|---|---|---|
| 715 | P-O, P=O | Luschtinetz et al., 2007 |
| 781 | P-O, P=O | Luschtinetz et al., 2007 |
| 931 | P-O, P=O | Luschtinetz et al., 2007 |
| 1005 | P-O, P=O | Kim et al., 2007 |
| 1074 | P-O, P=O | Lim et al., 2010 |
| 1213 | P=O | Kim et al., 2007 |
| 1400 | C-H deformation | Lafont, 2009 |
| 1471 | C-H deformation | Lafont, 2009 |
| 2116 | P-O-H | Yah et al., 2012 |
| 2341 | P-O-H | Yah et al., 2012 |
| 2359 | P-O-H | Yah et al., 2012 |
| 2848 | C-H stretching | Kim et al., 2007, Lim et al., 2010, Lafont, 2009 |
| 2914 | C-H stretching | Kim et al., 2007, Lim et al., 2010, Lafont, 2009 |

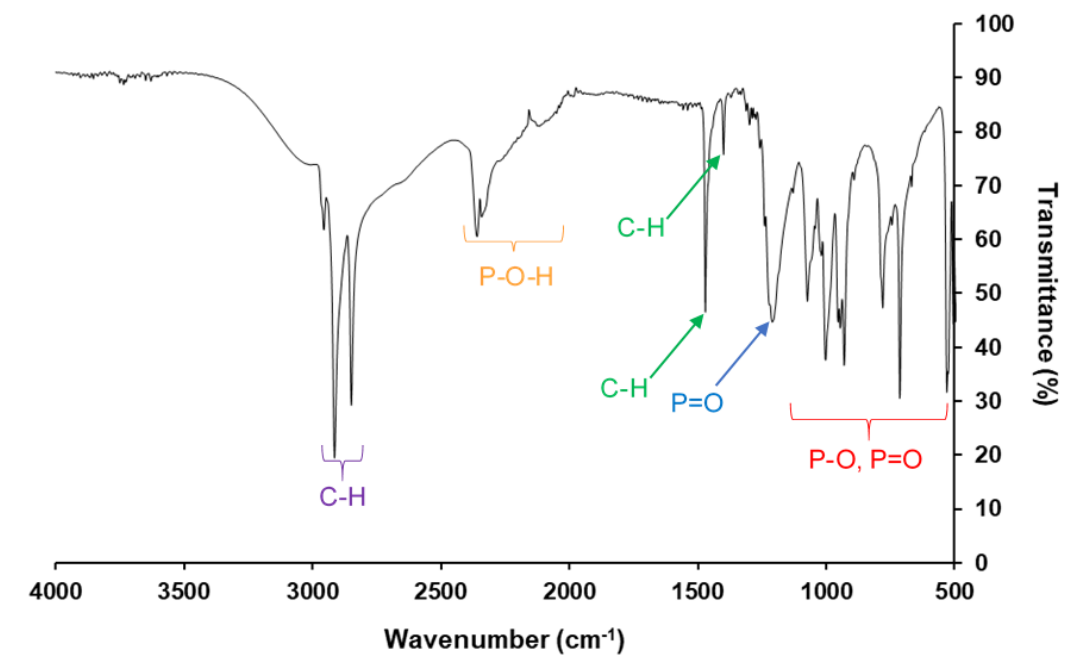


**Figure 4.2. Representative FTIR spectrum of ODPA powder.**

Ti6Al4V surfaces were coated with ODPA in different conditions and analysed by FTIR (n = 1). In a first experiment, surfaces investigated were immersed for 1 h and 24 h in 1 mM ODPA solution prior to baking and rinsing steps, as stated in 4.2.3.1.

The spectra of the coated surfaces were compared to ODPA powder and the untreated Ti6Al4V spectrum (Figure 4.3). Untreated Ti6Al4V surfaces presented bands at 582 $cm^{-1}$, 627 $cm^{-1}$ and 641 $cm^{-1}$, corresponding to Ti-O (Ba-Abbad *et al.*, 2012; Zhao *et al.*, 2013). The ODPA-coated surfaces presented some of the characteristic peaks of the ODPA powder spectrum, however a shift in wavenumbers was noticed. According to several FTIR analyses, the band found at 1022 $cm^{-1}$ corresponded to P-O and the two peaks observed at 2330 $cm^{-1}$ and 2353 $cm^{-1}$ to the vibration of P-O-H (Luschtinetz *et al.*, 2007; Ding *et al.*, 2010; Lim *et al.*, 2010; Yah *et al.*, 2012; Dai *et al.*, 2014). Finally, the bands found at 2839 $cm^{-1}$ and 2908 $cm^{-1}$ potentially corresponded to the C-H stretching (Gawalt *et al.*, 2001; Gouzman *et al.*, 2006; Luschtinetz *et al.*, 2007; Lim *et al.*, 2010; Yah *et al.*, 2012).

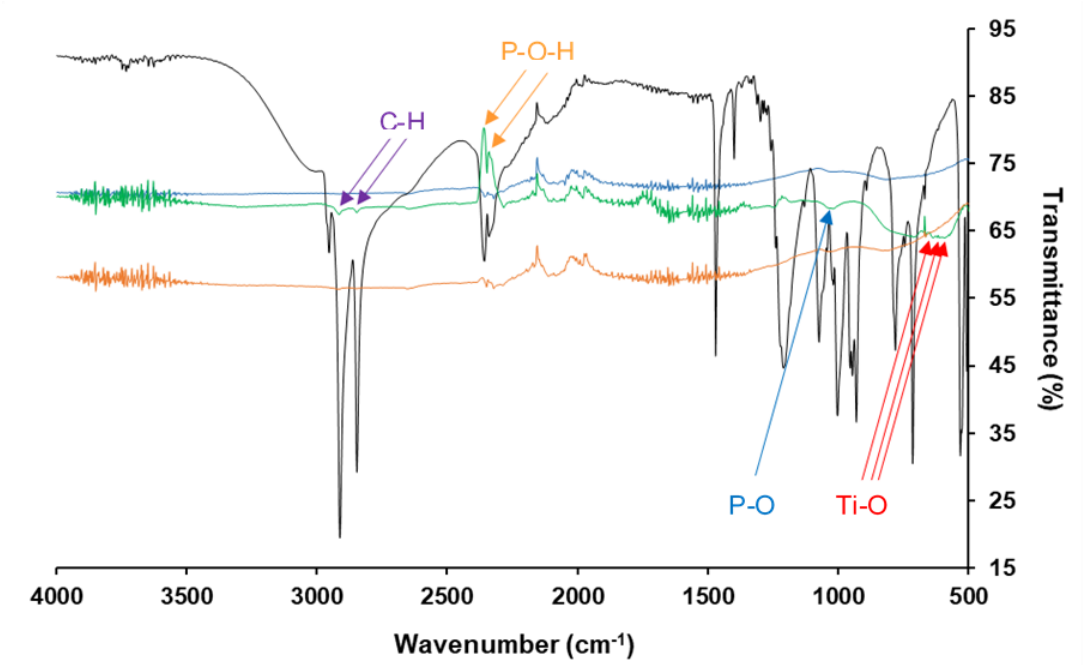


**Figure 4.3. Representative FTIR spectra of ODPA powder (black), untreated Ti6Al4V (blue), ODPA-coated Ti6Al4V 1 h incubation (green), and ODPA-coated Ti6Al4V 24 h incubation (orange).**

In a second experiment, the necessity of the baking step was investigated. Surfaces were steeped in 1 mM ODPA solution for 1 h or 24 h. Half the surfaces tested were then rinsed without undergoing the baking step and subsequently analysed by FTIR, whilst the other half were baked, rinsed, then analysed by FTIR. The FTIR spectra of the discs coated with ODPA without baking step were compared to their corresponding baked surfaces. After 1 h incubation, the surfaces which did not experience the baking step were very similar to the untreated Ti6Al4V and no ODPA-

related peaks were observed. The surfaces that underwent the baking step however presented two peaks at 2846 $cm^{-1}$ and 2914 $cm^{-1}$ corresponding to the C-H stretch in the ODPA spectrum (Figure 4.4). This was the only difference detected between surfaces that underwent the baking step compared with untreated and unbaked surfaces. At 24 h incubation, no ODPA peak was identified with or without baking step (Figure 4.5).

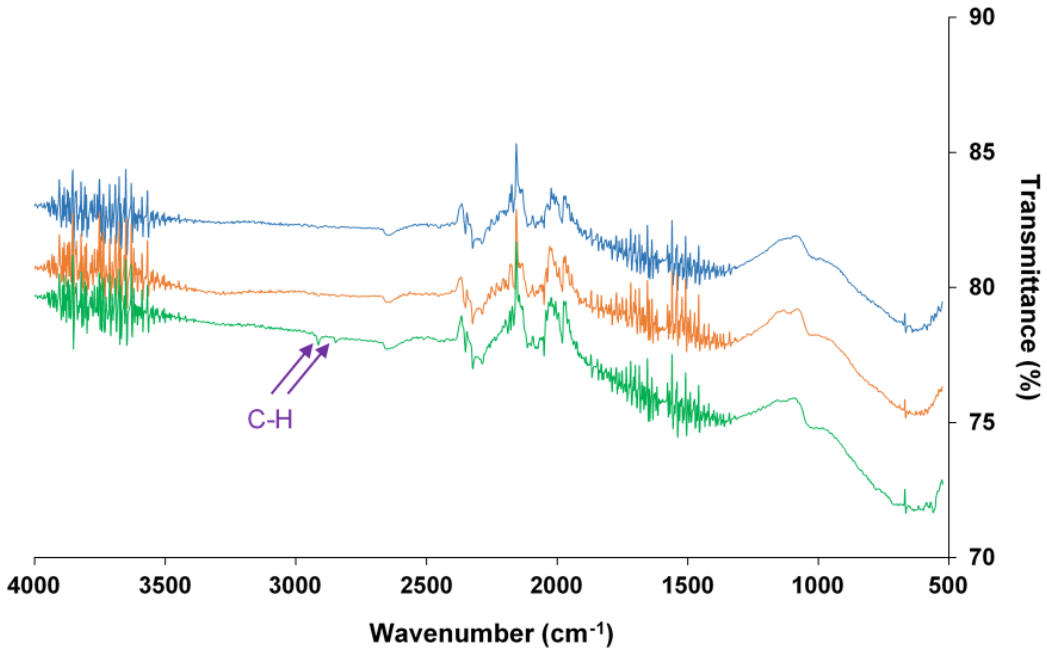


**Figure 4.4. Representative FTIR spectra of Ti6Al4V surfaces with and without baking step, after 1 h incubation in 1 mM ODPA solution. The spectra presented correspond to untreated Ti6Al4V (blue), ODPA-coated Ti6Al4V without baking step (orange), ODPA-coated Ti6Al4V with baking and rinsing steps (green).**

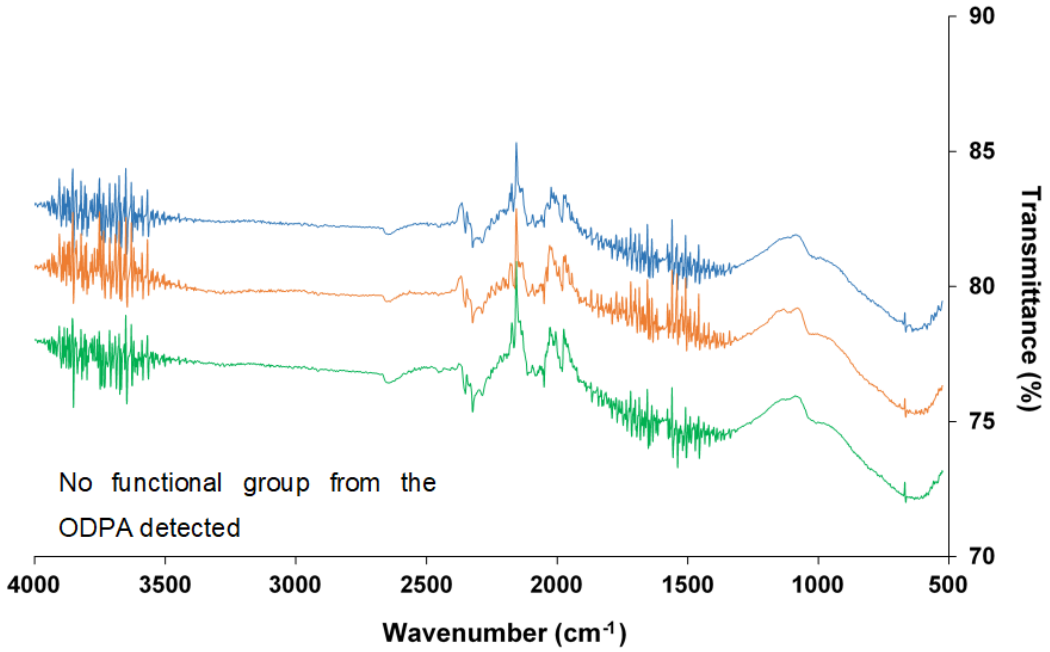


**Figure 4.5. Representative FTIR spectra of Ti6Al4V surfaces with and without baking step, after 24 h incubation in 1 mM ODPA solution. The spectra presented correspond to untreated Ti6Al4V (blue), ODPA-coated Ti6Al4V without baking step (orange), ODPA-coated Ti6Al4V with baking and rinsing steps (green).**

Ti6Al4V surfaces were also analysed by XPS. They were first incubated for 1 h or 24 h in ODPA. Half the surfaces were then baked for 1 h at 180 °C and rinsed, while the other half was rinsed without baking. All samples were then analysed by XPS (n = 1). Baked surfaces presented more phosphorus on their surface than unbaked surfaces: for 1 h incubation 1.76 versus 0.18 atomic percentages were detected, and for 24 h incubation 4.18 and 0.07 atomic percentages were found, respectively (Figure 4.6). Discs incubated in ODPA solution for 24 h and baked presented more phosphorus than discs incubated for 1 h and baked, which was contrary to the FTIR results. Finally, unbaked untreated discs showed 0.51 phosphorus atomic percentage at the disc surface, whilst the untreated and baked disc did not show any phosphorus content.

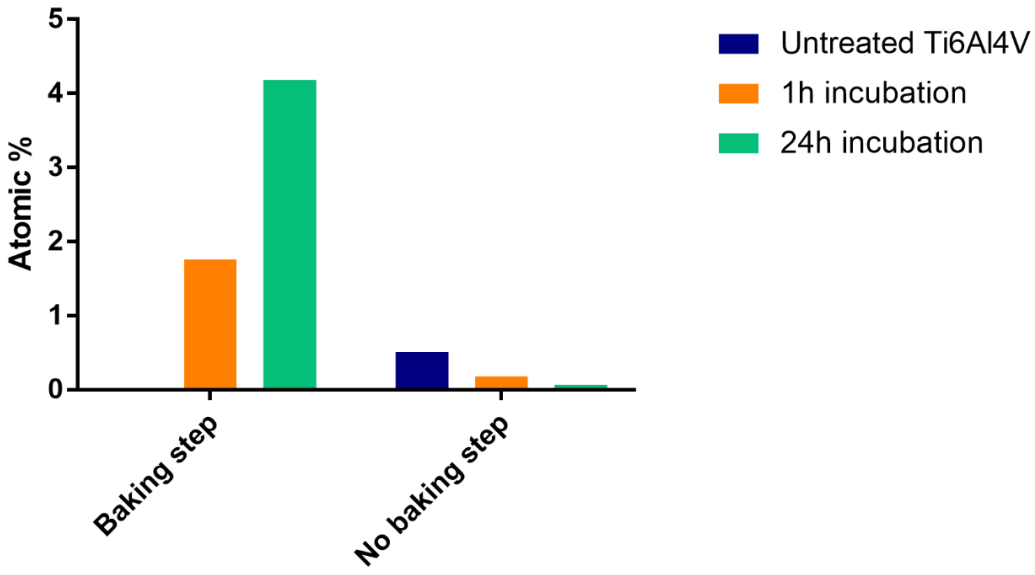


**Figure 4.6. Atomic percentage of phosphorus on Ti6Al4V surfaces detected by XPS.**

Oxygen and carbon content of the surfaces were analysed during these experiments. The oxygen content at the Ti6Al4V surface remained constant for the unbaked surfaces: the untreated disc presented 30.55 oxygen atomic percentage, whilst the discs incubated for 1 h and 24 h showed 29.94 and 29.12 oxygen atomic percentage, respectively (Figure 4.7). The untreated, baked disc presented a lower oxygen content with 23.52 atomic percentage, compared with the untreated unbaked disc, with 30.55 oxygen atomic percentage. However, the discs incubated in ODPA solution and baked demonstrated a higher oxygen content with 38.65 and 39.91 atomic percentage, respectively.

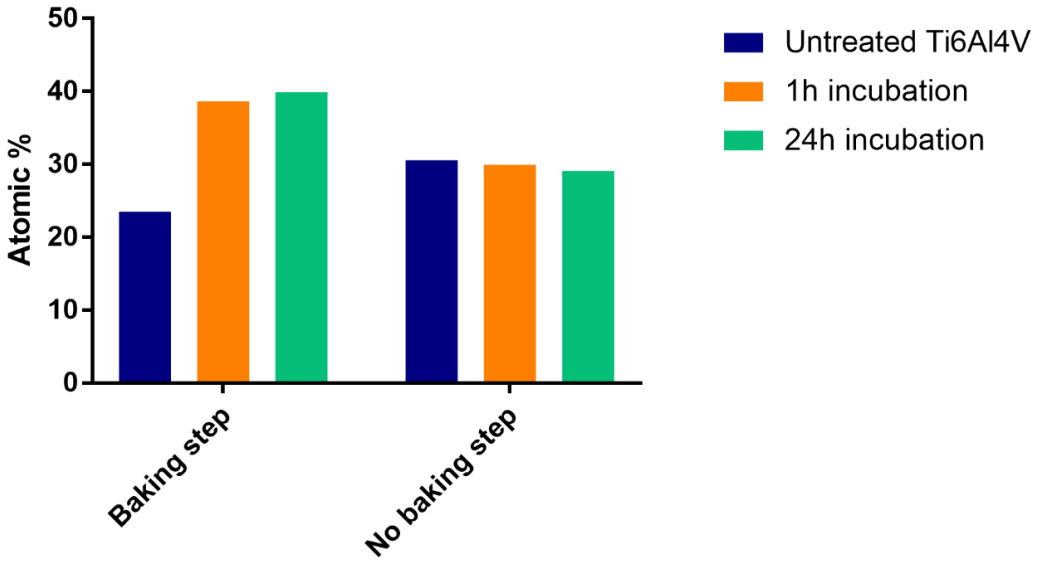


**Figure 4.7. Atomic percentage of oxygen on Ti6Al4V surfaces detected by XPS.**

The carbon content (Figure 4.8) remained constant for the unbaked surfaces: the untreated disc presented 44.51 carbon atomic percentage, similar to the discs incubated for 1 h and 24 h, with 46.52, and 47.52 carbon atomic percentage, respectively. However, the carbon content decreased with the increase exposure to ODPA: the untreated disc showed a carbon atomic percentage of 52.42, the discs incubated for 1 h and 24 h presented a carbon atomic percentage of 43.28 and 33.5.

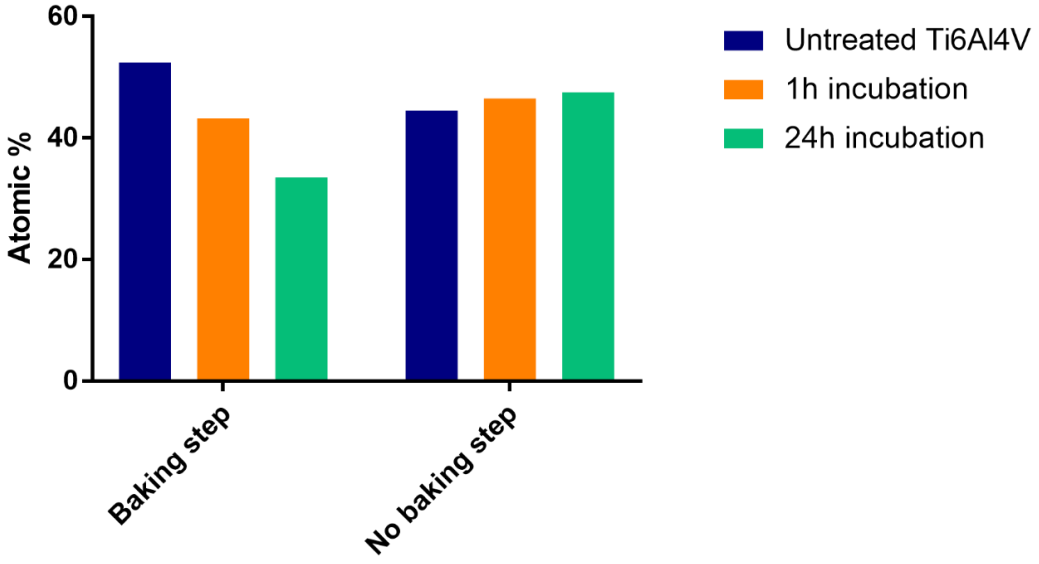


**Figure 4.8. Atomic percentage of carbon on Ti6Al4V surfaces detected by XPS.**

#### 4.3.1.2 Design of experiments and characterisation by XPS

ODPA-coated surfaces were analysed by XPS. One surface per condition was analysed, however in order to study the homogeneity of the ODPA coating three different areas per surface were analysed.

The effects of the different factors were calculated according to Equation 1:

$$\alpha = \frac{3.79 + 3.70 + 2.54 + 2.34}{4} - \frac{1.63 + 1.75 + 2.16 + 2.08}{4} = 1.1875$$

$$\beta = \frac{1.75 + 3.70 + 2.08 + 2.34}{4} - \frac{1.63 + 3.79 + 2.16 + 2.54}{4} = -0.0625$$

$$\gamma = \frac{2.16 + 2.54 + 2.08 + 2.34}{4} - \frac{1.63 + 3.79 + 1.75 + 3.70}{4} = -0.4375$$

α, the effect of the factor A (i.e. concentration of ODPA) was positive and slightly above 1, meaning that the concentration of ODPA influenced positively the outcome. This suggests that increasing the concentration of ODPA in the solution led to a higher attachment of ODPA to the Ti6Al4V surface. On the contrary, β and γ were negative, however close to zero. According to these calculations, their impact appears to be less crucial than the concentration of ODPA. The effect of each concentration was calculated: 0.05 mM had an effect of +1.92, 1 mM + 2.98 and 5 mM +3.16. These results suggest that the concentration of 5 mM ODPA could lead to a higher attachment of ODPA.

After analysis by XPS, a high variability in phosphorus content was detected on each Ti6Al4V surface (Table 4.6, Figure 4.9). The highest variation found was in experiment 5: a mean of 2.31 phosphorus percentage was detected with a standard deviation of ± 1.112. It was hypothesised that the ODPA attachment may have been heterogenous on the surfaces.

**Table 4.6. Matrix of experiments from the DoE.**

| Experiment number | Concentration of ODPA (mM) | Incubation time | Baking time | Mean atomic % of phosphorus (SD) |
|---|---|---|---|---|
| **1** | 0.5 | 1 h 30 min | 1 h 30 min | 1.63 (± 0.132) |
| **2** | 0.5 | 4 h 30 min | 1 h 30 min | 1.75 (± 0.308) |
| **3** | 0.5 | 1 h 30 min | 4 h 30 min | 2.16 (± 0.641) |
| **4** | 0.5 | 4 h 30 min | 4 h 30 min | 2.08 (± 0.543) |
| **5** | 1 | 1 h | 3 h | 2.31 (± 1.112) |
| **6** | 1 | 5 h | 3 h | 4.07 (± 0.499) |
| **7** | 1 | 3 h | 1 h | 2.19 (± 0.751) |
| **8** | 1 | 3 h | 5 h | 3.78 (± 1.453) |
| **9** | 1 | 3 h | 3 h | 2.16 (± 0.483) |
| **10** | 5 | 1 h 30 min | 1 h 30 min | 3.79 (± 0.432) |
| **11** | 5 | 4 h 30 min | 1 h 30 min | 3.70 (± 0.920) |
| **12** | 5 | 1 h 30 min | 4 h 30 min | 2.54 (± 0.312) |
| **13** | 5 | 4 h 30 min | 4 h 30 min | 2.34 (± 0.153) |
| **14** | 5 | 1 h | 3 h | 3.68 (± 0.130) |
| **15** | 5 | 3 h | 1 h | 2.74 (± 0.340) |
| **16** | 5 | 3 h | 3 h | 3.98 (± 0.641) |

SD: Standard deviation

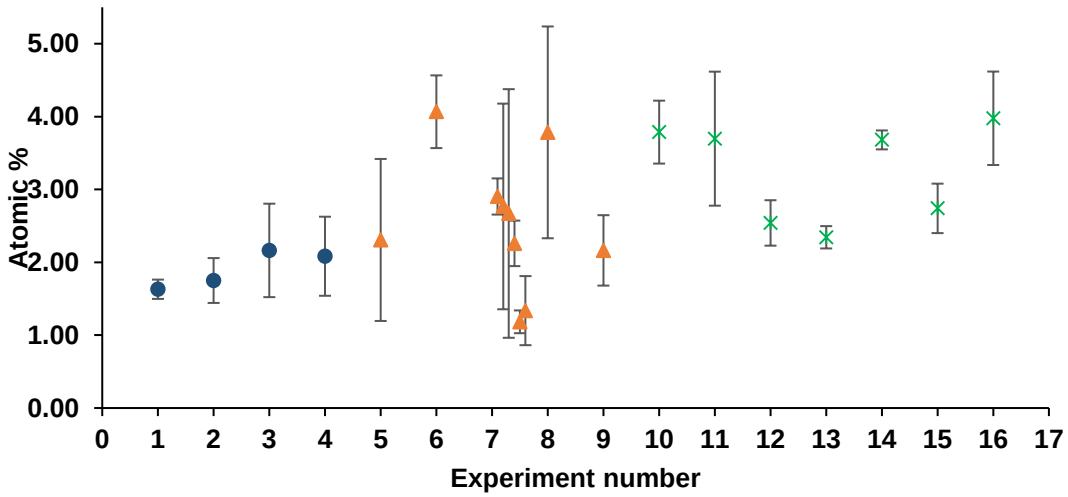


**Figure 4.9. XPS analysis of the Ti6Al4V surfaces coated with ODPA at concentrations of 0.5 mM (blue circles), 1 mM (orange triangles), 5 mM (green crosses), and incubation and baking times of 1 h, 1 h 30 min, 3 h, 4 h 30 min, 5 h. One experiment was performed. Three randomly chosen fields of view were analysed. Error bars represent standard deviation.**

Finally, the variation between experiments was analysed by repeating the experiment number 7 five times. The XPS analysis was performed three times on a randomly selected area of each surface. The intra- and inter-experiment variability was found to be high (Figure 4.10). As an example of the intra-experimental variability, the replicate number 3 presented 1.14 phosphorus atomic percentage during the first analysis. This number quadrupled during the second analysis with 4.51 phosphorus atomic percentage. Regarding the inter-experimental variability, the mean of the replicate number one was 2.90 phosphorus atomic percentage, whilst a mean of 1.18 and 1.33 phosphorus atomic percentage were calculated for the replicates number five and six, respectively.

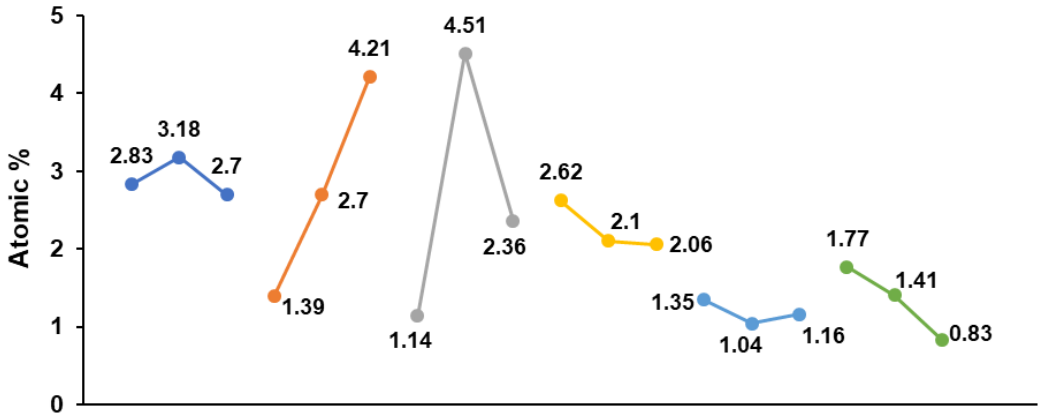


**Figure 4.10. XPS analysis of the atomic percentage of phosphorus found on the Ti6Al4V surfaces after replicating experiment number 7. Each independent replicate is represented by a colour. Three linked points of the same colour indicate three XPS analyses of the same surface.**

#### 4.3.1.3 Contact angle measurement

As stated in Chapter 2, Section 2.3.4, untreated discs presented a mean contact angle of 48 ° (± 1.178) after autoclaving. The ODPA coating increased the contact angle to 73 ° (± 7.267) meaning that the Ti6Al4V surfaces were more hydrophobic after treatment with ODPA.

### 4.3.2 Characterisation of liposomes

#### 4.3.2.1 Size and polydispersity

The size and polydispersity of the liposomes were characterised. After re-suspension, liposomes were not extruded. They presented a mean size of 1296 nm (± 515, Figure 4.11). Due to the high variability in size, the mean index of polydispersity was 0.757 (± 0.007).

#### 4.3.2.2 Zeta potential

The liposomes were negatively charged and presented a mean zeta potential of -23.6 mV (± 1.299, Figure 4.11).

#### 4.3.2.3 Liposome stability in heat

The stability of the liposomes in a hot environment was assessed in order to ensure that the formulation would remain intact once poured in molten agar to perform the MIC testing.

Liposomes showed a non-significant ($p = 0.5976$) increase in size from 1296 nm (± 515) before heating to 1679 nm (± 426) after heating at 80 °C for 10 min (Figure 4.11). An increase in PDI was also observed from 0.757 (± 0.007) before heating to 0.816 (± 0.020). No modification of the zeta potential was noted: the liposomes presented a mean zeta potential of -23.6 mV (± 1.299) before heating and -23.1 mV (± 1.198) after heating.

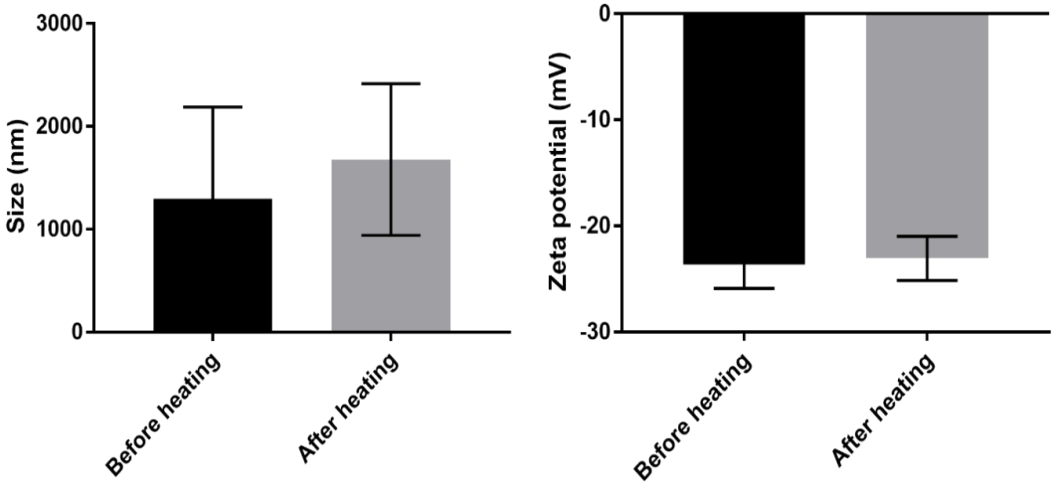


**Figure 4.11. Size and zeta potential before and after heat treatment at 80 °C for 10 min. Mean values of 3 independent experiments are shown. Error bars represent standard error of the mean.**

#### 4.3.2.4 Phospholipid concentration

The standard curve was produced (Figure 4.12) from the standard concentrations of phosphatidylcholine and their corresponding absorbance at 570 nm. The standard curve was linear with a $R^2$ of 0.9994 and the equation was: $y = 0.003954x + 0.08793$. The concentration of phosphatidylcholine in the liposomes was calculated from the absorbance at 570 nm using the equation of the standard curve. The mean concentration of phosphatidylcholine was 2.538 mg/mL, corresponding to 96 % of the total amount of phosphatidylcholine weighed.

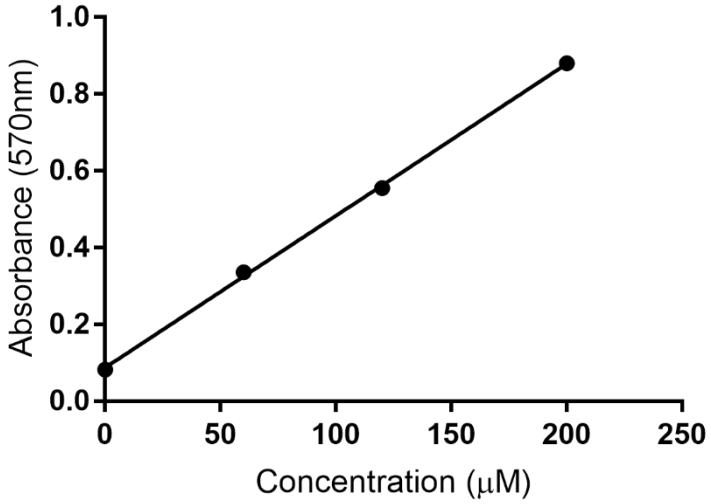


**Figure 4.12. Standard curve produced from known phospholipid concentrations and their corresponding absorbance at 570 nm. Mean values of 3 independent experiments are shown. Error bars represent standard error of the mean.**

#### 4.3.2.5 Triclosan concentration

The standard solutions of triclosan presented a single elution peak at 9 min. The AUC was calculated and correlated to the known concentration of triclosan. This produced the linear calibration curve presenting a $R^2$ of 0.996 and the following equation: $y = 9.117x - 0.6397$ (Figure 4.13).

A single peak at 9 min was also observed from the liposomal formulations. The triclosan concentration within the liposomes was calculated using the calibration curve produced. A mean triclosan concentration of 281 µg/mL was found in the liposomes, corresponding to a mean encapsulation efficiency of 94 %. As the liposomes were composed of 3 mg/mL lipids and 281 µg/mL triclosan, the loading capacity of the liposomes found to be of 9 %.

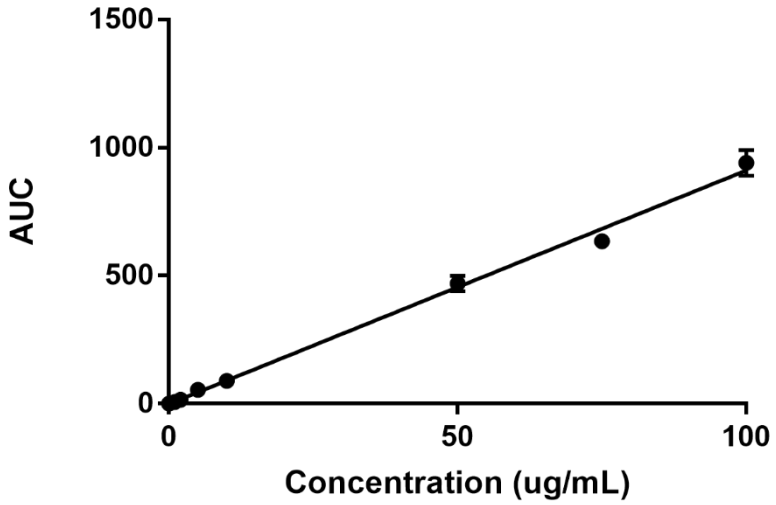


**Figure 4.13. Standard curve produced from known concentrations of triclosan and their corresponding AUC detected by HPLC. Mean values of 3 independent experiments are shown. Error bars represent standard error of the mean.**

### *4.3.2.6* Intrinsic activity of triclosan against *Fusobacterium nucleatum* and *Porphyromonas gingivalis*

The intrinsic activity of the triclosan and triclosan liposomes was investigated firstly by culture (Figure 4.14, Figure 4.15). A non-significant decrease in viability ($p > 0.9999$) was observed in *F. nucleatum* suspensions placed in 1 % IPA in PBS (v/v) compared with *F. nucleatum* in PBS only, with $5.44x10^6$ CFU/mL (± $1.43x10^6$) and $6.29x10^6$ CFU/mL (± $1.77x10^6$), respectively. After incubation in blank liposome suspensions (1 mg/mL and 3 mg/mL), *F. nucleatum* also showed a non-significant reduction in colonies ($p > 0.9999$) with $5.49x10^6$ CFU/mL (± $1.36x10^6$) CFU/mL and $5.60x10^6$ CFU/mL (± $1.56x10^6$), respectively, compared with PBS. *F. nucleatum* placed in the presence of triclosan liposomes (100 µg/mL triclosan, 1 mg/mL lipids and 300 µg/mL triclosan, 3 mg/mL lipids) presented a significant decrease in viability with $1.36x10^5$ CFU/mL (± $7.12x10^4$, $p = 0.0048$) and 240 CFU/mL (± 47.3, $p = 0.0040$), respectively. After incubation in free triclosan no colony was found on the plates, the reduction in CFU/mL was consequently significant ($p = 0.0040$).

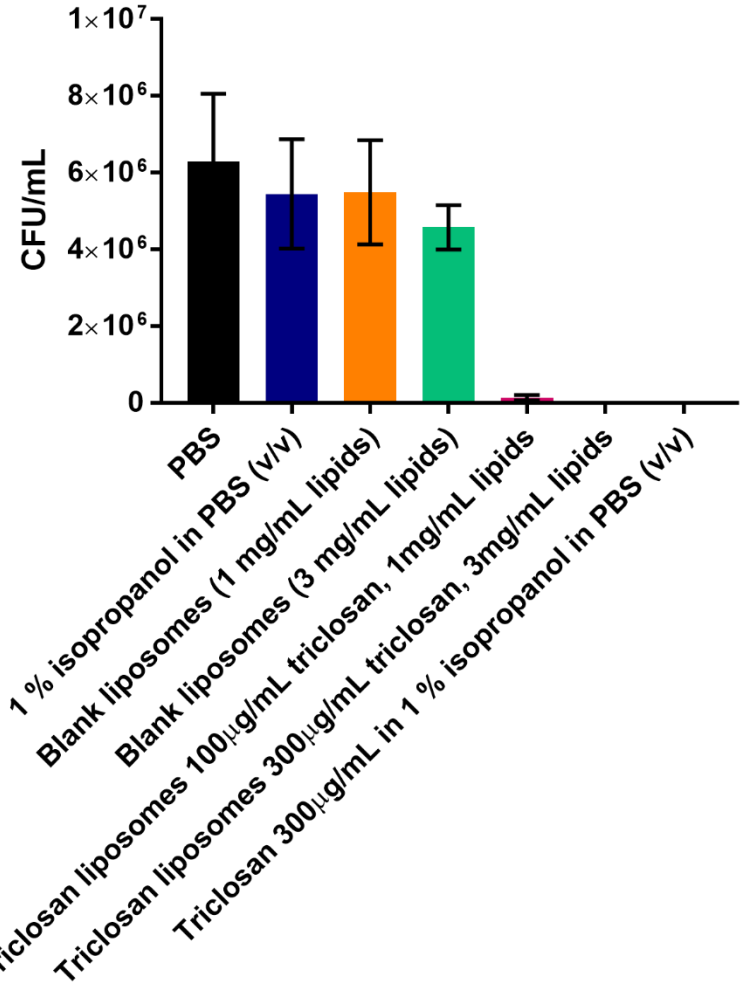


**Figure 4.14. Intrinsic activity of triclosan liposomes and free triclosan on *F. nucleatum*. Mean values of 3 independent experiments in triplicate are shown. Error bars represent standard error of the mean.**

*P. gingivalis* showed a significant decrease in viability ($p = 0.0010$) after incubation in 1 % IPA in PBS (v/v), with $1.07 \times 10^9$ CFU/mL ($\pm 1.94 \times 10^7$) counted, compared with *P. gingivalis* in PBS showing $1.34 \times 10^9$ CFU/mL ($\pm 5.41 \times 10^7$). A dose-dependent effect of the triclosan-loaded liposomes was observed: incubation in liposomal suspension of concentration 100 µg/mL triclosan and 1 mg/mL lipids led to a significant ($p < 0.0001$) decrease in viability ($5.02 \times 10^8$ CFU/mL; $\pm 4.87 \times 10^7$). A further significant reduction was noticed, with *P. gingivalis* presenting 11.1 CFU/mL (± 5.88) after incubation in the liposomal suspension of concentration 300 µg/mL triclosan, 3 mg/mL lipids. The significance was as follows: $p < 0.0001$ compared with bacterial suspensions incubated in PBS, $p = 0.0092$ compared with bacterial suspensions incubated in liposomal suspension of concentration 100 µg/mL triclosan and 1 mg/mL

lipids. Finally, after incubation in free triclosan, no colony was observed on the agar plate ($p < 0.0001$).

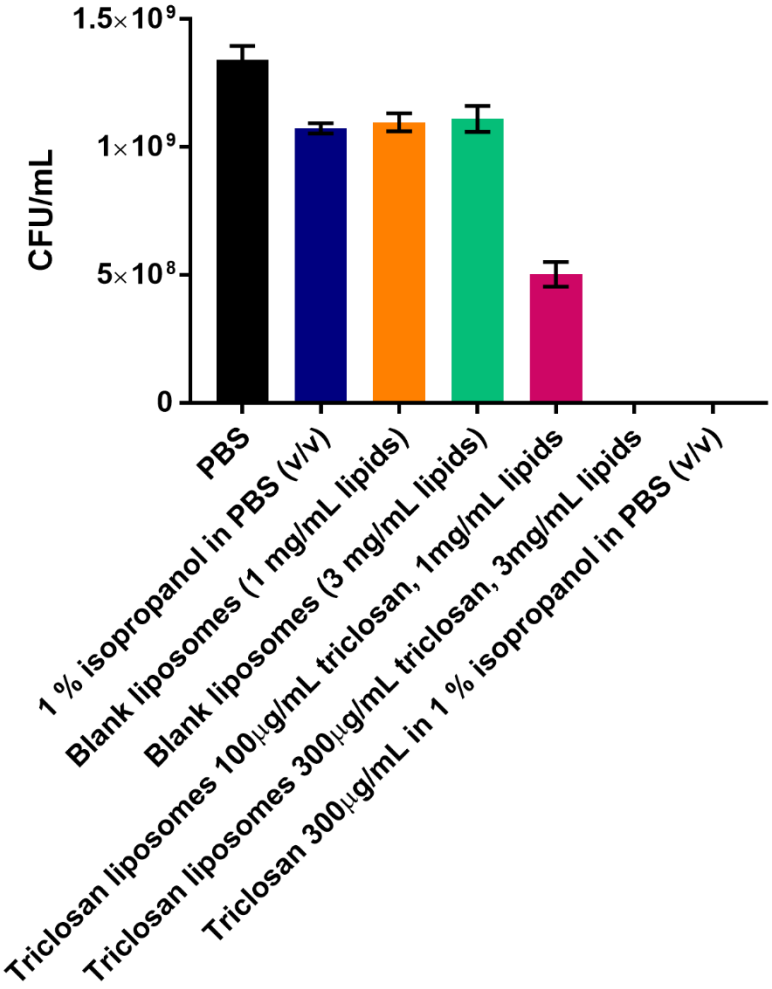


**Figure 4.15. Intrinsic activity testing of triclosan liposomes and free triclosan on *P. gingivalis*. Mean values of 3 independent experiments in triplicate are shown. Error bars represent standard error of the mean.**

Issues were encountered during the imaging of the bacterial suspensions placed in contact with the liposomes. The liposomes appeared green after staining with SYTO9, the green fluorophore used in the LIVE/DEAD™ BacLight™ kit (Figure 4.16, Figure 4.17). Images of unstained liposomes and liposomes stained with SYTO9 were taken to confirm that no autofluorescence was involved in this phenomenon (Figure 4.18). Consequently, the quantification of viable and dead bacteria could not be performed. The ratios of viable/dead bacteria were however calculated for bacterial suspensions incubated in 1 % IPA in PBS and free triclosan. Similar to the culture data, *F. nucleatum* viability decreased in a non-significant manner ($p = 0.1910$) with

addition of 1 % IPA to PBS with 74 % (± 5.29 %) viable bacteria against 83 % (± 3.92) in PBS (Figure 4.19). Likewise, *P. gingivalis* viability reduced in the presence of 1 % IPA in PBS with 82 % (± 1.99 %) viability versus 88 % (± 2.76 %) viability in PBS (Figure 4.20), however, this reduction in viability was significant ($p = 0.0480$) The free triclosan demonstrated a significant bactericidal effect ($p < 0.0001$) on *F. nucleatum* and *P. gingivalis* with a mean live ratio of 6 % (± 1.15 %) and 4 % (± 0.48), respectively.

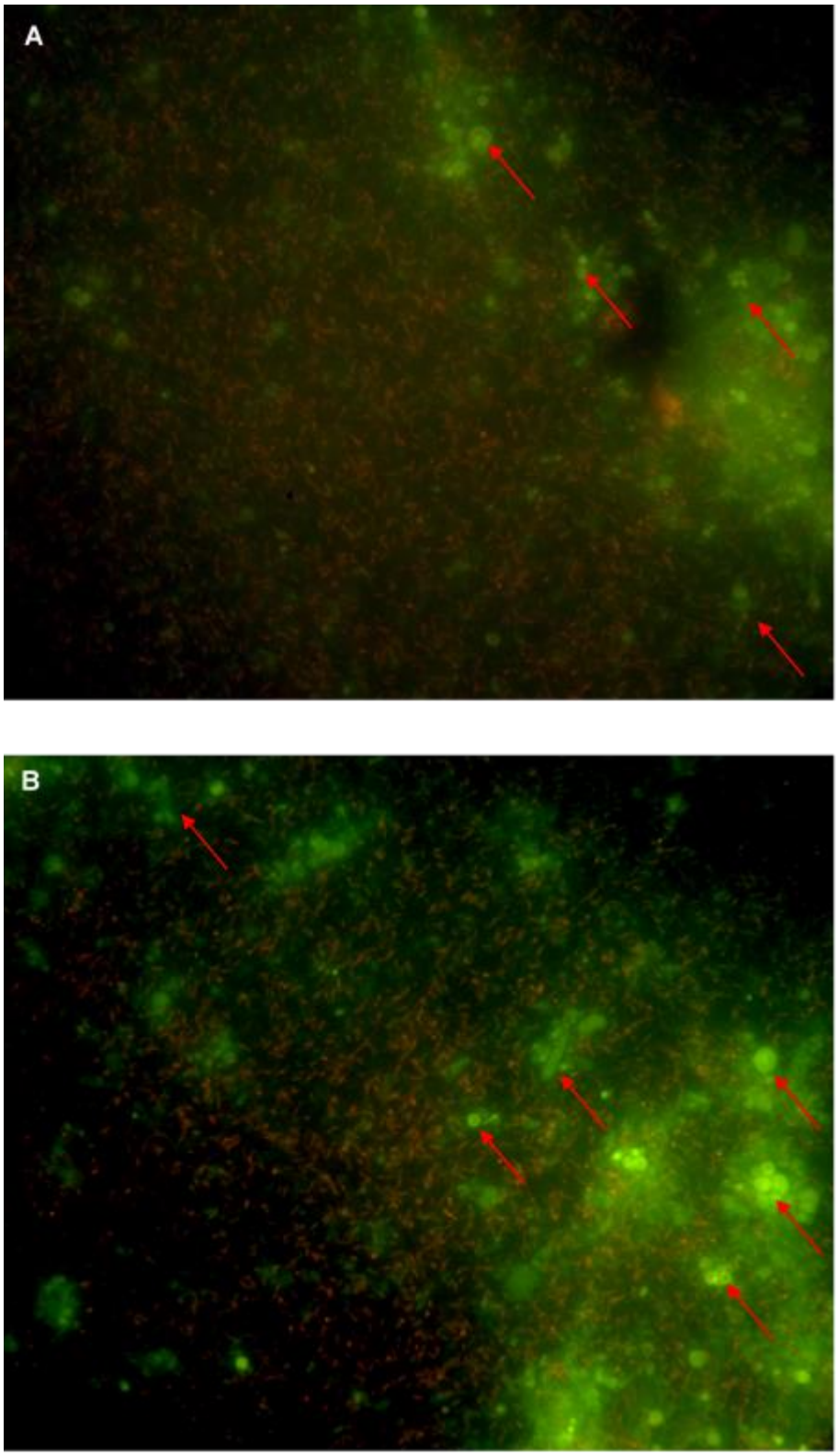


**Figure 4.16. Representative fluorescent images of *F. nucleatum* (A, B, magnification x60) incubated in triclosan liposomes and imaged using the LIVE/DEAD™ BacLight™ kit. The red arrows show liposomes.**

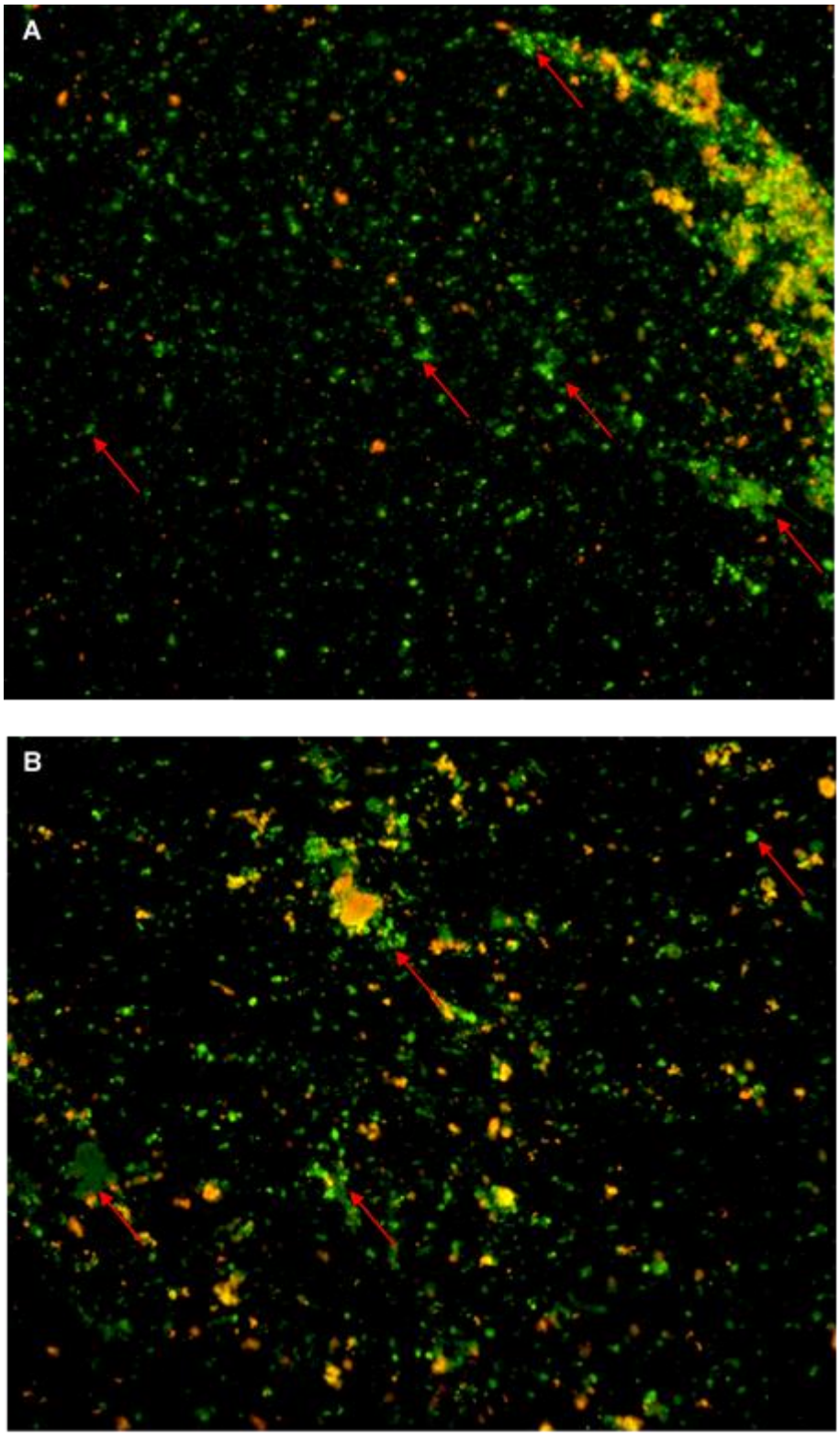


**Figure 4.17. Representative fluorescent images of *P. gingivalis* (A, B, magnification x20) incubated in triclosan liposomes and imaged using the LIVE/DEAD™ BacLight™ kit. The red arrows show liposomes.**

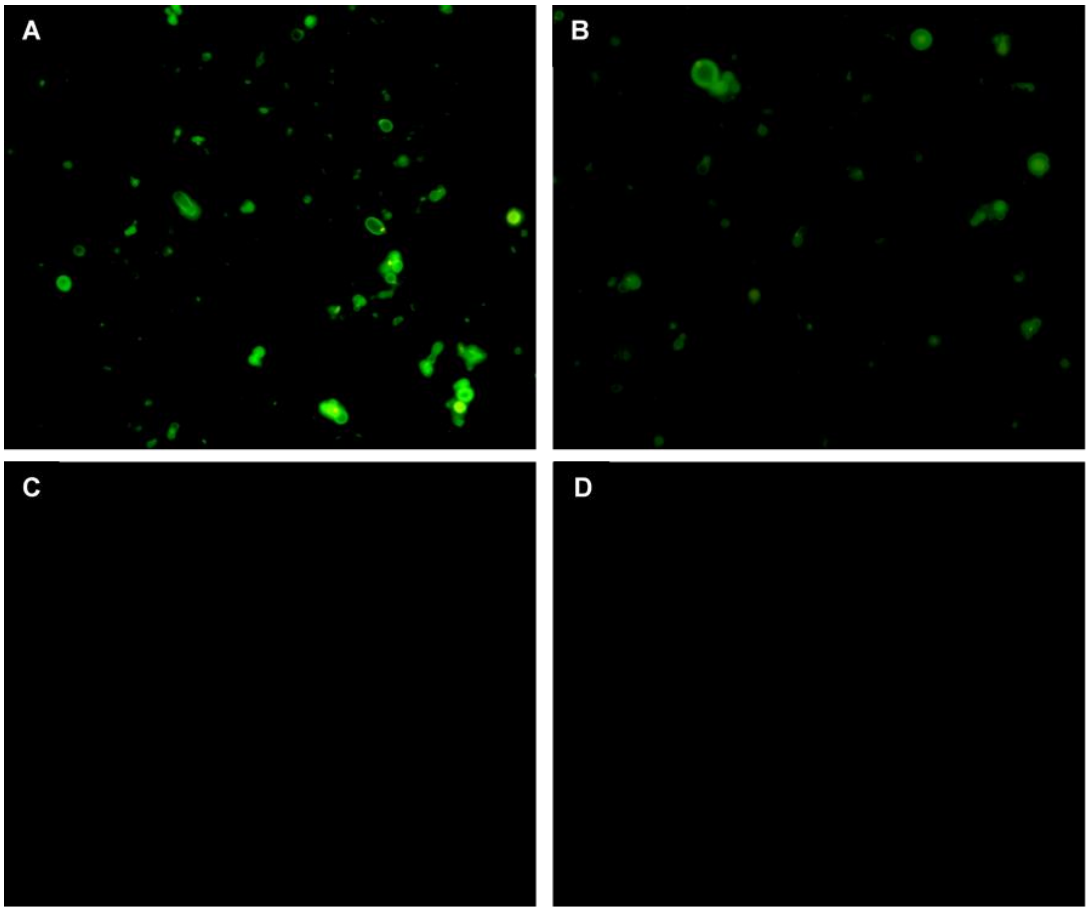


**Figure 4.18. Representative fluorescent images of liposomes stained with SYTO9 (A and B) and unstained liposomes (C and D) at magnification x60.**

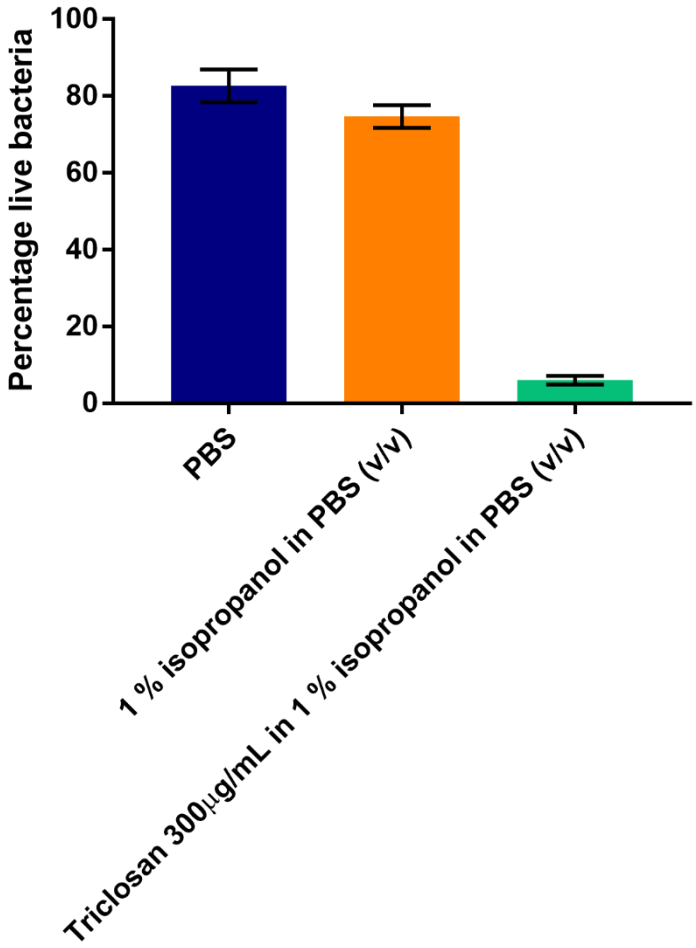


**Figure 4.19. *F. nucleatum* viability after 1 h incubation in PBS, 1 % IPA in PBS (v/v), and free triclosan in 1 % IPA in PBS. Mean values of 3 independent experiments in triplicate are shown. Error bars represent standard error of the mean.**

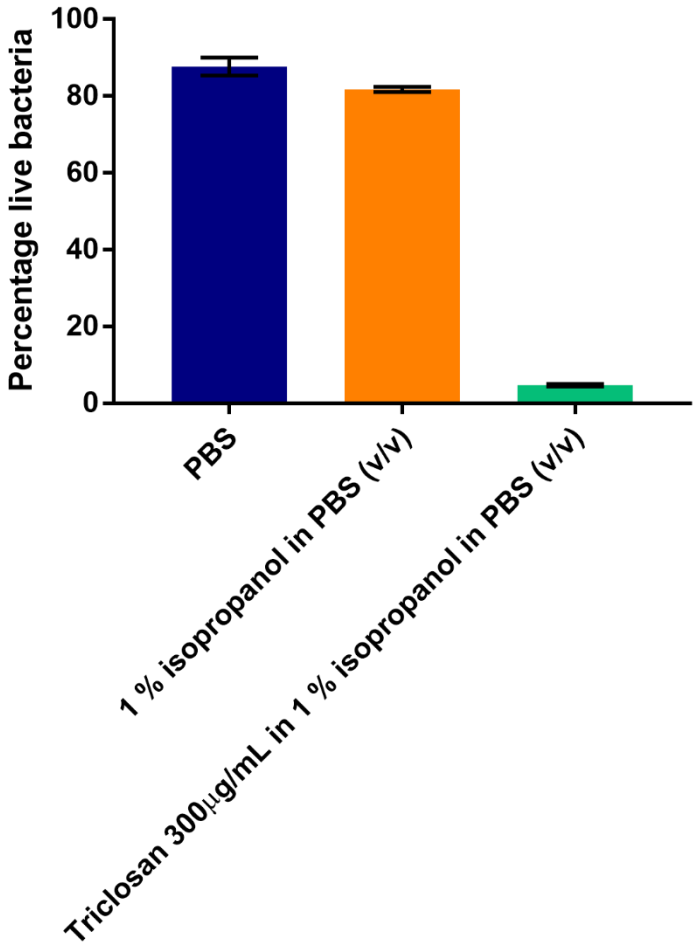


**Figure 4.20. *P. gingivalis* viability after 1 h incubation in PBS, 1 % IPA in PBS (v/v), and free triclosan in 1 % IPA in PBS. Mean values of 3 independent experiments in triplicate are shown. Error bars represent standard error of the mean.**

#### 4.3.2.7 Minimum inhibitory concentrations

The MIC testing was performed on agar, as recommended to identify the MIC of a compound against anaerobes (Clinical and Laboratory Standards Institute, 2012). Triclosan liposomes showed an MIC of 300 µg/mL for *F. nucleatum* (Figure 4.21), which was higher than for *P. gingivalis*, found to be 75 µg/mL (Figure 4.22). No MIC was identified for free triclosan and blank liposomes for *F. nucleatum*. Free triclosan presented an MIC of 100 µg/mL for *P. gingivalis* and no MIC was detected for blank liposomes. Both bacteria colonised the plain agar and the agar containing 1 % IPA.

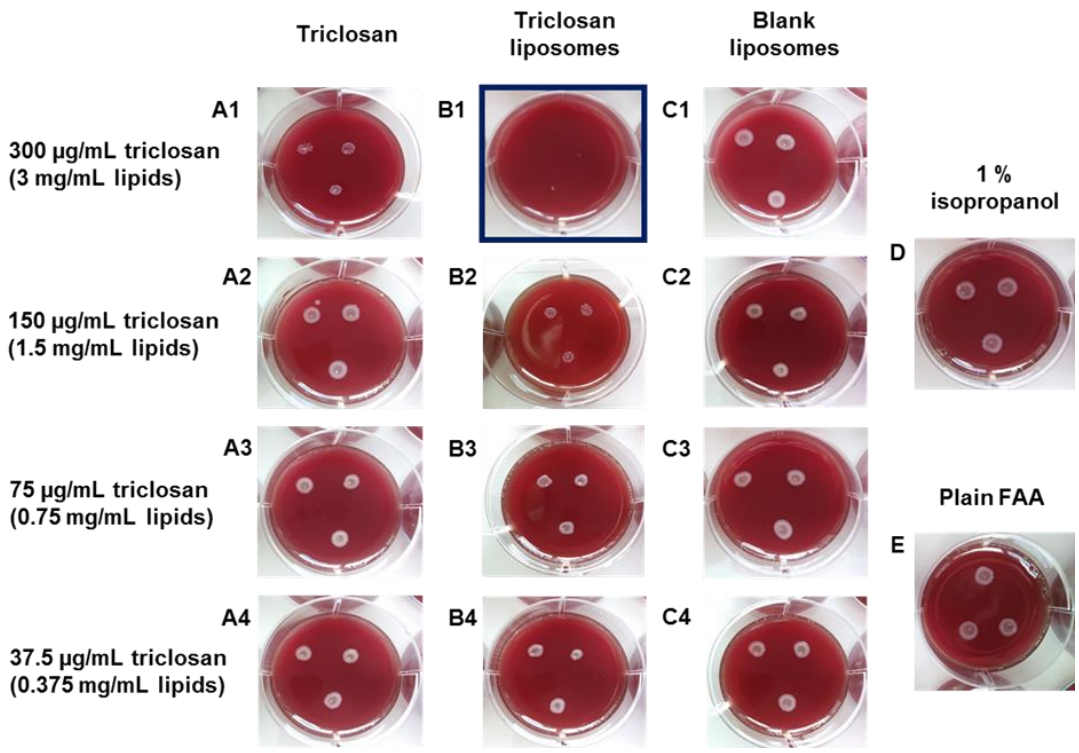


**Figure 4.21. Representative images of MIC testing of *F. nucleatum* on FAA. Triclosan (column A), triclosan-loaded liposomes (column B), blank liposomes (column C), and isopropanol (image D) were incorporated into FAA and tested. 300 µg/mL (A1, B1), 150 µg/mL (A2, B2), 75 µg/mL (A3, B3) and 37.5 µg/mL (A4, B4) of triclosan were tested. The blue rectangle (B1) indicates the MIC of triclosan-loaded liposomes against *F. nucleatum*. Plain FAA was used as a control.**

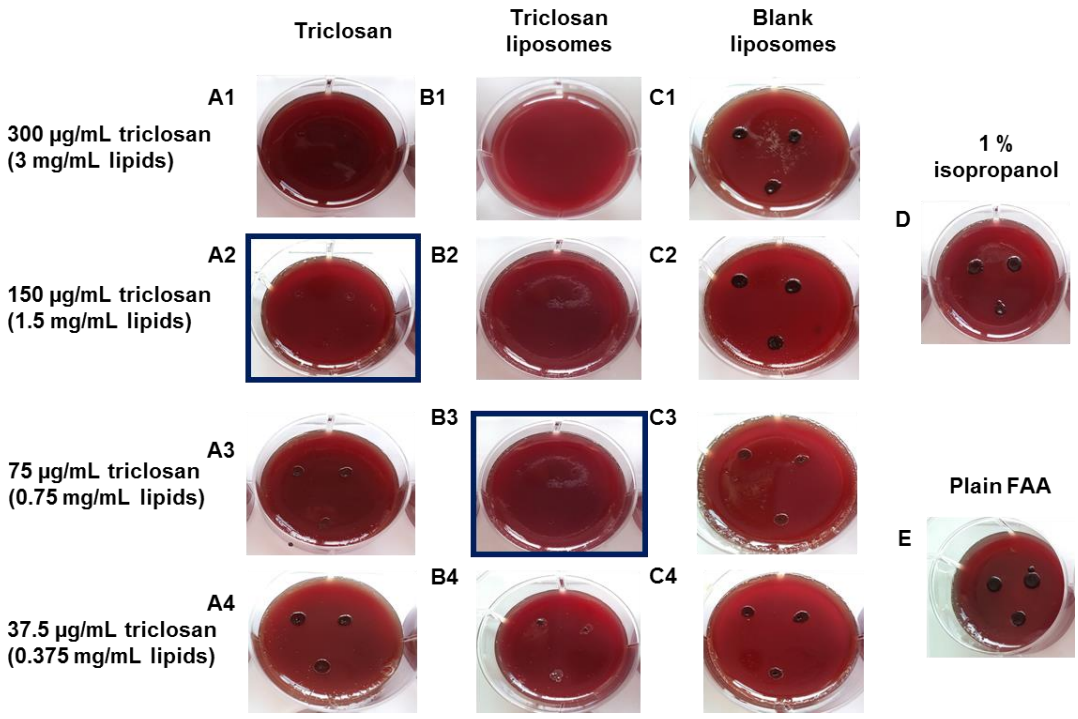


**Figure 4.22. Representative images of MIC testing of *P. gingivalis* on FAA. Triclosan (column A), triclosan-loaded liposomes (column B), blank liposomes (column C), and isopropanol (image D) were incorporated into FAA and tested. 300 µg/mL (A1, B1), 150 µg/mL (A2, B2), 75 µg/mL (A3, B3) and 37.5 µg/mL (A4, B4) of triclosan were tested. The blue rectangles indicate the MIC of triclosan (A2) and triclosan-loaded liposomes (B3) against *P. gingivalis*. Plain FAA was used as a control.**

## 4.3.3 Attachment of triclosan-loaded liposomes to ODPA-coated Ti6Al4V

### 4.3.3.1 Quantification of liposomal coverage by CSLM

Liposomal percentage coverage on Ti6Al4V was calculated. In order to investigate the potential influence of ODPA coating concentrations on liposomal coverage, Ti6Al4V surfaces were coated with different concentrations of ODPA: 0.5 mM, 1 mM and 5 mM.

A similar liposomal coverage was observed between untreated surfaces and surfaces coated with 0.5 mM and 1 mM ODPA, with 0.17 % (± 0.01), 0.19 % (± 0.02) and 0.71 % (± 0.11), respectively ($p > 0.9999$, Figure 4.23). Significant differences were however detected between the surfaces coated with 5 mM ODPA, presenting 2.03 %

(± 0.49) coverage, compared with untreated Ti6Al4V ($p = 0.0047$), Ti6Al4V coated with 0.5 mM ODPA ($p = 0.0050$), and Ti6Al4V coated with 1 mM ODPA ($p = 0.0350$).

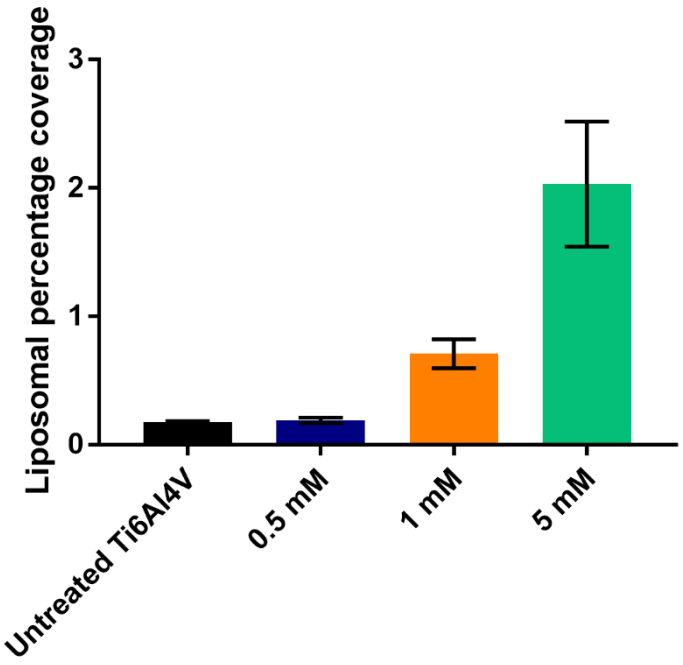


**Figure 4.23. Liposomal percentage coverage depending on the ODPA concentration used to coat the Ti6Al4V surfaces. Mean values of 3 independent experiments in triplicate are shown. Error bars represent standard error of the mean.**

The association between incubation time of ODPA-coated surfaces in liposomal suspension and liposomal coverage was also studied. Discs coated with 5 mM ODPA were incubated in liposomal suspensions for 1 h, 5 h and 24 h. A reduction in liposomal coverage was observed with increase in incubation time for the ODPA-coated surfaces (Figure 4.24). The surfaces presenting 6.82 % (± 3.39), 5.96 % (± 2.77) and 5.21 % (± 2.07) liposomal coverage for 1 h, 5 h and 24 h incubation, respectively. No trend could however be determined for the plain surfaces: an increase in liposomal coverage was detected between 1 h and 5 h incubation, showing respectively 2.48 % (± 0.21) and 6.48 % (± 0.89), followed by a decrease in coverage after 24 h incubation corresponding to 3.55 % (± 1.46). No significant difference was observed between incubation times or between coated and untreated surfaces.

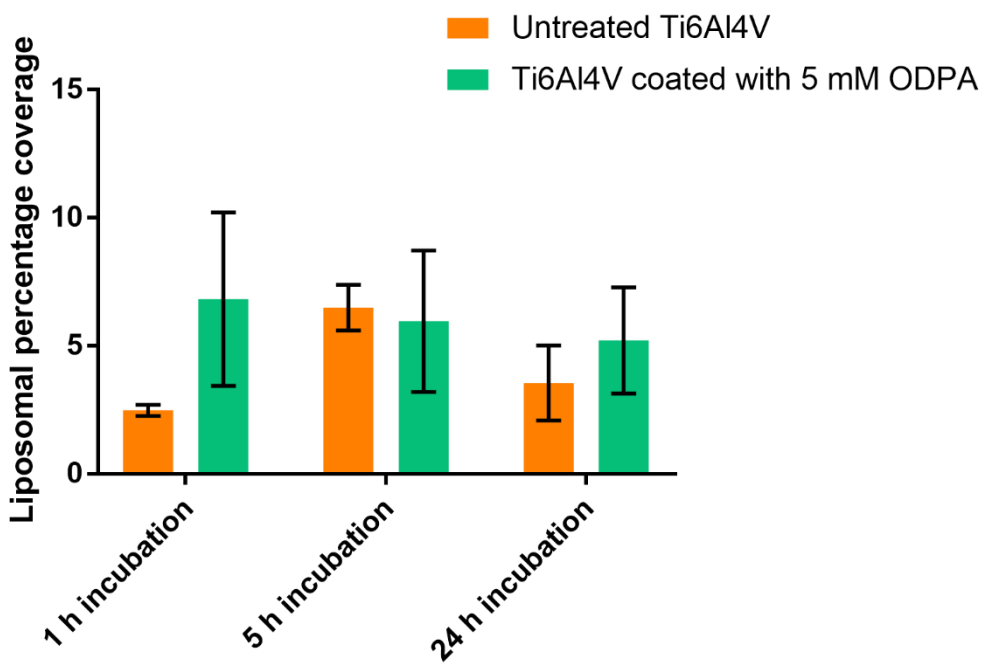


**Figure 4.24. Liposomal percentage coverage depending on the Ti6Al4V incubation time in liposomal suspensions. Mean values of 3 independent experiments in triplicate are shown. Error bars represent standard error of the mean.**

The overall liposomal coverage was low. However, liposomes showed a tendency to form aggregates while attaching to the surfaces at all concentrations (Figure 4.25) and for all incubation times (Figure 4.26). Ti6Al4V surfaces appeared bare between liposomal aggregates. Discs coated with 0.5 mM ODPA presented smaller liposomes and less aggregates. Dye alone did not attach to the untreated and ODPA-coated surfaces (Figure 4.27).

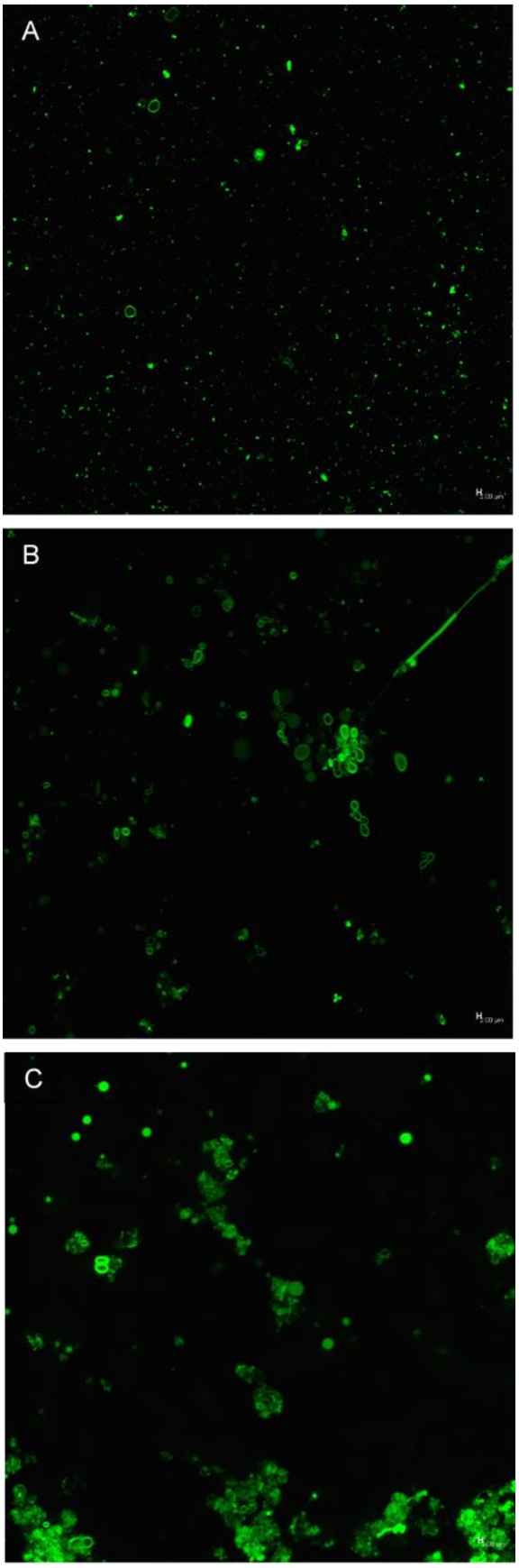


**Figure 4.25. Representative fluorescent liposomes attached to the Ti6Al4V surfaces coated with 0.5 mM (A), 1 mM (B), and 5 mM (C) ODPA.**

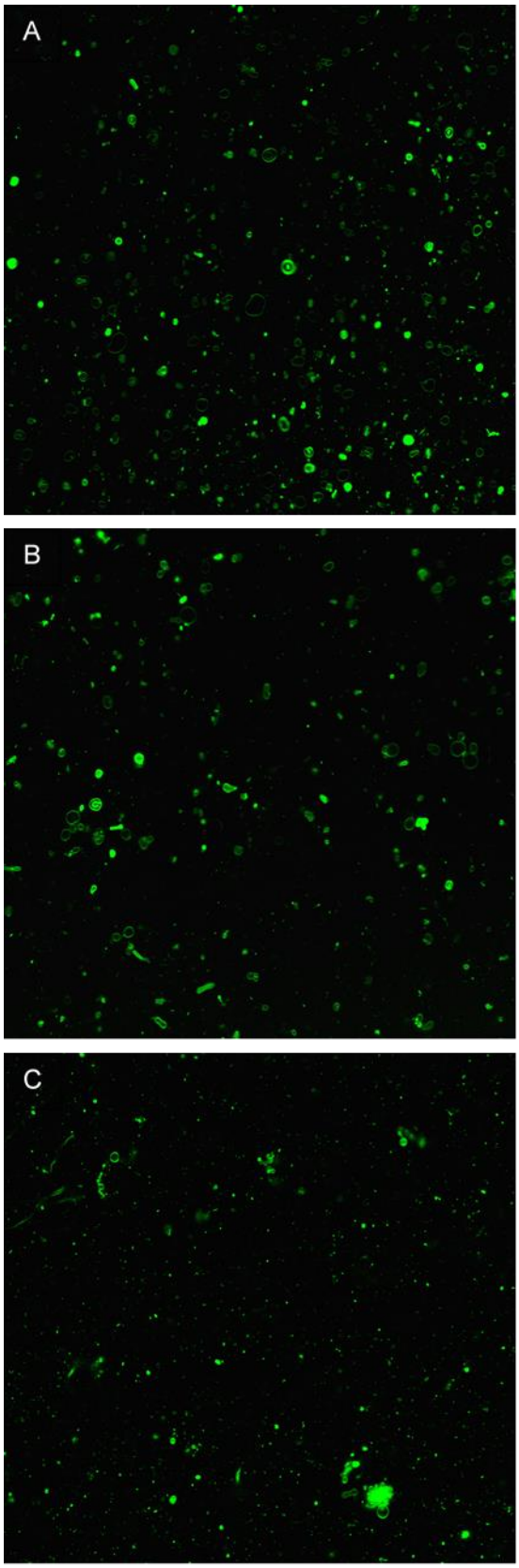


**Figure 4.26. Representative fluorescent liposomes attached to the ODPA-coated Ti6Al4V (5 mM) incubated for 1 h (A), 5 h (B), and 24 h (C) in liposomal suspensions (300 µg/mL triclosan, 3 mg/mL lipids).**

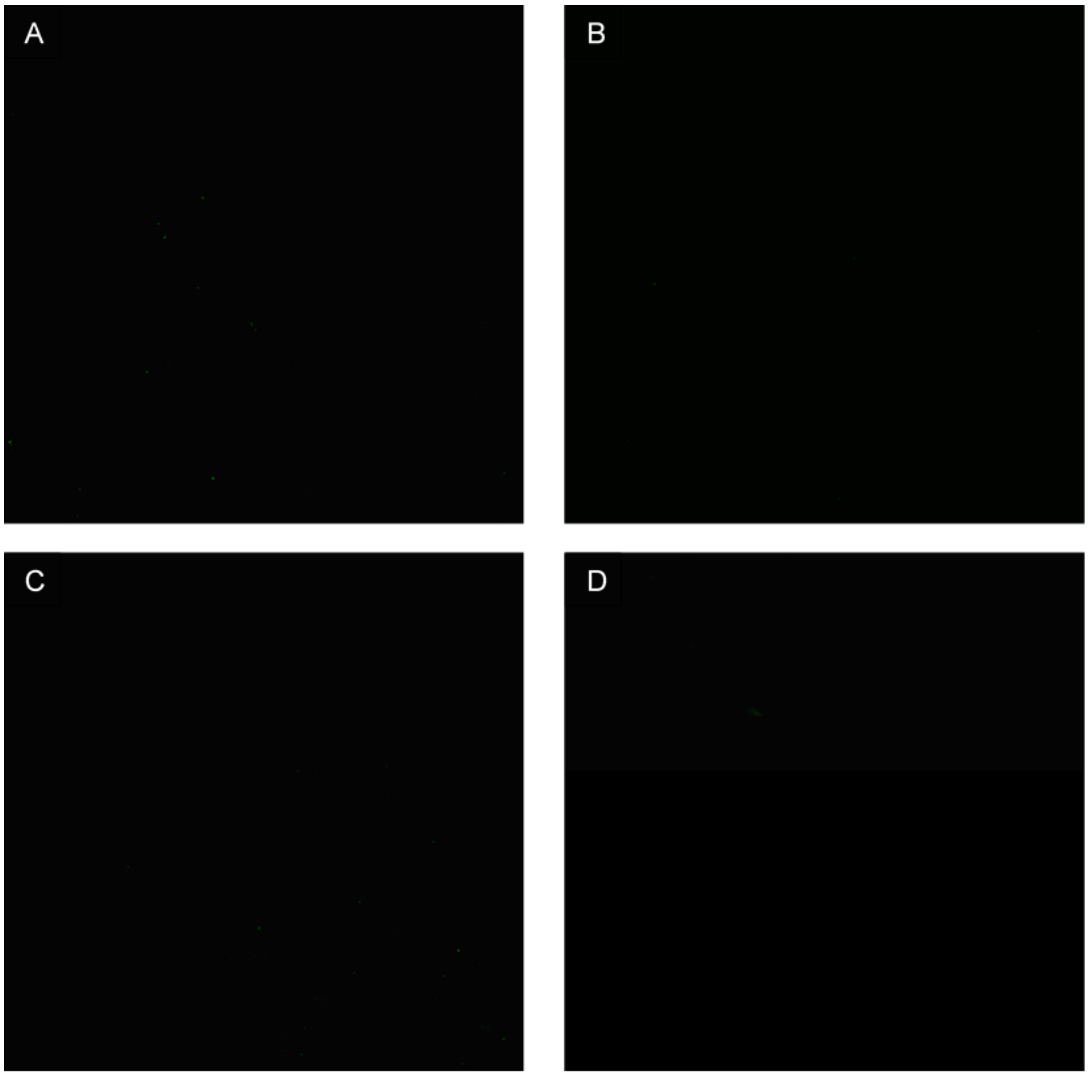


**Figure 4.27. Representative images of controls: Dye alone on surfaces coated with 0.5 mM (A), 1 mM (B), 5 mM (C) ODPA and on untreated Ti6Al4V (D).**

#### 4.3.3.2 Quantification of total triclosan coverage by HPLC

The total amount of triclosan on the coated Ti6Al4V surfaces was measured by HPLC. As found in earlier experiments, the standard solutions of triclosan, as well as the liposomal formulations presented a single elution peak at 9 min. The AUC was calculated and correlated to the known concentration of triclosan in the standard solutions. This produced the linear calibration curve presenting a $R^2$ of 0.9991 and the following equation: $y = 0.174x - 0.1382$ (Figure 4.28).

The total amount of triclosan on each sample was dissolved in methanol and analysed, the amount detected by HPLC was therefore the total mass of triclosan present on each surface: 0.0819 µg/mm$^2$ were detected on the liposome-coated

Ti6Al4V surfaces, whilst 0.0028 µg/mm$^2$ were found on the triclosan-coated discs. No triclosan peak was detected for untreated surfaces.

#### 4.3.3.3 Release study

The release of triclosan from liposomes was studied from 1 h to 140 h. Each sample was in an individual well and underwent the full incubation time in water. The whole water sample was taken for analysis at each time point. An initial burst release could be observed: 0.319 µg/mL triclosan was released at 1 h, whilst 2.01 µg/mL was detected at 24 h (Figure 4.28). No further release was observed after 24 h in water, with 1.46 µg/mL, 1.50 µg/mL and 0.73 µg/mL detected at 48 h, 72 h and 140 h, respectively. The total amount of triclosan released from the system was lower than 10 % of the total amount of triclosan entrapped in liposomes on the Ti4Al6V surfaces at all time points. No triclosan peak was detected for the blank liposomes.

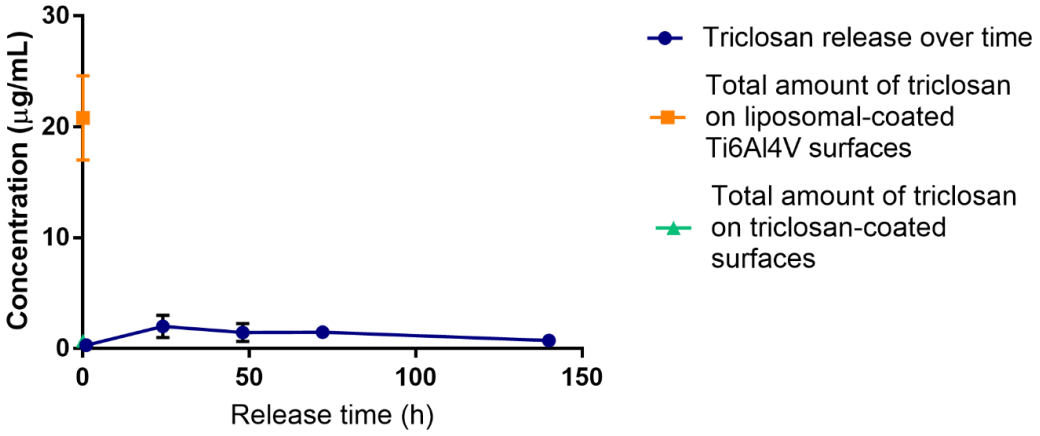


**Figure 4.28. Triclosan release profile in water from liposome-coated Ti6Al4V surfaces (blue circles), compared to the total amount of triclosan detected on the liposome-coated (orange square) and triclosan-coated surface (green triangle). Mean values of 3 independent experiments are shown. Error bars represent standard error of the mean.**

## 4.4 Discussion

Coating medical device surfaces has been shown to have a valuable impact on clinical outcomes, such as coated cardiac stents that prevent restenosis. These stents are

coated with polymers, such as poly(lactic-co-glycolic acid), polylactic acid, and polylysine. The polymers are linked to anticancer agents such as paclitaxel, or immunosuppressants, including sirolimus (Lee *et al.*, 2018). Based on the important progress in avoiding complications through stent coatings, high expectations are currently placed in this technology. Medical device coatings are seen as a multifunctional platform that can enhance the overall performance of the medical device and increase patient quality of life (Khan *et al.*, 2014). Antibiotic and antimicrobial coatings are especially investigated (Zhao *et al.*, 2009; Salwiczek *et al.*, 2014) due to the risk of failure caused by bacterial infections (Schierholz and Beuth, 2001; Pye *et al.*, 2009). Some orthopaedic implants use antibiotic loaded bone cement to treat osteomyelitis (Espehaug *et al.*, 1997; Bistolfi *et al.*, 2011). The use of local antibiotics, such as gentamicin and erythromycin, leads to a constant and high antibiotic concentration around the affected zone that would not be attained using systemic administration. The combination of both types of administration showed the best outcomes (Espehaug *et al.*, 1997), however, some studies showed that antibiotic-loaded bone cements have similar or better effects than systemic administration of antibiotics alone (Josefsson and Kolmert, 1993; Chiu *et al.*, 2002).The development of a safe, long-lasting localised antimicrobial coating on medical device surfaces would therefore be a valuable method to keep the implant free of bacterial colonisation and subsequently decrease the likelihood of peri-implant infections (Goodman *et al.*, 2013).

In this chapter, the development of an antimicrobial coating on laser melted Ti6Al4V was investigated. The coating was composed of a self-assembled layer of ODPA, covalently bound to the $TiO_2$ layer through the phosphate heads. Triclosan-loaded liposomes were then attached to the ODPA layer. It was hypothesised that the attachment occurred via hydrophobic forces: the ODPA aliphatic chains are thought to have formed a hydrophobic bond with the phospholipids of the liposomes (Figure 4.29). Physicochemical characterisations and antimicrobial activity assessment were performed to evaluate this coating.

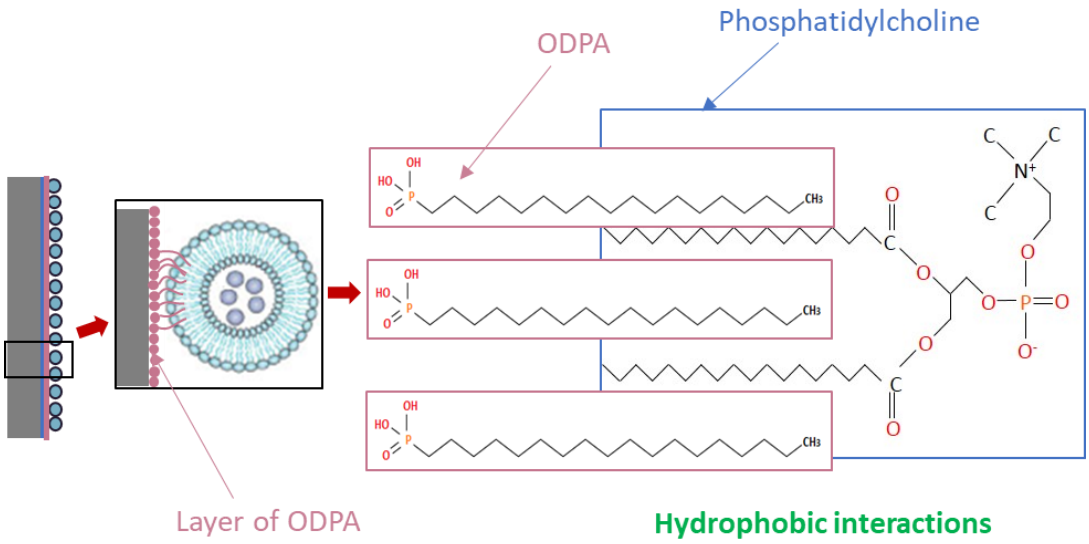


**Figure 4.29. Hydrophobic interactions between the ODPA alkyl chains and the liposomal phosphatidylcholine**

Characterisation of the discs in Chapter 1 showed the presence of an oxide layer at the surface. The $TiO_2$ layer allowed the attachment of ODPA to the surface via the self-assembled monolayers (SAM) method and stabilisation by heating. Studies have shown the simple attachment of alkanephosphonic acids to a number of metals and alloys, such as Al, Cu, Ti, or stainless steel (Adden *et al.*, 2006; Luschtinetz *et al.*, 2007; Ding *et al.*, 2010; Lim *et al.*, 2010; Dai *et al.*, 2014; Ayre *et al.*, 2016). Most studies used an organic solvent, such as THF or toluene, to obtain an ODPA solution in which substrates were immersed. ODPA is an amphiphilic molecule constituted of a phosphorus polar head and an alkyl chain, however, due to its long alkyl chain composed of 18 carbons, its solubility in aqueous solutions is poor, with a logP of 7.2 according to the open chemistry database PubChem (2018). ODPA attaches to metals by forming bonds between the metallic atoms and the polar head $PO_3^-$ through oxygen (Gawalt *et al.*, 2001). The unheated molecules appear to adhere to the surface through hydrogen bonds. Heating transforms the phosphonic acid into phosphonate by dehydration, resulting in a covalent interaction (Gawalt *et al.*, 2001). This was confirmed in the present study: the unheated molecules were washed off by the rinsing solution, and no phosphorus was detected by XPS, whilst phosphorus was detected when a heat treatment was performed before rinsing. The necessity of heating was also observed by Lim and co-workers (2010). The polar head can attach to the surface according to three configurations: mono-, bi-, or tri-dentate interactions with the oxide layer (Gouzman *et al.*, 2006). In a monodentate interaction, one oxygen

links the $PO_3^-$ to the oxide layer, whilst in bi- and tri-dentate interactions, two and three oxygens bind the polar head, respectively (Figure 4.30).

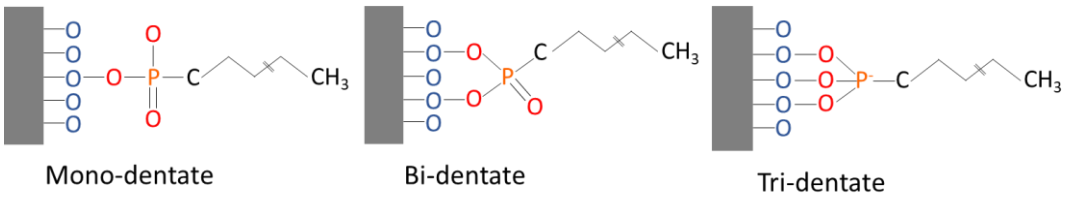


**Figure 4.30. Configurations of covalent binding of ODPA to $TiO_2$.**

Outcomes from studies differ greatly: Luschtinetz's team (2007) and Lim et al (2010) showed that mono- and bi-dentate interactions were predominantly taking place, whilst Gouzman and co-workers (2006), and Yah et al (2012) detected the disappearance of P-O and P=O bonds, concluding that a tridentate interaction was predominant. High resolution XPS and FTIR were used to obtain these results. Although Ding et al (2010) and Dai and co-workers (2014) did not mention the configuration of attachment, the FTIR spectra presented peaks corresponding to P-O and P=O, leading to the suggestion that the majority of interactions were composed of mono- and bi-dentate bonds. In the present study, P-O-H bonds were found. This shows that monodentate interactions may have taken place. The covalent attachment of ODPA molecules to $TiO_2$ appears to be achieved in two steps. A monodentate interaction takes place first, followed by bi- and tridentate (Lafont, 2009). However, the study of the phosphonic acid interactions with metal atoms is recognised to be difficult to assess (Lafond *et al.*, 2003). Studies showed an increase in surface contact angle after ODPA coating. An increase in surface contact angle was also observed in this study, indicating a more hydrophobic surface. This increase can be explained by the configuration taken by the molecules of ODPA at the substrate surface: the polar head is covalently bound to the metallic oxide layer, whilst the hydrophobic alkyl chain faces outward. The surrounding molecules are consequently in contact with the alkyl chains. Studies incubated substrates for various periods of time, from dip-coating (D. Chen *et al.*, 2014) to 240 h (Balaur *et al.*, 2005). By analysing the results using DoE, this research showed that the concentration in ODPA had a positive impact on attachment to the substrate: an increase in concentration was correlated to an increase in phosphorus percentage at the surface. A greater positive effect in attachment was found between 0.5 mM and 1 mM ODPA, than between 1 mM and 5 mM ODPA. This may show that a concentration limit in ODPA exists above which

no further increase in attachment would occur. Numerous studies have used low concentrations of ODPA (Woodward *et al.*, 1996; Kim *et al.*, 2002; Balaur *et al.*, 2005; Gouzman *et al.*, 2006; Dai *et al.*, 2014), the highest investigated concentration being 2 mM (Woodward *et al.*, 1997). The attachment of ODPA to the surface was, however, not homogenous and high variability was observed on different areas of the same surface. This can be expected, as the SAM method is not controlled.

The attachment of liposomes to the functionalised surfaces was successful. It is thought that the liposomes attached to the ODPA layer through lipophilic interactions between the alkyl chains of the ODPA and the phosphatidylcholine (Zheng *et al.*, 2014). Chandrawati et al (2009) showed attachment of liposomes to surfaces via cholesterol and formulated the same hypothesis. The imaging showed an increase in liposomal coverage with increased ODPA concentration during the disc coating process. The coverage obtained was low, reaching a maximum of 6.82 % coverage of the disc surface. The liposomal attachment to the Ti6Al4V surface was not uniform: aggregates of liposomes were observed in some areas of the discs whilst no liposomes were detected in other areas. It was hypothesised that this may be a consequence of the heterogeneity of ODPA coverage on the surface. Woodward and colleagues (1996) found similar results and described the attachment of ODPA to mica as “dense islands” presenting “a compact, rounded morphology”, and surrounded by areas of bare mica. The team described this attachment as the first step “prior to forming a complete monolayer”. Woodward and co-workers incubated mica discs in 0.2 mM ODPA in THF for 1 min, 2 min, 5 min, 10 min, 30 min and 120 min and measured the attachment using AFM. Before 30 min, images showed aggregates of ODPA that grew larger with increased incubation time. At 30 min and 120 min, a dense coverage could be observed on the AFM images. The static water contact angle reached a maximum of 89 °, which is similar to the dynamic contact angle results this study observed. Woodward et al also observed a high variation in molecular adsorption between experiments, which is consistent with the high inter-experiment variability found in this study. The control of the coating process may allow a better uniformity of ODPA coverage on the disc surface and enhance the homogeneity of the liposomal coating, leading to a denser liposomal attachment. This control may be achieved through active covalent binding of an antimicrobial to the linking molecule.

The total amount of triclosan contained in the liposomal coating, as well as its release profile were measured by HPLC. The total amount of triclosan on the coated surfaces was low, with 20.82 µg detected. This corresponds to the low liposomal coverage

measured by fluorescence. The release study showed that less than 10 % of the total amount of triclosan was detected after 140 h incubation in water. It can be hypothesized that the triclosan, a highly hydrophobic molecule, remained predominantly within the liposomes. Everett (2017) also observed this outcome using a methylcellulose hydrogel containing triclosan liposomes. The release of triclosan reached 20 % and plateaued over 168 h in water. A burst release profile was noticed between 0 h and 24 h, followed by a plateau from 24 h to 168 h release.

MLVs were used during this study, their size and polydispersity were consequently high. After heating the liposomal suspensions at 80 °C for 10 min, the liposomes presented a non-significant increase in size and an unaffected zeta potential. This suggested that liposomes could withstand temperatures as high as 80 °C for 10 min and remain stable during their incorporation into molten agar at 60 °C. Studies have shown that liposomes can be autoclaved (Kikuchi *et al.*, 1991; Zuidam *et al.*, 1993). The process resulted in a low degradation of the phosphatidylcholine and no loss of hydrophobic molecules. This result confirmed the hypothesis that the triclosan-loaded liposomes did not release their contents whilst heated to 80 °C for 10 min.

Triclosan was chosen as a drug model in this research project due to its high hydrophobicity and its efficacy against a wide range of bacteria, including microbes involved in the pathogenesis of peri-implantitis. Its encapsulation was performed using the thin film hydration method. The encapsulation efficiency of triclosan into liposomes was high, with a mean encapsulation efficiency of 94 %. This parameter is influenced by the structure of the molecule to be encapsulated, as well as by the liposome constituents and method of preparation of the liposomes (Kulkarni and Vargha-Butler, 1995; Lee *et al.*, 2005; Liu and Park, 2009). Kulkarni and Vargha-Butler (1995) investigated the encapsulation of four hydrophobic compounds in MLVs. They showed that the encapsulation efficiency increased with increasing hydrophobic properties of the molecule to be encapsulated. This may explain the high encapsulation efficiency of triclosan into liposomes, as triclosan presents a high hydrophobicity with a logP of 4.76, according to PubChem (PubChem, 2018b). The activity of free triclosan and triclosan-loaded liposomes was tested using *F. nucleatum* and *P. gingivalis*. No growth was observed in suspensions that were incubated with free triclosan. This shows that 300 µg/mL was an effective concentration against *F. nucleatum* and *P. gingivalis*. Bacterial suspensions cultured after incubation with triclosan-loaded liposomes showed a significant reduction in growth compared with bacteria in PBS. These data suggest that for the same concentration in triclosan, liposomal triclosan and free triclosan presented a similar antimicrobial activity. El-

Zawawy and colleagues (2015b) observed a higher antimicrobial activity with liposomal triclosan compared with free triclosan against the parasite *Toxoplasma gondii*. Another concentration of triclosan-loaded liposomes was tested: 100 µg/mL triclosan, 1 mg/mL lipids. A step-like reduction was observed for *P. gingivalis* between the 300 µg/mL triclosan, 3 mg/mL lipids and 100 µg/mL triclosan, 1 mg/mL lipids. This phenomenon was also observed by Everett (2017) against *E. faecalis* and *S. anginosus*. *F. nucleatum*, however, did not show a step-like reduction between both concentrations. The reduction was as high after incubation with 100 µg/mL triclosan, 1 mg/mL lipids, as after incubation with 300 µg/mL triclosan, 3 mg/mL lipids. This suggests that *F. nucleatum* was more sensitive to triclosan than *P. gingivalis* in PBS. The culture results could not determine if 300 µg/mL triclosan had a bactericidal or bacteriostatic effect and if the presence of liposomes modified this effect. To investigate this, bacterial imaging after incubation in free triclosan 300 µg/mL and triclosan-loaded liposomes 300 µg/mL, 3 mg/mL was performed. Bacteria appeared red after incubation in both conditions. This suggests that the concentration of 300 µg/mL triclosan had a bactericidal effect on *P. gingivalis* and *F. nucleatum* in NaCl solution. The interpretation and quantification of the imaging of the bacterial suspensions incubated in liposomes was challenging as SYTO9, the green fluorophore from the LIVE/DEAD™ BacLight™ kit, bound in a non-specific manner to the liposomes.

The MICs of free triclosan and triclosan-loaded liposomes were investigated using the agar dilution method. Triclosan liposomes presented an MIC of 300 µg/mL for *F. nucleatum* and 75 µg/mL for *P. gingivalis*. This suggests that *P. gingivalis* was more sensitive to triclosan liposomes than *F. nucleatum* on agar. This result is in contradiction with the experiment performed in PBS and NaCl solution. *F. nucleatum* is a faster growing bacterium than *P. gingivalis*. The presence of nutrients within the agar may have helped *F. nucleatum* to proliferate despite the presence of triclosan up to 300 µg/mL. No MIC was found for free triclosan against *F. nucleatum* in the concentration range of 37.5 µg/mL to 300 µg/mL. The free triclosan MIC was higher than the triclosan-loaded liposome MIC for *P. gingivalis*. Furthermore, the MICs detected for free and encapsulated triclosan were higher than the MICs showed in the literature, which ranged from 3 µg/mL to 50 µg/mL for *P. gingivalis* and 6 µg/mL to 50 µg/mL for *F. nucleatum* (Bradshaw *et al.*, 1993; Villalaín *et al.*, 2001; McBain *et al.*, 2003; Nudera *et al.*, 2007; Cullinan *et al.*, 2014). It was hypothesised that while the agar was setting, free triclosan may have precipitated due to its high hydrophobicity or may have bound to agar proteins as a way to increase its hydrophilicity (Grove *et*

*al.*, 2003). Both phenomena would hinder the antimicrobial activity of the compound. Blank liposomes as well as agar containing 1 % IPA did not show a reduction in bacterial growth.

## 4.5 Conclusion

This research has demonstrated the possibility to develop an antimicrobial coating on laser melted Ti6Al4V. The attachment of ODPA to Ti6Al4V and of liposomes to the ODPA-coated Ti6Al4V was successful. A low attachment of ODPA, and consequently of liposomes, to the surfaces was detected, however, a better control over the ODPA attachment process may lead to a denser and more homogenous liposomal coverage. The encapsulation of triclosan within the liposomes was high. During the release studies, the triclosan appeared to remain within the liposomes, however its antimicrobial activity was not hindered by its retention, according to the high reduction in bacterial viability observed.

This piece of research is a proof of concept showing the feasibility of coating laser melted Ti6Al4V using antimicrobial liposomes. The assessment of the coating antimicrobial activity and robustness is needed to carry this work further.

# Chapter 5. Antimicrobial coating assessment

## 5.1 Introduction

Since the success of cardiac stents coated with anti-cancerous and immunosuppressive agents to avoid cell colonisation of the stent and restenosis, novel medical device coatings have triggered great interest among clinicians and researchers. Due to the prevalence of implant infections, a substantial amount of research currently focuses on antimicrobial coatings. Some of these coatings are already commercially available, such as the central venous catheter Cook Spectrum® lined with minocycline and rifampicin, DAC® (Defensive Antimicrobial Coating; Drago *et al.*, 2014; Malizos *et al.*, 2017), or UTN PROtect® (Fuchs *et al.*, 2011). DAC® is a powder composed of hyaluronic and poly-lactic acids, which form a hydrogel when in contact with water or water-containing antibiotics. This hydrogel can be subsequently used to coat medical devices. UTN PROtect® is a titanium alloy tibial nail coated with gentamicin. Although some antimicrobial coatings have obtained regulatory authorisation, the vast majority have not yet proved sufficient antimicrobial activity *in vitro* or *in vivo* to justify clinical trials.

Several methods can be used to assess the surface antimicrobial activity *in vitro*, including international standards as well as non-standardised techniques. The ASTM E2149-01 standard involves the immersion of the antimicrobial surface in a bacterial suspension under dynamic conditions, followed by the culture and enumeration of CFUs of the surviving bacteria (ASTM, 2013). The AATCC standards, used in textile industries, comprise several protocols including:

- the culture and the CFU enumeration of the surviving bacteria after pouring a known volume of bacterial suspension on the antimicrobial fabric (Kugel *et al.*, 2011);
- the deposition of the material onto seeded agar to measure the subsequent zone of inhibition (AATCC, 2016b);

- the deposition of the test material onto agar previously streaked with several concentrations of the relevant inoculum to observe the area of inhibited growth around test material (AATCC, 2016a).

Other techniques are frequently used, such as live/dead staining followed by fluorescent imaging (Grapski and Cooper, 2001; Park *et al.*, 2006; Edupuganti *et al.*, 2007; Huang *et al.*, 2008); optical density monitoring (Alt *et al.*, 2004); the imprint of the non-textile material on agar and subsequent CFU enumeration (Thorn *et al.*, 2005; Park *et al.*, 2006); and techniques based on tetrazolium salts (Chen *et al.*, 2010; De L. Rodríguez López *et al.*, 2019).

Bacteria commonly used to assess antimicrobial activity in dental-related research are *S. aureus*, *S. epidermidis*, *S. mutans*, *A. actinomycetemcomitans*, and *P. gingivalis* (Kim *et al.*, 2008; Gallardo-Moreno *et al.*, 2009; Huang *et al.*, 2010; Kizuki, Matsushita and Kokubo, 2014; Lv *et al.*, 2014; Zhao *et al.*, 2014; Winkel *et al.*, 2015; Gallardo-Moreno *et al.*, 2009; Norowski *et al.*, 2011; Winkel *et al.*, 2015; Yucesoy *et al.*, 2015; Lin *et al.*, 2011; He *et al.*, 2014; Kawabe *et al.*, 2014; Ji *et al.*, 2015; Kos *et al.*, 2015; Yucesoy *et al.*, 2015; Lin *et al.*, 2011; Norowski *et al.*, 2011; Park *et al.*, 2014; K. V. Holmberg *et al.*, 2013; Mei *et al.*, 2014; Park *et al.*, 2014; Ji *et al.*, 2015). Although *S. aureus*, *S. epidermidis*, and *S. mutans* are commonly employed to test antimicrobial activity in dental research, they are not relevant pathogens in the context of dental implant infections (Mombelli and Décaillet, 2011).

### 5.1.1 Aims and Ojectives

This chapter assessed the antimicrobial activity of the triclosan liposomal coating against *F. nucleatum* and *P. gingivalis* with and without preconditioning for 1 h and 24 h incubation.

## 5.2 Materials and methods

### 5.2.1 Materials

ODPA, anhydrous THF, L-α-phosphatidylcholine (extracted from egg yolk, Type XVI-E), and cholesterol were obtained from Sigma Aldrich-Merck (Haverhill, UK). Chloroform, $K_2CO_3$ and ethanol were purchased from ThermoFisher Scientific (Eugene, Oregon, USA).

*F. nucleatum* subsp. *vincentii* ATCC® 49256™ (originally isolated from a human periodontal pocket) and *P. gingivalis* NCTC 11834 (originally isolated from a human gingival sulcus) were used in these studies. FAA and FAB were obtained from Lab M (Lancashire, UK).

Defibrinated horse blood was obtained from TCS Biosciences (Buckingham, UK). The LIVE/DEAD™ BacLight™ Bacterial Viability Kit stain was purchased from ThermoFisher Scientific (Eugene, Oregon, USA). Glass beads (500-750 µm) were obtained from Acros Organics (Thermo Fisher Scientific, Geel, Belgium).

### 5.2.2 Disc preparation

Five surface treatments with and without preconditioning were tested against *F. nucleatum* and *P. gingivalis*:

- Untreated Ti6Al4V
- Untreated Ti6Al4V preconditioned with AS
- ODPA-coated Ti6Al4V
- ODPA-coated Ti6Al4V preconditioned with AS
- Liposomal-coated Ti6Al4V (blank liposomes, 3 mg/mL lipids)
- Liposomal-coated Ti6Al4V (triclosan liposomes, 300 µg/mL triclosan, 3 mg/mL lipids)
- Liposomal-coated Ti6Al4V preconditioned with AS (blank liposomes, 3 mg/mL lipids)
- Liposomal-coated Ti6Al4V preconditioned with AS (triclosan liposomes, 300 µg/mL triclosan, 3 mg/mL lipids)
- Triclosan-coated Ti6Al4V

- Triclosan-coated Ti6Al4V preconditioned with AS.

The conditioning processes are described below.

Prior to any use, the Ti6Al4V discs were brushed for 30 seconds each side under tap water to remove any adherent particles. The discs were then immersed three times in 70 % ethanol for 30 seconds, followed by three rinses in sterile water. The samples were finally sterilised by autoclaving. The untreated discs did not undergo any further handling and remained in a sealed and sterile environment until further use.

All the other discs were ODPA coated. The discs were incubated in 5 mM ODPA-THF solution for 1 h (five discs in 10 mL), as determined in Chapter 4. The samples were air-dried prior to baking for 1 h at 180 °C. The discs were then immersed in the rinsing solution containing 5 mL 1.5 M $K_2CO_3$ in 10 mL ethanol for 20 min, followed by three washes in water. The ODPA-coated discs were air-dried.

Liposomal suspensions were prepared as described in Chapter 4, Section 4.2.4.1. The liposomal-coated discs were first ODPA-coated as mentioned above, were then incubated in liposomal solution for 1 h followed by a rinsing step in sterile water to remove loosely attached liposomes. The blank liposomal coating was obtained by incubating discs in 3 mg/mL blank liposomes, whilst the triclosan liposomal coating was obtained by immersing the discs in 3 mg/mL liposomes containing 300 µg/mL triclosan.

The triclosan-coated discs were first ODPA-coated as mentioned above, then incubated in 300 µg/mL triclosan in 1 % IPA in sterile water for 1 h followed by a rinsing step in sterile water.

Half the total number of discs from each condition described above (untreated, ODPA-coated blank liposome-coated, triclosan liposome-coated and triclosan-coated discs) were preconditioned with AS. AS was prepared as described in Chapter 3, Section 3.2.7.1. Discs were incubated in AS for 15 h prior to use.

### 5.2.3 Culture

All bacteria were initially cultured under anaerobic conditions (anaerobic gas mixture: 10 % $CO_2$, 10 % $H_2$, 80 % $N_2$) on FAA supplemented with 5 % (v/v) defibrinated horse blood, at 37 °C for 72 h to 96 h. A loop of bacterial colonies was transferred to 5 mL pre-reduced FAB at 37 °C for 15 h without agitation. Broth cultures were then diluted

in 20 mL of pre-reduced FAB to an $OD_{600}$ of 0.08 and further diluted to an optimal starting concentration.

Bacterial suspensions were cultured in FAB to mid-log phase. Ti6Al4V discs were incubated in suspension for 1 h, rinsed in sterile PBS and placed in a bijou bottle. The discs were vortexed for 1 min with 200 mg of sterile glass beads (500-750 µm) in 1 mL of sterile PBS. The resulting bacterial suspension was serially diluted and plated on to FAA using a spiral plater (Whitley Automatic Spiral Plater, Don Whitley Scientific, West Yorkshire, UK). *F. nucleatum* and *P. gingivalis* were then cultured anaerobically at 37 °C for 3 and 7 days, respectively. Colony forming units (CFU/mL) from the Ti6Al4V discs were enumerated. The experiment was performed with single species as well as both species mixed together (dual species). Both species were differentiated by colony morphology: *F. nucleatum* forms white colonies, whilst *P. gingivalis* colonies appear black.

### 5.2.4 Live/dead stain

Bacterial suspensions were cultured in FAB to mid-log phase. Ti6Al4V discs were incubated in suspension for 1 h and 24 h then rinsed in 0.9 % (w/v) NaCl. Adherent bacteria were stained using the LIVE/DEAD™ BacLight™ kit. Three images of randomly selected fields of view (658x551 µm, magnification x100) were obtained using a fluorescent microscope. The percentage coverage and bacterial viability were then assessed by image analysis using Comstat2 software as stated in Chapter 3, Section 3.2.5.

### 5.2.5 Statistical analysis

All experiments involving CFU enumeration were performed three times and included internal triplicates. Experiments involving bacterial imaging were performed three times but did not include internal replicates. Two-way analysis of variance (ANOVA) was performed for the experiments presented in this chapter. When a p value of $< 0.05$ was found, a Bonferroni multiple comparisons post-test was performed between all groups.

## 5.3 Results

### 5.3.1 Culture

#### 5.3.1.1 *Fusobacterium nucleatum*

Unconditioned surfaces showed a high number of *F. nucleatum* colonies (Figure 5.1): untreated and ODPA-coated Ti6Al4V surfaces presented $1.18 \times 10^8$ CFU/mL ($\pm 5.39 \times 10^6$) and $1.05 \times 10^8$ CFU/mL ($\pm 9.75 \times 10^6$) respectively. A significant reduction in colonies was observed in the presence of the blank liposome coating and triclosan liposome coating, with $8.02 \times 10^7$ CFU/mL ($\pm 2.38 \times 10^7$; $p = 0.0169$) and $6.71 \times 10^7$ CFU/mL ($\pm 3.49 \times 10^7$; $p = 0.0006$) respectively. The CFU/mL further decreased after contact with the triclosan-coated Ti6Al4V with $1.68 \times 10^7$ CFU/mL ($\pm 1.10 \times 10^7$; $p = 0.0006$ compared with triclosan liposome-coated surfaces).

Preconditioning decreased the total number of colonies recovered from most surfaces: $3.07 \times 10^7$ CFU/mL ($\pm 1.76 \times 10^6$; $p < 0.0001$) were recovered from untreated Ti6Al4V, $2.98 \times 10^7$ CFU/mL ($\pm 2.99 \times 10^6$; $p < 0.0001$) from ODPA-coated Ti6Al4V, $2.73 \times 10^7$ CFU/mL ($\pm 3.15 \times 10^6$; $p = 0.0171$) from blank liposome-coated surface and $1.47 \times 10^7$ CFU/mL ($\pm 5.09 \times 10^6$; $p = 0.0188$) from triclosan liposome-coated surfaces. A reduction in CFU/mL was also observed between unconditioned triclosan-coated surfaces and preconditioned triclosan-coated surfaces, however this reduction was not significant, with $3.27 \times 10^6$ CFU/mL ($p > 0.9999$) recovered from triclosan-coated Ti6Al4V. In the presence of AS, neither liposomal or triclosan coatings decreased the colony counts in a significant manner.

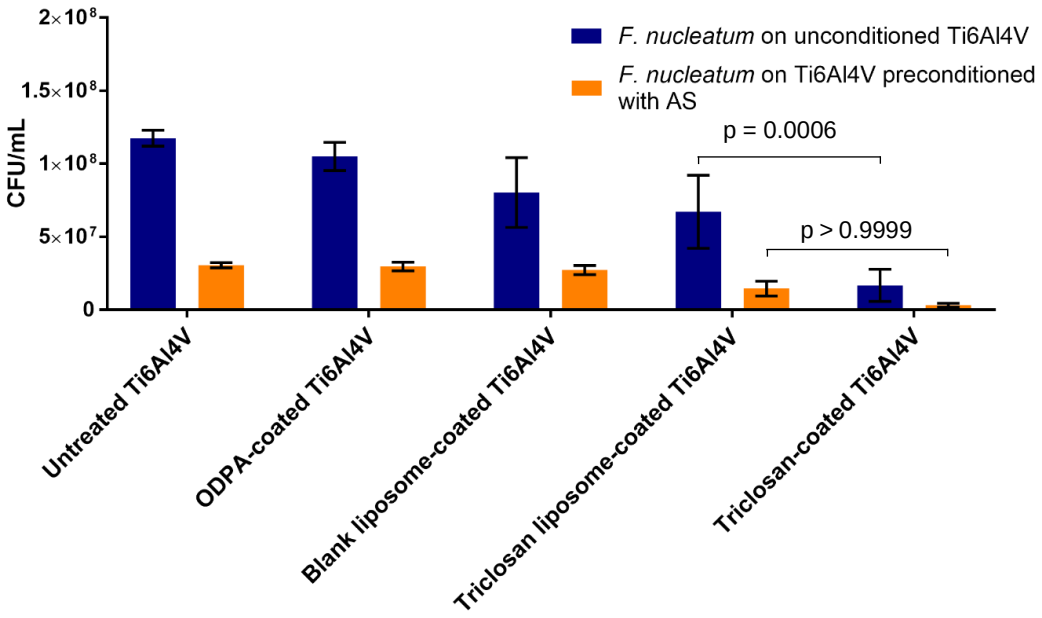


**Figure 5.1. *F. nucleatum* colony counts on unconditioned and AS-preconditioned Ti6AL4V. Mean values of 3 independent experiments in triplicate are shown. Error bars represent standard error of the mean.**

### 5.3.1.2 *Porphyromonas gingivalis*

*P. gingivalis* presented a similar colony count on unconditioned untreated and unconditioned ODPA-coated surfaces (Figure 5.2) with $7.93 \times 10^7$ CFU/mL ($\pm 8.67 \times 10^6$) and $6.56 \times 10^7$ CFU/mL ($\pm 8.99 \times 10^6$) respectively. A significant reduction in viability was observed when *P. gingivalis* was in the presence of blank liposome-coated, triclosan liposome-coated and triclosan-coated Ti6Al4V surfaces, with $4.09 \times 10^7$ CFU/mL ($\pm 5.97 \times 10^6$; $p = 0.0129$), $3.00 \times 10^7$ CFU/mL ($\pm 3.15 \times 10^6$; $p = 0.0008$) and $1.06 \times 10^7$ CFU/mL ($\pm 4.80 \times 10^6$; $p < 0.0001$), respectively. However, no significance was detected between triclosan liposome-coated and triclosan-coated Ti6Al4V.

Preconditioning with AS increased the number of *P. gingivalis* colonies to $1.64 \times 10^8$ CFU/mL ($\pm 1.57 \times 10^7$; $p < 0.0001$ compared with unconditioned untreated samples) and $1.53 \times 10^8$ CFU/mL ($\pm 1.08 \times 10^7$; $p < 0.0001$ compared with unconditioned ODPA-coated samples) for untreated and ODPA-coated Ti6Al4V surfaces, respectively. The AS inhibited the antimicrobial/antifouling activity of the blank and triclosan liposomes: $1.56 \times 10^8$ CFU/mL ($\pm 1.74 \times 10^7$) and

1.58 x $10^8$ CFU/mL (± 1.77 x $10^7$) were recovered, respectively. With 6.93 x $10^7$ CFU/mL (± 3.82 x $10^7$), the total number of colonies recovered from the triclosan-coated surfaces was significantly reduced compared with preconditioned untreated Ti6Al4V, which showed 1.64 x $10^8$ CFU/mL (± 1.57 x $10^7$; $p < 0.0001$). The reduction was also significant compared with preconditioned triclosan liposome coated Ti6Al4V ($p < 0.0001$).

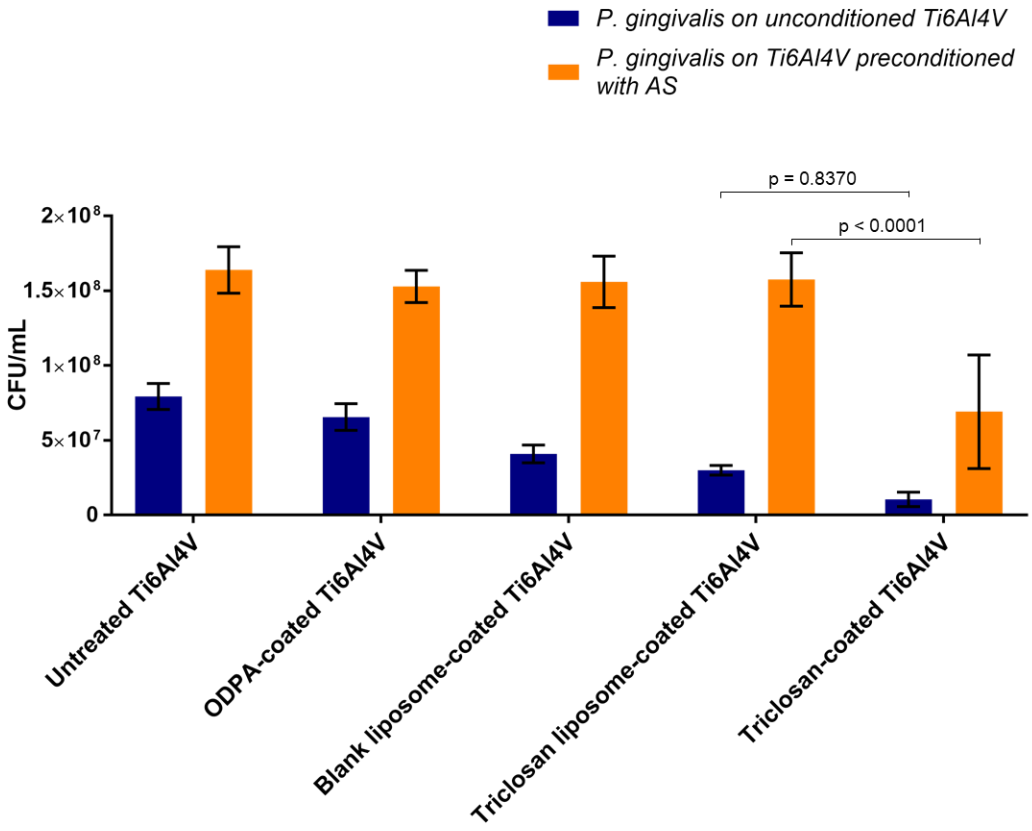


**Figure 5.2. *P. gingivalis* colony counts on unconditioned and AS-preconditioned Ti6Al4V. Mean values of 3 independent experiments in triplicate are shown. Error bars represent standard error of the mean.**

### 5.3.1.3 Dual species

The incubation of *F. nucleatum* and *P. gingivalis* together resulted in an overall reduction in both species colony counts on all unconditioned surfaces (Figure 5.3). *F. nucleatum* presented 2.36 x $10^7$ CFU/mL (± 6.63 x $10^6$), 2.22 x $10^7$ CFU/mL (± 1.98 x $10^6$), 1.62 x $10^7$ CFU/mL (± 4.95 x $10^6$), 1.56 x $10^7$ CFU/mL (± 8.26 x $10^6$) and 9.31 x $10^6$ CFU/mL (± 5.88 x $10^6$) for untreated, ODPA-coated, blank liposome-

coated, triclosan liposome-coated, and triclosan-coated Ti6Al4V surfaces, respectively. *P. gingivalis* showed a similar reduction with $4.67 \times 10^6$ CFU/mL ($\pm 1.92 \times 10^6$), $4.86 \times 10^6$ CFU/mL ($\pm 2.19 \times 10^6$), $4.00 \times 10^6$ CFU/mL ($\pm 1.76 \times 10^6$), $2.22 \times 10^6$ CFU/mL ($\pm 4.44 \times 10^5$) and $1.58 \times 10^6$ CFU/mL ($\pm 5.84 \times 10^5$) for untreated, ODPA-coated, blank liposome-coated, triclosan liposome-coated, and triclosan-coated Ti6Al4V surfaces, respectively.

The preconditioning further decreased the overall colony count for both species in a non-significant manner compared with unconditioned surfaces (all p values were above 0.9999). *F. nucleatum* presented similar colony counts for untreated and ODPA-coated Ti6Al4V with $1.69 \times 10^7$ CFU/mL ($\pm 8.44 \times 10^6$) and $1.56 \times 10^7$ CFU/mL ($\pm 7.78 \times 10^6$), respectively, whilst a non-significant decrease was detected for blank liposome-coated, triclosan liposome-coated, and triclosan-coated Ti6Al4V, with $9.78 \times 10^6$ CFU/mL ($\pm 4.89 \times 10^6$; $p > 0.9999$), $8.89 \times 10^6$ CFU/mL ($\pm 4.44 \times 10^6$; $p > 0.9999$) and $4.16 \times 10^6$ CFU/mL ($\pm 3.60 \times 10^6$; $p > 0.9999$), respectively. *P. gingivalis* presented $6.67 \times 10^5$ CFU/mL ($\pm 3.85 \times 10^5$) and $1.33 \times 10^6$ CFU/mL ($\pm 6.67 \times 10^5$), on untreated and ODPA-coated surfaces respectively. Few *P. gingivalis* colonies were recovered from blank liposome-coated, triclosan liposome-coated and triclosan-coated surfaces leading to low total colony counts, with $4.44 \times 10^5$ CFU/mL ($\pm 2.22 \times 10^5$), $4.44 \times 10^5$ CFU/mL ($\pm 2.22 \times 10^5$), and $4.44 \times 10^4$ CFU/mL ($\pm 2.22 \times 10^4$), respectively. The antimicrobial coatings had no significant effect on the bacteria incubated together with or without preconditioning with AS. This may be due to the high variability that can be observed between repeats for each condition.

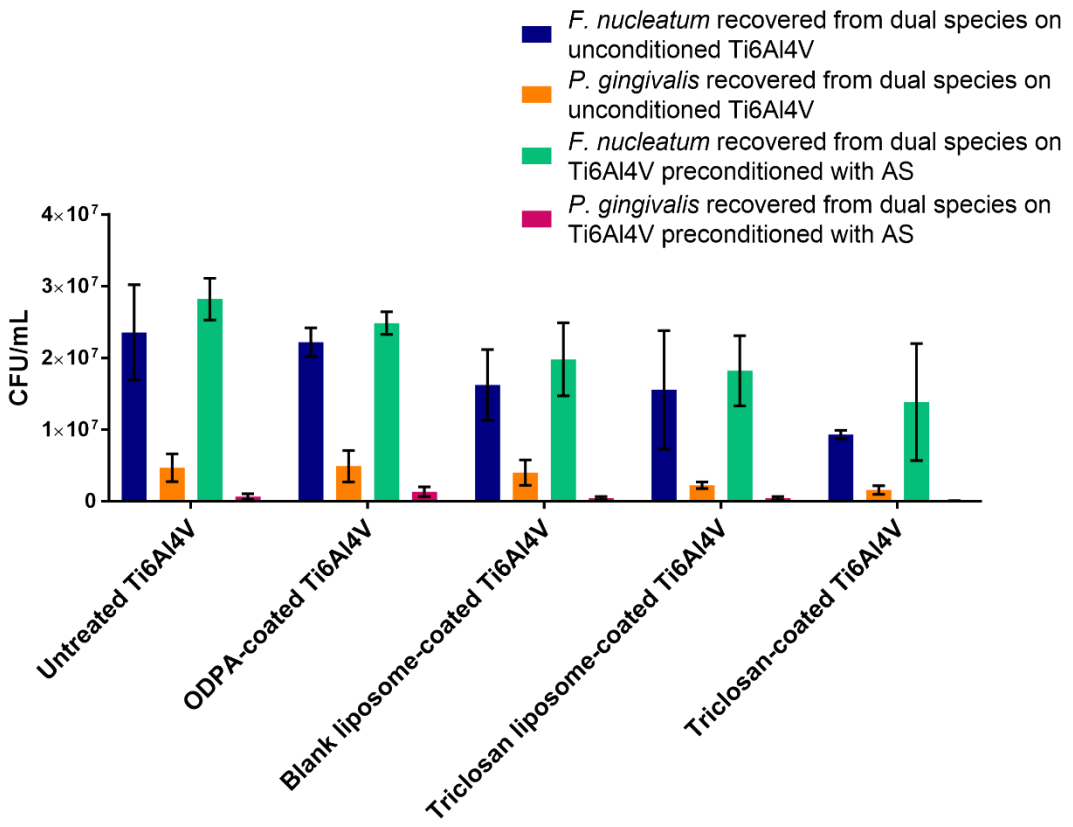


**Figure 5.3. *F. nucleatum* and *P. gingivalis* colony counts on unconditioned and AS-preconditioned Ti6Al4V after incubation together. Mean values of 3 independent experiments in triplicate are shown. Error bars represent standard error of the mean.**

### 5.3.2 Live/dead stain

Similar to Chapter 4, the liposomes present on the liposomal coating were stained by the SYTO9, the green fluorophore found in the LIVE/DEAD™ BacLight™ kit (Figure 5.4 and Figure 5.5). Consequently, the quantification of attachment as well as viable and dead bacteria could not be performed. These two parameters were however calculated for untreated, ODPA-coated and triclosan-coated surfaces.

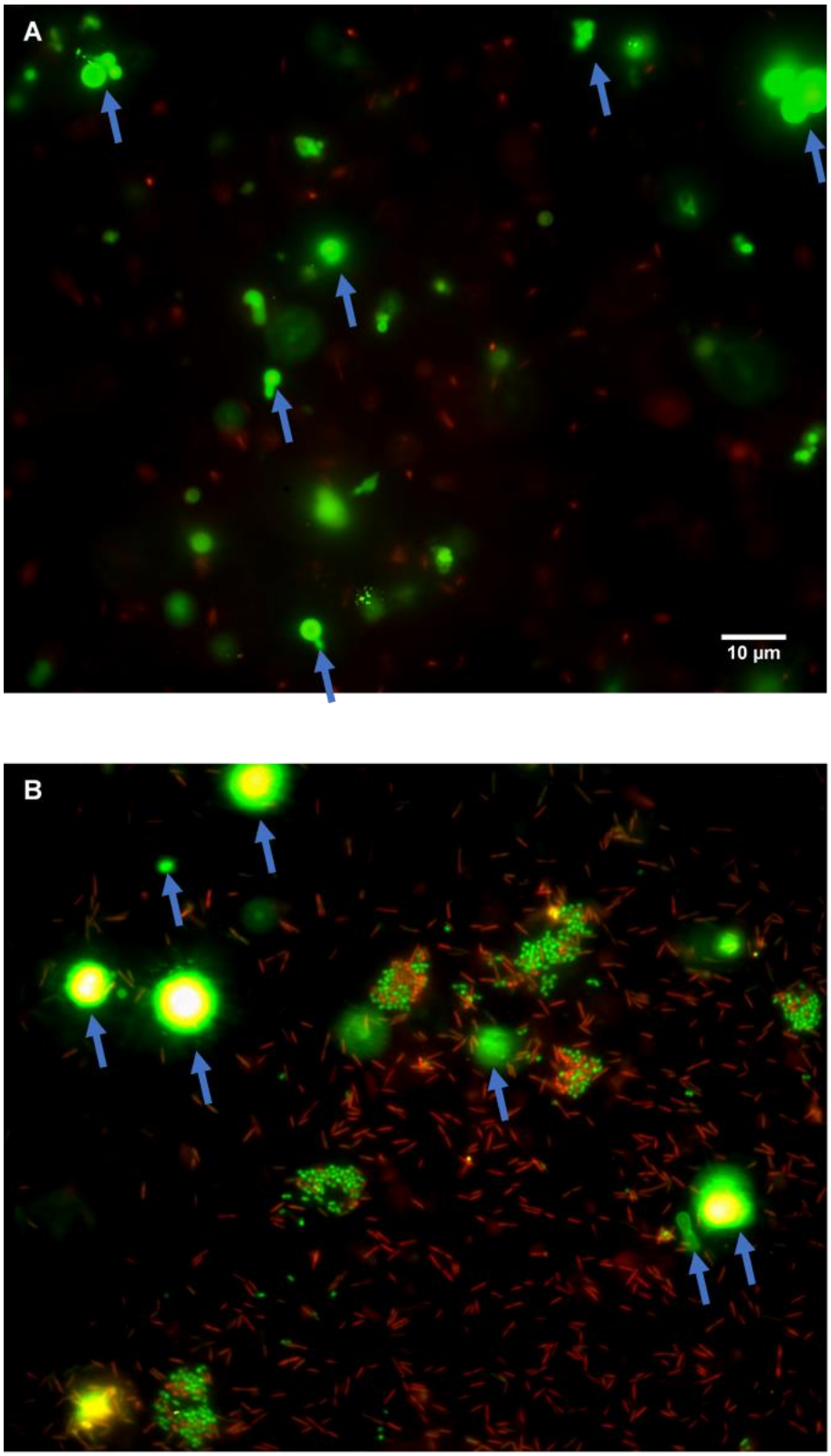


**Figure 5.4. Liposomes stained by the SYTO9 fluorophore (magnification x100). The images were focused on the bacteria, which led to the blurry appearance of the liposomes, indicated by the blue arrows.**

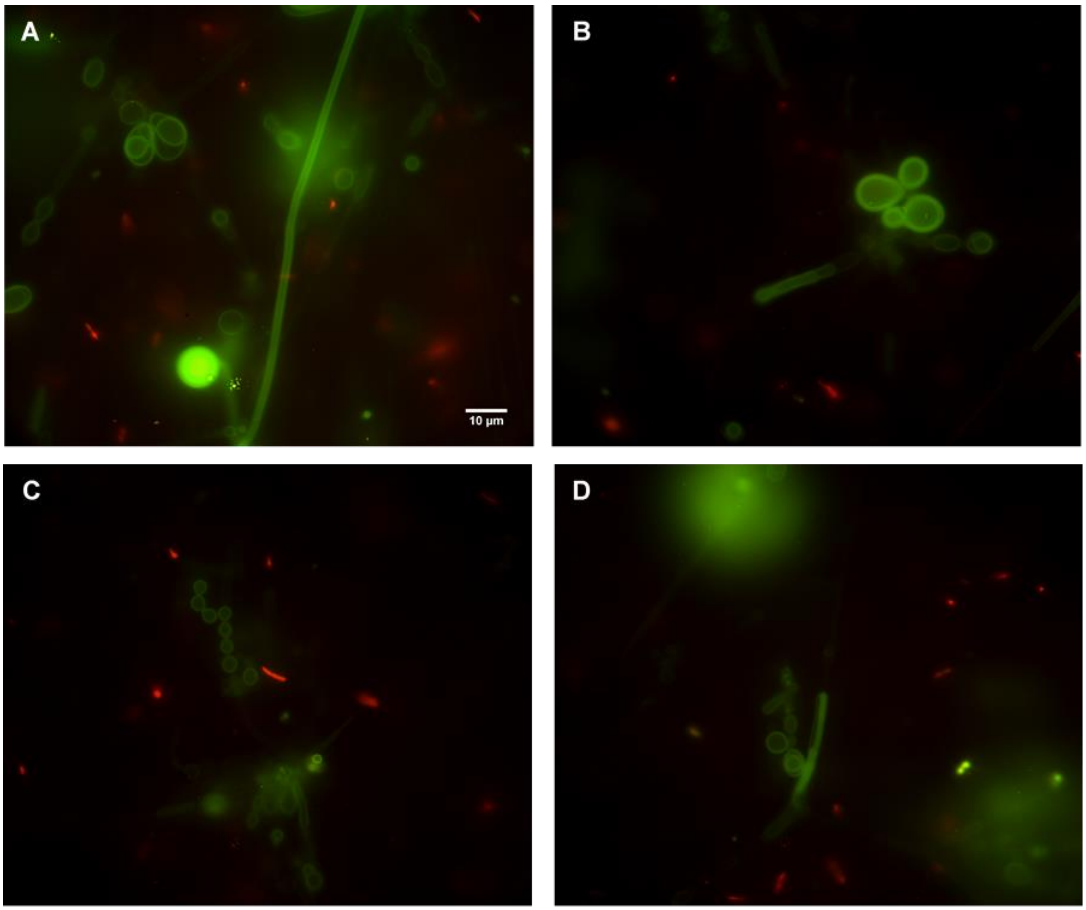


**Figure 5.5. Liposomes stained by the SYTO9 fluorophore (magnification x100). The images were focused on the liposomes, which led to the disappearance of the bacteria, which were not on the same depth as the liposomes.**

#### 5.3.2.1 *Fusobacterium nucleatum*

At 1 h incubation on unconditioned surfaces, *F. nucleatum* presented 25 % (± 4.90) coverage and 94 % (± 3.53) viability on untreated Ti6Al4V and 25 % (± 2.23) coverage and 95 % (± 2.53) viability on ODPA-coated Ti6Al4V (Figure 5.6 and Figure 5.7). Triclosan-coated Ti6Al4V showed a significant increase in attachment compared with untreated and ODPA-coated Ti6Al4V, with 41 % (± 3.99; $p = 0.0284$) coverage. The detected viability, however, significantly fell to 9 % (± 0.63; $p < 0.0001$). Preconditioning with AS appeared to have caused a significant reduction in *F. nucleatum* attachment on untreated Ti6Al4V with 8 % coverage (± 0.18; $p = 0.0161$), however the viability remained similar with 90 % (± 5.09; $p > 0.9999$) viable bacteria. A significant reduction in attachment was also detected on the triclosan-coated surfaces with 8 % coverage (± 1.39; $p = 0.0161$) after preconditioning, whilst the viability increased to 29 % (± 13.75; $p > 0.9999$). Finally,

no significant modification was observed for *F. nucleatum* in contact with the ODPA-coated surfaces with 15 % coverage (± 6.25; p = 0.5681) and 89 % viability (± 2.86; p > 0.9999) after preconditioning.

At 24 h incubation on unconditioned surfaces, attachment reached 31 % (± 2.83) coverage on untreated surfaces, 39 % (± 3.90) coverage on ODPA-coated Ti6Al4V, and 23 % (± 0.61) coverage on triclosan-coated surfaces (Figure 5.8). *F. nucleatum* showed a viability of 91 % (± 1.05), 81 % (± 3.14) and 0 % (± 0.02) in contact to untreated, ODPA-coated and triclosan-coated surfaces, respectively (Figure 5.9). Preconditioning did not modify significantly *F. nucleatum* attachment, with 39 % (± 4.91; p > 0.9999), 25 % (± 5.52; p = 0.4093) and 33 % (± 2.28; p > 0.9999) coverage for untreated, ODPA-coated and triclosan-coated surface, respectively. Viability also remained constant with 95 % (± 0.97; p > 0.9999), 97 % (± 0.78; p = 0.1344) and 6 % (± 1.10; p > 0.9999) viable bacteria detected in the presence of untreated, ODPA-coated and triclosan-coated Ti6Al4V, respectively.

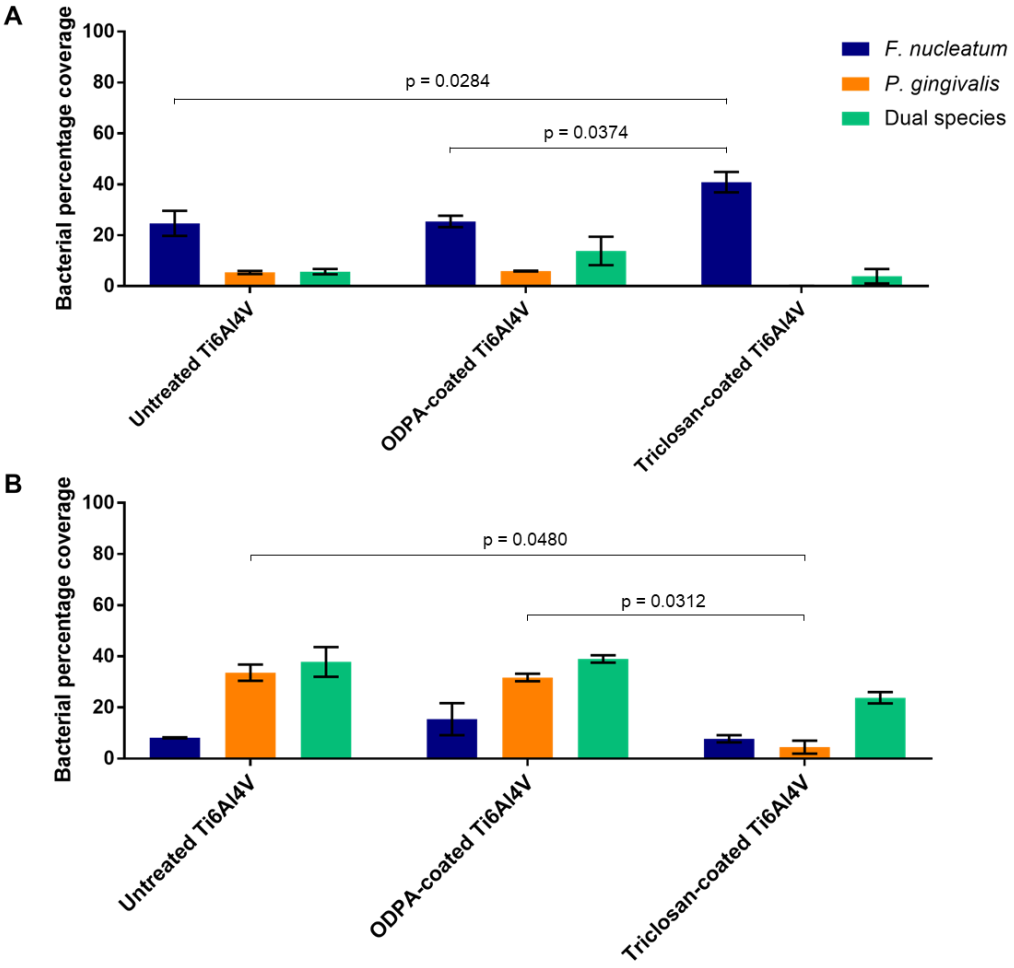


**Figure 5.6. Bacterial percentage coverage on unconditioned (A) and AS-preconditioned (B) Ti6Al4V surfaces after 1 h incubation. Mean values of 3 independent experiments are shown. Error bars represent standard error of the mean.**

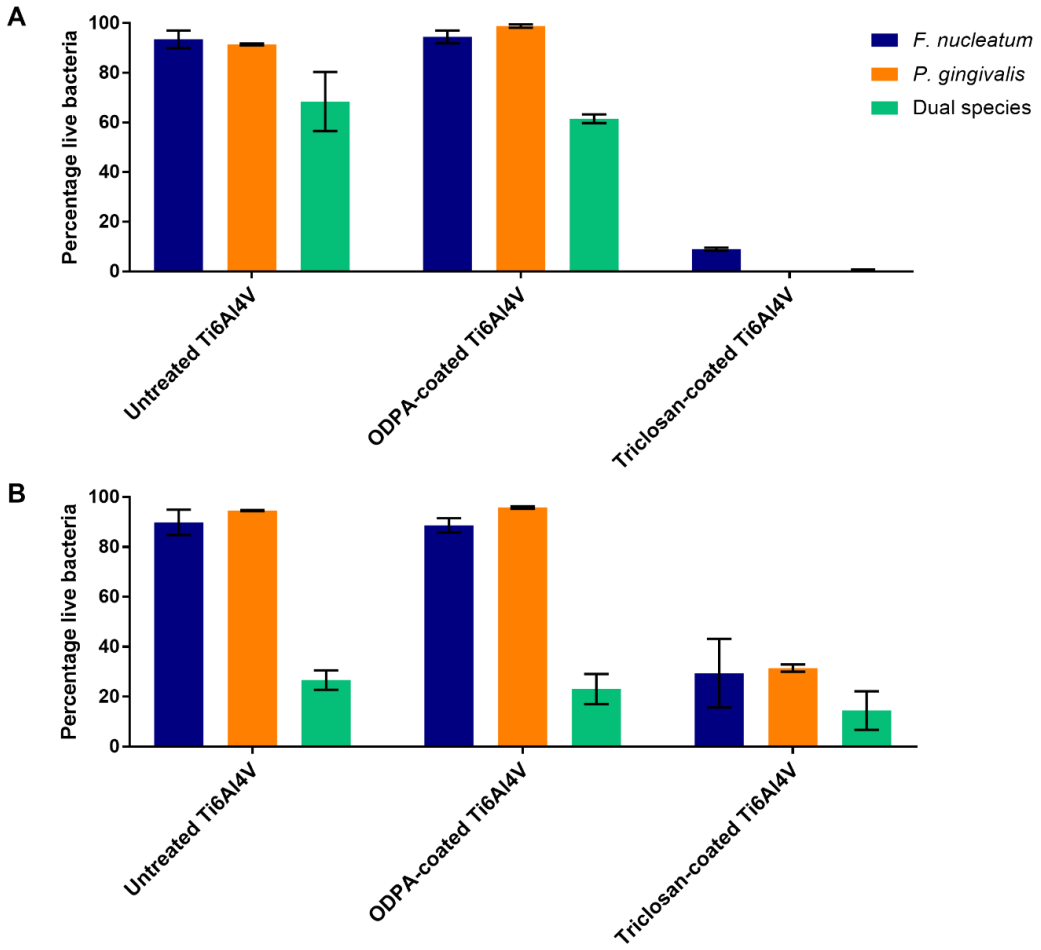


**Figure 5.7. Bacterial viability on unconditioned (A) and preconditioned with AS (B) Ti6Al4V surfaces after 1 h incubation. Mean values of 3 independent experiments are shown. Error bars represent standard error of the mean.**

### 5.3.2.2 *Porphyromonas gingivalis*

At 1 h incubation on unconditioned surfaces, *P. gingivalis* presented 5 % (± 0.60), 6 % (± 0.17) and 0 % (± 0.02) coverage on untreated, ODPA-coated and triclosan-coated Ti6Al4V respectively (Figure 5.6). *P. gingivalis* was also found to be viable at 92 % (± 0.38) and 99 % (± 0.71) on untreated and ODPA-coated Ti6Al4V. The triclosan-coated surfaces demonstrated a 0 % (± 0.00) viability. The preconditioning with AS increased the overall coverage of *P. gingivalis* to 34 % (± 3.13), 32 % (± 1.44) and 5 % (± 2.54) on untreated, ODPA-coated and triclosan-coated surfaces, respectively. No significant impact ($p > 0.9999$) on viability was observed in the presence of untreated and ODPA-coated surfaces, with 95 % (± 0.23) and 96 % (± 0.51) bacteria

viable. However, preconditioning with AS significantly increased *P. gingivalis* viability on triclosan-coated surfaces to 31 % (± 1.47; p = 0.0110).

At 24 h incubation on unconditioned surfaces, coverage was detected at 24 % (± 3.06), 11 % (± 7.93) and 1 % (± 0.51) on untreated, ODPA-coated and triclosan-coated surfaces respectively, whilst 15 % (± 2.99), 8 % (± 7.05) and 1 % (± 0.20) coverage were detected on untreated, ODPA-coated and triclosan-coated surfaces respectively after preconditioning with AS (Figure 5.8). No significance between unconditioned and preconditioned surfaces was detected (p > 0.9999 for all unconditioned versus preconditioned surfaces). Similar to 1 h incubation, preconditioning with AS did not affect viability on untreated and ODPA-coated surfaces at 24 h incubation with 98 % (± 1.01) and 100 % (± 0.13; p > 0.9999) *P. gingivalis* viable respectively, compared with 100 % viability on unconditioned untreated (± 0.00; p > 0.9999) and unconditioned ODPA-coated surfaces (± 0.19; p > 0.9999). A significant increase from 14 % (± 1.26) viable bacteria on unconditioned triclosan-coated Ti6Al4V to 31 % (± 6.23; p = 0.0420) was however observed (Figure 5.9).

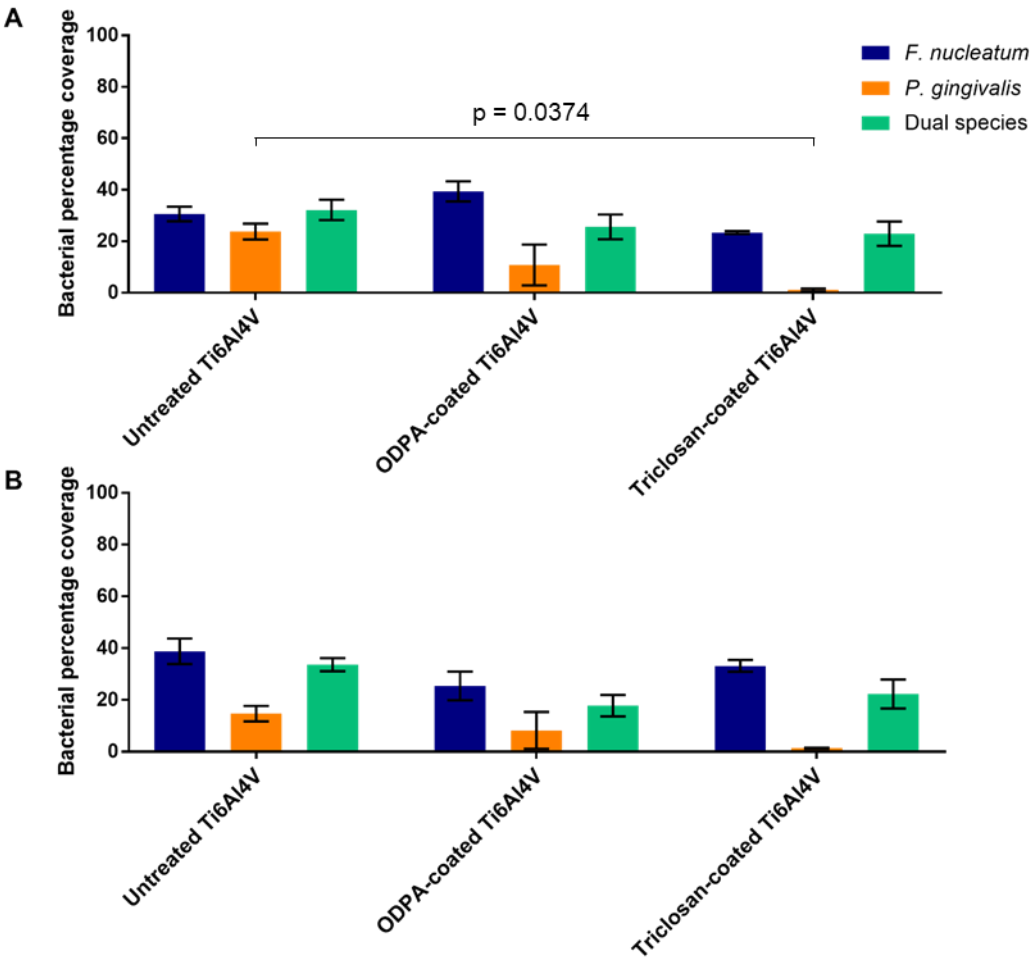


**Figure 5.8. Bacterial percentage coverage on unconditioned (A) and AS-preconditioned (B) Ti6Al4V surfaces after 24 h incubation. Mean values of 3 independent experiments are shown. Error bars represent standard error of the mean.**

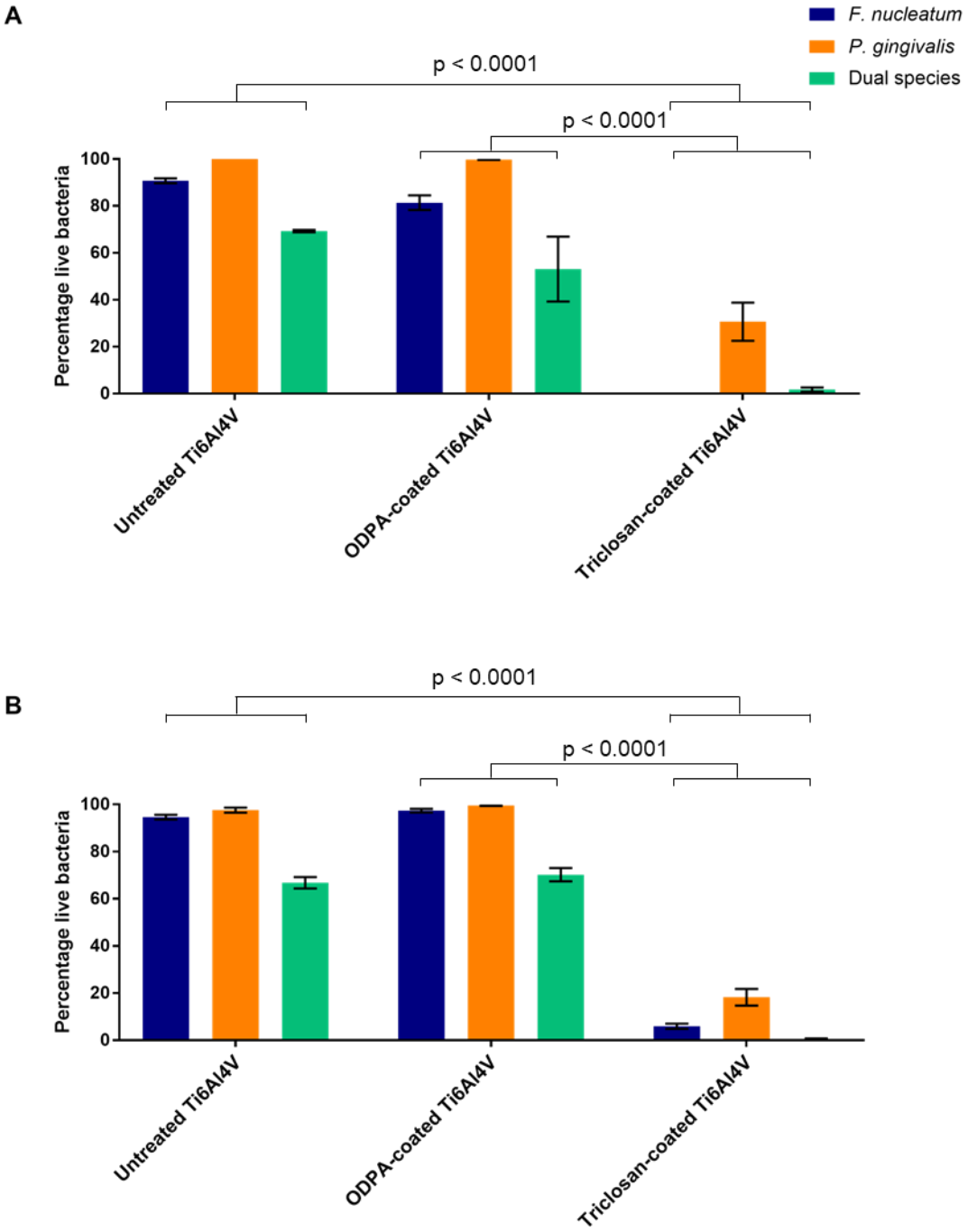


**Figure 5.9. Bacterial viability on unconditioned (A) and preconditioned with AS (B) Ti6Al4V surfaces after 24 h incubation. Mean values of 3 independent experiments are shown. Error bars represent standard error of the mean.**

#### 5.3.2.3 Dual species

At 1 h incubation on unconditioned surfaces, the overall attachment detected was much lower than during single species experiments: untreated, ODPA-coated and triclosan-coated surfaces respectively presented 6 % (± 1.07), 14 % (± 5.58) and 4 % (± 2.82) attachment to Ti6Al4V (Figure 5.6). The viability also decreased to 68 % (± 11.85), 62 % (± 1.77) and 1 % (± 0.29; $p < 0.0001$) when in contact to untreated, ODPA-coated and triclosan-coated Ti6Al4V respectively (Figure 5.7). The preconditioning of surfaces with AS appeared to increase the overall attachment on all tested surfaces significantly: 38 % ($p < 0.0001$), 39 % ($p < 0.0001$) and 24 % ($p = 0.0020$) coverage were observed on untreated, ODPA-coated and triclosan-coated Ti6Al4V respectively. Despite the overall increase in attachment on all surfaces, a significant difference in attachment was observed between untreated and triclosan-coated surfaces ($p = 0.0480$). A significant reduction in viability however, was noticed on untreated and ODPA-coated surfaces after preconditioning with AS with 27 % (± 3.84; $p = 0.0001$) and 23 % (± 6.03; $p = 0.0004$) viable bacteria, whilst a non-significant increase reaching 15 % (± 7.72) viability was found on triclosan-coated Ti6Al4V.

At 24 h incubation, attachment was very similar between all surfaces, indifferent of the presence or absence of AS (Figure 5.8). Unconditioned surfaces presented 32 % (± 3.95), 26 % (± 4.79) and 23 % (± 4.72) coverage, whilst preconditioned surfaces showed 34 % (± 2.51; $p > 0.9999$), 18 % (± 4.20; $p > 0.9999$) and 22 % (± 5.60; $p > 0.9999$) coverage for untreated, ODPA-coated and triclosan-coated Ti6Al4V respectively. Viability was also unaffected by the presence or absence of preconditioning: untreated, ODPA-coated and triclosan-coated Ti6Al4V presented 69 % (± 0.50), 53 % (± 13.85) and 2 % (± 0.87) viability respectively on unconditioned surfaces and 67 % (± 2.41; $p > 0.9999$), 70 % (± 2.83; $p = 0.0822$) and 1 % (± 0.17; $p > 0.9999$) viability after preconditioning (Figure 5.9).

## 5.4 Discussion

Interest in antimicrobial coatings is increasing as the number of implant placements and subsequently the number of implant infections increase (Albrektsson *et al.*, 2014). A high dose of antimicrobials and antibiotics can be administered locally while

avoiding the adverse toxic effects that the same dose would trigger after systemic administration. Antimicrobial coatings allow the delivery of a high local concentration of antimicrobials for a prolonged period of time, leading to a healthier environment surrounding the implant (Goodman *et al.*, 2013; Cyphert and von Recum, 2017). In this chapter, the antimicrobial coating developed during this project was assessed using different conditions: incubation in single and dual species of *F. nucleatum* and *P. gingivalis* suspensions for 1 h or 24 h in the presence or absence of preconditioning with AS. Two methods were used to assess the antimicrobial coating efficacy: culture, the discs were vortexed after 1 h incubation and the bacteria plated onto FAA; and imaging, the bacteria were directly stained on the discs with the LIVE/DEAD™ BacLight™ Bacterial Viability kit to assess attachment and viability.

The culture results showed that the triclosan liposome coating and the triclosan coating significantly reduced the total number of colonies found in single species experiments. The blank liposome coating also presented a reduction in bacteria. The liposomes prepared during this project were composed of cholesterol and phosphatidylcholine. Phosphatidylcholine is known for its antifouling properties, though the mechanisms are not fully understood. Ishihara's team (Ishihara *et al.*, 1992; Ishihara and Iwasaki, 1998) had hypothesised that the antifouling property does not come from 'no interaction' with proteins, but rather the fact that it allows constant reversible interactions. This appears to come from the high level of hydration of the phosphatidylcholine molecule which allows the environmental proteins to interact with the surface through weak, easily desorbed van der Waals forces. In another study, Ishihara et al (1998) noticed that the proteins adsorbing weakly to the phosphatidylcholine-containing polymer experienced little configuration change from the native state, whereas proteins adsorbed to a polymer that did not contain phosphatidylcholine underwent a considerable conformation modifications. It was also hypothesised that the fluidity and mobility of the phosphatidylcholine and other antifouling molecules may play a role in keeping protein-surface interactions weak. Jeon and colleagues (1991) worked with polyethylene oxide and explained that the approach of a protein toward the polymer induces a contraction of the chains, which leads to a steric repulsion of the chains between themselves and of the approaching protein. The steric repulsion force overtakes the weak van der Waals attractive forces and the protein is repelled. High density polymer coating and longer polymer chains exhibit stronger repulsion forces due to the increase in chain compression. The triclosan-loaded liposomes may therefore demonstrate two properties: an anti-fouling and an antimicrobial activity. When comparing the imaged unconditioned triclosan-

coated surfaces to the unconditioned untreated surfaces, the prior presented a significantly lower viability but a higher attachment of *F. nucleatum* at 1 h incubation. *P. gingivalis* however showed a significant reduction in viability and attachment in the presence of triclosan-coated surfaces. This is consistent with the findings in Chapter 3, in which it was observed that after preconditioning the Ti6Al4V surfaces with AS, *F. nucleatum* attachment decreased, whilst *P. gingivalis* surface coverage increased. It was hypothesised that this result was due to the increase in hydrophilicity of the surface after preconditioning. Due to the highly hydrophobic nature of triclosan, the Ti6Al4V surfaces may have become much more hydrophobic than untreated Ti6Al4V, leading to a decrease in *P. gingivalis* attachment and an increase in *F. nucleatum* attachment. Overall, the preconditioning with AS modified bacterial attachment after 1 h incubation. After 24 h incubation however, little difference was observed between unconditioned and AS preconditioned surfaces. It was hypothesised that a shift from electrostatic attachment to adhesion involving membrane proteins and appendages occurred, as this transition is usually considered to start after several hours of contact (Tuson and Weibel, 2013). The mechanisms of adhesion however, may have been adapted to the type of proteins available at the Ti6Al4V surface by the functionalisation. Rzhepishevska and colleagues (2013) found that the charge of the abiotic surface modified bacterial cell surfaces and the amount of extracellular matrix secreted, which led to the modification of the biofilm architecture. This shows the rapid adaptability of bacteria to their environment. Marshall and Cruickshank (1973), showed a modification in bacterial configuration during adhesion to surfaces and suggested that the orientation resulted from the repulsion of hydrophobic moieties of the cell from the surrounding aqueous phase. This implies that electrostatic interactions remain essential in bacterial adhesion involving proteins. It is also known that bacteria will employ some adhesins rather than others depending on the proteins available at the substrate surface (Tuson and Weibel, 2013). Overall, despite similar coverage between unconditioned and preconditioned surfaces after 24 h incubation, the mechanisms of adhesion may have differed. It would be interesting to incubate the surfaces for longer and study the biofilm structure using a confocal microscope, as well as investigating the proteins secreted by *F. nucleatum* and *P. gingivalis* for each type of surface.

It is interesting to note that *F. nucleatum* viability on unconditioned triclosan-coated surfaces decreased between 1 h and 24 h incubation, whilst attachment increased. It is hypothesised that the increase in bacterial mass did not hinder the contact between triclosan and the bacteria. Coating triclosan to Ti6Al4V did not reduce its antimicrobial

activity against *F. nucleatum*. *P. gingivalis* did not attach to the unconditioned triclosan-coated surfaces. After 24 h incubation, however the preconditioning enabled a higher rate of bacterial survival. AS may have inhibited the antimicrobial activity of triclosan by conjugation of the triclosan molecules to amphiphilic proteins of the AS. This phenomenon could happen due to the hydrophobic character of triclosan (PubChem, 2018a). The triclosan would not be free to diffuse across the protein layer and consequently would not make contact with the bacteria. Verifying if the triclosan does diffuse through the layer of adhered bacteria could be performed by staining the adhered bacteria and using the time lapse setting of a confocal microscope to observe in real time the effect of triclosan on the bacteria. If the triclosan can diffuse, the bacteria will lose their membrane integrity and the fluorophore will be released (Takenaka *et al.*, 2008; Davison *et al.*, 2010).

## 5.5 Conclusion

In conclusion, both culture and live/dead staining showed that on unconditioned surfaces, the triclosan liposome-coated surface had a noticeable and promising effect however, after preconditioning with AS no or little antimicrobial activity was observed. It is hypothesised that the AS may hinder the contact between triclosan and the bacteria, reducing the possibility for the triclosan to disrupt the bacterial fatty acid production or destabilise the bacterial membrane. This information is critical in terms of clinical outcomes: saliva contains bacteria and many more protein types than AS produced in laboratory. If a reduction in the antimicrobial efficacy of the coating was observed with AS, the contact with saliva in the patient's buccal cavity will potentially hinder the antimicrobial activity as well. This hypothesis strengthens the need for testing novel coatings in conditions close to or mimicking physiological conditions.

# Chapter 6: General summary and future work

Peri-implantitis is a progressive and irreversible disease characterised by an inflammation of the soft tissues surrounding the dental implant, an increase of pocket formation and a loss of supporting bone (Lindhe and Meyle, 2008; Renvert *et al.*, 2018; Schwarz *et al.*, 2018b). Its prevalence is currently estimated at 22 % (Derks and Tomasi, 2015). In 5 % to 20 % of cases, peri-implantitis leads to implant failure, requiring implant removal (Rosenberg *et al.*, 2004; Moy *et al.*, 2005). The continued inflammation is due to a prolonged bacterial infection and a modification in the composition of the microbiota: a complex and heterogenous infection takes place including an increase in Gram negative anaerobes number such as *F. nucleatum* and *P. gingivalis* (Persson and Renvert, 2014). Opportunistic pathogens such as *P. aeruginosa* and *S. aureus* are also detected (Leonhardt *et al.*, 1999; Mombelli and Décaillet, 2011), as well as fungi, such as *Candida spp* or *Penicillum spp* (Leonhardt *et al.*, 1999; Albertini *et al.*, 2015; Schwarz *et al.*, 2015), and viruses, including human cytomegalovirus and Epstein-Barr virus (Jankovic *et al.*, 2011; Akram *et al.*, 2019). In studies investigating the histopathology of this condition, inflammatory lesions biopsied from peri-implantitis presented a high number of neutrophil granulocytes, lymphocytes and plasma cells (Sanz *et al.*, 1991; Cornelini *et al.*, 2001; Bullon *et al.*, 2004). A secretion of pro-inflammatory cytokines, such as IL-1α, IL-1β and TNFα, and an activation of osteoclasts was also detected (Konttinen *et al.*, 2006; Faot *et al.*, 2015). The progression of peri-implantitis tends to follow an accelerating pattern (Fransson *et al.*, 2010) and present large inflammatory lesions (Carcuac *et al.*, 2012). Due to the complex and not yet fully understood aetiology of peri-implantitis, multiple treatment protocols exist (Roccuzzo *et al.*, 2018). No consensus has currently been reached regarding the use of antimicrobials and antibiotics: numerous antibiotics and antimicrobials are used and their administration can be local or systemic according to the protocol used and clinician preference (Mombelli *et al.*, 2001; De Araújo Nobre *et al.*, 2006; Renvert *et al.*, 2006; Salvi *et al.*, 2007; Renvert *et al.*, 2008). A Cochrane meta-analysis conducted by Esposito and co-workers (2012) demonstrated that none

of the current treatments proves significantly better outcomes than the others. Despite the efforts made in finding treatment methods, Heitz-Mayfield and Mombelli (2014) showed cases of progression, recurrence and non-resolution of peri-implantitis in their systematic review.

The main aim of this project was to develop an antimicrobial coating onto laser melted Ti6Al4V in order to prevent biofilm formation *in vitro*. In a clinical setting, the main advantage of antimicrobial coatings is the ability to deliver high concentrations of antimicrobials locally by bypassing the systemic administration. The local delivery avoids the adverse effects the same high dose would trigger after systemic administration (Goodman *et al.*, 2013; Cyphert and von Recum, 2017).
The proposed antimicrobial comprised three main components: ODPA, triclosan, and liposomes composed of phosphatidylcholine and cholesterol. ODPA was used to link the liposomes to the Ti6Al4V surface through its amphiphilic properties: the polar head, composed of phosphorus and oxygen forms a covalent bond with $TiO_2$ (Gawalt *et al.*, 2001), whilst its aliphatic chain forms a hydrophobic bond with the phospholipids of the liposomes. Liposomes were chosen for their biocompatibility, their capacity to encapsulate several, hydrophilic and lipophilic molecules and the possibility to anchor them to surfaces. Liposomes also enable a prolonged and controlled drug delivery and may in some cases enhance the drug activity (Lian and Ho, 2001; Samad *et al.*, 2007; El-Zawawy *et al.*, 2015d). Triclosan was selected due to its broad-spectrum antimicrobial activity and its wide use in oral health products, such as toothpastes and mouth rinses. Its efficacy against Gram negative bacteria was demonstrated by several studies (Jones *et al.*, 2000; Cullinan *et al.*, 2003; McBain *et al.*, 2004; Nudera *et al.*, 2007; Sreenivasan *et al.*, 2011).
The laser melted and milled surfaces were compared in order to investigate the effect of the manufacturing process on the material surface properties. No significant difference was detected between surfaces from both manufacturing processes in terms of material characterisation. This project found that *F. nucleatum* and *P. gingivalis* were able to attach directly to unconditioned and AS-preconditioned Ti6Al4V without the aid of early colonisers. This is a clinically crucial finding as biofilm formation on metallic surfaces may differ from the traditional scientific belief: late colonisers may take part of the early colonisation of the metallic surfaces, especially in parts that are shielded from oxygen and saliva flow such as the abutment. The biofilm structure and composition may consequently differ at the peri-implant mucosa margin. Investigation employing in situ hybridization techniques such as fluorescent

in situ hybridization, such as the experiments conducted by Mark Welch and colleagues (2016) on the oral microbiome is needed to analyse the structure of plaque formed on abutments in humans. During this study, it was observed that *F. nucleatum* attachment increased over time indifferent of the presence or absence of preconditioning with AS. The presence of AS did however cause a decrease in *F. nucleatum* attachment. *F. nucleatum* viability increased over time on unconditioned surfaces but remained low and constant on preconditioned surfaces. *P. gingivalis* attachment was low and constant on unconditioned Ti6Al4V, whilst it increased significantly on preconditioned surfaces. Its viability was high regardless of surface preconditioning. It was hypothesised that the difference in *F. nucleatum* and *P. gingivalis* patterns of attachment and viability in the presence or absence of preconditioning originated from their membrane charge. *F. nucleatum* presented a membrane charge closer to neutral whereas a negatively charged membrane was detected for *P. gingivalis*. Preconditioning increased the surface charge as an increase in hydrophilicity was detected, caused by the adsorption of proteins contained in AS. Preconditioning may consequently have facilitated *P. gingivalis* attachment through an increase in electrostatic interactions between its protein membrane and the proteins adsorbed to the Ti6Al4V surface. This hypothesis was confirmed after attachment of triclosan to the metallic surfaces: it is hypothesised that the attachment of triclosan decreased the surface hydrophilicity. This reduction is thought to have led to the significant increase in *F. nucleatum* attachment, whilst *P. gingivalis* did not attach to triclosan-coated surfaces. No viability was observed on triclosan-coated surfaces. When incubated together, *F. nucleatum* and *P. gingivalis* did not present a synergistic effect during attachment. The attachment and viability remained constant regardless of preconditioning. It was hypothesised that their concomitant incubation may have increased their survival capacity during modulation of their environment (Mukherjee and Chandra, 2004; Harriott and Noverr, 2009; Lee *et al.*, 2014; Beardmore *et al.*, 2018; Estrela and Brown, 2018).

The liposomes were successfully attached to the ODPA-coated Ti6Al4V, however the attachment was not homogenous and aggregates were visualised. Woodward and colleagues (1996, 1997) showed that the aggregates formed by the ODPA molecules were the first step before the formation of a complete monolayer onto the surface. It is hypothesised that a longer incubation of the Ti6Al4V surfaces in ODPA solution may lead to the formation of a more uniform monolayer of ODPA and a higher attachment of liposomes. Woodward and colleagues however performed their experiments on mica, which may also affect the attachment of ODPA compared with

Ti6Al4V. The ODPA molecules appeared to have attached to the $TiO_2$ via mono- and bi-dentate interactions. According to Lafont (2009), the mono-dentate interactions are the first step of attachment of the ODPA molecules to the oxide layer. A longer baking time may consequently lead to a full bi-dentate or a tri-dentate interaction between the oxygens of the ODPA and $TiO_2$. Future work is needed to investigate these two hypotheses. The use of AFM would allow the visualisation of the ODPA coating to assess the uniformity.

Triclosan was successfully encapsulated into the liposomes at concentrations of 300 µg/mL into 3 mg/mL lipids and 100 µg/mL into 1 mg/mL lipids with a high encapsulation efficiency. Incubated in PBS, the triclosan liposomes significantly reduced the bacterial colony counts for both species at both concentrations. The MIC testing showed a MIC of 300 µg/mL and 75 µg/mL for *F. nucleatum* and *P. gingivalis*, respectively. The MIC detected for *P. gingivalis* was consistent with the previous experiment. The MIC found for *F. nucleatum* was however high and not consistent with the results from the culture experiment. It is hypothesised that *F. nucleatum* presented a high MIC value due to the presence of nutrients in the FAA compared with PBS. *F. nucleatum* tends to grow quickly on FAA and the presence of proteins may have helped it overcome the antimicrobial activity by proliferating fast. Imaging experiments showed that triclosan coated on the surfaces was bactericidal at a concentration of 300 µg/mL in NaCl solution. Free triclosan did not inhibit *F. nucleatum* and *P. gingivalis* growth at all tested concentrations. It is hypothesised that due to its hydrophobicity, free triclosan precipitated or complexed with the proteins in the molten agar. When attached to Ti6Al4V, the antimicrobial liposomal coating presented a significant antimicrobial activity on unconditioned surfaces, however the presence of AS on the coated surfaces decreased its antimicrobial activity. It is hypothesised that the proteins contained in the AS hindered the antimicrobial activity.

During the attachment to laser melted unconditioned Ti6Al4V, *F. nucleatum* presented branching patterns after 2 h incubation. It is hypothesised that *F. nucleatum* exploited modifications present at the surface and adhered primarily within the contours designed by the grain boundaries formed during laser melting. Two hypotheses were raised: the grain boundaries affected the surface topography despite the finely polishing process the surfaces underwent, or the composition of the surface at the grain boundary was different and influenced *F. nucleatum* attachment. Further investigation is required to elucidate this phenomenon.

In conclusion, a novel antimicrobial coating was developed that showed promising results against *F. nucleatum* and *P. gingivalis* when used on unconditioned Ti6Al4V. Optimisation is needed however in order for this coating to reach a higher efficacy in the presence of saliva and for this technology to be effective in a clinical context. The potential of this coating has not been fully explored as only one antimicrobial was tested. Future optimisation should include longer incubation in ODPA and baking time to investigate the possibility of the formation of a full monolayer at the surface. A greater number of liposomes may attach to a fully formed monolayer of ODPA. As the aetiology of peri-implantitis is bacterial accumulation, numerous antimicrobials or antibiotics efficient against pathogens involved in peri-implantitis could be encapsulated and their efficacy assessed. The cause however of peri-implantitis and its associated bone loss is the constant inflammatory response of the host. To further support the resolution of the inflammation, anti-inflammatory molecules could also be encapsulated along with antimicrobials within the liposomes.

# Bibliography


Aas, J. A. *et al.* (2005) 'Defining the Normal Bacterial Flora of the Oral Cavity', *Journal of Clinical Microbiology*, 43(11), pp. 5721–5732.

AATCC (2016a) *AATCC TM147-2016. Antibacterial Activity Assessment of Textile Materials: Parallel Streak Method*. USA: AATCC.

AATCC (2016b) *AATCC TM90-2016. Antibacterial Activity Assessment of Textile Materials: Agar Plate Method*. USA: AATCC.

Abrahamsson, I., Berglundh, T., Lindhe, J., *et al.* (1998) 'Soft tissue response to plaque formation at different implant systems. A comparative study in the dog.', *Clinical Oral Implants Research*, 9, pp. 73–79.

Abrahamsson, I., Berglundh, T., Glantz, P., *et al.* (1998) 'The mucosal attachment at different abutments. An experimental study in dogs.', *Journal of clinical periodontology*, 25(9), pp. 721–7.

Abrahamsson, I. and Cardaropoli, G. (2007) 'Peri-implant hard and soft tissue integration to dental implants made of titanium and gold', *Clinical Oral Implants Research*, 18, pp. 269–274.

Adams, L. K., Lyon, D. Y. and Alvarez, P. J. J. (2006) 'Comparative eco-toxicity of nanoscale TiO2, SiO2, and ZnO water suspensions', *Water Research*, 40(19), pp. 3527–3532.

Adden, N. *et al.* (2006) 'Phosphonic acid monolayers for binding of bioactive molecules to titanium surfaces', *Langmuir*, 22(19), pp. 8197–8204.

Akram, Z. *et al.* (2019) 'Current weight of evidence of viruses associated with peri-implantitis and peri-implant health: A systematic review and meta-analysis', *Reviews in Medical Virology*, 29(3), pp. 1–8.

Al-Askar, M. *et al.* (2018) 'Clinical and Radiographic Peri-Implant Parameters and Whole Salivary Interleukin-1β and Interleukin-6 Levels among Type-2 Diabetic and Nondiabetic Patients with and without Peri-Implantitis', *Medical Principles and Practice*, 27(2), pp. 133–138.

Al-Majid, A. *et al.* (2018) 'Matrix Metalloproteinase-8 as an Inflammatory and Prevention Biomarker in Periodontal and Peri-Implant Diseases', *International Journal of Dentistry*, 2018, pp. 1–27.

Al-Nawas, B. *et al.* (2001) 'Validation of three-dimensional surface characterising methods: scanning electron microscopy and confocal laser scanning microscopy', *Scanning*, 23(4), pp. 227–231.

Albertini, M. *et al.* (2015) 'Assessment of periodontal and opportunistic flora in patients with peri-implantitis', *Clinical Oral Implants Research*, 26(8), pp. 937–941.

Albrektsson, T. *et al.* (2014) 'Is marginal bone loss around oral implants the result of a provoked foreign body reaction?', *Clinical Implant Dentistry and Related Research*, 16(2), pp. 155–165.

Allen, T. M. *et al.* (2006) 'Phosphatidylserine as a determinant of reticuloendothelial recognition of liposome models of the erythrocyte surface.', *Proceedings of the National Academy of Sciences*, 85(21), pp. 8067–8071.

Allen, T. M. and Cullis, P. R. (2013) 'Liposomal drug delivery systems: From concept to clinical applications', *Advanced Drug Delivery Reviews*. Elsevier B.V., 65(1), pp. 36–48.

Aloise, J. P. *et al.* (2010) 'Microbial leakage through the implant-abutment interface of morse taper implants in vitro', *Clinical Oral Implants Research*, 21(3), pp. 328–335.

Alt, V. *et al.* (2004) 'In Vitro Testing of Antimicrobial Activity of Bone Cement', *Antimicrobial Agents and Chemotherapy*, 48(11), pp. 4084–4088.

American Type Culture Collection (2019) *Fusobacterium nucleatum subsp. vincentii Dzink et al. (ATCC® 49256™)*. Available at: https://www.lgcstandards-atcc.org/products/all/49256.aspx?geo_country=fr (Accessed: 29 March 2019).

Amoroso, P.-F. *et al.* (2006) 'Titanium surface modification and its effect on the adherence of Porphyromonas gingivalis: An in vitro study', *Clinical Oral Implants Research*, 17(6), pp. 633–637.

Aradigm (2019a) *Aradigm Announces Detailed Third Party Evaluation Results for Apulmiq (FDA)/Linhaliq (EMA)*. Available at: https://aradigm.gcs-web.com/news-releases/news-release-details/aradigm-announces-detailed-third-party-evaluation-results (Accessed: 2 May 2019).

Aradigm (2019b) *Product Pipeline: Inhalation Drug Treatments to Prevent and Treat Severe Respiratory Diseases*. Available at: http://www.aradigm.com/products_pipeline.html (Accessed: 2 May 2019).

Araujo, M. G. and Lindhe, J. (2017) 'Peri-implant health', *Journal of Periodontology*, 89(Suppl1), pp. 249–256.

De Araújo Nobre, M. *et al.* (2006) 'Non-surgical treatment of peri-implant pathology.', *International journal of dental hygiene*, 4(2), pp. 84–90.

Arhakis, A. *et al.* (2017) 'Social and Psychological Aspects of Dental Trauma,

Behavior Management of Young Patients Who have Suffered Dental Trauma', *The Open Dentistry Journal*, 11(1), pp. 41–47.

Arweiler, N. B. *et al.* (2001) 'Alcohol-free mouthrinse solutions to reduce supragingival plaque regrowth and vitality. A controlled clinical study.', *Journal of clinical periodontology*, 28(2), pp. 168–74.

Arweiler, N. B. *et al.* (2002) 'Effect of an amine-fluoride-triclosan mouthrinse on plaque regrowth and biofilm vitality', *Journal of Clinical Periodontology*, 29(4), pp. 358–363.

Asadishad, B., Ghoshal, S. and Tufenkji, N. (2011) 'Method for the Direct Observation and Quantification of Survival of Bacteria Attached to Negatively or Positively Charged Surfaces in an Aqueous Medium', *Environmental Science and Technhology*, pp. 8345–8351.

Ashok, C. *et al.* (2015) 'Synthesis and Characterization of MgO/TiO2 Nanocomposites', *Journal of Nanomedicine & Nanotechnology*, 6(6), p. 329.

Aspen Dental (2017) *Dental Implants Alternative to Dentures*. Available at: https://aspendds.com/content/dental-implants-alternative-dentures (Accessed: 16 April 2019).

ASTM (2013) *ASTM E2149 − 13a. Standard Test Method for Determining the Antimicrobial Activity of Antimicrobial Agents Under Dynamic Contact Conditions*. USA: ASTM.

ASTM International (2011) 'Standard Specification for Titanium and Titanium Alloy Bars and Billets'.

De Avila, E. D. *et al.* (2014) 'The relationship between biofilm and physical-chemical properties of implant abutment materials for successful dental implants', *Materials*, 7(5), pp. 3651–3662.

Ayre, W. N. *et al.* (2016) 'Fluorophosphonate-functionalised titanium via a pre-adsorbed alkane phosphonic acid: a novel dual action surface finish for bone regenerative applications', *Journal of Materials Science: Materials in Medicine*. Springer US, 27(2), p. 36.

Ba-Abbad, M. *et al.* (2012) 'Synthesis and Catalytic Activity of TiO2 Nanoparticles for Photochemical Oxidation of Concentrated Chlorophenols under Direct Solar Radiation', *Int. J. Electrochem. Sci.*, 7, pp. 4871–88.

Bachrach, G. *et al.* (2005) 'Fluorescence based measurements of Fusobacterium nucleatum coaggregation and of fusobacterial attachment to mammalian cells', *FEMS Microbiology Letters*, 248(2), pp. 235–240.

Baier, R. E. *et al.* (1982) 'Degradative effects of conventional steam sterilization on biomaterial surfaces', *Biomaterials*, 3(4), pp. 241–245.

Balaur, E. *et al.* (2005) ‘Tailoring the wettability of TiO2 nanotube layers’, *Electrochemistry Communications*, 7(10), pp. 1066–1070.

Barbour, M. E. *et al.* (2009) ‘Differential adhesion of Streptococcus gordonii to anatase and rutile titanium dioxide surfaces with and without functionalization with chlorhexidine’, *Journal of Biomedical Materials Research. Part A.*, 90(4), pp. 993–8.

Bayoudh, S. *et al.* (2006) ‘Quantification of the adhesion free energy between bacteria and hydrophobic and hydrophilic substrata’, *Materials Science and Engineering C*, 26(2–3), pp. 300–305.

Beardmore, R. E. *et al.* (2018) ‘Drug-mediated metabolic tipping between antibiotic resistant states in a mixed-species community’, *Nature Ecology and Evolution*. Springer US, 2(8), pp. 1312–1320.

Becker, S. T. *et al.* (2014) ‘Peri-Implantitis versus Periodontitis: Functional Differences Indicated by Transcriptome Profiling’, *Clinical Implant Dentistry and Related Research*, 16(3), pp. 401–411.

Behneke, A. *et al.* (2000) ‘Treatment of peri-implantitis defects with autogenous bone grafts: six-month to 3-year results of a prospective study in 17 patients.’, *The International journal of oral & maxillofacial implants*, 15(1), pp. 125–38.

Berglundh, T. *et al.* (1991) ‘The soft tissue barrier at implants and teeth’, *Clinical Oral Implants Research*, 2, pp. 81–90.

Berglundh, T. *et al.* (2004) ‘Histopathological observations of human periimplantitis lesions’, *Journal of Clinical Periodontology*, 31(5), pp. 341–347.

Berglundh, T. *et al.* (2011) ‘Are peri-implantitis lesions different from periodontitis lesions?’, *Journal of Clinical Periodontology*, 38(SUPPL. 11), pp. 188–202.

Berridge, M., Herst, P. and Tan, A. (2005) ‘Tetrazolium dyes as tools in cell biology: New insights into their cellular reduction’, *Biotechnology Annual Review*, 11, pp. 127–52.

Bikas, H. *et al.* (2016) ‘Additive manufacturing methods and modeling approaches: A critical review’, *International Journal of Advanced Manufacturing Technology*, 83(1–4), pp. 389–405.

Bistolfi, A. *et al.* (2011) ‘Antibiotic-Loaded Cement in Orthopedic Surgery: A Review’, *ISRN Orthopedics*, 2011, pp. 1–8.

Blinkhorn, A. *et al.* (2009) ‘Is there a role for triclosan/copolymer toothpaste in the management of periodontal disease?’, *British Dental Journal*. Nature Publishing Group, 207(3), pp. 117–125.

Bollen, C. M. *et al.* (1996) ‘The influence of abutment surface roughness on plaque accumulation and peri-implant mucositis.’, *Clinical oral implants research*, pp. 201–

211.
Bollen, C. M. L. *et al.* (1997) 'Comparison of surface roughness of oral hard materials to the threshold surface roughness for bacterial plaque retention: A review of the literature', *Dental Materials*, 13(4), pp. 258–269.
Bollen, C. M. L., Lambrechts, P. and Quirynen, M. (1997) 'Comparison of surface roughness of oral hard materials to the threshold surface roughness for bacterial plaque retention: A review of the literature', *Dental Materials*, 13, pp. 258–269.
Bolstad, A. I., Jensen, H. B. and Bakken, V. (1996) 'Taxonomy , biology , and periodontal aspects of Fusobacterium nucleatum . These include : Taxonomy , Biology , and Periodontal Aspects of Fusobacterium nucleatum', *Clinical Microbiology Reviews*, 9(1), pp. 55–71.
Boonsongrit, Y. *et al.* (2008) 'Controlled release of bovine serum albumin from hydroxyapatite microspheres for protein delivery system', *Materials Science and Engineering B: Solid-State Materials for Advanced Technology*, 148(1–3), pp. 162–165.
Boulange-Petermann, L. *et al.* (1993) 'The influence of metallic surface wettability on bacterial adhesion', *Journal of Adhesion Science and Technology*, 7(3), pp. 221–230.
Bozzuto, G. and Molinari, A. (2015) 'Liposomes as nanomedical devices', *International Journal of Nanomedicine*, 10, pp. 975–999.
Bradshaw, D. J. *et al.* (1993) 'The Effects of Triciosan and Zinc Citrate, Alone and in Combination, on a Community of Oral Bacteria Grown in vitro', *Journal of Dental Research*, 72(1), pp. 25–30.
Brazier, J. S. *et al.* (1990) 'Fastidious anaerobe agar compared with Wilkins-Chalgren agar, brain heart infusion agar, and brucella agar for susceptibility testing of Fusobacterium species', *Antimicrobial Agents and Chemotherapy*, 34(11), pp. 2280–2282.
Broggini, N. *et al.* (2003) 'Persistent acute inflammation at the implant-abutment interface', *Journal of Dental Research*, 82(3), pp. 232–237.
Brunette, D. M. *et al.* (2001) *Titanium in Medicine: Material Science, Surface Science, Engineering, Biological Responses, and Medical Applications*. Heidelberg: Springer.
Bulbake, U. *et al.* (2017) 'Liposomal formulations in clinical use: An updated review', *Pharmaceutics*, 9(2), pp. 1–33.
Bullon, P. *et al.* (2004) 'Immunohistochemical analysis of soft tissues in implants with healthy and peri-implantitis condition, and aggressive periodontitis', *Clinical Oral Implants Research*, 15(5), pp. 553–559.
Bürgers, R. *et al.* (2010) 'Adhesion of Candida albicans to various dental implant

surfaces and the influence of salivary pellicle proteins', *Acta Biomaterialia*. Acta Materialia Inc., 6(6), pp. 2307–2313.

Callister, W. and Rethwisch, D. (2007) *Materials science and engineering: an introduction*, *Materials Science and Engineering*. New York: John Wiley & Sons, Inc.

Campoccia, D. *et al.* (2013) 'A review of the biomaterials technologies for infection-resistant surfaces', *Biomaterials*. Elsevier Ltd, 34(34), pp. 8533–8554.

Campoccia, Davide *et al.* (2006) 'The significance of infection related to orthopedic devices and issues of antibiotic resistance', *Biomaterials*, 27(11), pp. 2331–2339.

Canullo, L. *et al.* (2018) 'What is the Impact of Epstein-Barr Virus in Peri-implant Infection?', *The International Journal of Oral & Maxillofacial Implants*, 33(1), pp. 58–63.

Capestany, C. A. *et al.* (2006) 'Role of the Porphyromonas gingivalis InlJ protein in homotypic and heterotypic biofilm development', *Infection and Immunity*, 74(5), pp. 3002–3005.

Carcuac, O. *et al.* (2012) 'Experimental periodontitis and peri-implantitis in dogs', *Clinical Oral Implants Research*, 24(4), pp. 363–371.

Carcuac, O. and Berglundh, T. (2014) 'Composition of human peri-implantitis and periodontitis lesions', *Journal of Dental Research*, 93(11), pp. 1083–1088.

Caton, J. *et al.* (2018) 'A new classification scheme for periodontal and peri-implant diseases and conditions – Introduction and key changes from the 1999 classification', *Journal of Clinical Periodontology*, 45(March), pp. S1–S8.

Catuogno, C. and Jones, M. N. (2003) 'The antibacterial properties of solid supported liposomes on Streptococcus oralis biofilms', *International Journal of Pharmaceutics*, 257(1–2), pp. 125–140.

Cecchinato, D. *et al.* (2013) 'A cross-sectional study on the prevalence of marginal bone loss among implant patients', *Clinical Oral Implants Research*, 24(1), pp. 87–90.

Chandra, J., Mukherjee, P. K. and Ghannoum, M. A. (2008) 'In vitro growth and analysis of candida biofilms', *Nature Protocols*, 3(12), pp. 1909–1924.

Chandrawati, R. *et al.* (2009) 'Cholesterol-mediated anchoring of enzyme-loaded liposomes within disulfide-stabilized polymer carrier capsules', *Biomaterials*, 30(30), pp. 5988–5998.

Chellappa, M. *et al.* (2015) 'Preparation and evaluation of the cytotoxic nature of TiO2 nanoparticles by direct contact method', *International Journal of Nanomedicine*, pp. 31–41.

Chen, D. *et al.* (2014) 'An extremely rapid dip-coating method for self-assembly of

octadecylphosphonic acid and its thermal stability on an aluminum film', *Journal of Materials Chemistry C*. Royal Society of Chemistry, 2(46), pp. 9941–9948.

Chen, W. *et al.* (2004) 'FTIR study of vanadium oxide nanotubes from lamellar structure', *Journal of Materials Science*, 39(7), pp. 2625–2627.

Chen, X. *et al.* (2014) 'Antimicrobial GL13K Peptide Coatings Killed and Ruptured the Wall of Streptococcus gordonii and Prevented Formation and Growth of Biofilms', *PLoS ONE*, 9(11), p. e111579.

Chen, Z. *et al.* (2010) 'Novel, UV-curable coatings containing a tethered biocide: Synthesis, characterization, and antimicrobial activity', *J Biomed Mater Res A*, 95(2), pp. 486–494.

Chiu, F. *et al.* (2002) 'Cefuroxime-impregnated cement in primary total knee arthroplasty: a prospective, randomized study of three hundred and forty knees.', *The journal of bone and joint surgery. American volume*, 84(5), pp. 759–62.

Chrcanovic, B. R. *et al.* (2014) 'Flapless versus conventional flapped dental implant surgery: A meta-analysis', *PLoS ONE*, 9(6), p. e100624.

Clinical and Laboratory Standards Institute (2012) *Methods for Antimicrobial Susceptibility Testing of Anaerobic Bacteria; Approved Standard – Eighth Edition. CLSI document M11-A8. Clinical and Laboratory Standards Institute, 950 West Valley Road, Suite*.

Cochran, D. L. *et al.* (2009) 'Bone Response to Loaded Implants With Non-Matching Implant-Abutment Diameters in the Canine Mandible', *Journal of Periodontology*, 80(4), pp. 609–617.

Corbin, A. *et al.* (2011) 'Antimicrobial penetration and efficacy in an in vitro oral biofilm model', *Antimicrobial Agents and Chemotherapy*, 55(7), pp. 3338–3344.

Cornelini, R. *et al.* (2001) 'Vascular endothelial growth factor and microvessel density around healthy and failing dental implants.', *The International journal of oral & maxillofacial implants*, 16(3), pp. 389–93.

Cortizo, M. C. *et al.* (2012) 'Chlorhexidine delivery system from titanium/polybenzyl acrylate coating: Evaluation of cytotoxicity and early bacterial adhesion', *Journal of Dentistry*, 40(4), pp. 329–337.

Costa, F. O. *et al.* (2012) 'Peri-implant disease in subjects with and without preventive maintenance: A 5-year follow-up', *Journal of Clinical Periodontology*, 39(2), pp. 173–181.

Costerton, J. W. *et al.* (1999) 'Bacterial biofilms: A common cause of persistent infections', *Science*, 284(5418), pp. 1318–1322.

Cullinan, M. P. *et al.* (2003) 'The effect of a triclosan-containing dentifrice on the

progression of periodontal disease in an adult population', *Journal of Clinical Periodontology*, 30(5), pp. 414–419.

Cullinan, M. P. *et al.* (2014) 'No evidence of triclosan-resistant bacteria following long-term use of triclosan-containing toothpaste', *Journal of Periodontal Research*, 49(2), pp. 220–225.

Del Curto, B. *et al.* (2005) 'Decreased bacterial adhesion to surface-treated titanium', *International Journal of Artificial Organs*, 28(7), pp. 718–730.

Cyphert, E. L. and von Recum, H. A. (2017) 'Emerging technologies for long-term antimicrobial device coatings: advantages and limitations', *Experimental Biology and Medicine*, 242(8), pp. 788–798.

Dai, C. *et al.* (2014) 'Fast formation of superhydrophobic octadecylphosphonic acid (ODPA) coating for self-cleaning and oil/water separation', *Soft Matter*. Royal Society of Chemistry, 10(40), pp. 8116–8121.

Dammer, U. *et al.* (1995) 'Binding Strength Between Cell Adhesion Proteoglycans Measured by Atomic Force Microscopy', *Science*, 267(5201), pp. 1173–5.

Daubert, D. M. *et al.* (2015) 'Prevalence and Predictive Factors for Peri-Implant Disease and Implant Failure: A Cross-Sectional Analysis', *Journal of Periodontology*, 86(3), pp. 337–347.

Davey, M. E. and Duncan, M. J. (2006) 'Enhanced biofilm formation and loss of capsule synthesis: Deletion of a putative glycosyltransferase in Porphyromonas gingivalis', *Journal of Bacteriology*, 188(15), pp. 5510–5523.

Davidson, H. *et al.* (2015) 'Tetracycline tethered to titanium inhibits colonization by Gram-negative bacteria', *Journal of Biomedical Materials Research. Part B, Applied Biomaterials*, 103(7), pp. 1381–9.

Davies, R. M. *et al.* (2004) 'The effectiveness of a toothpaste containing Triclosan and polyvinyl-methylether maleic acid copolymer in improving plaque control and gingival health: A systematic review', *Journal of Clinical Periodontology*, 31(12), pp. 1029–1033.

Davison, W. M. *et al.* (2010) 'Spatial and temporal patterns of biocide action against Staphylococcus epidermidis biofilms', *Antimicrobial Agents and Chemotherapy*, 54(7), pp. 2920–2927.

Deng, J.-Y. *et al.* (2010) 'Role of Chloride Formed on Anodized Titanium Surfaces Against an Oral Microorganism', *Journal of Biomaterials Applications*, 25, pp. 179–189.

Derks, J *et al.* (2016) 'Effectiveness of Implant Therapy Analyzed in a Swedish Population: Prevalence of Peri-implantitis', *Journal of Dental Research*, 95(1), pp. 43–

49.
Derks, Jan *et al.* (2016) ‘Peri-implantitis - Onset and pattern of progression’, *Journal of Clinical Periodontology*, 43(4), pp. 383–388.
Derks, J. and Tomasi, C. (2015) ‘Peri-implant health and disease. A systematic review of current epidemiology’, *Journal of Clinical Periodontology*, 42(S16), pp. S158–S171.
Dibart, S. *et al.* (2005) ‘In vitro evaluation of the implant-abutment bacterial seal: the locking taper system.’, *The International journal of oral & maxillofacial implants*, 20(5), pp. 732–737.
Ding, J. *et al.* (2010) ‘n-Octadecylphosphonic acid grafted mesoporous magnetic nanoparticle: Preparation, characterization, and application in magnetic solid-phase extraction’, *Journal of Chromatography A*, 1217(47), pp. 7351–7358.
Divakar, D. D. *et al.* (2018) ‘International Journal of Biological Macromolecules Enhanced antimicrobial activity of naturally derived bioactive molecule chitosan conjugated silver nanoparticle against dental implant pathogens’, *International Journal of Biological Macromolecules*. Elsevier B.V., 108, pp. 790–797.
Donlan, R. M. (2001) ‘Biofilm Formation: A Clinically Relevant Microbiological Process’, *Clinical Infectious Diseases*, 33(8), pp. 1387–1392.
Dorkhan, M. *et al.* (2012) ‘Effects of saliva or serum coating on adherence of Streptococcus oralis strains to titanium’, *Microbiology*, 158(2), pp. 390–397.
Dorobantu, L. S. and Gray, M. R. (2010) ‘Application of atomic force microscopy in bacterial research’, *Scanning*, 32(2), pp. 74–96.
Drago, L. *et al.* (2014) ‘Does Implant Coating With Antibacterial-Loaded Hydrogel Reduce Bacterial Colonization and Biofilm Formation in Vitro ?’, *Clin Orthop Relat Res*, 472, pp. 3311–3323.
Duan, Y. *et al.* (2018) ‘Investigation on the Nanomechanics of Liposome Adsorption on Titanium Alloys: Temperature and Loading Effects’, *Polymers*, 10(4), p. 383.
Duarte, P. M. *et al.* (2009) ‘Bacterial Adhesion on Smooth and Rough Titanium Surfaces After Treatment With Different Instruments’, *Journal of Periodontology*, 80(11), pp. 1824–1832.
Duarte, P. M. *et al.* (2016) ‘Could cytokine levels in the peri-implant crevicular fluid be used to distinguish between healthy implants and implants with peri-implantitis? A systematic review’, *Journal of Periodontal Research*, 51(6), pp. 689–698.
Dufrene, Y. (2002) ‘Atomic Force Microscopy , a Powerful Tool in Microbiology’, *Journal of Bacteriology*, 184(19), pp. 5205–5213.
Dufrene, Y. F. (2014) ‘Atomic Force Microscopy in Microbiology: New Structural and Functional Insights into the Microbial Cell Surface’, *mBio*, 5(4), pp. e01363-14-

e01363-14.
Ebadian, A. R. *et al.* (2012) 'Bacterial Analysis of Peri-implantitis and Chronic Periodontitis in Iranian Subjects', (4).
Edupuganti, O. P. *et al.* (2007) 'Covalent bonding of vancomycin to Ti6Al4V alloy pins provides long-term inhibition of Staphylococcus aureus colonization', *Bioorganic & Medicinal Chemistry Letters*, 17, pp. 2692–2696.
El-Zawawy, L. A. *et al.* (2015a) 'Preventive prospective of triclosan and triclosan-liposomal nanoparticles against experimental infection with a cystogenic ME49 strain of Toxoplasma gondii', *Acta Tropica*. Elsevier B.V., 141(Part A), pp. 103–111.
El-Zawawy, L. A. *et al.* (2015b) 'Preventive prospective of triclosan and triclosan-liposomal nanoparticles against experimental infection with a cystogenic ME49 strain of Toxoplasma gondii', *Acta Tropica*. Elsevier B.V., 141(Part A), pp. 103–111.
El-Zawawy, L. A. *et al.* (2015c) 'Triclosan and triclosan-loaded liposomal nanoparticles in the treatment of acute experimental toxoplasmosis', *Experimental Parasitology*. Elsevier Inc., 149, pp. 54–64.
El-Zawawy, L. A. *et al.* (2015d) 'Triclosan and triclosan-loaded liposomal nanoparticles in the treatment of acute experimental toxoplasmosis', *Experimental Parasitology*. Elsevier Inc., 149, pp. 54–64.
Eli, I. *et al.* (2001) 'At first glance: Social meanings of dental appearance', *Journal of Public Health Dentistry*, 61(3), pp. 150–154.
EOS (2019) *Additive Manufacturing, Laser-Sintering and industrial 3D printing - Benefits and Functional Principle*. Available at: https://www.eos.info/additive_manufacturing/for_technology_interested (Accessed: 27 April 2019).
Ericsson, I. *et al.* (1995) 'Different types of inflammatory reactions in peri-implant soft tissues', *Journal of Clinical Periodontology*, 22(3), pp. 255–261.
Ericsson, I. and Lindhe, J. (1993) 'Probing depth at implants and teeth - an experimental study in the dog', *Journal of Clinical Periodontology*, 20, pp. 623–627.
Espehaug, B. *et al.* (1997) 'Antibiotic prophylaxis in total hip arthroplasty. Review of 10905 primary total hip replacements reported to the Norwegian arthroplasty register, 1987 to 1995', *J Bone Joint Surg [Br]*, 79(4), pp. 590–5.
Espinosa-Cristobal, L. *et al.* (2013) 'Toxicity , distribution , and accumulation of silver nanoparticles in Wistar rats Toxicity , distribution , and accumulation of silver nanoparticles in Wistar rats', *Journal of Nanomedicine & Nanotechnology*, 15, p. 1702.
Esposito, M. *et al.* (1998) 'Biological factors contributing three major determinants for

late implant failures in the Brånemark system', *Eur J Oral Sci*, 106, pp. 527–551.
Esposito, M. *et al.* (2011) 'Interventions for replacing missing teeth: Dental implants in fresh extraction sockets (immediate, immediate-delayed and delayed implants): Commentary', *Australian Dental Journal*, 56(1), pp. 100–102.
Esposito, M., Maghaireh, H., *et al.* (2012) 'Intervention for replacing missing teeth: management of soft tissues for dental implants', *Cochrane Database Syst Rev*, 15(2), p. CD006697.
Esposito, M., Grusovin, M., *et al.* (2012) 'Interventions for replacing missing teeth: treatment of peri-implantitis', *Cochrane Database Syst Rev*.
Esposito, M. *et al.* (2013) 'Interventions for replacing missing teeth: different times for loading dental implants.', *Cochrane database of systematic reviews*, (3), p. CD003815.
Esposito, M. *et al.* (2014) 'Interventions for replacing missing teeth: different types of dental implants', *Cochrane Database of Systematic Reviews*, (7).
Estrela, S. and Brown, S. P. (2018) 'Community interactions and spatial structure shape selection on antibiotic resistant lineages', *PLOS Computanional Biology*, 14(6), p. e1006179.
European Commission (2007) *Medical Devices Directive 93/42/EEC - Annex IX*.
European Medicines Agency (2013) *Public summary of opinion on orphan designation: Tobramycin (liposomal) for the treatment of Pseudomonas aeruginosa lung infection in cystic fibrosis*. Available at: https://www.ema.europa.eu/en/documents/orphan-designation/eu/3/06/366-public-summary-positive-opinion-orphan-designation-tobramycin-liposomal-treatment-pseudomonas_en.pdf (Accessed: 2 May 2019).
Everett, E. P. (2017) *Novel Antimicrobial Restorative Materials for the Control of Dental Disease*.
Facchini, L. *et al.* (2010) 'Ductility of a Ti-6Al-4V alloy produced by selective laser melting of prealloyed powders', *Rapid Prototyping Journal*, 16(6), pp. 450–459.
Fakhravar, Z. *et al.* (2015) 'Nanoliposomes: Synthesis methods and applications in cosmetics', *Journal of Cosmetic and Laser Therapy*, 18(3).
Fan, F. and Wood, K. V. (2007) 'Bioluminescent Assays for High-Throughput Screening', *ASSAY and Drug Development Technologies*, 5(1), pp. 127–136.
Fang, H. H. ., Chan, K.-Y. and Xu, L.-C. (2000) 'Quantification of bacterial adhesion forces using atomic force microscopy (AFM)', *Journal of Microbiological Methods*, 40(1), pp. 89–97.
Faot, F. *et al.* (2015) 'Can Peri-Implant Crevicular Fluid Assist in the Diagnosis of Peri-

Implantitis? A Systematic Review and Meta-Analysis', *Journal of Periodontology*, 86(5), pp. 631–645.

Farsi, D. and Tanner, A. (2016) 'In vitro resistance testing of porphyromonas gingivalis, Prevotella intermedia, and Tannerella forsythia to triclosan', *Journal of Contemporary Dental Practice*, 17(4), pp. 282–285.

Food and Drug Administration (2018) *Highlights of prescribing information*. Available at: https://www.accessdata.fda.gov/drugsatfda_docs/label/2018/207356s000lbl.pdf (Accessed: 2 May 2019).

Foster, H. A. *et al.* (2011) 'Photocatalytic disinfection using titanium dioxide: Spectrum and mechanism of antimicrobial activity', *Applied Microbiology and Biotechnology*, 90(6), pp. 1847–1868.

Fransson, C. *et al.* (2010) 'Severity and pattern of peri-implantitis-associated bone loss', *Journal of Clinical Periodontology*, 37(5), pp. 442–448.

Froum, S. and Summerford, K. L. (2015) *Dollars and sense: Saving teeth vs. placing implants*, *Dental Economics*. Available at: https://www.dentaleconomics.com/articles/print/volume-105/issue-2/science-tech/dollars-and-sense-saving-teeth-vs-placing-implants.html (Accessed: 25 March 2019).

Fu, G., Vary, P. S. and Lin, C.-T. (2005) 'Anatase TiO2 Nanocomposites for Antimicrobial Coatings', *The Journal of Physical Chemistry B*, 109(18), pp. 8889–8898.

Fuchigami, K. *et al.* (2017) 'A diversity of peri-implant mucosal thickness by site', *Clinical Oral Implants Research*, 28(2), pp. 171–176.

Fuchs, T. *et al.* (2011) 'The use of gentamicin-coated nails in the tibia : preliminary results of a prospective study', *Arch Orthop Trauma Surg*, 131, pp. 1419–1425.

Furuichi, Y. and Birkhed, D. (1999) 'Retention of fluoride/triclosan in plaque following different modes of administration.', *Journal of clinical periodontology*, 26(1), pp. 14–18.

Gaisinskaya-Kipnis, A. and Klein, J. (2016) 'Normal and Frictional Interactions between Liposome-Bearing Biomacromolecular Bilayers', *Biomacromolecules*, 17(8), pp. 2591–2602.

Gallardo-Moreno, A. M. *et al.* (2009) 'In vitro biocompatibility and bacterial adhesion of physico-chemically modified Ti6Al4V surface by means of UV irradiation', *Acta Biomaterialia*, 5(1), pp. 181–192.

Gallucci, G. *et al.* (2014) 'Consensus Statements and Clinical Recommendations for Implant Loading Protocols', *The International Journal of Oral & Maxillofacial Implants*,

29(Suppl), pp. 287–290.
Gammon, L. M. *et al.* (2004) 'Metallography and Microstructures of Titanium and its Alloys', *Materials Park, OH: ASM International, 2004.*, 9, pp. 899–917.
Ganly, S. *et al.* (2013) 'Liposomal surface coatings of metal stents for efficient non-viral gene delivery to the injured vasculature', *Journal of Controlled Release*. Elsevier B.V., 167(2), pp. 109–119.
Garrett, T. R., Bhakoo, M. and Zhang, Z. (2008) 'Characterisation of bacterial adhesion and removal in a flow chamber by micromanipulation measurements', *Biotechnology Letters*, 30(3), pp. 427–433.
Gawalt, E. S. *et al.* (2001) 'Self-assembly and bonding of alkanephosphonic acids on the native oxide surface of titanium', *Langmuir*, 17(19), pp. 5736–5738.
Gay, I. C. *et al.* (2016) 'Role of supportive maintenance therapy on implant survival: a university-based 17 years retrospective analysis', *International Journal of Dental Hygiene*, 14(4), pp. 267–271.
Gebhardt, A. (2012) 'Layer Manufacturing Processes', in *Understanding Additive Manufacturing*. Cincinnati: Hanser Publications, pp. 31–63.
Geens, T. *et al.* (2012) 'Distribution of bisphenol-A, triclosan and n-nonylphenol in human adipose tissue, liver and brain', *Chemosphere*. Elsevier Ltd, 87(7), pp. 796–802.
Geidel, A. *et al.* (2017) 'Control of Plaque and Gingivitis by an Herbal Toothpaste - A Randomised Controlled Study', *Oral Health and Preventive Dentistry*, 5, pp. 407–13.
George, S. *et al.* (2010) 'Use of a Rapid Cytotoxicity Screening Approach To Engineer a Safer Zinc Oxide Nanoparticle through Iron Doping', *ACS Nano*, 4(1), pp. 15–29.
Gerits, E., Verstraeten, N. and Michiels, J. (2017) 'New approaches to combat Porphyromonas gingivalis biofilms', *Journal of Oral Microbiology*. Taylor & Francis, 9(1).
Gilbert, P. *et al.* (2007) 'Common therapeutic approaches for the control of oral biofilms: Microbiological safety and efficacy', *Clinical Microbiology and Infection*. European Society of Clinical Infectious Diseases, 13(SUPPL. 4), pp. 17–24.
Gogniat, G. and Dukan, S. (2007) 'TiO2 photocatalysis causes DNA damage via fenton reaction-generated hydroxyl radicals during the recovery period', *Applied and Environmental Microbiology*, 73(23), pp. 7740–7743.
Goldberg, R., Schroeder, A., Silbert, G., *et al.* (2011) 'Boundary Lubricants with Exceptionally Low Friction Coefficients Based on 2D Close-Packed Phosphatidylcholine Liposomes', *Advanced Materials*, 23(31), pp. 3517–3521.
Goldberg, R., Schroeder, A., Barenholz, Y., *et al.* (2011) 'Interactions between

adsorbed hydrogenated soy phosphatidylcholine (HSPC) vesicles at physiologically high pressures and salt concentrations', *Biophysical Journal*. Biophysical Society, 100(10), pp. 2403–2411.

Gómez-Moreno, G. *et al.* (2015) 'Peri-implant evaluation in type 2 diabetes mellitus patients: A 3-year study', *Clinical Oral Implants Research*, 26(9), pp. 1031–1035.

Goodman, S. B. *et al.* (2013) 'The future of biologic coatings for orthopaedic implants', *Biomaterials*. Elsevier Ltd, 34(13), pp. 3174–3183.

Goulbourne, P. A. and Ellen, R. P. (1991) 'Evidence that Porphyromonas (Bacteroides) gingivalis fimbriae function in adhesion to Actinomyces viscosus', *Journal of Bacteriology*, 173(17), pp. 5266–5274.

Gouzman, I. *et al.* (2006) 'Monolayer vs. multilayer self-assembled alkylphosphonate films: X-ray photoelectron spectroscopy studies', *Surface Science*, 600(4), pp. 773–781.

Grapski, J. A. and Cooper, S. L. (2001) 'Synthesis and characterization of non-leaching biocidal polyurethanes', *Biomaterials*, 22, p. 2239}2246 Synthesis.

Gregoriadis, Gregory and Florence, A. (1993) 'Liposomes in Drug Delivery: Present and Future', *Liposome Dermatics*, 45(I), pp. 346–352.

Gregoriadis, G and Florence, A. (1993) 'Liposomes in drug delivery', *Drugs*, 45(1), pp. 15–28.

Grischke, J. *et al.* (2016) 'Antimicrobial dental implant functionalization strategies — A systematic review', *Dental Materials Journal*, 35(4), pp. 545–558.

Gross, M. *et al.* (2000) 'Microleakage at the abutment-implant interface of osseointegrated implants: a comparative study.', *The International journal of oral & maxillofacial implants*, 14(1), pp. 94–100.

Grossmann, Y. and Levin, L. (2007) 'Success and Survival of Single Dental Implants Placed in Sites of Previously Failed Implants', *Journal of Periodontology*, 78(9), pp. 1670–1674.

Grove, C. *et al.* (2003) 'Improving the aqueous solubility of triclosan by solubilization, complexation, and in situ salt formation.', *Journal of Cosmetic Science*, 54(6), pp. 537–550.

Grusovin, M. *et al.* (2010) 'Interventions for replacing missing teeth: maintaining and re-establishing healthy tissues around dental implants', *Cochrane Database of Systematic Reviews*, (8), p. CD003069.

Gualini, F. and Berglundh, T. (2003) 'Immunohistochemical characteristics of inflammatory lesions at implants', *Journal of Clinical Periodontology*, 30(1), pp. 14–18.

Gulati, M. *et al.* (2014) 'Implant Maintenance: A Clinical Update', *International Scholarly Research Notices*. Hindawi Publishing Corporation, 2014, pp. 1–8.

Haas, R. *et al.* (2000) 'Lethal photosensitization, autogenous bone, and e-PTFE membrane for the treatment of peri-implantitis: preliminary results.', *The International journal of oral & maxillofacial implants*, 15(3), pp. 374–82.

Hajishengallis, G., Darveau, R. and Curtis, M. (2012) 'The Keystone Pathogen Hypothesis', *Nat Rev Microbiol*, 10(10), pp. 717–725.

Hämmerle, C. H. F. *et al.* (1995) 'Successful Bone Fill in Late Peri-Implant Defects Using Guided Tissue Regeneration. A Short Communication', *Journal of Periodontology*, 66, pp. 303–308.

Hämmerle, C. H. F. *et al.* (2004) 'Consensus statements and recommended clinical procedures regarding the placement of implants in extraction sockets.', *The International journal of oral & maxillofacial implants*, 19(Suppl), pp. 26–8.

Handelsman, M. (2006) 'Surgical guidelines for dental implant placement', *British Dental Journal*, 201(3), pp. 139–152.

Hannig, C. *et al.* (2010) 'Visualization of adherent micro-organisms using different techniques', *Journal of Medical Microbiology*, 59, pp. 1–7.

Hanson, E. L. *et al.* (2003) 'Bonding Self-Assembled, Compact Organophosphonate Monolayers to the Native Oxide Surface of Silicon', *Journal of the American Chemical Society*, 125(51), pp. 16074–16080.

Harriott, M. M. and Noverr, M. C. (2009) 'Candida albicans and Staphylococcus aureus form polymicrobial biofilms: Effects on antimicrobial resistance', *Antimicrobial Agents and Chemotherapy*, 53(9), pp. 3914–3922.

Hashimoto, M. *et al.* (2003) 'Binding of Porphyromonas gingivalis fimbriae to Treponema denticola dentilisin', *FEMS Microbiology Letters*, 226(2), pp. 267–271.

Haworth, C. S. *et al.* (2019) 'Inhaled liposomal ciprofloxacin in patients with non-cystic fibrosis bronchiectasis and chronic lung infection with Pseudomonas aeruginosa (ORBIT-3 and ORBIT-4): two phase 3, randomised controlled trials', *The Lancet Respiratory Medicine*. Elsevier Ltd, 7(3), pp. 213–226.

He, S. *et al.* (2014) 'Antibiotic-decorated titanium with enhanced antibacterial activity through adhesive polydopamine for dental/bone implant', *Journal of The Royal Society Interface*, 11(95).

Heath, R. J. *et al.* (1999) 'Mechanism of triclosan inhibition of bacterial fatty acid synthesis', *Journal of Biological Chemistry*, 274(16), pp. 11110–11114.

Heitz-Mayfield, L. J. A. (2008) 'Peri-implant diseases: Diagnosis and risk indicators', *Journal of Clinical Periodontology*, 35(SUPPL. 8), pp. 292–304.

Heitz-Mayfield, L. J. A. and Lang, O. N. P. (2004) ‘Antimicrobial Treatment of Peri-implant Diseases’, *The International Journal of Oral & Maxillofacial Implants*, 19(Suppl), pp. 128–139.

Heitz-Mayfield, L. J. A. and Salvi, G. E. (2018) ‘Peri-implant mucositis’, *Journal of Clinical Periodontology*, 45(Suppl20), pp. S237–S245.

Heitz-Mayfield, L. and Mombelli, A. (2014) ‘The Therapy of Peri-implantitis: A Systematic Review’, *The International Journal of Oral & Maxillofacial Implants*, 29(Supplement), pp. 325–345.

Heydorn, A. *et al.* (2000) ‘Quantification of biofilm structures by the novel computer program COMSTAT’, *Microbiology*, 146(May), pp. 2395–2407.

Holmberg, K. *et al.* (2013) ‘Acta Biomaterialia Bio-inspired stable antimicrobial peptide coatings for dental applications’, *Acta Biomaterialia*. Acta Materialia Inc., 9, pp. 8224–8231.

Holmberg, K. V. *et al.* (2013) ‘Bio-inspired stable antimicrobial peptide coatings for dental applications’, *Acta Biomaterialia*. Acta Materialia Inc., 9(9), pp. 8224–8231.

Hoppe, A. D., Seveau, S. and Swanson, J. A. (2010) ‘Live Cell Fluorescence Microscopy to Study Microbial Pathogenesis’, *Cell Microbiology*, 11(4), pp. 540–550.

Hori, K. and Matsumoto, S. (2010) ‘Bacterial adhesion: From mechanism to control’, *Biochemical Engineering Journal*, 48(3), pp. 424–434.

Hu, X. *et al.* (2010) ‘An in vitro assessment of titanium functionalized with polysaccharides conjugated with vascular endothelial growth factor for enhanced osseointegration and inhibition of bacterial adhesion’, *Biomaterials*. Elsevier Ltd, 31(34), pp. 8854–8863.

Huang, H. L. *et al.* (2010) ‘Antibacterial TaN-Ag coatings on titanium dental implants’, *Surface and Coatings Technology*. Elsevier B.V., 205(5), pp. 1636–1641.

Huang, J. *et al.* (2008) ‘Nonleaching Antibacterial Glass Surfaces via “ Grafting Onto ”: The Effect of the Number of Quaternary Ammonium Groups on Biocidal Activity’, *Langmuir*, 24(13), pp. 6785–6795.

Huang, S. L. and MacDonald, R. C. (2004) ‘Acoustically active liposomes for drug encapsulation and ultrasound-triggered release’, *Biochimica et Biophysica Acta - Biomembranes*, 1665(1–2), pp. 134–141.

Hultin, M. *et al.* (2012) ‘Neutrophil Response and Microbiological Findings Around Teeth and Dental Implants’, *Journal of Periodontology*, 69(12), pp. 1413–1418.

Humphrey, S. (2006) ‘Implant Maintenance’, *Dental Clinics of North America*, 50(3), pp. 463–478.

Huynh-Ba, G. *et al.* (2008) ‘Association of the composite IL-1 genotype with peri-

implantitis: A systematic review', *Clinical Oral Implants Research*, 19(11), pp. 1154–1162.

Ignjatovi, N. *et al.* (2016) 'Chitosan-PLGA polymer blends as coatings for hydroxyapatite nanoparticles and their effect on antimicrobial properties , osteoconductivity and regeneration of osseous tissues', *Materials Science and Engineering C*, 60, pp. 357–364.

Immordino, M., Dosio, F. and Cattel, L. (2006) 'Stealth liposomes: review of the basic science, rationale, and clinical applications, existing and potential', *International Journal of Nanomedicine 2006:1(3)*, 1(3), pp. 297–315.

Insua, A. *et al.* (2017) 'Patient-Centered Perspectives and Understanding of Peri-implantitis', *Journal of Periodontology*, (May), pp. 1–15.

Irache, J. M. *et al.* (2005) 'Bioadhesive properties of pegylated nanoparticles', *Molecules*, 10, pp. 126–145.

Ishihara, K. *et al.* (1992) 'Hemocompatibility of human whole blood on polymers with a phospholipid polar group and its mechanism', *Journal of Biomedical Materials Research*, 26, pp. 1543–1552.

Ishihara, K. *et al.* (1998) 'Why do phospholipid polymers reduce protein adsorption?', *Journal of Biomedical Materials Research*, 39, pp. 323–330.

Ishihara, K. and Iwasaki, Y. (1998) 'Reduced Protein Adsorption on Novel Phospholipid Polymers', *Journal of Biomaterials Applications*, 13, pp. 111–127.

Jacobs, R. and van Steenberghe, D. (1994) 'Role of periodontal ligament receptors in the tactile function of teeth: a review.', *Journal of Periodontal Research*, pp. 153–67.

Janani, K. and Kumar, M. P. S. (2018) 'Triclosan-coated sutures in oral and maxillofacial surgery - An overview', *Drug Invention Today*, 10(10), pp. 2029–2032. Available at: https://www.scopus.com/inward/record.uri?eid=2-s2.0-85054268544&partnerID=40&md5=db94d848630b2b5e97900c073ff29db7%0Ahttp://www.embase.com/search/results?subaction=viewrecord&from=export&id=L624079904.

Janković, A. *et al.* (2015) 'Structural and biological evaluation of lignin addition to simple and silver-doped hydroxyapatite thin films synthesized by matrix-assisted pulsed laser evaporation', *Journal of Materials Science: Materials in Medicine*, 26(17).

Jankovic, S. *et al.* (2011) 'Prevalence of human cytomegalovirus and Epstein-Barr virus in subgingival plaque at peri-implantitis, mucositis and healthy sites. A pilot study', *International Journal of Oral and Maxillofacial Surgery*. International Association of Oral and Maxillofacial Surgery, 40(3), pp. 271–276.

Jannesson, L. *et al.* (2002) 'Effect of a triclosan-containing toothpaste supplemented with 10% xylitol on mutans streptococci in saliva and dental plaque. A 6-month clinical study.', *Caries research*, 36(1), pp. 36–39.

Jeng, H. A. and Swanson, R. J. (2006) 'Toxicity of Metal Oxide Nanoparticles in Mammalian Cells', *Journal of Environmental Science and Health Part A*, 41, pp. 2699–2711.

Jeon, S. *et al.* (1991) 'Protein-Surface Interactions in the Presence of Polyethylene Oxide', *Journal of colloid and interface science*, 142(1), pp. 149–158.

Ji, M. *et al.* (2015) 'Evaluation of antibacterial activity and osteoblast-like cell viability of TiN, ZrN and (Ti1-xZrx)N coating on titanium.', *The journal of advanced prosthodontics*, 7(2), pp. 166–71.

Jones, M. N. *et al.* (1993) 'Targeting and delivery of bactericide to adsorbed oral bacteria by use of proteoliposomes', *BBA - Biomembranes*, 1147(2), pp. 251–261.

Jones, M. N. *et al.* (1994) 'The use of phospholipid liposomes for targeting to oral and skin-associated bacteria', *Journal of Drug Targeting*, 2(5), pp. 381–389.

Jones, M. N. *et al.* (1997) 'The interaction of phospholipid liposomes with bacteria and their use in the delivery of bactericides', *J.Drug Target*, 5(1), pp. 25–34.

Jones, R. D. *et al.* (2000) 'Triclosan: A review of effectiveness and safety in health care settings', *American Journal of Infection Control*, 28(2), pp. 184–196.

Jordan, R. *et al.* (2016) 'An assessment of early colonisation of implant-abutment metal surfaces by single species and co-cultured bacterial periodontal pathogens', *Journal of Dentistry*, 53, pp. 64–72.

Josefsson, G. and Kolmert, L. (1993) 'Prophylaxis with systematic antibiotics versus gentamicin bone cement in total hip arthroplasty: A ten-year survey of 1688 hips', *Clinical Orthopaedics and Related Research*, (292), pp. 210–214.

Kajale, A. and Mehta, D. (2014) 'Interleukin-1β level in peri-implant crevicular fluid and its correlation with the clinical and radiographic parameters', *J Indian Soc Periodontol*, 18(2), pp. 220–225.

Kalykakis, G. K. *et al.* (1998) 'Clinical and microbial findings on osseo-integrated implants; comparisons between partially dentate and edentulous subjects', *Eur.J Prosthodont.Restor.Dent*, 6(0965-7452 (Print)), pp. 155–159.

Kang, M.-K. *et al.* (2012) 'The biomimetic apatite-cefalotin coatings on modified titanium', *Dental Materials Journal*, 31(1), pp. 98–105.

Kapatral, V. *et al.* (2003) 'Genome analysis of F. nucleatum sub spp vincentii and its comparison with the genome of F. nucleatum ATCC 25586', *Genome Research*, 13(6), pp. 1180–1189.

Kapos, T. and Evans, C. (2014) ‘CAD/CAM Technology for Implant Abutments, Crowns, and Superstructures’, 29(Suppl), pp. 117–136.

Karacan, I. *et al.* (2017) ‘Antibiotic Containing Poly Lactic Acid / Hydroxyapatite Biocomposite Coatings for Dental Implant Applications’, *Key Engineering Materials*, 758, pp. 120–125.

Karbach, J. *et al.* (2009) ‘Comparison of five parameters as risk factors for peri-mucositis.’, *The International journal of oral & maxillofacial implants*, 24(3), pp. 491–6.

Kawabe, A. *et al.* (2014) ‘Evaluation of biofilm formation in the presence of saliva on poly(ethylene glycol)deposited titanium’, *Dental Materials Journal*, 33(5), pp. 638–647.

Kazuhisa, M. (2002) *Surface Characterization Techniques: An Overview*.

Keservani, R. *et al.* (2016) ‘Liposomes: Properties and therapeutic applications’, in *Novel Approaches for Drug Delivery*. Hershey: IGI Global, pp. 27–51.

Khan, W. *et al.* (2014) ‘Focal Controlled Drug Delivery’, in *Focal Controlled Drug Delivery*. New York: Springer US, pp. 33–59.

Khoury, F. and Buchmann, R. (2001) ‘Surgical Therapy of Peri-Implant Disease : A 3-Year Follow-Up Study of Cases Treated With 3 Different Techniques of Bone Regeneration.’, *Journal of periodontology*, 72(11), pp. 1498–1508.

Kikuchi, H. *et al.* (1991) ‘Possibility of heat sterilisation of liposomes’, *Chem Pharm Bull*, 39(4), pp. 1018–22.

Kim, J. *et al.* (2002) ‘Preparation and characterization of Triclosan-containing vesicles’, *Colloids and Surfaces B: Biointerfaces*, 26, pp. 235–241.

Kim, P. *et al.* (2007) ‘Phosphonic acid-modified barium titanate polymer nanocomposites with high permittivity and dielectric strength’, *Advanced Materials*, 19(7), pp. 1001–1005.

Kim, W. H. *et al.* (2008) ‘The release behavior of CHX from polymer-coated titanium surfaces’, *Surface and Interface Analysis*, 40(3–4), pp. 202–204.

Kim, Y. K. *et al.* (2010) ‘Prognosis of the implants replaced after removal of failed dental implants’, *Oral Surgery, Oral Medicine, Oral Pathology, Oral Radiology and Endodontology*. Elsevier Inc., 110(3), pp. 281–286.

Kiwi, J. and Nadtochenko, V. (2005) ‘Evidence for the Mechanism of Photocatalytic Degradation of the Bacterial Wall Membrane at the TiO Interface by ATR-FTIR and Laser Kinetic Spectroscopy Evidence for the Mechanism of Photocatalytic Degradation of the Bacterial Wall Membrane at the TiO 2 In’, *Langmuir*, 21, pp. 4631–4641.

Kizuki, T., Matsushita, T. and Kokubo, T. (2014) 'Antibacterial and bioactive calcium titanate layers formed on Ti metal and its alloys', *Journal of Materials Science: Materials in Medicine*, 25(7), pp. 1737–1746.

Klinge, B. *et al.* (2018) 'Peri-implant diseases', *European Journal of Oral Sciences*, 126(10), pp. 88–94.

Koldsland, O. C. *et al.* (2010) 'Prevalence of Peri-Implantitis Related to Severity of the Disease With Different Degrees of Bone Loss', *Journal of Periodontology*, 81(2), pp. 231–238.

Kolenbrander, P. and Andersen, R. (1989) 'Inhibition of Coaggregation between Fusobacterium nucleatum and Porphyromonas (Bacteroides) gingivalis by Lactose and Related Sugars', *Infection and Immunity*, 57(10), pp. 3204–3209.

Kolenbrander, P. E. *et al.* (2006) 'Bacterial interactions and successions during plaque development', *Periodontology 2000*, 42(1), pp. 47–79.

Kolenbrander, P. E. *et al.* (2010) 'Oral multispecies biofilm development and the key role of cell-cell distance.', *Nature reviews. Microbiology*. Nature Publishing Group, 8(7), pp. 471–480.

Kolenbrander, P. E. and London, J. (1993) 'Adhere today, here tomorrow: Oral bacterial adherence', *Journal of Bacteriology*, 175(11), pp. 3247–3252.

Konstantinidis, I. K. *et al.* (2015) 'Cross-sectional study on the prevalence and risk indicators of peri-implant diseases', *International Journal of Implantology*, 1, pp. 75–88.

Konttinen, Y. *et al.* (2006) 'Immunohistochemical Evaluation of Inflammatory Mediators in Failing Implants.', *International Journal of Periodontics & Restorative Dentistry*, 26(2), pp. 134–141.

Kos, M. *et al.* (2015) 'Bisphosphonates enhance bacterial adhesion and biofilm formation on bone hydroxyapatite', *Journal of Cranio-Maxillofacial Surgery*. Elsevier Ltd, 43(6), pp. 863–869.

Koyanagi, T. *et al.* (2013) 'Comprehensive microbiological findings in peri-implantitis and periodontitis', pp. 218–226.

Kubacka, A. *et al.* (2014) 'Understanding the antimicrobial mechanism of TiO 2 -based nanocomposite films in a pathogenic bacterium', *Scientific Reports*, 4, pp. 1–9.

Kuboniwa, M. *et al.* (2009) 'Distinct roles of long/short fimbriae and gingipains in homotypic biofilm development by porphyromonas gingivalis', *BMC Microbiology*, 9, pp. 1–13.

Kugel, A. *et al.* (2011) 'Progress in Organic Coatings Antimicrobial coatings produced by " tethering " biocides to the coating matrix : A comprehensive review', *Progress in*

*Organic Coatings*. Elsevier B.V., 72(3), pp. 222–252.
Kulkarni, S. B. and Vargha-Butler, E. I. (1995) 'Study of liposomal drug delivery systems 2. Encapsulation efficiencies of some steroids in MLV liposomes', *Colloids and Surfaces B: Biointerfaces*, 4(2), pp. 77–85.
Kyriakides, T. R. (2015) *Molecular Events at Tissue–Biomaterial Interface*, *Host Response to Biomaterials*. Elsevier Inc.
De L. Rodríguez López, A. *et al.* (2019) 'Acta Biomaterialia Preventing S . aureus biofilm formation on titanium surfaces by the release of antimicrobial b -peptides from polyelectrolyte multilayers q', *Acta Biomater.*, [Epub ahea.
Lafond, V. *et al.* (2003) '17O MAS NMR Study of the Bonding Mode of Phosphonate Coupling Molecules in a Titanium Oxo-Alkoxo-Phosphonate and in Titania-Based Hybrid Materials', *Chemistry of Materials*, 15(21), pp. 4098–4103.
Lafont, U. (2009) *Oxydes de titane mésoporeux : Synthèse , caractérisation et modification de surface*.
Lambert, F. (2018) *The Importance of Preserving the Peri-Implant Soft Tissue Barrier*, *Dental Asia*. Available at: http://www.dentalasia.net/en/news-archive/the-importance-of-preserving-the-peri-implant-soft-tissue-barrier/1683 (Accessed: 27 April 2019).
Lamont, R. J. *et al.* (1993) 'Involvement of Porphyromonas gingivalis fimbriae in adherence to Streptococcus gordonii', *Oral Microbiology and Immunology*, 8(5), pp. 272–276.
Laouini, A. *et al.* (2012) 'Preparation, Characterization and Applications of Liposomes: State of the Art', *Journal of Colloid Science and Biotechnology*, 1(2), pp. 147–168.
Lapovok, R. and Tomus, D. (2007) *Productionof dense compact billet from Ti-alloy powder using equal channel angular extrucion*. Available at: http://www.dtic.mil/docs/citations/ADA473093 (Accessed: 18 September 2017).
Lee, J. *et al.* (2013) 'Modification of TiO 2 nanotube surfaces by electro-spray deposition of amoxicillin combined with PLGA for bactericidal effects at surgical implantation sites', *Acta Oncologica Scandinavia*, 71, pp. 168–174.
Lee, J. H. *et al.* (2018) 'Analysis of trends and prospects regarding stents for human blood vessels', *Biomaterials Research*. Biomaterials Research, 22(1), pp. 1–10.
Lee, K. W. K. *et al.* (2014) 'Biofilm development and enhanced stress resistance of a model, mixed-species community biofilm', *ISME Journal*. Nature Publishing Group, 8(4), pp. 894–907.
Lee, S. C. *et al.* (2005) 'The effect of cholesterol in the liposome bilayer on the stabilization of incorporated retinol', *Journal of Liposome Research*, 15(3–4), pp. 157–166.

Lemos, C. A. A. *et al.* (2018) ‘Comparison between flapless and open-flap implant placement: a systematic review and meta-analysis’, *International Journal of Oral and Maxillofacial Surgery*. Elsevier, S0901-5027(18), pp. 30132–2.

Leonhardt, A. *et al.* (1999) ‘Microbial findings at failing implants’, *Clinical Oral Implants Research*, 10, pp. 339–345.

Levin, L. (2008) ‘Dealing with dental implant failures’, *Journal of Applied Oral Science*, 16(3), pp. 171–175.

Lewis, K. (2010) ‘Persister cells.’, *Annual review of microbiology*, 64, pp. 357–372.

Li, J. *et al.* (2015) ‘A review on phospholipids and their main applications in drug delivery systems’, *Asian Journal of Pharmaceutical Sciences*. Elsevier Ltd, 10(2), pp. 81–98.

Li, R., Stevens, C. A. and Cho, S. S. (2017) ‘Molecular Dynamics Simulations of Biocorona Formation’, in *Modeling, Methodologies and Tools for Molecular and Nano-scale Communications*. Springer, Cham, pp. 241–256.

Li, T. *et al.* (2017) ‘Antibacterial activity and cytocompatibility of an implant coating consisting of TiO 2 nanotubes combined with a GL13K antimicrobial peptide’, *International Journal of Nanomedicine*, 12, pp. 2995–3007.

Lian, T. and Ho, R. J. Y. (2001) ‘Trends and developments in liposome drug delivery systems’, *Journal of Pharmaceutical Sciences*. Elsevier Masson SAS, 90(6), pp. 667–680.

Lim, M. S. *et al.* (2010) ‘Thermally Driven Stability of Octadecylphosphonic Acid Thin Films Grown on SS316L’, *Scanning*, 32(5), pp. 304–311.

Lin, D.-J. *et al.* (2011) ‘In vitro antibacterial activity and cytocompatibility of bismuth doped micro-arc oxidized titanium’, *Journal of Biomaterials Applications*, 27(5), pp. 553–563.

Lin, Y. (2000) ‘Buccal absorption of triclosan following topical mouthrinse application.’, *American Journal of Dentistry*, 13(4), pp. 215–7.

Lindh, L. *et al.* (2014) ‘Salivary pellicles’, *Saliva: Secretion and Functions*, 24, pp. 30–39.

Lindhe, J. and Berglundh, T. (1998) ‘The interface between the mucosa and the implant.’, *Periodontology 2000*, 17, pp. 47–54.

Lindhe, J., Lang, N. and Karring, T. (2008) *Clinical Periodontology and Clinical Dentistry - Fifth Edition*. Oxford: Blackwell Publishing.

Lindhe, J. and Meyle, J. (2008) ‘Peri-implant diseases : Consensus Report of the Sixth European Workshop on Periodontology’, *Journal of Clinical Periodontology*, 35(Suppl. 8), pp. 282–285.

Linkevicius, T. and Apse, P. (2008) ‘Influence of abutment material on stability of peri-implant tissues: a systematic review.’, *The International journal of oral & maxillofacial implants*, 23(3), pp. 449–456.

Lira-Junior, R. *et al.* (2019) ‘CSF-1 and IL-34 levels in peri-implant crevicular fluid and saliva from patients having peri-implant diseases’, *Clinical Oral Investigations*. Clinical Oral Investigations, epub ahead.

Listgarten, M. A. and Lai, C. (1999) ‘Comparative Microbiological Characteristics of Failing Implants and Periodontally Diseased Teeth *’, (April), pp. 431–437.

Liu, N. and Park, H. J. (2009) ‘Chitosan-coated nanoliposome as vitamin e carrier’, *Journal of Microencapsulation*, 26(3), pp. 235–242.

Liu, S. and Shin, Y. C. (2019) ‘Additive manufacturing of Ti6Al4V alloy : A review’, *Materials & Design*. The Authors, 164, p. 107552.

van Loosdrecht, M. C. *et al.* (1987) ‘Electrophoretic mobility and hydrophobicity as a measured to predict the initial steps of bacterial adhesion.’, *Applied and Environmental Microbiology*, 53(8), pp. 1898–1901.

Lopes de Chaves e Mello Dias, E. *et al.* (2017) ‘Association Between Implant-Abutment Microgap and Implant Circularity to Bacterial Leakage: An In Vitro Study Using Tapered Connection Implants’, *The International Journal of Oral & Maxillofacial Implants*, pp. 505–511.

Lorenzetti, M. *et al.* (2015) ‘The influence of surface modification on bacterial adhesion to titanium-based substrates’, *ACS Applied Materials and Interfaces*, 7(3), pp. 1644–1651.

Luschtinetz, R. *et al.* (2007) ‘Infrared spectra of alkylphosphonic acid bound to aluminium surfaces’, *Macromolecular Symposia*, 254, pp. 248–253.

Lv, H. *et al.* (2014) ‘Layer-by-layer self-assembly of minocycline-loaded chitosan/alginate multilayer on titanium substrates to inhibit biofilm formation’, *Journal of Dentistry*. Elsevier Ltd, 42(11), pp. 1464–1472.

Ma, M. *et al.* (2011) ‘Local delivery of antimicrobial peptides using self-organized TiO 2 nanotube arrays for peri-implant infections’, *Journal of Biomedical Materials Research A*, 100(A), pp. 278–285.

Mabboux, F. *et al.* (2004) ‘Surface free energy and bacterial retention to saliva-coated dental implant materials - An in vitro study’, *Colloids and Surfaces B: Biointerfaces*, 39(4), pp. 199–205.

Machtei, E. E. *et al.* (2011) ‘Third attempt to place implants in sites where previous surgeries have failed’, *Journal of Clinical Periodontology*, 38(2), pp. 195–198.

Madni, M. A. *et al.* (2014) ‘Liposomal drug delivery: A versatile platform for challenging

clinical applications', *Journal of Pharmacy and Pharmaceutical Sciences*, 17(3), pp. 401–426.

Maeda, K. *et al.* (2004) 'Glyceraldehyde-3-phosphate dehydrogenase of Streptococcus oralis functions as a coadhesin for Porphyromonas gingivalis major fimbriae', *Infection and Immunity*, 72(3), pp. 1341–8.

Malizos, K. *et al.* (2017) 'Fast-resorbable antibiotic-loaded hydrogel coating to reduce post-surgical infection after internal osteosynthesis : a multicenter randomized controlled trial', *J Orthop Traumatol*, 18, pp. 159–169.

Marcus, I. M. *et al.* (2012) 'Pseudomonas aeruginosa attachment on QCM-D sensors: The role of cell and surface hydrophobicities', *Langmuir*, 28(15), pp. 6396–6402.

Mardinger, O. *et al.* (2008) 'Factors Affecting the Decision to Replace Failed Implants: A Retrospective Study', *Journal of Periodontology*, 79(12), pp. 2262–2266.

Mardinger, O. *et al.* (2012) 'A retrospective analysis of replacing dental implants in previously failed sites', *Oral Surgery, Oral Medicine, Oral Pathology and Oral Radiology*. Elsevier, 114(3), pp. 290–293.

Mark Welch, J. L. *et al.* (2016) 'Biogeography of a human oral microbiome at the micron scale', *Proceedings of the National Academy of Sciences*, 113(6), pp. E791–E800.

Marmur, A. (2009) 'Solid-Surface Characterization by Wetting', *Annual Review of Materials Research*, 39(1), pp. 473–489.

Marrone, A. *et al.* (2013) 'Prevalence and risk factors for peri-implant disease in Belgian adults', *Clinical Oral Implants Research*, 24(8), pp. 934–940.

Marsh, P. *et al.* (2016) *Marsh and Martin's Oral Microbiology*. 6th Editio. London: Churchill Livingstone.

Marsh, P. D. (2004) 'Dental plaque as a microbial biofilm', *Caries Research*, 38(3), pp. 204–211.

Marshall, K. C. *et al.* (1971) 'Mechanism of the Initial Events in the Sorption of Marine Bacteria to Surfaces', *Journal of General Microbiology*, 68(3), pp. 337–348.

Marshall, K. C. and Cruickshank, R. H. (1973) 'Cell surface hydrophobicity and the orientation of certain bacteria at interfaces', *Archiv für Mikrobiologie*, 91(1), pp. 29–40.

Maruyama, N. *et al.* (2014) 'Intraindividual variation in core microbiota in peri-implantitis and periodontitis', pp. 1–10.

Mattheos, N. *et al.* (2012) 'Specialists' management decisions and attitudes towards mucositis and peri-implantitis.', *British dental journal*. Nature Publishing Group, 212(1), p. E1.

Mattos Corrêa, J. *et al.* (2015) 'Silver nanoparticles in dental biomaterials', *International Journal of Biomaterials*, 2015, p. 485275.

McBain, A. J. *et al.* (2003) 'Effects of Triclosan-Containing Rinse on the Dynamics and Antimicrobial Susceptibility of In Vitro Plaque Ecosystems', *Antimicrobial Agents and Chemotherapy*, 47(11), pp. 3531–3538.

McBain, A. J. *et al.* (2004) 'Selection for high-level resistance by chronic triclosan exposure is not universal', *Journal of Antimicrobial Chemotherapy*, 53(5), pp. 772–777.

McMillan, J., Batrakova, E. and Gendelman, H. E. (2011) *Cell delivery of therapeutic nanoparticles*. 1st edn, *Progress in Molecular Biology and Translational Science*. 1st edn. Elsevier Inc.

McMurry, L. M., Oethinger, M. and Levy, S. B. (1998) 'Triclosan targets lipid synthesis', *Nature*, 394(6693), pp. 531–532.

van Meer, G. *et al.* (2008) 'Membrane lipids: where they are and how they behave.', *Nature reviews. Molecular cell biology*, 9(2), pp. 112–124.

Mei, S. *et al.* (2014) 'Antibacterial effects and biocompatibility of titanium surfaces with graded silver incorporation in titania nanotubes', *Biomaterials*. Elsevier Ltd, 35(14), pp. 4255–4265.

Metzger, Z. *et al.* (2009) 'Characterization of Coaggregation of Fusobacterium nucleatum PK1594 with Six Porphyromonas gingivalis Strains', *Journal of Endodontics*. American Association of Endodontists, 35(1), pp. 50–54.

Mîndroiu, M. *et al.* (2013) 'Applied Surface Science The effect of deposition electrolyte on polypyrrole surface interaction with biological environment', *Applied Surface Science*. Elsevier B.V., 276, pp. 401–410.

Minisini, K. (2016) *Development of thermoresponsive liposomes as a delivery system of HRP*. Ecole Polytechnique Federale de Lausanne.

Misch, C. E. *et al.* (2008) 'Implant success, survival, and failure: the International Congress of Oral Implantologists (ICOI) Pisa Consensus Conference.', *Implant dentistry*, 17(1), pp. 5–15.

Mo, A. *et al.* (2008) 'Applied Surface Science Preparation and antibacterial effect of silver – hydroxyapatite / titania nanocomposite thin film on titanium', 255, pp. 435–438.

Mo, S. Di and Ching, W. Y. (1995) 'Electronic and optical properties of three phases of titanium dioxide: Rutile, anatase, and brookite', *Physical Review B*, 51(19), pp. 13023–13032.

Mohseni, E., Zalnezhad, E. and Bushroa, A. R. (2014) 'Comparative investigation on

the adhesion of hydroxyapatite coating on Ti-6Al-4V implant: A review paper', *International Journal of Adhesion and Adhesives*. Elsevier, 48, pp. 238–257.

Molecular Probes Inc (2011) *Vybrant™ Cell-Labeling Solutions*. Available at: https://www.thermofisher.com/document-connect/document-connect.html?url=https%3A%2F%2Fassets.thermofisher.com%2FTFS-Assets%2FLSG%2Fmanuals%2Fmp22885.pdf&title=VnlicmFudCBDZWxsLUxhYmVsaW5nIFNvbHV0aW9ucw== (Accessed: 29 March 2019).

Mombelli, A. *et al.* (2001) 'Treatment of peri-implantitis by local delivery of tetracycline: Clinical, microbiological and radiological results', *Clinical Oral Implants Research*, 12(4), pp. 287–294.

Mombelli, A. and Décaillet, F. (2011) 'The characteristics of biofilms in peri-implant disease', *Journal of Clinical Periodontology*, 38(SUPPL. 11), pp. 203–213.

Monov, G. *et al.* (2006) 'Soluble RANKL in crevicular fluid of dental implants: A pilot study', *Clinical Implant Dentistry and Related Research*, 8(3), pp. 135–141.

Monteiro, N. *et al.* (2014) 'Liposomes in tissue engineering and regenerative medicine Liposomes in tissue engineering and regenerative medicine', *Journal of The Royal Society Interface*, 11, p. 20140459.

Moon, S.-K. *et al.* (2012) 'Synthesis and evaluation of tetracycline encapsulated in poly (lactic-co-glycolic acid) on porous titania formed by using plasma electrolytic oxidation', *Journal of the Korean Physical Society*, 60(6), pp. 954–958.

Moran, J. *et al.* (2000) 'A study to assess the plaque inhibitory activity of a new triclosan mouthrinse formulation.', *Journal of clinical periodontology*, 27(11), pp. 806–809.

Moran, J. *et al.* (2010) 'A study to assess the plaque inhibitory action of a newly formulated triclosan toothpaste', *Journal of Clinical Periodontology*, 28(1), pp. 86–89.

Moss, T. *et al.* (2000) 'Percutaneous penetration and dermal metabolism of triclosan (2,4,4'- trichloro-2'-hydroxydiphenyl ether)', *Food and Chemical Toxicology*, 38(4), pp. 361–370.

Moy, P. K. *et al.* (2005) 'Dental implant failure rates and associated risk factors.', *International Journal of Oral & Maxillofacial Implants*, 20(4), pp. 569–77.

Mukherjee, P. K. and Chandra, J. (2004) 'Candida biofilm resistance', *Drug Resistance Updates*, 7(4–5), pp. 301–309.

Muller, R. *et al.* (2007) 'Fluorescence-Based Bacterial Overlay Method for Simultaneous In Situ Quantification of Surface-Attached Bacteria □', *Applied and Environ*, 73(8), pp. 2653–2660.

Murata, M. *et al.* (2002) 'Osteocalcin , deoxypyridinoline and interleukin- 1 b in peri-

implant crevicular fluid of patients with peri- implantitis', *Clinical Oral Implants Research*, 13, pp. 637–643.

Nabi, N. *et al.* (1989) 'In vitro and in vivo studies on triclosan/PVM/MA copolymer/NaF combination as an anti-plaque agent.', *American Journal of Dentistry*, 2, pp. 197–206.

Nanci, A. (2012) 'Chapter 1: Structure of the Oral Tissues', in *Ten Cate's Oral Histology*. 8th Editio. St. Louis: Mosby, pp. 1–13.

National Collection of Type Cultures (2019) *Bacteria collection: Porphyromonas gingivalis*. Available at: https://www.phe-culturecollections.org.uk/products/bacteria/detail.jsp?refId=NCTC+11834&collection=nctc (Accessed: 29 March 2019).

Norambuena, G. A. *et al.* (2017) 'Antibacterial and Biocompatible Titanium-Copper Oxide Coating May Be a Potential Strategy to Reduce Periprosthetic Infection: An In Vitro Study', *Clinical Orthopaedics and Related Research*®. Springer US, 475(3), pp. 722–732.

Norowski, P. A. *et al.* (2011) 'Chitosan coatings deliver antimicrobials from titanium implants: A preliminary study', *Implant Dentistry*, 20(1), pp. 56–67.

Norville, I. H. *et al.* (2014) 'Efficacy of Liposome-Encapsulated Ciprofloxacin in a Murine Model of Q Fever', *Antimicrobial Agents and Chemotherapy*, 58(9), pp. 5510–5518.

Nudera, W. J. *et al.* (2007) 'Antimicrobial Effect of Triclosan and Triclosan with Gantrez on Five Common Endodontic Pathogens', *Journal of Endodontics*, 33(10), pp. 1239–1242.

O'Toole, G., Kaplan, H. and Kolter, R. (2000) 'Biofilm Formation as Microbial Development', *Annual review of microbiology*, 54, pp. 49–79.

Öhman, M. *et al.* (2006) 'In situ ATR-FTIR studies of the aluminium/polymer interface upon exposure to water and electrolyte', *Progress in Organic Coatings*, 57, pp. 78–88.

Oliveira Eloy, J. *et al.* (2014) 'Liposomes as carriers of hydrophilic small molecule drugs: Strategies to enhance encapsulation and delivery', *Colloids and Surfaces B: Biointerfaces*. Elsevier B.V., 123, pp. 345–363.

Osman, R. and Swain, M. (2015) 'A Critical Review of Dental Implant Materials with an Emphasis on Titanium versus Zirconia', *Materials*, 8(3), pp. 932–958.

van Oss, C. J. (1995) 'Hydrophobicity of biosurfaces - Origin, quantitative determination and interaction energies', *Colloids and Surfaces B: Biointerfaces*, 5(3–4), pp. 91–110.

Van Oss, C. J. (1989) 'Energetics of Cell-Cell and Celi-Biopolymer Interactions', *Cell*

*Biophysics*, 14.

Park, Daewon *et al.* (2006) 'One-Step , Painting-Like Coating Procedures To Make Surfaces Highly and Permanently Bactericidal', *Biotechnol. Prog*, 22, pp. 584–589.

Park, J. *et al.* (2016) 'Characterization of Fusobacterium nucleatum ATCC 23726 adhesins involved in strain-specific attachment to Porphyromonas gingivalis', *International Journal of Oral Science*. Nature Publishing Group, 8(3), pp. 138–144.

Park, J. H. *et al.* (2011) 'Effect of cleaning and sterilization on titanium implant surface properties and cellular response', *Acta Materialia*, 8(5).

Park, S. W. *et al.* (2014) 'Mesoporous TiO2 implants for loading high dosage of antibacterial agent', *Applied Surface Science*. Elsevier B.V., 303, pp. 140–146.

Patil, Y. P. and Jadhav, S. (2014) 'Novel methods for liposome preparation', *Chemistry and Physics of Lipids*. Elsevier Ireland Ltd, 177, pp. 8–18.

Pattni, B. S. *et al.* (2015) 'New Developments in Liposomal Drug Delivery', *Chemical Reviews*, 115(19), pp. 10938–10966.

Pedersen, A. M. *et al.* (2002) 'Saliva and gastrointestinal functions of taste, mastication, swallowing and digestion', *Oral Diseases*, 8, pp. 117–129.

Peeters, E., Nelis, H. J. and Coenye, T. (2008) 'Comparison of multiple methods for quantification of microbial biofilms grown in microtiter plates', *Journal of Microbiological Methods*, 72(2), pp. 157–165.

Pegueroles, M. *et al.* (2008) 'The influence of blasting and sterilization on static and time-related wettability and surface-energy properties of titanium surfaces', *Surface and Coatings Technology*, 202(15), pp. 3470–3479.

Pereni, C. I. *et al.* (2006) 'Surface free energy effect on bacterial retention', *Colloids and Surfaces B: Biointerfaces*, 48(2), pp. 143–147.

Peres Pimentel, S. *et al.* (2019) 'Triclosan-containing fluoride toothpaste on clinical parameters and osteo-inflammatory mediators when applied in a stent during experimental peri-implant mucositis in smokers', *Clinical Oral Implants Research*, Epub.

Persson, G. R. and Renvert, S. (2014) 'Cluster of bacteria associated with peri-implantitis', *Clinical Implant Dentistry and Related Research*, 16(6), pp. 783–793.

Petrini, P. *et al.* (2006) 'Antibacterial activity of zinc modified titanium oxide surface', *The International Journal of Artificial Organs*, 29(4), pp. 434–442.

Pontoriero, R. *et al.* (1994) 'Experimentally induced peri-implant mucositis. A clinical study in humans.', *Clinical Oral Implants Research*, pp. 254–259.

Poon, C. Y. and Bhushan, B. (1995) 'Comparison of surface roughness measurements by stylus profiler, AFM and non-contact optical profiler', *Wear*, 190(1),

pp. 76–88.

Provencher, G. *et al.* (2014) ‘Determination of bisphenol A, triclosan and their metabolites in human urine using isotope-dilution liquid chromatography-tandem mass spectrometry’, *Journal of Chromatography A*, 1348, pp. 97–104.

PubChem (2018a) *Compound Summary - Triclosan*. Available at: https://pubchem.ncbi.nlm.nih.gov/compound/triclosan#section=Top (Accessed: 20 March 2019).

PubChem (2018b) *Compound Summary for CID 5564: Triclosan*. Available at: https://www.google.co.uk/search?safe=off&rlz=1C1CHBF_en-GBGB785GB785&ei=uwn7W5TaDujWgAbqrIyACg&q=triclosan+logp&oq=triclosan+logp&gs_l=psy-ab.3..0i22i30l2.17702.18432..18686...0.0..0.265.523.1j1j1.....0....1..gws-wiz.....0j0i71j35i39j0i20i263j0i22i10i3 (Accessed: 18 November 2018).

PubChem (2018c) *Compound Summary for CID 78451: Octadecylphosphonic acid*. Available at: https://pubchem.ncbi.nlm.nih.gov/compound/Octadecylphosphonic_acid#section=Top (Accessed: 8 November 2018).

Pye, A. D. *et al.* (2009) ‘A review of dental implants and infection’, *Journal of Hospital Infection*. Elsevier Ltd, 72(2), pp. 104–110.

Rafi, H. K. *et al.* (2013) ‘Microstructures and Mechanical Properties of Ti6Al4V Parts Fabricated by Selective Laser Melting and Electron Beam Melting’, *Journal of Materials Engineering and Performance*, 22(12), pp. 3872–3883.

Regos, J. *et al.* (1979) ‘Antimicrobial Spectrum of Triclosan, a Broad-Spectrum Antimicrobial Agent for Topical Application’, *Dermatologica*, 158, pp. 72–79.

Renvert, S. *et al.* (2006) ‘Topical minocycline microspheres versus topical chlorhexidine gel as an adjunct to mechanical debridement of incipient peri-implant infections: A randomized clinical trial’, *Journal of Clinical Periodontology*, 33(5), pp. 362–369.

Renvert, S., Lessem, J., *et al.* (2008) ‘Mechanical and Repeated Antimicrobial Therapy Using a Local Drug Delivery System in the Treatment of Peri-Implantitis: A Randomized Clinical Trial’, *Journal of Periodontology*, 79(5), pp. 836–844.

Renvert, S., Roos-Jansåker, A. M., *et al.* (2008) ‘Non-surgical treatment of peri-implant mucositis and peri-implantitis: A literature review’, *Journal of Clinical Periodontology*, 35(SUPPL. 8), pp. 305–315.

Renvert, S. *et al.* (2018) ‘Peri-implant health, peri-implant mucositis, and peri-implantitis: Case definitions and diagnostic considerations’, *Journal of Clinical*

*Periodontology*, 45(January), pp. S278–S285.

Renvert, S. and Birkhed, D. (1995) 'Comparison between 3 triclosan dentifrices on plaque, gingivitis and salivary microflora', *Journal of Clinical Periodontology*, 22, pp. 63–70.

Ribeiro, F. V. *et al.* (2018) 'Impact of a triclosan-containing toothpaste during the progression of experimental peri-implant mucositis: Clinical parameters and local pattern of osteo-immunoinflammatory mediators in peri-implant fluid', *Journal of Periodontology*, 89(2), pp. 203–212.

Ribeiro, Marta *et al.* (2012) 'Infection of orthopedic implants with emphasis on bacterial adhesion process and techniques used in studying bacterial-material interactions', *BioMatter*, 2(4), pp. 176–194.

Riley, P. and Lamont, T. (2013) 'Triclosan / copolymer containing toothpastes for oral health (Review)', *Cochrane Database of Systematic Reviews*, (12), p. CD010514.

Riley, P *et al.* (2013) 'Triclosan / copolymer containing toothpastes for oral health', *Cochrane Database Syst Rev*, (12), pp. 12–15.

Rimondini, L. *et al.* (1997) 'The Effect of Surface Roughness on Early In Vivo Plaque Colonization on Titanium', *Journal of Periodontology*, 68(6), pp. 556–562.

Rinke, S. *et al.* (2011) 'Prevalence of periimplant disease in partially edentulous patients: A practice-based cross-sectional study', *Clinical Oral Implants Research*, 22(8), pp. 826–833.

Rinner, M. *et al.* (2000) 'Formation of titanium oxide films on titanium and Ti6Al4V by O2-plasma immersion ion implantation', *Surface and Coatings Technology*, 132(2–3), pp. 111–116.

Robinson, A. M. *et al.* (2001) 'The interaction of phospholipid liposomes with mixed bacterial biofilms and their use in the delivery of bactericide', *Colloids and Surfaces A: Physicochemical and Engineering Aspects*, 186(1–2), pp. 43–53.

Roccuzzo, M. *et al.* (2018) 'Clinical outcomes of peri-implantitis treatment and supportive care: A systematic review', *Clinical Oral Implants Research*, 29(March), pp. 331–350.

van Rooijen, N. (1998) 'Liposomes', in *Encyclopedia of Immunology*. 2nd ed. Cambrigde, MA: Academic Press, p. 391.

Rosan, B. and Lamont, R. J. (2000) 'Dental plaque formation', *Microbes and Infection*, 2, pp. 1599–1607.

Rosen, G. and Sela, M. N. (2006) 'Coaggregation of Porphyromonas gingivalis and Fusobacterium nucleatum PK 1594 is mediated by capsular polysaccharide and lipopolysaccharide', *FEMS Microbiology Letters*, 256(2), pp. 304–310.

Rosenberg, E. S. *et al.* (2004) 'A comparison of characteristics of implant failure and survival in periodontally compromised and periodontally healthy patients: a clinical report.', *The International journal of oral & maxillofacial implants*, 19(6), pp. 873–879.
Russell, A. D. (2004) 'Whither triclosan?', *Journal of Antimicrobial Chemotherapy*, 53(5), pp. 693–695.
Rzhepishevska, O. *et al.* (2013) 'The surface charge of anti-bacterial coatings alters motility and biofilm architecture', *Biomaterials Science*, 1(6), p. 589.
Sachdeo, A. *et al.* (2008) 'Biofilms in the edentulous oral cavity', *Journal of Prosthodontics*, 17, pp. 348–356.
Salvi, G. E. *et al.* (2007) 'Adjunctive local antibiotic therapy in the treatment of peri-implantitis II: Clinical and radiographic outcomes', *Clinical Oral Implants Research*, 18(3), pp. 281–285.
Salvi, G. E. *et al.* (2012) 'Reversibility of experimental peri-implant mucositis compared with experimental gingivitis in humans', *Clinical Oral Implants Research*, 23(2), pp. 182–190.
Salwiczek, M. *et al.* (2014) 'Emerging rules for effective antimicrobial coatings', *Trends in Biotechnology*. Elsevier Ltd, 32(2), pp. 82–90.
Samad, A. *et al.* (2007) 'Liposomal Drug Delivery Systems: An Update Review', *Current Drug Delivery*, 4(4), pp. 297–305.
Sandberg, M. E. *et al.* (2009) 'Pros and cons of using resazurin staining for quantification of viable Staphylococcus aureus biofilms in a screening assay', *Journal of Microbiological Methods*. Elsevier B.V., 78(1), pp. 104–106.
Sandborgh-Englund, G. *et al.* (2006) 'Pharmacokinetics of triclosan following oral ingestion in humans', *Journal of Toxicology and Environmental Health - Part A: Current Issues*, 69(20), pp. 1861–1873.
Sanz, M. *et al.* (1991) 'Histo-pathologic characteristics of peri-implant soft tissues in Branemark implants with 2 distinct clinical and radiological patterns.', *Clinical Oral Implants Research*, 2, pp. 28–134.
Sarker, M. A. R. (2014) 'Optical Properties of Al- and Zr-Doped Rutile Single Crystals Grown by Tilting-Mirror-Type Floating Zone Method and Study of Structure-Property Relationships by First Principle Calculations', *Journal of Inorganic Chemistry*, 2014, pp. 1–11.
Schierholz, J. M. and Beuth, J. (2001) 'Implant infections: A haven for opportunistic bacteria', *Journal of Hospital Infection*, 49(2), pp. 87–93.
Schrand, A. M. *et al.* (2010) 'Metal-based nanoparticles and their toxicity assessment', *WIREs Nanomedicine and Nanobiotechnology*, 2, pp. 21–24.

Schwarz, F. *et al.* (2015) 'Real-time PCR analysis of fungal organisms and bacterial species at peri-implantitis sites', *International Journal of Implant Dentistry*, 1(1), pp. 1–7.

Schwarz, F. *et al.* (2018a) 'Peri-implantitis', *Journal of Clinical Periodontology*, 45(June 2016), pp. S246–S266.

Schwarz, F. *et al.* (2018b) 'Peri-implantitis', *Journal of Clinical Periodontology*, 89(Suppl 1), pp. S246–S266.

Serro, A. P. and Saramago, B. (2003) 'Influence of sterilization on the mineralization of titanium implants induced by incubation in various biological model fluids', *Biomaterials*, 24(26), pp. 4749–4760.

Severino, V. O. *et al.* (2016) 'Expression of IL-6, IL-10, IL-17 and IL-33 in the peri-implant crevicular fluid of patients with peri-implant mucositis and peri-implantitis', *Archives of Oral Biology*. Elsevier Ltd, 72(8), pp. 194–199.

Shaniztki, B. *et al.* (1997) 'Identification of a Fusobacterium nucleatum PK1594 galactose-binding adhesin which mediates coaggregation with periopathogenic bacteria and hemagglutination', *Infection and Immunity*, 65(12), pp. 5231–5237.

Shi, Z. *et al.* (2006) 'Antibacterial and mechanical properties of bone cement impregnated with chitosan nanoparticles', *Biomaterials*, 27(11), pp. 2440–2449.

Sigma-Aldrich (2018) *Phospholipid Assay Kit (MAK122) - Technical Bulletin*. Available at: https://www.sigmaaldrich.com/content/dam/sigma-aldrich/docs/Sigma/Bulletin/2/mak122bul.pdf (Accessed: 23 November 2018).

Simões, S. *et al.* (2001) 'On the mechanisms of internalization and intracellular delivery mediated by pH-sensitive liposomes', *Biochimica et Biophysica Acta - Biomembranes*, 1515(1), pp. 23–37.

Sing, S. L. *et al.* (2016) 'Laser and electron-beam powder-bed additive manufacturing of metallic implants: A review on processes, materials and designs', *Journal of Orthopaedic Research*, 34(3), pp. 369–385.

Singhal, N. *et al.* (2015) 'MALDI-TOF mass spectrometry: An emerging technology for microbial identification and diagnosis', *Frontiers in Microbiology*, 6(AUG), pp. 1–16.

Smith, D. C. *et al.* (1991) 'Dental implant materials. I. Some effects of preparative procedures on surface topography', *Journal of Biomedical Materials Research*, 25(9), pp. 1045–1068.

Sorkin, R. *et al.* (2013) 'Origins of extreme boundary lubrication by phosphatidylcholine liposomes', *Biomaterials*. Elsevier Ltd, 34(22), pp. 5465–5475.

Sorkin, R. *et al.* (2016) 'Soft Matter', *Soft Matter*, 12(10), pp. 2773–2784.

Srakaew, V. *et al.* (2011) 'Sodium-phosphorylated chitosan/zinc oxide complexes and evaluation of their cytocompatibility : An approach for periodontal dressing', *Journal of Biomaterials Applications*, 27(4), pp. 403–412.

Sreenivasan, P. K. *et al.* (2011) 'A 6-month study of the effects of 0.3% triclosan/copolymer dentifrice on dental implants', *Journal of Clinical Periodontology*, 38(1), pp. 33–42.

Stern, I. B. (1981) 'Current Concepts of the Dentogingival Junction: The Epithelial and Connective Tissue Attachments to the Tooth', *Journal of Periodontology*, 52(9), pp. 465–476.

Stewart, B. *et al.* (2018) 'Effects of a toothpaste containing 0.3% triclosan in the maintenance phase of peri-implantitis treatment: 2-Year randomized clinical trial', *Clinical Oral Implants Research*, 29(10), pp. 973–985.

Stigter, M. *et al.* (2004) 'Incorporation of different antibiotics into carbonated hydroxyapatite coatings on titanium implants, release and antibiotic efficacy', *Journal of Controlled Release*, 99(1), pp. 127–137.

Stone, N. R. H. *et al.* (2016) 'Liposomal Amphotericin B (AmBisome®): A Review of the Pharmacokinetics, Pharmacodynamics, Clinical Experience and Future Directions', *Drugs*, 76(4), pp. 485–500.

Sułkowski, W. W. *et al.* (2005) 'The influence of temperature, cholesterol content and pH on liposome stability', *Journal of Molecular Structure*, 744–747(SPEC. ISS.), pp. 737–747.

Suzuki, J. B. and Misch, C. E. (2018) 'Periodontal and Maintenance Complications', in *Misch's Avoiding Complications in Oral Implantology*. Atlanta: Elsevier Inc., pp. 771–826.

Takenaka, S. *et al.* (2008) 'Direct visualization of spatial and temporal patterns of antimicrobial action within model oral biofilms', *Applied and Environmental Microbiology*, 74(6), pp. 1869–1875.

Tanaka, Y. *et al.* (2010) 'Effects of electrodeposited poly ( ethylene glycol ) on biofilm adherence to titanium', pp. 1105–1113.

Tavares, L. J. *et al.* (2018) 'An in vitro model of Fusobacterium nucleatum and Porphyromonas gingivalis in single- and dual-species biofilms.', *Journal of periodontal & implant science*, 48(1), pp. 12–21.

Thorn, R. M. S. *et al.* (2005) 'In vitro method to assess the antimicrobial activity and potential efficacy of novel types of wound dressings', *Journal of Applied Microbiology*, 99, pp. 895–901.

Todescan, S. *et al.* (2012) 'Guidance for the maintenance care of dental implants:

Clinical review', *Journal of the Canadian Dental Association*, 78(1).

Trapalis, C. C. *et al.* (2003) 'TiO2(Fe3+) nanostructured thin films with antibacterial properties', *Thin Solid Films*, 433(1-2 SPEC.), pp. 186–190.

Truong, V. K. *et al.* (2010) 'The influence of nano-scale surface roughness on bacterial adhesion to ultrafine-grained titanium', *Biomaterials*. Elsevier Ltd, 31(13), pp. 3674–3683.

Tuson, H. H. and Weibel, D. B. (2013) 'Bacteria-surface interactions', *Soft Matter*, 9(17), pp. 4368–4380.

U.S. National Library of Medicine (2019) *Compound summary: Triclosan*, *PubChem*. Available at: https://pubchem.ncbi.nlm.nih.gov/compound/triclosan (Accessed: 3 May 2019).

Varghese, D. *et al.* (2015) 'Management of a Failing Implant-a case report', *IOSR Journal of Dental and Medical Sciences*, 14(10), pp. 2279–861.

Vélez, M. A. *et al.* (2017) 'Soy PC liposomes as CLA carriers for food applications: Preparation and physicochemical characterization', *Journal of Food Engineering*, 212, pp. 174–180.

van Velzen, F. J. J. *et al.* (2015) '10-year survival rate and the incidence of peri-implant disease of 374 titanium dental implants with a SLA surface: A prospective cohort study in 177 fully and partially edentulous patients', *Clinical Oral Implants Research*, 26(10), pp. 1121–1128.

Venza, I. *et al.* (2010) 'Proinflammatory Gene Expression at Chronic Periodontitis and Peri-Implantitis Sites in Patients With or Without Type 2 Diabetes', *Journal of Periodontology*, 81(1), pp. 99–108.

Verdugo, F. *et al.* (2015) 'Epstein–Barr virus associated peri-implantitis: a split-mouth study', *Clinical Oral Investigations*, 19(2), pp. 535–543.

Villalaín, J. *et al.* (2001) 'Membranotropic effects of the antibacterial agent triclosan', *Archives of Biochemistry and Biophysics*, 390(1), pp. 128–136.

Vogel, K. *et al.* (2014) 'Dental implants coated with a durable and antibacterial film', *Surface Innovations*, 3(SI1), pp. 27–38.

Vorburger, T. V *et al.* (1998) 'Characterization of Surface Topography', in Plenum Press (ed.) *Beam Effects, Surface Topography, and Depth Profiling in Surface Analysis*. New York, pp. 275–354.

Vorregaard, M. (2008) 'Comstat2 - a modern 3D image analysis environment for biofilms', *Technical University of Denmark: Kongens Lyngby, Denmark*.

Vrancken, B. *et al.* (2012) 'Heat treatment of Ti6Al4V produced by Selective Laser Melting : Microstructure and Mechanical properties', *Journal of Alloys and*

*Compounds*, 541(0), pp. 177–185.

Wadhwa, B. *et al.* (2015) 'Flapless vs open flap techniques of implant placement', *Indian Journal of Dental Research*, 26(4), pp. 372–377.

Wang, B. *et al.* (2006) 'Acute toxicity of nano- and micro-scale zinc powder in healthy adult mice', *Toxicology Letters*, 161, pp. 115–123.

Wang, W. C. *et al.* (2017) 'Management of peri-implantitis – A contemporary synopsis', *Singapore Dental Journal*. Elsevier (Singapore) Pte Ltd., 38, pp. 8–16.

Wara-Aswapati, N. *et al.* (2005) 'The effect of a new toothpaste containing potassium nitrate and triclosan on gingival health, plaque formation and dentine hypersensitivity', *Journal of Clinical Periodontology*, 32(1), pp. 53–58.

Watts, J. F. and Wolstenholme, J. (2005) 'Comparison of XPS and AES with Other Analytical Techniques', in *An Introduction to Surface Analysis by XPS and AES*. 2nd ed. Chichester: John Wiley & Sons, Ltd., pp. 165–182.

Welk, A. *et al.* (2005) 'The effect of a polyhexamethylene biguanide mouthrinse compared with a triclosan rinse and a chlorhexidine rinse on bacterial counts and 4-day plaque re-growth', *Journal of Clinical Periodontology*, 32(5), pp. 499–505.

Wenzel, R. N. (1936) 'Resistance of solid surfaces to wetting by water', *Industrial and Engineering Chemistry*, 28(8), pp. 988–994.

Wilson, M. (1999) 'Use of constant depth film fermentor in studies of biofilms of oral bacteria.', *Methods in Enzymology*, 310, pp. 264–279.

Winkel, A. *et al.* (2015) 'Introducing a Semi-Coated Model to Investigate Antibacterial Effects of Biocompatible Polymers on Titanium Surfaces', *International Journal of Molecular Sciences*, 16(2), pp. 4327–4342.

Wong, M. L. and Medrano, J. F. (2005) 'Real Time PCR for mRNA quantitation', *BioTechniques*, 39(1), pp. 1–11.

Wood, N. J. *et al.* (2015) 'Chlorhexidine hexametaphosphate nanoparticles as a novel antimicrobial coating for dental implants', *Journal of Materials Science: Materials in Medicine*. Springer US, 26(6), pp. 1–10.

Woodward, J. T. *et al.* (1996) 'Self-Assembled Monolayer Growth of Octadecylphosphonic Acid on Mica', *Langmuir*, 12(15), pp. 3626–3629.

Woodward, J. T. *et al.* (1997) 'Kinetics of self-assembled monolayer growth explored via submonolayer coverage of incomplete films', *Journal of Physical Chemistry B*, 101(38), pp. 7535–7541.

Wu, J. *et al.* (2010) 'Determination of triclosan metabolites by using in-source fragmentation from high-performance liquid chromatography/negative atmospheric pressure chemical ionization ion trap mass spectrometry', *Rapid Commun. Mass*

*Spectrom.*, 24, pp. 1828–1834.

Wu, X. S. *et al.* (1992) 'Conjugation of phosphatidylethanolamine to poly(N-isopropylacrylamide) for potential use in liposomal drug delivery systems', *Polymer*, 33(21), pp. 4659–4662.

Wu, X. S. *et al.* (1993) 'Effect of conjugation of phospholipid to poly(N-isopropylacrylamide) on its critical solution temperature.', *Makromolekulare Chemie, Rapid Communications*, 14(5), pp. 309–314.

Wu, Y. *et al.* (2017) 'Cytochrome P450-mediated metabolism of triclosan attenuates its cytotoxicity in hepatic cells', *Archives of Toxicology*. Springer Berlin Heidelberg, 91(6), pp. 2405–2423.

Xiao, J. *et al.* (2012) 'The exopolysaccharide matrix modulates the interaction between 3D architecture and virulence of a mixed-species oral biofilm', *PLoS Pathogens*, 8(4), pp. 7–9.

Xie, H., Rj, G. and Di, H. (1991) 'Adhesive properties of strains of Fusobacterium nucleatum of the subspecies nucleatum , vincentii and polymorphum', *Oral Microbiology Immunology*, 6(42), pp. 257–263.

Yaghobee, S. *et al.* (2014) 'Assessment of interleukin-1beta and interleukin-6 in the crevicular fluid around healthy implants, implants with peri-implantitis, and healthy teeth: a cross-sectional study', *Journal of the Korean Association of Oral and Maxillofacial Surgeons*, 40(5), p. 220.

Yah, W. O. *et al.* (2012) 'Selective modification of halloysite lumen with octadecylphosphonic acid: New inorganic tubular micelle', *Journal of the American Chemical Society*, 134(3), pp. 1853–1859.

Yakar, N. *et al.* (2019) 'Evaluation of gingival crevicular fluid and peri-implant crevicular fluid levels of sclerostin, TWEAK, RANKL and OPG', *Cytokine*, 113(March 2018), pp. 433–439.

Yang, L. *et al.* (2017) 'Comparisons of the biodistribution and toxicological examinations after repeated intravenous administration of silver and gold nanoparticles in mice', *Nature Scientific Reports*. Springer US, 7, pp. 1–12.

Yaseen, M. *et al.* (2017) 'Photocatalytic Studies of Tio2/Sio2 Nanocomposite Xerogels', *Journal of Analytical & Bioanalytical Techniques*, 08(01), pp. 8–11.

Yatvin, M. *et al.* (1978) 'Design of liposomes for enhanced local release of drugs by hyperthermia.', *Science*, 202(4374), pp. 1290–3.

Yeagle, P. L. (1985) 'Cholesterol and the cell membrane', *BBA - Reviews on Biomembranes*, 822(3–4), pp. 267–287.

Yeh, H. C. *et al.* (2019) 'Identification of microbiota in peri-implantitis pockets by

matrix-assisted laser desorption/ionization time-of-flight mass spectrometry', *Scientific Reports*. Springer US, 9(1), pp. 1–9.

Yoshinari, M. *et al.* (2010) 'Biofouling : The Journal of Bioadhesion and Biofilm Prevention of biofilm formation on titanium surfaces modified with conjugated molecules comprised of antimicrobial and titanium-binding peptides', *Biofouling*, 26, pp. 103–110.

Yucesoy, D. T. *et al.* (2015) 'Chimeric Peptides as Implant Functionalization Agents for Titanium Alloy Implants with Antimicrobial Properties', *Jom (1989)*, 67(4), pp. 754–766.

Yue, C. *et al.* (2009) 'Bioactive titanium metal surfaces with antimicrobial properties prepared by anodic oxidation treatment', *Science in China Series E: Technological Sciences*, 52(8), pp. 2269–2274.

Zani, S. R. *et al.* (2016) 'Peri-implant crevicular fluid biomarkers as discriminants of peri-implant health and disease', *Journal of Clinical Periodontology*, 43(10), pp. 825–832.

Zeza, B. and Pilloni, A. (2012) 'Peri-implant mucositis treatments in humans: a systematic review', *Annali di stomatologia*, III(3/4), pp. 83–89.

Zhao, L. *et al.* (2009) 'Antibacterial coatings on titanium implants', *Journal of Biomedical Materials Research - Part B Applied Biomaterials*, 91(1), pp. 470–480.

Zhao, M. *et al.* (2013) 'Electronic Supplementary Information ( ESI ) available for : A facile strategy to large-scale uniform brookite TiO 2 nanospindles with high thermal stability and superior electrical properties', pp. 1–14.

Zhao, S. *et al.* (2014) 'The construction of hierarchical structure on Ti substrate with superior osteogenic activity and intrinsic antibacterial capability', *Scientific Reports*, 4(1), pp. 1–10.

Zheng, R. *et al.* (2014) 'Liposomes tethered to a biopolymer film through the hydrophobic effect create a highly effective lubricating surface', *Soft Matter*, 10(46), pp. 9226–9229.

Zhou, C. *et al.* (2017) 'Personal Care Products and Cosmetics', in *Reproductive and Developmental Toxicology*. Cambridge, MA: Academic Press, pp. 857–899.

Zhou, W. *et al.* (2016) 'Feasibility of Dental Implant Replacement in Failed Sites: A Systematic Review', *The International Journal of Oral & Maxillofacial Implants*, (May), pp. 535–545.

Zhou, X. and Li, Y. (2015) *Subgingival Microbes*, *Atlas of Oral Microbiology: From Healthy Microflora to Disease*. London: Elsevier Science & Technology Books.

Zitzmann, N. U. *et al.* (2001) 'Experimental peri-implant mucositis in man', *Journal of*

*Clinical Periodontology*, 28(6), pp. 517–523.
Zuidam, N. *et al.* (1993) 'Sterilization of Liposomes by Heat Treatment', *Pharmaceutical research*, 10(11), pp. 1591–6.